MECHANICAL PROPERTIES OF POLYESTER NANO-COMPOSITES EXPOSED TO LIQUID MEDIA

MOHD SHAHNEEL BIN SAHARUDIN

A thesis submitted in partial fulfilment
of the requirements of the
University of Northumbria at Newcastle
for the degree of
Doctor of Philosophy

Research undertaken in the Faculty of
Engineering and Environment

November 2017

Declaration

I declare that the work contained in this thesis has not been submitted for any other award and that it is all my own work. I also confirm that this work fully acknowledges opinions, ideas and contributions from the work of others. This thesis fully complies with the regulations set by the Northumbria University.

I declare that the Word Count for this thesis is 38,892 words

Name: Mohd Shahneel Saharudin

Signature:

Date: 15/11/2017

Abstract

Halloysite nanotubes (HNTs) offer excellent improvements in wide range of physical and engineering properties at low filler content. Due to their outstanding properties such as large aspect ratio, high surface area, flame retardant and good optical clarity, HNTs polymer nanocomposites are widely used in automotive, coating, packaging and medical devices. The results showed that the incorporation of halloysite nanotubes (HNTs) into polyester significantly improved dynamic mechanical properties of the nanocomposites including the glass transition temperature (T_g), storage moduli, microhardness, tensile properties, flexural properties and impact toughness. The mechanical properties of polyester-based nanocomposites were degraded after water-methanol exposure. The maximum microhardness, tensile, flexural and impact toughness values were measured at 1 wt% of HNTs reinforcement and the results also showed that HNTs improved the liquid barrier properties of polymers due to an increase in the tortuosity path. Several deterioration effects are likely to take place concurrently after seawater exposure. Plasticization reduced the mechanical properties of the nanocomposites and microorganisms such as microbes entered through microvoids to further increase the deterioration in mechanical properties of the nanocomposites. Microbes can cause chemical degradation and the breakage of hydrocarbons using seawater molecules. Nanocomposite biodegradation is highly undesirable for material integrity as these are mostly used in structural designs of marine applications. Structural damage may result in premature weakening which is often translated into system failure and enormous economic losses. The influence of short-term water absorption on the mechanical properties of HNTs-multi layer graphene-reinforced polyester hybrid nanocomposites was also investigated. After short-term water exposure, the maximum microhardness, tensile, flexural and impact toughness values were observed in case of polyester-multi-layer graphene (MLG) nanocomposites. It was also found that synergistic effects were not effective at a concentration of 0.1 wt % in producing considerable improvement in the mechanical properties of the hybrid nanocomposites.

Table of contents

Contents Page

List of technical abbreviations

CNTs	Carbon nanotubes
DMA	Dynamic mechanical analysis
ESC	Environmental stress cracking
GO	Graphene oxide
GP	Graphene platelets
GnPs	Graphene nano-platelets
HDPE/EVA	High density polyethylene/Ethylene-vinyl acetate
HNTs	Halloysite nanotubes
LDPE/EVA	Low density polyethylene/Ethylene-vinyl acetate
MLG	Multi-layer graphene
MMT	Montmorillonite
MP	Monolithic polyester
MIC	Microbially influenced corrosion
NaOH	Sodium hydroxide
PC	Polycarbonate
R_a	Roughness average
R_q	Surface roughness root mean square
R_z	Highest and lowest point of profile
SCC	Stress corrosion cracking
SEM	Scanning electron microscopy
UP	Unsaturated polyester

Preface

Nanocomposite materials have been commonly used to replace not only steel but also alloys in the production of numerous products and structures in automotive, aircraft, sporting goods, civil and marine structures [1, 2]. Their excellent properties have made them superior and more popular than other materials. Resistance to expected forces during operation and exposure to environment are two main aspects that should be taken into account when selecting the materials used for product design [3]. Available data is insufficient and makes it hard to predict the deterioration in the mechanical properties of nano-particle reinforced polymers in the presence of liquid media. The understanding of how materials degrade could contribute to improvements in the existing mechanical properties of polymers, particularly for application that are exposed to liquid media. A comprehensive literature review on the deterioration in mechanical properties is given in chapter 1. Halloysite nanotubes (HNTs) have gained great attention due their capability to enhance the mechanical properties of polymers with low filler loading. However, the application of HNTs in the reinforcement of polyester/clay nanocomposites exposed to aggressive environments has not yet been fully studied, and this is the subject of this thesis. HNTs were used as the main nano-filler reinforcement while multi-layer graphene is used as a second filler in this study. Adding a little graphene makes a significant difference. It can make stronger, lighter and more durable. Common products such as light bulbs, aircrafts and cars can be tailored to use minimum energy. HNTs and graphene can transform our world; however, the future is unknown because it is difficult to predict their impact over time.

Acknowledgements

I would like to express my sincere gratitude and appreciation to my supervisor, Dr. Fawad Inam and co-supervisor Dr. Islam Shyha. It has been an honour to be their PhD student. They have taught me how good research is done. I appreciate all their contributions of time, ideas, and support during my PhD journey. I am also indebted to my research colleagues Atif Rasheed and Jiacheng Wei for helping me in every possible manner in my research. My time at Northumbria University was made enjoyable in large part due to the many friends and groups that became part of my life. Special acknowledgements go to Kuala Lumpur University and Majlis Amanah Rakyat (MARA) for financially supporting my PhD study. I am also very thankful to Professor Dr. Mohd Razif Idris and Haji Azmi Mohamad for the opportunity and trust that they gave to me to pursue my PhD at Northumbria University. I wish to thank my wife Syafawati Hasbi, and our children Hanzhalah and Nusaybah as well as my parents Saharudin Salleh and Norazien Ramli for their love, moral support and encouragement. Finally, I wish to thank my parents-in-law Hasbi Yahya and Julia Bakar for their support and concern. The PhD experience has brought me and my family to a very special unforgettable journey.

Mohd Shahneel Saharudin

Northumbria University, October 2017.

1. Introduction to materials failure

The integration of reinforcement into polymers at nanoscale can provide a significant increase in numerous physical and mechanical properties of polymer nanocomposites [4–8]. The high strength-to-weight ratio of polymer nanocomposites and the ability to exhibit flexibility by manipulating their mechanical properties are the main reasons attracting the interest of researchers. Extensive research has been dedicated to this field in the past couple of decades [9, 10]. The mechanical properties of polymers can be modified using numerous fibres and particulates, and smaller nano-filler reinforcements have surpassed the larger counterparts [11, 12].

Material failure which leads to catastrophic consequences can result in the loss of life and injuries and inflict costly damage. The sinking of the Titanic and the Boston Molasses are classic examples of engineering disasters caused by material failure [13]. Material failure is defined as any change in properties that makes the material or component functionally, structurally or aesthetically unacceptable. Over the last few decades, polymers have effectively replaced other materials in most commercialised applications. It is crucial to understand the reasons behind polymer failure in order to prevent its occurrence.

The main drawback of polymeric composite materials is the loss of inherent mechanical properties mainly caused by exposure to liquid media. Such exposure results in plasticization, matrix cracking and also resulting in premature failure [14]. Polymeric materials are also prone to defects during manufacturing process and sometimes can be affected by the environment that they are exposed to. At relatively low stress levels, far below tensile strength, failure in polymer components is inevitable

due to long-term stress (creep rupture), cyclic stresses (fatigue failure) or even due to contact with aggressive chemical solutions contact.

In marine environments, the properties of polymers are strongly influenced by seawater, which contains having a mixture of various salts [15–18]. Similarly, organic liquids can cause cracking at very low stress levels in semi-crystalline, amorphous, and highly cross-linking polymers [19–21]. In the last few years, the effect of water or chemical media on the mechanical properties of thermosets have been studied particularly in the field of piping and the marine, medical, coating and automotive industries [1, 22–27]. For example, unsaturated polyesters are brittle due to their high cross-linking level and vulnerable to stress cracking failure and deterioration in mechanical properties in applications where contact with liquid is unavoidable [28]. There are many applications in which polymer nanocomposites are either directly or indirectly exposed to certain liquid media conditions. Immersion or direct contact with a fluid medium as in the case of bottles, vessels, and pipes are common sources of fluid contact that can cause deterioration in mechanical properties [29, 30]. Depending on the application and type of fluids involved, the primary source of fluid contact will accelerate the stress cracking failure of polymers. In some cases, there are also sources of secondary fluid contact, usually through detergents, lubricants, paints and coatings [31].

Although various review articles are available on the mechanical properties of polymer nanocomposites, however, no article has been published where the mechanical properties of polymer nanocomposites are correlated with the presence of liquid media and their influence on the stress-cracking properties of polymer nanocomposites. Therefore, this review chapter discusses in detail on how the

polymer nanocomposites behave in the presence of liquid media and provides a rationale for their peculiar behaviour.

Failures in materials are major concerns in many applications because the consequences can lead to disasters and catastrophes as well as loss of life. However, such failures also motivate researchers to investigate the failed materials further. Failures in materials are also known as deterioration in their properties which cause undesirable effects on part function, structure or aesthetic value [32, 33].

Engineering polymers have prospered as an alternative to metals in countless applications, such as in the automotive, aircraft, construction and bio-medicine sectors [1, 2, 34–36]. Failures in polymers are always of significant interest for researchers, and it is essential to identify the causes so that suitable actions can be carried out to avoid or control reoccurrence. Polymeric-based materials are considerably influenced by the processing technique used and also vulnerable to environment such as liquid media, high temperature and storage time, making their operational life cycle unpredictable [32, 37, 38].

1.1. Fundamentals of fracture type after liquid exposure

The failure of engineering products through fracture can have catastrophic consequences and much effort among engineers has been put to develop materials and designing structures that are resistant to premature failure. By definition, a fracture is the creation of new surfaces within a body through the application of external forces [39]. In general, there are two common terms which are used to explain polymer fracture after liquid contact; ESC (environmental stress cracking) and SCC (stress corrosion cracking).

ESC is a specific term used to demonstrate brittle failure phenomenon in thermoplastics-based polymers which are exposed to aggressive solvents; mainly alcohols and oils. In many publications, SCC is commonly used to explain problems in thermoset-based polymers exposed to various acidic solutions. However, under environmental attack, crack propagation is quicker for materials exposed to water than air. In the literature, ESC only occurs in thermoplastic polymers, while SCC occurs in thermoset-based polymers, metals and ceramics. The use of terms ESC and SCC has slightly changed over time based on more recent publications. Most recent studies categorize thermoset-based polymers exposed to acidic liquids and alcohols under ESC [40–44]. The SCC term has been reserved to define faults in metal and ceramic materials exposed to corrosive environments [45–50].

Adding halloysite nanotubes (HNTs) to polymers has been shown to increase the mechanical properties of nanocomposites. However, very little is known about the effect of HNTs-polymer nanocomposites being exposed to liquid environments. This study provides new insights into mechanical properties of the HNT-polyester durability.

The objectives of this research are:

i) To achieve a better dispersion of HNTs in the polyester matrix. This will include processing optimization by using sonication.
ii) To analyse the deterioration of mechanical properties in HNTs-polyester nanocomposites exposed to aggressive environment (water-methanol).
iii) To investigate the effect of HNTs on the mechanical properties of polyester exposed to a seawater environment.

iv) To analyse the effect of short-term water absorption on the mechanical properties of polyester-based nanocomposites reinforced with HNTs, multi-layer graphene (MLG) and HNTs-MLG (hybrid fillers).

1.1.1. Environmental stress cracking (ESC)

ESC typically takes place in amorphous polymers because of their loose structure which enables fluids to permeate into the polymer [31, 51]. Amorphous thermoplastics have also shown high sensitivity to ESC. The locally dissolved aggressive liquid can cause crazing, cracking, and plasticization [52]. Crazes are extended areas covered by highly drawn fibrils which link the micro-cracks and stop their movement and combination [53]. Gent [54] proposed a hypothetical mechanism of crazing is associated with the stress-activated devitrification of a small amount of material at the tip of a flaw to a softer rubbery state. This mechanism is similar to the process reported by Knight [55]. The following points can be drawn from the existing reported research on the mechanism of ESC:

a) The application of hydrostatic pressure can stop craze development [54]

b) Temperature influences crazing stress. Increasing temperature up to T_g will reduce the craze [31]

c) The tensile stress at which crazes form is much lower in the presence of certain active liquids and vapours

d) Crazes do not develop in materials with prominent molecular orientation of tension, but instead develop when it is perpendicular to the tension [55]

Hansen pointed out that the solubility parameters have three categories of interconnected forces; dispersive, polar, and hydrogen bonding [31, 56]. The presence of hydrocarbon liquid can significantly influence the viscoelastic properties of biodegradable polymers. Widiastuti *et al.* [57] reported that there is a consistent decrease in modulus with an increasing hydrocarbon liquid content even at 40^{o}C. In some cases, non-aggressive chemicals can also accelerate brittle failure [58]. It was shown that the porosity in unsaturated polyester creates space between matrix and fibre. Porosity allows the liquid media to diffuse into the nanocomposites, which can create large internal stresses before failure takes place [59–61].

ESC in polymers and nanocomposites has also been studied for biomedical applications such as surgical, respiratory, drug delivery and IV access devices [62–65]. Glassy polymers such as polycarbonate and PMMA are extensively used for biomedical applications. Wright [31] has shown that residual stresses during the injection moulding process are responsible for causing ESC in polymers. The residual thermal stresses are also found in polymers arising from temperature gradients during the fabrication process [66]. Isayev [67] revealed that the residual thermal stress is of parabolic shape with compression mode on the surface, which shifts to tension mode in the core. A number of molecular mechanisms have been proposed to be responsible for ESC, such as interlamellar failure [68] which is a rate-dependent process which is commonly observed in ESC [69].

Nano-size particle reinforcement, on the other hand, is a new approach that is worth exploration. Recent publications show that polycarbonate filled with nanoparticles leads to an improvement in environmental stress cracking (ESC)

resistance where the rate of growth of the damage decreases with increased nano-SiO_2 content.

1.1.2. Stress corrosion cracking (SCC)

Stress corrosion cracking (SCC) can be defined as crack formation in a corrosive environment which can lead to the catastrophic failure of metals and polymers [70, 71]. Over the years, metals have been substituted by composites because of their high strength and chemical resistance [72–74]. The characteristics of stress corrosion cracking on polymer composites have been studied over the years by Kumosa [75–84] and Shokrieh [85]. So far, there has been little discussion or research into the durability of fibre-reinforced polymers.

Composite suspension insulators are commonly used in overhead transmission lines with line voltages in the range of 69 kV to 735 kV [86]. The insulated pultruded glass fibre/polymer matrix rods are used as the principal load bearing components. The rubber housing materials with multiple weather sheds is used to cover the surface of the rod with two metal end fittings attached. However, the composite suspension insulators often undergo brittle fracture due to the stress corrosion cracking (SCC) of the composite rod material [77].

The growth of stress corrosion crack (SCC) on composites under its fracture strength can occur in diluted acid environments and severely affects the life time of composites [87, 88] [89, 90]. In the past, most studies of stress corrosion cracking (SCC) topic focused on glass fibre/polyester composites which are mainly used as materials in containers, pipes and pressure vessels. Stress corrosion crack growth

rates and other factors that affect crack growth are often taken into consideration when designing the glass/polymer composites. [91–94].

Megel *et al.* reported that the extent of stress corrosion damage on composite surfaces is strongly determined by the type of polymer resin used [77]. The process can be divided into three steps; crack initiation, sub-critical crack growth and stable propagation. Crack initiation and sub-critical crack growth are random processes. Different degrees of stress corrosion surface damage are noticed depending on the exposed surface area of the fibres. In terms of the sub-critical crack extension process, the E-glass/epoxy composite shows approximately 5 times better resistance than E-glass/modified polyester systems [77].

Friedrich carried out stress corrosion tests for glass fibre/polyester composites [95]. He revealed that the crack resistance of the materials can deteriorate faster either or slower under environmental attack; for instance, the cracks propagate faster in water compared to in air. Microstructural parameters such as fibre fraction and the local orientation of fibres to the propagating crack contribute to crack propagation [95]. The attack only happens at the fibre matrix interfaces and at the fibres, while the matrix shows insensitivity towards the aggressive medium in all cases.

1.1.3. Ageing mechanism

The assessment of the durability of polymer products exposed to marine environments has become increasingly crucial in industrial sectors such as the oil and gas industries, harbour and naval applications and renewable energy in terms of product certification, total lifetime and maintenance periods.

Polymer lifetime prediction in harsh environments includes three steps; First, the ageing mechanisms observed naturally are identified; and then the accelerated ageing tests are performed to reduce the test time and the kinetics of the ageing reactions are investigated. Finally, a time-temperature superposition rule is applied to evaluate the ageing consequences under service conditions. Ageing tests to accelerate the degradation kinetics need to be carry out without any modification to the degradation process to ensure long term integrity.

The generic term ageing can refer to the reversible physical ageing effects (for instance, swelling due to moisture absorption) as well as to the more serious and irreversible chemical ageing. The lack of data regarding the effects that such deterioration might have on the residual properties of such composites represents a major issue still hindering their wider use, especially in outdoor applications. Nonetheless, this represents an active field of research that is attracting increasing interest [96]. Polymer composites that absorb moisture and water molecules can act as plasticizers by influencing the fibres, the matrix and the interface, forming regions of poor transfer efficiency and thus reducing mechanical properties. Composites materials are prone to degradation due to humidity, as the absorption of water causing differential swelling between the fibres and the matrix [97].

The effects of water absorption can be understood by taking into account the influence exerted on each of the constituents (fibre and matrix) of the composite along with the fibre/matrix interface. Water entering composites results in the deterioration of jute fibres, stress corrosion of glass fibres [98] and weakening of the fibre/matrix bonding strength, as the effect of water on the polymeric matrix is considered only of minor importance (the plasticization effect) [60]. Prolonged exposure to water causing

the swelling of natural fibres leads to a decrease in the stiffness of the fibres and the development of shear stresses at the interface that cause debonding [15, 60, 96, 99, 100].

It is also noted that ageing results in significant reduction of the strength and stiffness of all composites. In general, the retention of the properties of hybrid composites is higher than that of jute fibre composites and therefore glass fibres had the effect of reducing the deterioration of jute fibre reinforced composites. The loss in tensile strength is as high as 54% for jute fibre composites, while it was equal to about 34% for JGC composites [101].

1.1.4. Summary

Undoubtedly, exposure to liquid media causes severe deterioration in the mechanical properties of polymers and polymer nanocomposites. The lowered mechanical properties and ESC are major concerns in applications of polymers and polymer nanocomposites in various sectors such as the medical, marine, automotive and coating industries. Non-aggressive liquid such as water can act as a plasticizer if exposed to polymers for a certain period of time, and also responsible for reductions in strength.

Swelling, plasticization, and the detachment of fibre and particulate reinforcement from the matrix are commonly observed phenomena in polymer nanocomposites when exposed to liquid media. The diffusion of liquid via micro-cracks leads to stress cracking which can be avoided by fibre and particulate reinforcement. It is interesting to study the stress cracking resistance of polymer nanocomposites under external stresses because complex phenomena happen simultaneously [102].

The existing information is definitely inadequate and the lack of sufficient data makes it hard to predict the stress cracking failure of nano-particle-reinforced polymers in the presence of liquid media. In this respect, research can be carried out by reinforcing the polymer matrix with different fibres and particulates to determine the resistance of polymer nanocomposites toward ESC. The understanding of these mechanisms will contribute to improvements in the existing mechanical properties of polymers, particularly for application that are exposed to liquid media.

Nanocomposites have not fulfilled the expectations due to several factors such as poor dispersion and interfacial load transfer, deficiencies during processing, poor alignment, poor load transfer to the interior of filler bundles and the fractal nature of filler clusters.

High quality dispersion is always a valuable property of a composite, and so one tries to optimise the dispersion of filler. The level of dispersion can be measured directly using scanning electron microscope (SEM). In thermoplastics, the greater part of the dispersion occurs in the melt zone where the pellets of polymer are just melting [103]. Apart from that, high viscosity resin incorporated with fillers requires a high energy input and sometimes encourages deagglomeration. Feeding the filler into the unmelted polymer may give good dispersion, but it also results in the higher wear of the extruder, so that this approach is only advisable for soft, surface-treated fillers [104]. As for thermosets, reducing resin viscosity and controlling sonication time may also be the solutions to produce desirable composites with moderate strength and ductility. When nanocomposites are exposed to liquid media, deterioration in mechanical properties is unavoidable unless the above-stated factors such as dispersion, agglomeration and deficiencies are tackled effectively.

1.2. Liquid media and polymer deterioration

The premature initiation of cracking and embrittlement of a plastic material is caused by both stress and strain as well as contact with aggressive fluids [31]. It is the leading cause of the failure of plastic components due to the unpredictable nature of the phenomenon because it occurs at stress levels below the mechanical strength of the material when the affected part is in contact with a strong chemical medium. The application of fibres and polymer blend technology are existing approach used to overcome the deterioration of mechanical properties caused by chemical attack. The polymer blend approach has proven to be good method to improve resistance to stress cracking failure [53, 105, 106] however, it is very expensive.

The in-service deterioration of the mechanical properties of polymers is an important aspect which limits the applications of these versatile materials.[107] Polymer deterioration involves the degradation properties caused by the environment and service conditions, and it normally limits the service lifetime [108, 109]. Polymer deterioration and failure caused by a liquid medium can cause life-threatening accidents. In 1996, a baby in hospital was fed via a Hickman line and suffered an infection, when new connectors were used [3]. The reason for this infection was the cracking and erosion of the connectors from the inner side due to contact with liquid media. It was reported that the baby suffered from brain damage and later the mother decided in 2002 to file a legal case of medical negligence for the usage of an inappropriate medical device [3]. Figure 1 shows a Hickman IV line fitted with a polycarbonate (PC) connector which undergoes brittle failure. Brittle failure caused by environmental stress cracking (ESC) can be life threatening to patients. The risk of stress cracking is always present when the product is subject to the simultaneous

effects of mechanical stresses and aggressive fluids [110]. Most recent studies report that ESC is a serious threat in the field of plastic products, being responsible for 25% of premature failures [111].

Poly(methyl methacrylate) (PMMA) is used when transparency or optical clarity is required in some products. Both PC and PMMA are prone to ESC failure due to their molecular chain structure that can be easily disentangled when subjected to stress and liquid media. Since the applications in medical devices are vital, any crack or damage will be life-threatening to users [3]. It can be observed that the cracks exist in the male of the luer connector (Figure 2) because of stress cracking failure after exposure to liquid media in the hospital. Although in certain cases secondary fluid contact is less severe than primary fluid contact; however, both can lead to catastrophic failure and the deterioration of polymer properties. For instance, moulded polystyrene eyes for teddy bears become clouded permanently. The eyes were held in by metal clips which were found to be coated with metal cutting fluid. The built-in stresses and fluid caused problems through crazing [31].

In another example of ESC, the failure of polyethylene-based components after exposure to liquid media has been identified and reported in several publications [106, 112, 113]. Various automotive components are made of polymers which undergo deterioration when exposed to liquid media, such as mirror housings, headlight lenses, latch handles and ignition modules [25]. Aggressive liquids such as diesel and unleaded fuel permeate slowly into the molecular structure of the polymer-based components and interfere with the intermolecular forces bonding the polymer chains. These conditions expedite molecular disentanglement and subsequent macroscopic

brittle-crack development. Thus, an unexpected brittle failure of polymeric-based products occurs during service.

It has been noted that the decrease in the surface energy of crack development exposed with organic solvent allows lower stress for craze or crack initiation [114]. The reduction in surface energy can be expressed in the following equation:

$$\gamma_{SL} = \gamma_S - \gamma_L \cos\theta \quad \text{.....Equation 1 [39]}$$

Where γ_{SL} Solid/liquid interfacial tension

γ_S Solid-air Surface tension

γ_L Solid-liquid Surface tension

The concept of solid and liquid interfacial tension presented in equation 1 only applies to cases of ESC. However, it is believed to have an insignificant effect in the overall mechanism where stress cracking take place [115]. Figure 3 and Figure 4 show a cracked mirror housing and headlight lens. Figure 5 shows an SEM image of the headlight lens with an intersecting network of cracks which indicate that the lens underwent brittle fracture after being exposed to windscreen washer liquid. Headlights lenses made from polycarbonates are brittle and the chemical agent responsible for the failure was thought to be from the windscreen washer liquid that contains methanol or possibly from vehicle fuel. The combination of built in stress and exposure with aggressive liquid have caused an ESC failure on the head light lens. SEM inspection showed the character of a brittle fracture where the cracking progressed into the lens base material. At high magnification, the craze fragments are obvious.

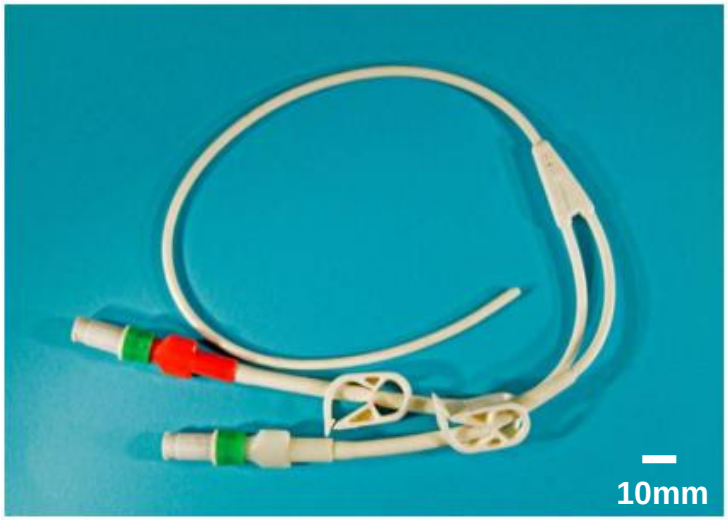

Figure 1. Hickman IV Line with fitted with polycarbonate connector [3].

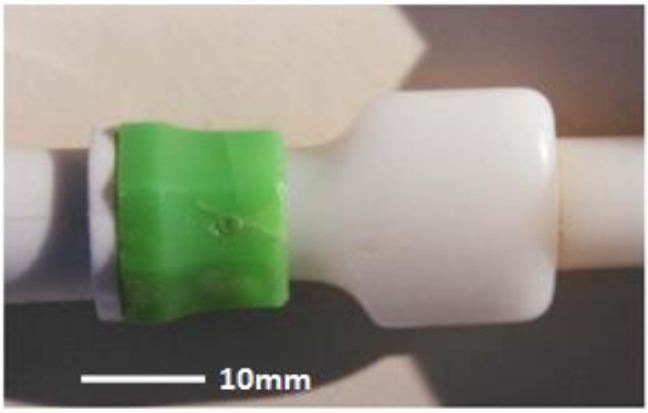

Figure 2. Macrograph of brittle cracks from gate in male luer connector [3].

Figure 3. Mirror housing exhibit stress cracking failure after liquid medium exposure [25].

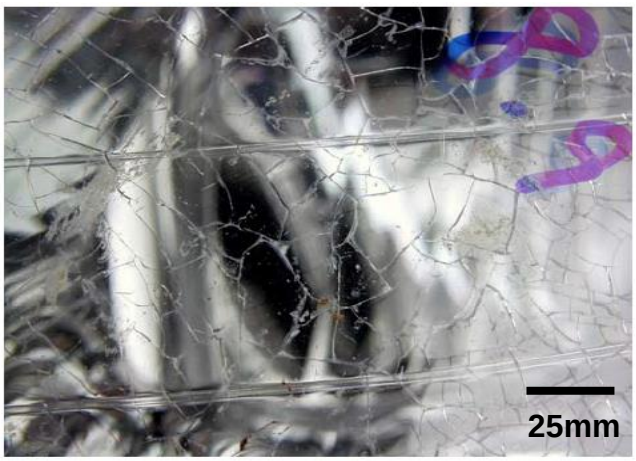

Figure 4. Windscreen washer effect on the headlight lens [25].

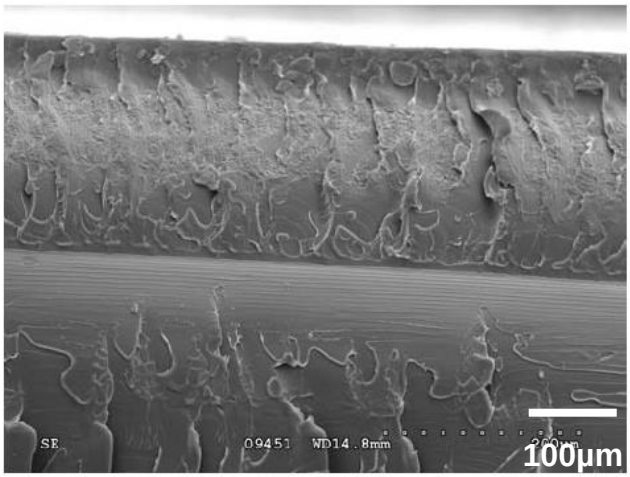

Figure 5. SEM image of intersecting network of cracks on headlight lens [25].

1.3. Effects of liquid media on mechanical properties of polymer nanocomposites

This section discusses the effect on the mechanical properties of polymer nanocomposites exposed to liquid media. In general, liquid media can be classified into three categories: non-aggressive, moderate, and aggressive media. Organic esters, ketones, aromatic hydrocarbons and chlorinated hydrocarbons have more severe effects than organic alcohols and aliphatic hydrocarbons [25]. Liquids with

hydrogen bonding are classified as aggressive media, organic alcohols are known to be moderately aggressive and water is a non-aggressive medium.

1.3.1. Water

Water has neutral pH due to its inherent hydrogen bonding but it can lower the mechanical properties of composites by plasticizing the matrix and reducing its interfacial strength of the reinforcing additive. In real applications, thermoset-based also suffer from deterioration in mechanical properties when exposed to water in the marine and automotive industries [1, 22–25], Water may penetrate into the polymers and polymer nanocomposites by capillary action and may significantly affect the polymer chains and interphases [116]. In cases of samples exposed to a water environment, many polymer matrix composites absorb water by instantaneous surface absorption and diffusion, and therefore degradation is strongly linked to water intake by composites. Several factors are known to affect the way in which composite materials absorb water [101, 117], such as temperature, fibre volume fraction, reinforcement architecture, fibre nature (permeable or impermeable), area of exposed surfaces, polarity of the molecular structure, and degrees of crosslinking and crystallinity [118].

Table 1 lists some of the prominent studies that have been carried out to study the effect of water on the mechanical properties of polymer composites. There is consensus in the reported literature that water can significantly degrade the properties of polymers and polymer nanocomposites. Normally, the absorption rate increases with longer immersion time. The reaction between water molecules and the polymer matrix causes the deterioration of the interphase which has a detrimental effect on the

mechanical properties. The primary reasons for the lower mechanical properties are, matrix swelling, interphase debonding, physical damage of the interphase, and hydrolysis of the material by water [18]. Garcia-Espinel *et al.* [119] have associated the reduction in tensile strength and flexural strength of epoxy/glass fibre with water absorption and reactions between water and the composite material. This finding has been supported by other researchers [101, 120, 121]. There are three categories of moisture diffusion:

a) Case I, where the liquid absorption equilibrium is quickly obtained
b) Case II, in which the boundary progresses at steady rate until equilibrium is reached
c) Case III, which Intermediate between case I and II

Three cases of diffusion can be theoretically represented by the following equation.

$$\frac{M_t}{M_\infty} = kt^n \quad \text{.....Equation 2 [122]}$$

Where M_t is liquid/moisture content at time t

M_∞ is equilibrium moisture content, k and n are constant

From the literature, it has been found that moisture absorption in natural fibre-reinforced polymer usually follows Case 1 Fickian behaviour. For Case II, the penetrant mobility is higher than in other relaxation processes. As for Case III, anomalous diffusion occurs if the penetrant mobility and the polymer segment are comparable. These three cases have been discussed by Espert *et al.* [122].

Table 1. Some prominent studies of the effect of water on the properties of polymer nanocomposites

Polymer	Filler	Finding	Author	Year
Epoxy	Glass fibre	After 30 days the degradation of mechanical properties slope decreases and become stabilized	Garcia-Espinel *et al.*	2015 [123]
Polyester	Glass fibre/clay	Chemical treatment improved clay dispersion, reduced water absorption and increase nanocomposites properties	Rull *et al.*	2015 [124]
Epoxy	Flax	Reduction in flexural and tensile properties	Yan *et al.*	2015 [120]
Polyester	Hyacinth	High moisture absorption of chemically treated nanocomposites Reduction in tensile and flexural strength	Abral *et al.*	2015 [121]
Polyester	Jute/glass fibre	Reduction in both strength and modulus was observed	Akil *et al.*	2014 [101]
PMMA	No filler	Reduction of tensile strength Water act as plasticizer weakening the mechanical properties	Moghbelli *et al.*	2014 [125]
Polyester	Bentonite	Clay fraction with more than 1% increased water absorption	Ollier *et al.*	2013 [22]
Epoxy	HNTs Nano silicon carbide	Flexural strength and modulus of all nanocomposites reduced due to plasticization effect Fracture toughness and impact strength improved caused by water absorption	Alamri and Low	2012 [126]
Polyester	Sisal and roselle	Tensile strength and flexural strength decreased after water immersion	Athijayamani *et al.*	2009 [127]
Polyester	Glass fibre	Reduction of tensile strength Matrix swelling, interface “debonding” caused by water diffusion	Huang and Sun	2007 [18]

Alamri and Low [126] produced nano-clay-epoxy and studied its swelling behaviour in over with time. They pointed out that the weight gain decreased with increasing nano-clay content. Ollier *et al.* [22] also reported a decrease in weight gain with increasing content of bentonite clay in polyester resin. The nano-clay acts as physical barrier and stops water molecules from penetrating [128, 129].

Another major study by Athijayamani *et al.* [127] found that water decreased the tensile and flexural strength of roselle-reinforced polyester. In comparison with unexposed composites, a 7 % reduction in tensile strength was observed in the case of 10 wt% roselle reinforcement. In the case of 30 wt% of roselle reinforcement, the tensile strength was decreased by 11.7%. The flexural strength of the composites also decreased when exposed to water. In the case of 10 wt% of roselle, a 5.7% reduction in flexural strength was observed. An approximately 8.6% decrease in flexural strength was also found with water uptake in 30 wt% roselle/polyester composites. In general, this study suggests that water reduces the tensile and flexural strength of composites.

Huang and Sun [18] reported that water can cause matrix swelling, interface debonding, physical damage to the interphase and the hydrolysis of the material. These are the main reasons for the deteriorating tensile strength of glass/polyester composites. Interface debonding occurs when fibre failure is suppressed at the matrix crack front. Moreover, fibre failure does not normally occur by deflection of the debonding through the fibre but is governed by the weakest-link statistics.

Rull *et al.*[124] were able to reduce the water absorption and increase the tensile and flexural strength of glass fibre-polyester in uniformly dispersed clay nanocomposites. A small fraction of nano-clay was used to provide resistance towards humidity and liquids. If the nano-clay used is more than 1wt% it tends to agglomerate and consequently increases the water absorption and reduces mechanical properties [22].

Table 2 shows the tensile strength of nanocomposites after certain periods of immersion in water. The breaking strength and tensile stress significantly reduced as the nanocomposites suffer physical damage. Huang and Sun, [18] demonstrated that water caused delamination between the fibre and matrix after water immersion. They found that hydrolysis caused by water reduced the tensile strength of glass/polyester composite material and caused physical damage to the interphase. This was caused by polymer debonding between the matrix and glass fibre. Figure 6 shows SEM images of broken samples before and after water immersion. Delamination between the fibre and matrix occurred which explains the reduction in tensile strength of glass/polyester nanocomposites [18]. Ishak *et al.*[130] studied Arenga Pinnata (sugar palm) fibre resistance to seawater. It was shown that polymers reinforced with natural fibre from the sugar palm showed improved mechanical properties and high resistance against seawater [131]. Sugar palm trunk fibre recorded the lowest seawater absorption of 0.39% [130]. However, this material (Arenga Pinnata) is unknown to many people because it is only available in Asian countries such as India, Malaysia, Indonesia and Philippines. Since this material is biodegradable, it would be fascinating to investigate whether or not it has the capability to be used in reducing the effect of premature failure caused by liquid media exposure.

Table 2. Tensile strength of glass/polyester after different periods of water immersion period. [18]

Immersion time (days)	Breaking strength (N)	Tensile stress (MPa)	Elongation at break (%)
0	3246.77	192	3.11
7	3098.26	181	3.07
14	3002.96	176	3.27
21	2754.11	162	3.15

Joseph *et al.* [118] have shown that, when exposed to water, sisal fibre reinforced polypropylene nanocomposites underwent interfacial failure detected through scanning electron micrography that can be attributed to plasticization caused by water which degraded the fibre-matrix interfacial interactions. All composites in this study showed a reduction in modulus values after immersion in boiling water due to the plasticization effect.

Failure in environmentally exposed composites is mainly dominated by matrix whereas the degradation of the fibre is minimal. Zainuddin *et al.*[14] have showed that the mechanical properties of epoxy nanocomposites filled with nano-clay degraded when exposed to water with a direct relationship to exposure time and temperature. It was found that 2wt% nano-clay reinforcement showed optimal mechanical properties compared to neat epoxy. This finding is in agreement with those in other research [61, 132–136]. Dhakal *et al.* [60] produced hemp-polyester nanocomposites and studied the effect of water in the mechanical properties. They observed that water uptake increased with increasing volume fraction of the fibres. High amounts of water cause

the swelling of fibres, which could fill the gaps between the fibre and the polymer-matrix. As a result, an increase in mechanical properties was observed compared to dry samples.

Figure 7 (a) shows the tensile strength of hemp fibre-polyester which increased by 22% for 2-layer hemp fibre after water immersion. The tensile stress was decreased by 38% and 15% for 3 and 4-layer-reinforced hemp respectively. For 5-layer-hemp, tensile strength was found to be higher than specimens tested in air. The gap between fibre and polymer was probably filled by the water therefore leading to the improvement in tensile properties as also reported in other studies [137]. Water molecules could also act as a plasticising agent in the composite material, which later subsequently increases the strain. When the strain increases, the stiffness of the composite decreases since the polymer chain is mobile. Further crosslinking is possibly takes place during environmental exposure in water with temperatures ranging between 25^{o}C to 100 ^{o}C which leads to improvements in tensile properties. Figure 7 (b) shows the flexural strength of composites. Water absorption causes a weaker fibre-matrix interface which can be associated with the decrease in flexural stress.

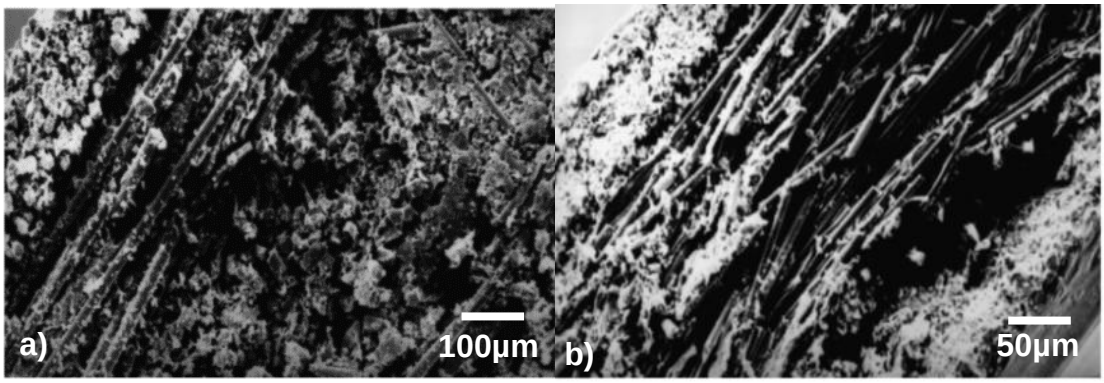

Figure 6. Broken section of glass/polyester composite sample before (a) and after water exposure (b) [18]

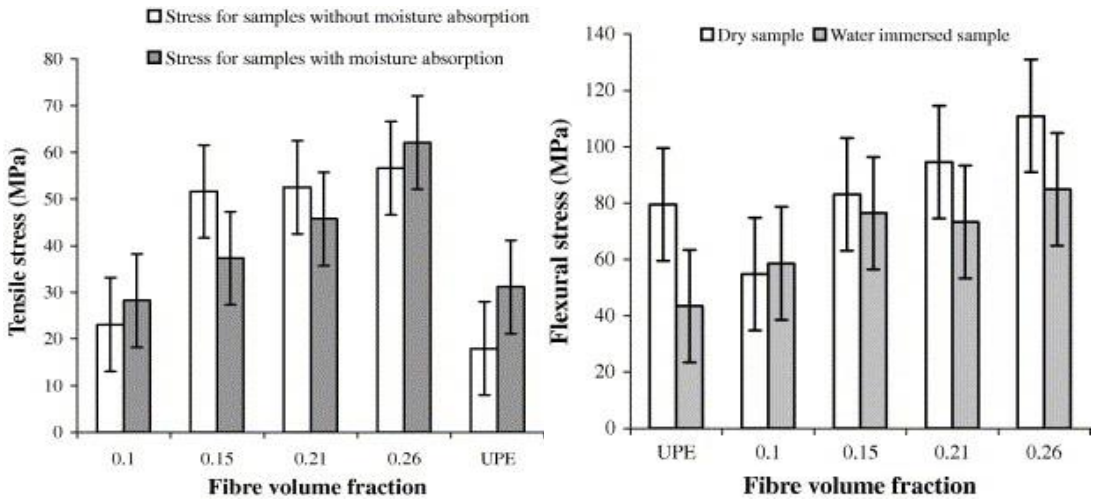

a) b)

Figure 7. The tensile strength and flexural strength of hemp fibre reinforced unsaturated polyester [60]

1.3.2. Aggressive liquids

In some applications, contact with aggressive liquid media is inevitable such as in automotive applications where the components are exposed to industrial chemicals (gasoline, windshield liquid and brake fluid) [66]. Residual stresses are generated during the injection moulding process to produce polymer components. A process-induced stress usually exists in a moulded part.

These residual stresses when combined with aggressive liquid media can cause unexpected brittle failure [138–142]. This phenomenon is known as environmental stress cracking (ESC) which is sometimes described as environmentally assisted cracking [53, 143, 144]. It is defined as the premature initiation of cracking and embrittlement of plastics as a result of the concurrent action of stress and strain in contact with certain fluids [25, 31]. In simpler terms, it is slow crack growth [102, 144–147]. As it involves liquids, it is also called the stress corrosion of polymer in solvents [148, 149]. For a given polymer, certain liquid media can cause ESC soon after they come into contact. Such liquid media are called ESC agents for those polymers. In general, liquid media with hydrogen bonding show a higher tendency to cause ESC in polymers, and therefore care must be taken to avoid the contact with such liquid media [25, 31]. Table 3 shows the research conducted to study the influence of liquid media on the deterioration phenomena in polymer nanocomposites. In general, the work carried out can be divided into two main categories;

a) The effect of liquid media on the engineering properties of polymer nanocomposites

b) The influence of particles and fibres in resisting stress cracking failure

Table 3 also summarises the key publications on the ESC of polymer composites. Interestingly, liquid natural rubber improves the stability of samples before it decreases over time. A strong interplay exists between morphological features and the environmental stress cracking behaviour of PE/EVAblends. EVA particles are capable of stopping crack propagation and lamellae can grow within the elastomeric phase.

Table 3. Polymer and nanocomposites exposed to different environments

Polymer type	Medium	Remarks	Author	Year
PHB	Sodium hydroxide	NaOH is severe stress cracking agent for PHB	Farias *et al.*	2015[150]
Epoxy	Acid and Base medium	Liquid natural rubber improves the stability of the sample but decrease over time due to detachment of the rubber particles.	Muhammad *et al.*	2015[151]
Polyester	Acetic acid, nitric acid and sodium hydroxide	Neat unsaturated polyester exerts better chemical resistant than the nanocomposites	Ruban *et al.*	2015[152]
Polyethylene	IGEPAL solution (detergent)	Homogenous dispersion provides good interfacial adhesion and resistance to stress cracking.	Chen *et al.*	2014 [105]
Polycarbonate	Toluene	Toluene found to promote stress cracking failure of polycarbonate	Alperstein *et al.*	2014 [153]
Rubber toughened Polyester-clay	Sodium hydroxide Hydrochloride acid	Acid medium affected nanocomposites more than base medium	Bonnia *et al.*	2012 [40]
Polystyrene	Sunflower oil	Sunflower oil proved to be an aggressive chemical agent	Grassi *et al.*	2011 [154]
Polyester-Kenaf	Acid medium Base medium	Acid medium rapidly weakened the nanocomposites more than base medium	Bonnia *et al.*	2010 [28]
HIPS/PE Blend	Sunflower oil	There is a close correlation between the morphology and fracture behaviour of HIPS, uncompatibilized and compatibilized HIPS/PE blends.	Khodabandelou *et al.*	2009 [44]
Polycarbonate	Butter	Non-absorbing chemicals can also cause ESC	Kjellander *et al.*	2008 [58]
Polyethylene	IGEPAL solution	Morphological features influenced stress cracking failure behaviour	Borisova and Kressler	2003 [53]

1.3.3. Organic solvents

The main characteristic of stress cracking agent is essentially identified as liquid diffusion through the craze fibril structure [143]. Once the liquid penetrates to the craze tip, it then starts to plasticise the polymer and permits the craze to develop. The degree of absorption of a liquid media into polymer is a function of solubility parameters of the liquid and the polymer [56]. Organic solvents can significantly deteriorate the mechanical properties of polymers. From the tensile tests performed, Alimi *et al.*[155] reported that the elastic modulus of high density polyethylene (HDPE) decreased up to 64% when exposed to toluene and methanol for seven days. The toluene-methanol mixture was significantly reduced the structural integrity of the specimens. Dashtizadeh *et al.*[156] measured the surface hardness, stress cracking resistance and glossiness of acrylic resin nanocomposites under severe environmental conditions. They observed that mechanical properties significantly deteriorated when the samples were exposed to acetone and toluene as a result of liquid penetration into the matrix.

1.3.4. Detergent

Detergents like Igepal have been used in many studies on environmental stress cracking. This liquid has been used widely to test the product durability in packaging and pipe applications [157]. This liquid has two significant effects:

a) It accelerates crazing by plasticizing the amorphous region of the bulk polymer [146]; and
b) Accelerates the fracture of the craze by plasticizing the crystalline region of the fibrils [53].

Exposure of polyethylene (PE) to stress cracking agents such as detergents will cause brittle fracture under external loading [143, 157]. The crack development under ESC environment is shown in Figure 8.These micro cracks combine with applied stress to cause brittle fracture [66] [158].

In thermoplastic polymers, the molecular chains are bonded via weak van der Waals forces or hydrogen bonding and exhibit high mobility and hence are easily disentangled when subjected to stress. This phenomenon is characterized by multiple cracks, smooth morphology, craze remnants, stretched fibrils, and alternating bands [25]. When an amorphous, semi-crystalline, and unsaturated polyester-based product is in contact with a fluid, it can crack instantly or even break at low stress.

Chen [105] investigated the effect of Igepal CA 630 solution on HDPE/EVA (ethylene-vinyl acetate) and LDPE/EVA blends using the Bell Telephone test. In this test, specimens were bent with the notch pointing upwards in a metal U-shaped specimen holder. The holder was placed in a glass tube containing a 10 vol.-% Igepal solution. The tubes were sealed and placed in a water bath at 50 ^{o}C. Failure was defined as the appearance of any crack visible to the naked eye. Five specimens were used for each test.

The solution caused the detachment of the EVA phase from the matrix. Stress concentration gives rise to cracking and formation of micro-pores inside the blend which produced higher stress concentration between the particles. The micro-porosity may hamper crack propagation as tip of the cracks is blunted when coming into contact with pores, as shown in Figure 9.

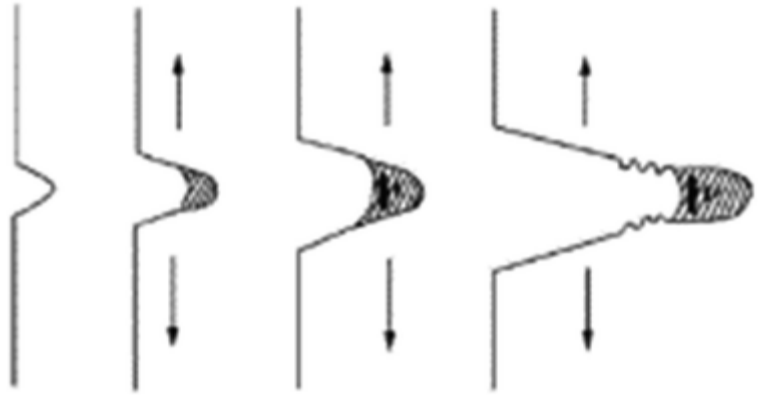

Figure 8. Crack development under ESC condition [31]

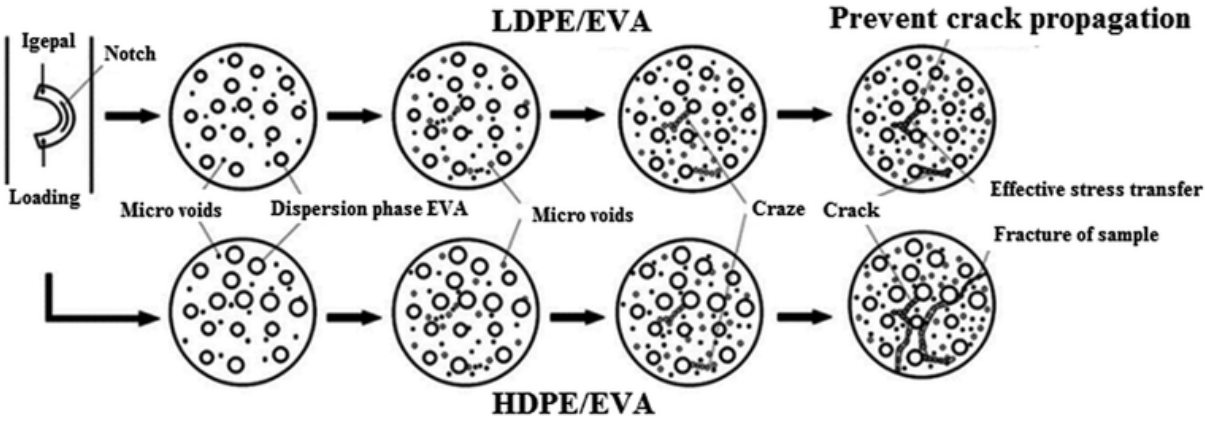

Figure 9. The failure mechanisms of LDPE/EVA and HDPE/EVA blends [105]

1.3.5. Alkaline and acid medium

In a recent study by Farias *et al.* [150] poly(3-hydroxbutyrate) (PHB) was immersed in a sodium hydroxide (NaOH) environment followed by tensile testing. The exposure to the sodium hydroxide did not significantly reduce the Young's modulus. Plasticization, which normally softens the polymer structure, did not occur as can be seen in polymers exposed to water. However, the significant effect of sodium hydroxide was observed to be on the tensile strength and strain-at-break. Compared to unexposed samples, tensile strength and strain were found to be decreased by 30% and 40% respectively as a result of sodium hydroxide exposure. In addition, when the

samples were tested at a slower crosshead speed, the tensile strength was reduced by 60% and the strain at break by 70%. The duration of liquid media exposure and stress facilitates crazes, cracking and a disentangled molecular structure [159]. Although ESC can occur in air, it is significantly increased in the presence of liquid media. Farias *et al.*[150] showed that NaOH solution caused a significant deterioration in the mechanical properties of poly(3-hydroxybutyrate). In their study of the mechanical properties of hybrid glass/kenaf fibre-reinforced epoxy. Analysis by Muhammad *et al.* [151] showed that alkaline exposure reduced the flexural and impact strength of epoxy/glass composites. This also accords with earlier observations by Bonnia *et al.*[28] who discovered the effect of alkaline on rubber reinforced polyester/kenaf composites. They reported on the comparison of the stress values of composites over time to failure between dry and immersed specimens in acid medium. In general, they agreed that, when the polymer composites were exposed to alkaline, the stress required to break the specimens was reduced compared to those tested in air. The combination of acid medium exposure and micro cracks tended to weaken the polymer matrix and the premature failure mechanism could be clearly observed.

Ruban *et al.* reported that unsaturated polyester without reinforcement showed higher resistance to liquid media (acetic acid, nitric acid, and sodium hydroxide) than when reinforced with nano-clay [152]. The expanded clay caused polymer swelling in nitric acid and aqueous ammonia. From their chemical resistance investigations, the increase in clay content was found to increase liquid absorption. Akdemir *et al.* [148] showed that crack proceeds along fiber-matrix interface causing delamination. The dimensions of the samples changed significantly due to the effect of liquid media, applied stress, crack growth and delamination [160]. The physical effect of the

environment on glass/polyester nanocomposites is indicated by liquid and gas absorption followed by the development of swelling at certain rates. Fibre/matrix debonding takes place due to swelling which subsequently increases internal stresses and results in a loss of structural integrity [18, 118, 161, 162]. Compared to the polymer matrix, the polymer-glass interface and the glass fibre reinforcement are considered to be more vulnerable to environmental deterioration [95]. ESC becomes feasible when the aggressive liquid diffuses through the polymer matrix via micro-cracks.

1.3.6. Sunflower oil and butter

Khodabandelou *et al.* [44] studied the phenomenon of ESC in the exposure to sunflower oil of HIPS/PE blends. ESC resistance was analysed in tensile creep tests and polyethylene (PE) was used to reinforce the composites. The first major finding indicated that the ESC resistance decreased with the addition of PE as a result of the incompatibility between these two polymers.

Another major finding which was observed from the morphological analysis suggested that, the polymer matrix and PE particles were easily disentangled as a consequence of weak bonding. Andena *et al.* [21] reported on the bending properties of high impact polystyrene (HIPS) exposed to sunflower oil. Before the bending test took place, all specimens were immersed in sunflower oil for minimum one hour. The time of crack initiation and propagation was significantly reduced when the polymers in contact with the sunflower oil environment. Fracture resistance was also lower compared to HIPS samples tested in air. Grassi *et al.* [154] studied the influence of rubber particles in high impact polystyrene (HIPS) in a mixture of sunflower oil and oleic mixture. Between these two-liquid media, sunflower oil was found to be a more

aggressive ESC agent. Interestingly with reinforcement small rubber particles reduced the effect of ESC. It was found that HIPS samples with a lower fraction of small particles exhibited better resistance to sunflower oil. A number of studies have been carried out to enhance the ESC resistance of numerous styrenic based polymeric materials.

The incorporation of rubber particles into polystyrene was found to be an efficient method to improve toughness [163, 164]. However further research needs to be carried out to study the effectiveness of rubber particles in reducing stress cracking failures caused by the environment. Kjellander *et al.* [58] exposed polycarbonate to butter and performed 3-point bend ESC testing. Non-absorbing chemicals like butter can cause ESC in polycarbonates. Butter was found to increase the amount of energetically favoured trans-trans conformation at the polycarbonate surface.

1.4. Polymers reinforced with conventional and natural fibres

Conventional fibres or synthetic fibres such as carbon fibre, glass fibre, Aramid and Kevlar are widely used in various engineering applications [165–171]. High stiffness and excellent strength properties are two important factors that make the applications of these fibres favourable. Natural fibres have a long history of serving mankind and are very important in a wide range of applications, and they compete and co-exist in the twenty-first century with man-made fibres, especially as far as quality, sustainability and the economics of production are concerned. The applications, advantages, and drawbacks of both types of fibres are illustrated in Figure 10.

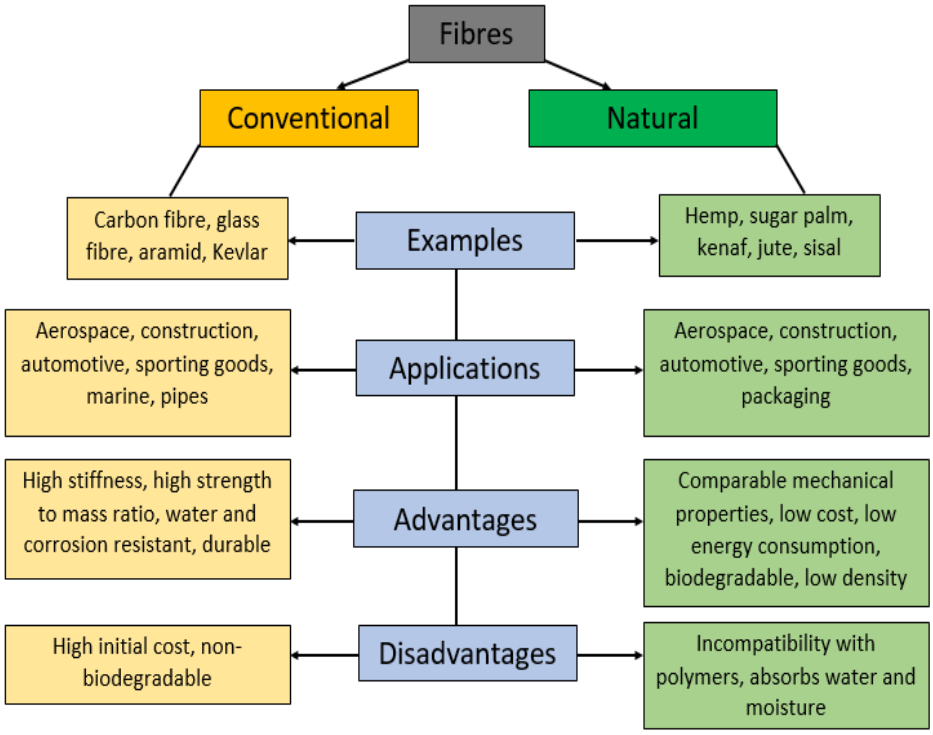

Figure 10. Characteristics of conventional fibres and natural fibres

Carbon fibre, glass fibre, Aramid and Kevlar are high-strength fibres and are found many applications such as aerospace, construction, automotive, sports, marine and pipes [172]. Carbon fibres were first developed in the United Kingdom in the 1960s and are widely used as reinforcements in polymer nanocomposites [39], being recognized for their high strength (3.5GPa). However, they show a high degree of brittleness having values of Young's modulus around 143GPa, and when they are used as reinforcement in polymers, the properties of the composite system are highly propitious carbon fibre-polymer composite systems are currently extensively used in automotive, aerospace, sporting goods and textiles applications [173–178].

Glass fibre is another fibrous reinforcement which is extensively used to produce polymer composite materials, due to its low cost and good mechanical properties [179,

180]. Glass fibres are usually added in the form of continuous or chopped fibres in a polymer matrix [181]. They are manufactured by extruding molten glass under gravity at high temperature through a series of holes in a platinum plate, and then the fine filaments are drawn mechanically downwards and wound at high speed on to a drum [39]. By controlling the processing conditions, the fibres produced have a diameter typically between 8 to 15 μm [39]. Despite their advantage of being easily processed advantage, this material also vulnerable to surface damage which causes a significant reduction in their strength. Glass fibre can be found in more than 90% of all composites, and more than five million tons used for reinforcement was consumed in 2015 [182].

Recently, graphene has attracted academic and industrial interest since it can produce good improvements in mechanical properties at very low content [183, 184]. Graphene has found applications in electronics devices, energy storage, sensors, and biomedical applications [34, 185–189]. Graphene may be preferred over other conventional fillers owing to its high surface area, tensile strength, thermal conductivity and electrical conductivity [190–195]. In the past, carbon nanotubes (CNTs) gained much attention due to their superior mechanical, thermal, and electrical properties compared to steel [196–200]. Moreover, CNTs have been broadly used in a range of applications such as biomedical devices, structural applications, electrical circuits, actuators, hydrogen storage and many other areas [201–204].The dispersion state of CNTs and interfacial interactions are most important parameters in CNTs-polymer nanocomposites [205–211].

It is widely believed that using nanofillers such as CNTs, HNTs and graphene can improve the mechanical properties of composites compared to neat polymers.

However, the reported values do not reflect the expected level of improvement. This can be attributed to the poor dispersion of the filler, agglomerates which act to increase stresses, and weak interfacial interactions.

Unlike HNTs and graphene, CNTs show several similarities to asbestos [212]. CNTs and asbestos induce similar molecular changes to develop fibro-proliferative and carcinogenic responses which are often linked to human lung disease after from prolonged exposure [213]. The CNTs have a special ability to stimulate mesenchymal cell growth and may cause granuloma formation and fibro-genesis [214]. Therefore, more studies need to be carried out to identify that pathogenic potential and carcinogenic potency.

Schaefer and Justice have studied in detail polymer nanocomposites and reported the presence of a large-scale morphology of the filler that is common in nanocomposites regardless of the level of dispersion, leading to substantial reductions in mechanical properties [215]. They further reported that, even in nanocomposites, microscale structures are present which significantly influence their mechanical properties. They stated that the large-scale morphology ubiquitous in nanocomposites regardless of the level of dispersion leads to substantial reductions in mechanical properties compared to predictions based on idealized filler morphology [215].

Over the last two decades, natural fibres have evolved as better options to replace conventional fibres in many applications [216]. Ecological and environmental concerns have also triggered an increased interest in natural fibres [101]. Natural fibres are also renewable, non-abrasive and non-toxic in nature [217]. Natural fibres are produced using traditional manufacturing techniques such as resin transfer moulding, vacuum

infusion, and injection moulding [216]. Natural fibres such as hemp,[60, 218] sugar palm, [130, 131, 219, 220] coir, sisal and jute [221–223] have attracted research to extend their usage in civil engineering applications due to their low cost, biodegradable and acceptable properties [224–229].

1.4.1. Introduction to particle reinforcement

Fibre and particulate reinforcements are commonly used to improve the mechanical properties of polymers [230–234]. It has been shown that fibrous reinforcement shows a greater ability to resist crack propagation than particulate reinforcement [95, 115, 235–237]. When stress is applied to fibre reinforced composites, the weakest fibre will break first. After this fibre has broken, the remaining fragment in the matrix bridges crack. The stress in the fibre then decreases and stops crack propagation. If the fibre does not break, fibre pull-out will occur immediately, which increases crack resistance since more energy is required for that process to occur and therefore crack propagation slows down.

Interest in materials filled with particulate has increased since polymer composites were first developed where initially, mineral particles were used as fillers. Reinforcement of polymers with rigid nano-fillers can alter the required properties. For instance, it is believed that particulate-filled materials can improve stiffness, fracture toughness and creep resistance [238]. However, a review by Robeson pointed out that particulate reinforced composites gave limited or no improvement [115].

It has been noted that the mechanical properties of polymer composites are influenced by several factors, such as shape, size, aspect ratio and the dispersion qualites of reinforcing particles [154, 239–241]. Many studies have indicated that

particulate based fillers have been used extensively since polymers were first invented due to their low cost. For instance, minerals that have layer structures such as mica and talc are commonly used and processed in the form of thin platelets [39]. They produce composites that are easy to process, such as by having shorter cycle times and allowing higher filler content, with significant increases in stiffness and strength compared to the pure polymer [39].

Various particles may be added to polymers for a variety of reasons. According to Ahmed and Jones [239], the distribution, size and shape of filler particles significantly influences the performance of nano-particle-reinforced composites, in terms of properties such as chemical resistance, being weatherproof and toughness [103, 239].

1.4.2. Particulate-reinforced polymers

The interest in particulate reinforced polymer nanocomposites has significantly increased, and the first such polymers used mineral particles as fillers [39]. Some of the earliest work on inorganic toughening at Toyota was published in 1987 [36, 242, 243]. Particulate reinforcements can improve the stiffness, creep resistance and fracture toughness of polymers [244, 245]. The mechanical properties of polymer nanocomposites have been shown to be influenced by several factors, such as shape, size, aspect ratio and the dispersion quality of the reinforcing particles [103, 154, 239–241, 246–248]. Mineral particles were first used as cheap fillers and additives since conventional polymers were first created. For example, talc and mica from silicate-based minerals with layer-type structures were used in the form of thin platelets [39]. The nanocomposites produced using mineral particles are easy to process and give significantly increased in polymers stiffness and strength [39]. In the development of polymer nanocomposites, the incorporation of nano-particles has been widely investigated employing numerous experimental setups and research methods [249–251].

Other materials used in the nano-reinforcement of polymers are layered silicates and ceramic nano-particles such as SiO_2, TiO_2 and $CaCO_3$ [252–254]. The addition of layered silicate to natural rubber and polyurethane was found to improve stiffness and strength [255]. Apart from that, it has been shown conclusively that the Young's modulus of nanocomposites improves five times with silicate based reinforcements [256].

3. Materials and experimental techniques

3.1. Introduction

This chapter provides detailed information about the materials, equipment and experimental procedures used in this study.

3.2. Materials

3.2.1. History of clay-based fillers

Clay is a fine material found in natural rocks or soil stuff that contains of one or more mineral with small amount of metal oxides and organic matter. It is made of chemically small crystallites of alumina-silicates of different sizes, with substitutions of iron and magnesium by alkalis and alkaline earth elements. During the period 1925 to 1940, clay mineral studies came into limelight in America. Heinrich Ries pioneered studies of clay in the eastern United States followed by Ross and Shannon in 1925 who continued to study the mineral composition of clays. Clay mineral research began in European countries in the 1940s and changed drastically in 1987 when Fukushima *et al.* identified the possibility of synthesizing polymer nanocomposites based on nylon-organophilic montmorillonite clay which showed distinct enhancement in material properties at very low fractions (below 5 wt%) of layered silicate [257, 258].

3.2.2. Introduction to clay/polymer composites

Clay/polymer is the most extensively studied and commercially in demand filler in polymer industry due to tremendous improvement offered in physical and engineering properties for polymers [243, 259]. For the last one and half decades, there has been a growing interest in the development of polymer/clay nanocomposites due to their

astounding properties compared to conventionally filled polymers even at very low fractions of filler addition. Commercial attention was attracted due to their easy availability, processability, low cost, non-toxicity and advancements in the processing of clay nanocomposites. Nevertheless, the enhancement of valued-added properties without compromising the properties of the pure polymer properties has attracted further interest in the polymer industry. To date, clay/polymer composites are used in medical and aerospace applications and even household items.

Clay/polymer nanocomposites use smectite-type clays such as hectorite, montmorillonite, and synthetic mica as fillers to improve the properties of polymers. Smectite-type clays have a layered structure. Each layer is constructed from tetrahedrally coordinated Si atoms fused into an edge-shared octahedral plane of either $Al(OH)_3$ or $Mg(OH)_2$. The layers should show excellent mechanical properties parallel to the layer direction based on the nature of the bonding between these atoms.

However, the exact mechanical properties of the layers are still unknown. In recent modelling work, the Young's modulus in the layer direction is estimated to be 50 to 400 times higher compared to typical polymer. The layers have a high aspect ratio with each being approximately 1 nm thick, while the diameter varies from 30 nm to several microns or larger. Clay particles are formed by hundreds or thousands of these layers stacked together with weak van der Waal's forces which makes it easy to shape them into various structures in polymer.

Clay particles have great advantages for use as reinforcement for polymeric materials due to their mechanical and chemical resistance [22]. Hussain pointed out that montmorillonite (MMT) has the widest acceptability for use in polymers because

of its high surface area and surface reactivity [238]. However, in a recent publication, Du *et al.* reported that HNTs have been an increasing focuse by researchers as showed in the rapid growth in relevant publications [260]. Scientists and engineers have also discovered a large range of exciting new applications for HNTs, as discussed in the next chapter.

3.2.3. Halloysite nanotubes (HNTs)

Halloysite nanotubes (HNTs) were used in the present study as reinforcement filler and were purchased from Sigma-Aldrich. The diameters are between 30 and 70 nm with lengths between 1 and 4 μm as shown in Figure 11.

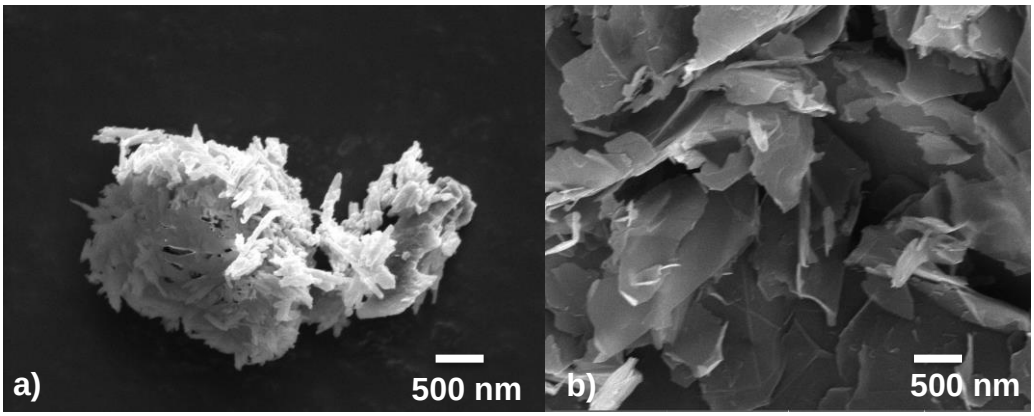

Figure 11. Image of halloysite nanotubes (HNTs) (a) and multi-layer graphene (MLG) (b)

Halloysite is a forgotten material compared to other clay-based particles. Only in recent years HNTs have been regarded as one of the most promising natural nanoscale materials [261]. It has been reported that approximately 30,000 tons of halloysite clay minerals are excavated worldwide annually and processed into dispersed nanotubes [262]. The unique crystal structure of HNTs is almost similar to CNTs which make them a potential candidate to replace expensive materials like CNTs since they have the tubular structure at nano-size.

Apart from being environmentally friendly and cost-effective, HNTs have gained popularity for use as reinforcement for polymeric materials due to their superior mechanical and chemical resistance [22]. Depending on chemical composition and nanoparticle morphology, nanoclays can be classified into numerous classes, such as montmorillonite, bentonite, kaolinite, hectorite, and halloysite [263, 264]. In general, the addition of HNTs can improve the tensile strength of the cured polyester resin as evident for other montmorillonite and bentonite-based clays [59, 61].

HNTs are 1:1 aluminosilicate [$Al_2Si_2O_5(OH)_4$] clay mineral, and has a tube-like morphology and strong hydrogen interactions with low electrical and thermal conductivity. HNTs are non-toxic in nature and have vast numbers of applications in anti-cancer therapy, sustained delivery of certain agents, and environment protection [265]. Schematic diagram of halloysite structure is shown in Figure 12, and it is chemically similar to kaolinite.

Its unique properties have led to HNTs gaining in popularity for use in the release of controlled drugs and other active molecules release [266]. They have been also used as nanoreactors and adsorbents [267]. The mechanical properties of systems with HNTs are certainly enhanced. In fact, the incorporation of HNTs enhances their thermal stability and flame and corrosion resistance of composites too [268]. In addition, Robeson [115] also reported that clay can improve gas and barrier properties.

A considerable number of studies have been published on the enhancement in the mechanical properties of polymer nanocomposites, especially when reinforced with montmorillonite and bentonite [14, 231, 258, 269, 270]. However, there has been only limited discussion of the mechanical properties of HNTs-polyester nanocomposites in

liquid media condition. According to Joussein *et al.*, the dominant morphology of halloysite is tubular [266]. The tubules can be long and thin or short and stubby commonly derived from crystalline minerals like feldspars and micas [271].

Table 4 illustrates a brief summary of the effect clay-based reinforcements including HNTs, on maximum improvements in K_{1C} values from several studies. Most polymers used in these studies were epoxy based-polymer. Unsaturated polyester was rarely used as polymer matrix. Clay-based reinforcements were used between 1 wt% to 10 wt%. However, clay dispersion was always an issue when higher concentrations were used. Wang *et al.* studied the rheological and mechanical properties of epoxy/clay nanocomposites with improved tensile and fracture toughness. The incorporation of 1 wt% montmorillonite can have produced an increase in 94% in fracture toughness (K_{1C} mode) [272].

Albdiry *et al.* reported an increase of 61% in the fracture toughness of HNTs/unsaturated polyester composites [273]. Ramsaroop *et al.* studied the fracture toughness of polypropylene-clay nanocomposites and glass fibre reinforced polypropylene composites. They revealed that the incorporation of Cloisite 15A (microgranuled nanoclay) improved fracture toughness up to 175% [181]. Kaynak *et al.* reported an increase of 140% in fracture toughness with only 0.5 wt% montmorillonite reinforcement. In general, clay reinforcement increases fracture toughness at low loading content, as evidently shown in Table 4.

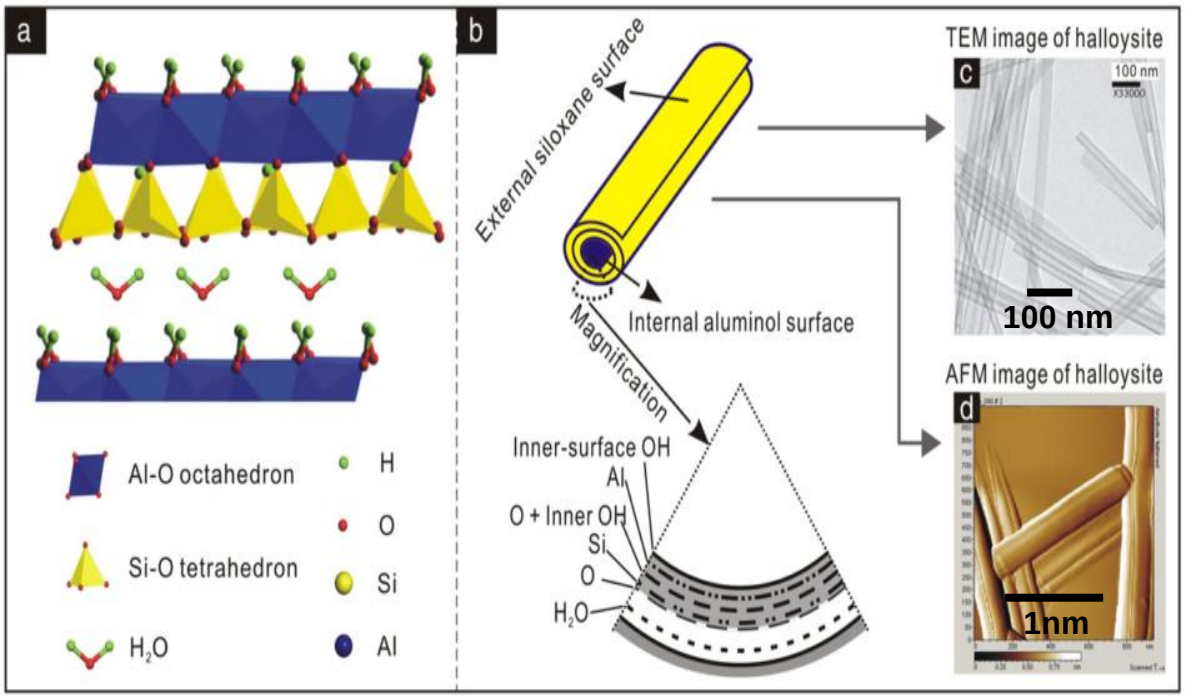

Figure 12. Diagram of halloysite crystalline structure (a) halloysite particle (b) and (c) TEM images of halloysite, and (d) AFM image of halloysite [274].

Table 5 on the other hand shows a brief list of the clay-based reinforcements in impact strength, Young's modulus and flexural modulus. The highest improvement in impact strength was obtained by Ye *et al.* at 413%. Lin *et al.* achieved 300% impact strength improvement later in 2011 [275] . Carli *et al.* observed remarkable improvement in Young's modulus (63% improvement) by incorporating HNTs into polyester [276]. The highest flexural modulus was reported by Pavlidou and co-workers who found 224% of flexural modulus improvement [277]. Manfredi *et al.* reported an increment of 29% higher in flexural modulus from the reinforcement of 5 wt% Cloisite clay. It can be observed that clay-based fillers can be utilized to improve the impact strength, Young's modulus and flexural modulus of polymers. Despite many researches reporting improvements in the mechanical properties of clay-polymers composites, the toughening mechanisms obtained with HNTs have been less studied.

Many factors like particle size, shape, distribution, type, aspect ratio, interface, particle concentration, and dispersion may strongly influence the toughening efficiency of nanoparticles. Nanoparticles with a high aspect ratio are likely to have negative toughening effects. Under external load, the large aspect ratio generates significantly high stress concentrations at the ends of particles leading to earlier crack initiation, and propagation and in the end causing adverse effects on material toughness [278]. HNTs are known to have high surface area, which offers more opportunities for filler-matrix interactions [279]. In summary, the incorporation of clay-based fillers can be used to improve the mechanical properties of polymer composites. However, most studies conducted here were using epoxy as polymer matrix. There is limited information on the reinforcement by HNTs into unsaturated polyester resin. Further work needs to be done to establish if clay-based particles such as HNTs have the same effect on unsaturated polyester.

Table 4. A brief record of maximum improvement in K_{1C} values in halloysite nanoclay

No.	Authors	Year	Reinforcement/ (wt%)	Polymer	Max. % increase in K_{1C} (MPa.m$^{1/2}$)	Ref.
1	Wang *et al.*	2015	MMT/1	Epoxy	94	[272]
2	Albdiry et al	2013	HNTs/3	Unsaturated polyester	61	[280]
3	Alamri and Low	2012	HNTs/1	Epoxy	57	[133]
4	Tang et al	2011	HNTs/10	Epoxy	78	[281]
5	Ramsaroop *et al.*	2011	Cloisite/5	PP	175	[181]
6	Kaynak *et al.*	2009	MMT/0.5	Epoxy	140	[282]
7	Bozkurt et al	2007	MMT/10	Epoxy	5	[283]
8	Qi et al	2006	Cloisite/5	Epoxy	25	[284]
9	Liu *et al.*	2005	Nanoclay/3	Epoxy	22	[132]
10	Ke Wang *et al.*	2004	Clay/2.5	Epoxy	80	[285]
11	Kinloch and Taylor	2003	Cloisite/5	Epoxy	70	[286]

Table 5. A brief record of maximum improvement in impact strength, Young's modulus and flexural values in halloysite nanoclay

Nr	Authors	Year	Reinforcement/ (wt%)	Polymer	Mechanical Properties	Max increase (%)	Ref.
1	Albdiry *et al.*	2013	HNTs/3	Unsaturated polyester	Impact strength	16	[273]
2	Lin *et al.*	2011	HNTs/5	Epoxy	Impact strength	300	[275]
3	Chozhan *et al.*	2008	Clay/3	Epoxy	Impact strength	19.2	[287]
4	Ye *et al.*	2007	HNTs/2.3	Epoxy	Impact strength	413	[288]
5	Sancaktar	2011	Nanoclay/1	Epoxy	Young's modulus	11	[269]
6	Carli *et al.*	2011	HNTs/5	Polyester	Young's modulus	63	[276]
7	Liu *et al.*	2001	Nanoclay/5	Epoxy	Young's modulus	40	[128]
8	Lepoittevin	2002	MMT/10	PCL(Poly(ε-caprolactone)	Young's modulus	54	[289]
9	Alamri and Low	2012	Halloysite/5	Epoxy	Flexural Modulus	88	[133]
10	Pavlidou *et al.*	2008	MMT/5	Epoxy	Flexural modulus	224	[277]
11	Manfredi *et al.*	2008	Cloisite/5	Epoxy	Flexural modulus	29	[290]
12	Wetzel *et al.*	2006	MMT/10	Epoxy	Flexural modulus	40	[291]

In certain applications of polymer nanocomposites, contact with liquid environments is inevitable, which leads to failure [292] that is caused by the swelling and deterioration of the polymer matrix as it interacts with the penetrating liquid environment. However, the degree of swelling and deterioration can be reduced by using nano-fillers such as HNTs. Alamri and Low [133] have reduced water absorption and increased the mechanical properties of epoxy through the use of uniformly dispersed clay.

The performance of clay often hindered by the environment to which the composites are exposed to. For instance, the presence of humidity had great influence in the failure of polymeric composites as the polymeric matrices are greatly affected by the presence of liquid media [293]. Therefore, the knowledge of the limitations of the polymeric matrices and ageing mechanisms in the presence of various liquid

media is significant to ensure successful composites application. Water diffusion, for instance, often hinders the use of fibre reinforced polymer composites [294].

Alamri and Low [133] studied the effect of water on the mechanical properties of HNTs-reinforced epoxy. They observed that the incorporation of HNTs was able to reduce water absorption and give improved mechanical properties of the nanocomposites after water immersion. Based on this observation, more severe environments were produced to examine the resistance of HNTs to more severe conditions. Some organic solvents, such as methanol, or a mixture of organic solvents may be considered to be severe environments.

HNTs as a filler in clay–polymer nanocomposites (CPN) was introduced by Du *et al.* in 2006 [268]. The effect of HNTs content on the mechanical properties of nanocomposites was investigated. The flexural strength of the nanocomposites increased from 2711 MPa (neat polypropylene) to 4557 MPa with 2wt% of HNTs addition. Deng *et al.* [295] reported on the fracture toughness of modified with HNTs particles epoxies. The highest improvement up to 50 % in K_{IC} and 127% in G_{IC} were discovered in comparison to monolithic epoxy. The remarkable improvement were attributed to the large aspect ratios [295]. Albdiry and Yousif [296] studied the tensile strength and modulus of UPE nanocomposites. In case of 3 wt.%. HNTs increased the tensile strength and tensile modulus by 7% and 12% respectively.

Tang *et al.* revealed that the incorporation of 10 wt% of HNTs into epoxy matrices considerably enhanced impact toughness by 78% [281]. In another study by Albdiry *et al.* an enhancement around 61% of fracture toughness was observed by

incorporating 3 wt% MMT. Vahedi revealed that a 240% improvement in impact toughness can be achieved by incorporating 3 wt% HNTs into epoxy [297].

Buvhana and Prabakaran recently reported that the addition of 4 wt% HNTs significantly increased the storage modulus of polyamide by 36% [298]. Last but not least, an improvement in Young's modulus up to 26% was reported by Gabr *et al.* when incorporating 5 wt% HNTs [61]. In previous work, Saharudin *et al.* studied the tensile properties of polyester nanocomposites reinforced with HNTs. We found that the incorporation of HNTs increased Young's modulus by 70% compared to unfilled polyester exposed to water-methanol [299]. Tensile strength and impact toughness increased by 17.4% and 184% respectively [299]. Other improvements in physical and engineering properties include those in fire retardancy [300, 301], barrier resistance [136] and ion conductivity [11].

Most studies seem to agree that the incorporation of HNTs into epoxy will increase its mechanical properties. In view of the above-mentioned research, there are great prospects for HNTs-based materials since they are now becoming the subject of intense consideration in global research, as shown in Figure 13. It can be concluded that a wide range of engineering properties can be improved with a low level of HNTs typically less than 5 wt% [11].

Another important character of clay nanocomposites is that the optical properties of the polymer are not considerably affected. This property is very useful for medical applications where optical clarity is vital such as catheter connectors, cardiac surgery products and intravenous infusion components [3, 115].

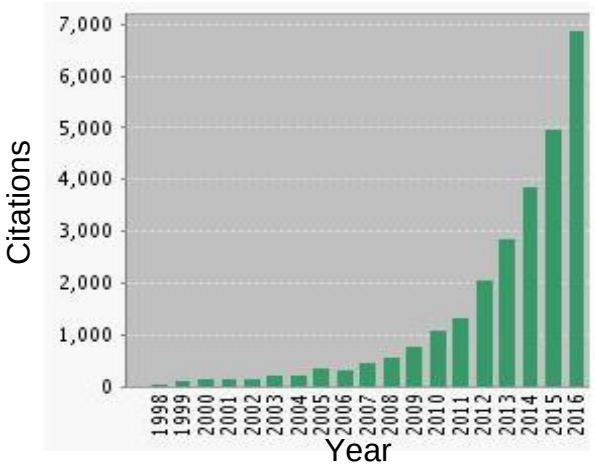

Figure 13. Number of citation using “halloysite nanotubes” as keyword searched in title from Web of Science (by 17/02/2017)

The incorporation of HNTs with tube-like morphology to resist the deterioration of mechanical properties of polymer nanocomposites exposed to aggressive liquid is a novel area in this research field [41]. Although clay-based particles have been used to enhance the mechanical properties of many polymers [135, 231], the influence of HNTs-based materials on the mechanical properties of polymer nanocomposites after exposure to liquid media has so far been overlooked [104, 124, 269, 302, 303].

In this research HNTs-polyester nanocomposites are evaluated through dynamic mechanical analysis to determine their microhardness, tensile strength, flexural strength, fracture toughness and impact properties. SEM has been used to investigate the morphology, microstructure, and failure modes of the produced nanocomposites.

3.2.4. Toxicological study of clay minerals

Clays are not only used in composites, construction, agriculture and environmental remediation but also commonly used in the packaging industry. In general clays are abundant, cheap and environmentally safer than other raw materials [304]. Oral exposure to clay minerals can happen deliberately or accidentally. Clay generally is non-toxic; however, prolonged exposure to mineral elements may have toxic effects [305].

Patel *et al.* reported that nanoclays with sorbents like activated carbon and alum can be used to treat industrial and municipal waste water [306]. The nanoclays are also better than any other water treatment and are very effective in filtering waste water containing significant amounts of oil and grease. Nanoclays have a synergistic affect with activated carbon and other unit processes such as reverse osmosis and work via partitioning phenomena [306].

Nanocarriers for anti-cancer drugs have gained much attention in nanomedicine. In cancer treatment, nanocarriers are useful to deliver drugs effectively to affected organs and cells but not to others. In a review, Guo suggested that HNTs can be used as a multifunctional nanovehicle for anticancer drug delivery [307]. They displaye high biocompatibility up to a concentration of 200 µg/mL of HNTs. Another interesting fact about halloysite is worth highlighting, in that research to produce functional nanometre-size containers has also experienced exponential growth due to high demand for their applications in the biomedical field [308]. The ideal criteria for such containers would be that they are relatively cheap materials that can be produced easily. Therefore, natural resources and nanotubes such as halloysite are definitely

suitable for this purpose. Halloysite biocompatibility studies need to be carried out for promising applications in polymer composites, bone implants, controlled drug delivery, and for anticorrosion in the coatings industry [308].

With good control of the concentrations used, clay-based particles can be very useful. From the early process of manufacturing and after being used, these alumosilicate nanotubes eventually return to the environment as waste in the form of nano-powder. Consequently, its toxicity assessment is always important. In one study conducted on common organisms, the low toxicity of halloysite to soil nematodes suggests that is likely to be environmentally safe [261].

Even though clay minerals have many benefits, toxicological assessments need to be carried out to prevent potential danger to human and environment [309]. Different treatments which include physical, chemical and thermal processes may be used to modify clays and clay minerals giving infinite scope for future applications, but a certain degree of caution should exercise to protect the environment [304].

3.3. Graphene

Multi-layer graphene (MLG) of 12 nm average thickness and 4.5 μm average lateral size with a surface area of 80 m^2/g was used as a second filler, and was purchased from the Graphene Supermarket. This particular material (MLG) has been widely used in nanocomposites, the aerospace industry, chemical biosensors and conductive coatings. An image of MLG is shown in Figure 11 (b).

3.3.1. History of graphene

The application of graphene started 6000 years ago in Europe to enhance the appearance of ceramics. Research into the isolated single-atom plane of graphite has rapidly increasing since the higher basal plan conductivity of graphite intercalation compounds compared to the original graphite was first revealed back in 1960s [190]. Scientists have noticed that graphite is made up of layers of completely 2D crystals called graphene for many years. However only in 2004, Andre Geim and Konstantin Novoselov managed to isolate graphene from graphite using sticky tape despite predictions that a single layer of carbon atoms could not possibly be stable. Even though the scientific community was excited about this finding, which promised a cheaper, lighter alternative to existing metal conductors, they were bewildered by the conductivity of graphite intercalation compounds and cautions about its possible utilization.

Explorations of graphene have developed gradually. Initially, the expectation was to study the remarkable electrical properties of thin graphite or graphene layers. Nicholas A. Kotov stated in a review that graphene is the answer when carbon fibres are not suitable and carbon nanotubes are too costly. In terms of cost, graphene

seems to be the best candidate for a practical conductive composite [310]. It has attracted significant attention due to its exceptional electron transport, mechanical properties, and high surface area [311]. Graphene has been used in various engineering applications including composites-coating, transport, energy, membranes, sensors, electronics and biomedical devices [183, 312]. When graphene is incorporated properly, its atomically thin carbon sheets can tremendously increase physical properties of host polymers even at small loading [185]. Due to its intrinsic properties, enormous interest is being shown to implement graphene in myriads of devices [313]. Single layer graphene was first observed in 2004. The thin carbon sheet has received attention and become a rapidly rising star in materials science research [183]. A 10-year project research with funding of 10 billion Euros has been provided by the European Commission to more than 140 academics and commercial institutions in 23 countries [314].

3.3.2. Introduction to graphene/polymer composites

Graphene and graphene oxide are gaining attention owing to applications envisioned in biomedical sciences, batteries, energy storage, the absorption of enzymes, drug delivery and solar cells [188, 312, 315]. Graphene is highly impermeable to water and also effective barrier. This makes it a potential perfect membrane for use in desalination to turn salty sea water into drinking water. This could have a great impact in certain countries which struggle to access clean drinking water. Adding graphene can make familiar things such as light bulbs, cars and aircrafts use less energy. Graphene also can filter water faster and more cheaply using less energy. In addition, graphene-based smart fabrics could be used to detect leaks in reservoirs.

Graphene has been used in a wide range of industrial applications due to its superior properties and specifically to prepare graphene-based composites. By combining both of these materials, graphene/polymer composites exhibit better mechanical, thermal, gas barrier, electrical and flame retardant properties when compared to the neat polymers [192, 193, 316]. Graphene has a large surface area (2630 m^2 g^{-1}) and an excellent thermal conductivity of 5000 W $m^{-1}s^{-1}$ which is twice the value of graphite. Graphene also has high resistance to the propagation of advancing crack in order to prevent failure [317].

Even at tiny fractions (below 1 wt%), graphene shows substantial enhancements in the fracture toughness of epoxy by deflecting cracks in the matrix [318]. To date, the strongest material discovered is a graphene nanosheet with a Young's modulus of 1 TPa and an ultimate strength of 130 GPa [319]. Graphene, in the case of 0.1 wt% reinforcement in epoxy, can increase fracture toughness by 131% [320]. The size, weight fraction, surface modification and dispersion mode of graphene have great influence on the improvement in fracture toughness values of epoxy–graphene nanocomposites. A brief list of graphene improvement in K_{1C} values is presented in Table 6. A recent study by Atif *et al.* reported an increase of 29% in fracture toughness [321] and Wan *et al.* reported an increase of 41% in K_{1C} of 0.25 wt% graphene oxide/epoxy. Meanwhile, Zaman reported the achievement of an improvement in fracture toughness by 86% with the incorporation of 4% of graphene platelets [322].

Table 6. A brief list of graphene improvements in K_{1C} values

No.	Authors	Year	Reinforcement/ (wt%)	Polymer	% Increase in K_{1C} (MPa.m$^{1/2}$)	Ref.
1	Atif *et al.*	2016	MLG/0.1	Epoxy	29.4	[323]
2	Wan *et al.*	2014	GO/0.25	Epoxy	41	[324]
3	Zhang *et al.*	2014	GnPs/0.3	Epoxy	50.5	[325]
4	Tang et al	2013	GO/0.2	Epoxy	52	[326]
5	Chatterjee *et al.*	2012	GP/2	Epoxy	82	[202]
6	Zaman *et al.*	2011	GP/4	Epoxy	86	[322]
7	Bortz *et al.*	2011	GO/0.1	Epoxy	111	[327]
8	Rafiee *et al.*	2010	GP/0.125	Epoxy	65	[328]
9	Rafiee *et al.*	2009	GP/0.1	Epoxy	53	[329]

The concentrations of graphene used in previous studies are normally below 5 wt%. Chatterjee *et al.* reported an improvement of K_{1C} by 82% achieved with 2 wt% graphene nanoplatelets reinforcement [202]. Zaman *et al.* studied K_{1C} of epoxy/graphene platelets. An increment of 82% was observed in the case of 4 wt% graphene-epoxy system. Rafiee and co-workers studied the mechanical properties of nanocomposites at low graphene content, revealing an increments of 65% and 53% in K_{1C} for 0.125 wt% and 0.1 wt% of graphene respectively [328, 329]. The high specific surface area and excellent matrix adhesion and interlocking from their rough surface can be associated with the remarkable fracture toughness (K_{1C}) improvement [191, 192, 330]. Bortz *et al.* studied fatigue life and fracture toughness improvements in graphene oxide/epoxy composites. An increment of 111% in fracture toughness was observed in the case of 0.1 wt% reinforcement. From the literature, graphene incorporated in epoxy at very low filler content significantly increases its fracture toughness by deflecting advancing cracks in the matrix. The strong graphene sheets

manage to impede crack propagation [318, 331]. However, the dispersion state and interfacial interactions with the epoxy matrix greatly influence the extent of matrix strengthening and crack bridging provided by graphene.

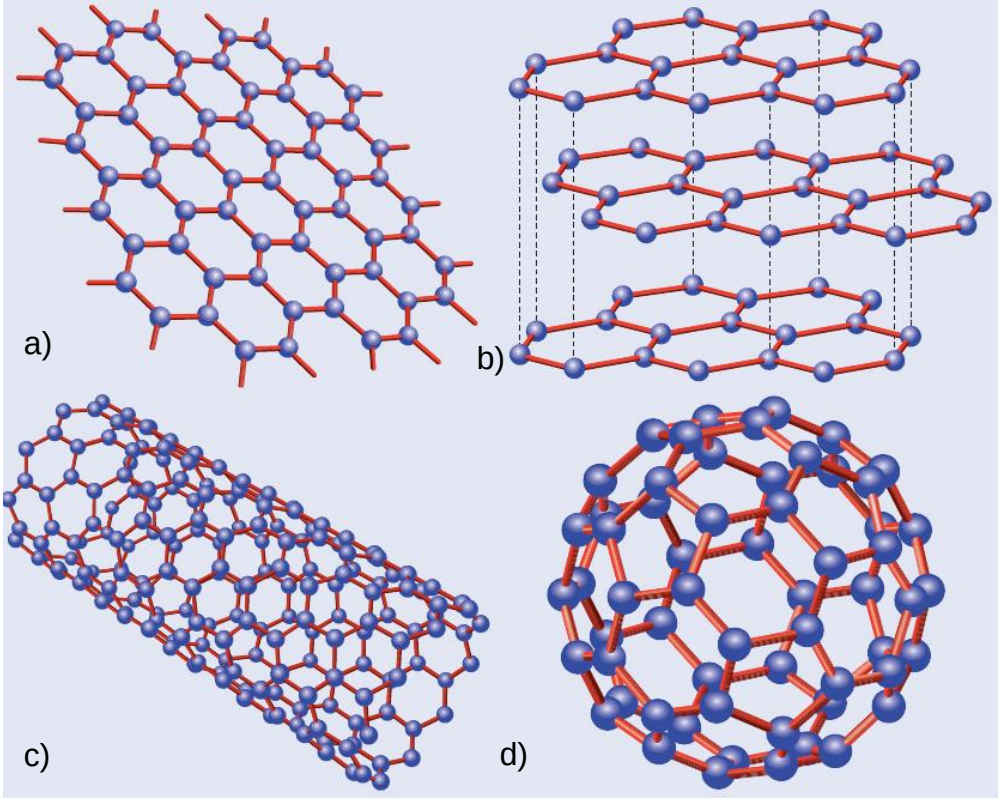

Figure 14. (a) Image of 2D hexagonal lattice of carbon atoms, (b) graphite as a stack of graphene layers, (c) carbon nanotubes as rolled up cylinders of graphene, (d) molecule consisting of graphene balled into sphere (introducing pentagons and hexagons into the lattice) [332]

Table 7. A brief list of graphene maximum improvements in values of impact strength, Young's modulus and flexural strength

No	Authors	Year	Reinforcement/ (wt%)	Polymer	Mechanical Properties	% Increase	Ref.
1	Rasheed *et al.*	2016	MLG/0.1	Epoxy	Impact strength	90	[323]
2	Ren *et al.*	2014	GO/0.7	Epoxy	Impact strength	31	[333]
3	Swain	2013	GnS/0.05	Polyester	Impact strength	32	[334]
4	Rafiq *et al.*	2010	Graphene/0.6	Nylon-12	Impact strength	175	[335]
5	Rasheed *et al.*	2016	MLG/0.1	Epoxy	Young's modulus	25.7	[323]
6	Bortz *et al.*	2012	GO/0.1	Epoxy	Young's modulus	12	[327]
7	Rasheed *et al.*	2016	MLG/0.3	Epoxy	Flexural modulus	47.1	[323]
8	Tang et al	2013	GO/0.1	Epoxy	Flexural modulus	14	[326]
9	Bortz *et al.*	2012	GO/0.1	Epoxy	Flexural modulus	9	[327]

3.3.3. Liquid barrier properties of graphene

Polymer-graphene nanocomposites have an amazing moisture barrier and undoubtedly have great potential in applications of permeation protection materials. Like clay-based particles, graphene is commonly used in anti-corrosive systems to protect coatings. Khyl *et al.* in their research proposed graphene-coated Pt (100) working as an anti-corrosion agent, and demonstrated that the graphene layer and the underlying surface reconstruction on the Pt (100) surface is insensitive to corrosion [336].

In packaging applications, graphene has been used in both the pharmaceutical and food sectors. Compton *et al.* used only 0.02 vol% of crumpled graphene nanosheets to reinforce polystyrene [337]. The graphene nanosheets were found to impede the permeation of oxygen molecules via the incorporation of graphene in a polymer nano-composite. The solubility of oxygen within the nano-composite contributed to the reduction in permeability caused by the densified graphene [337]. Kousalya *et al.* reported that, even under vigorous flow boiling conditions, a few layers or graphene work as a protective layer which proves that it can be used as an ultra-thin oxidation barrier coating [338].

Graphene-based/polymer nanocomposites can potentially act as barriers for organic electronics due to their superior barrier properties. It was found that polymer/graphene-based nanocomposites can offer tremendous enhancements in moisture barrier properties which makes them suitable for display devices in notebooks and computers which are vulnerable to the effects of moisture and oxygen.

The study of polyimide/graphene oxide nanocomposites has found that water vapour permeability decreases by 83% with 0.001wt% graphene oxide content [339]. However, for the same reduction in water vapour permeability in polyimide/montmorillonite nanocomposites, 8 wt% of nanoclay was needed [340]. This is due to the higher aspect ratio of the graphene-derived platelets compared to nanoclay. An appropriate surface modification of graphene oxide nano-sheets is required to achieve exfoliation and a well-dispersed graphene-based nano-composite.

3.3.4. Toxicological study of graphene

Current developments in nanoscience are creating a lot of industrial applications, particularly in medicine [188, 190]. With excellent physiochemical properties and superior electrical, thermal and mechanical properties, the application of nanoparticles in nanomaterials may increase dramatically in the near future, thus prompting concern regarding their toxic behaviour when exposed to the environment and living systems [341]. Exposure to graphene may have adverse toxic effects on health and the environment. Poor exposure control during the production or use of graphene could lead to inhalation, which cause pathological outcomes similar to those from asbestos as the graphene nanoparticles were capable of cutting or piercing cell membranes in human lung tissue [342].

Most recent studies agree that unmodified graphene is cytotoxic and/or genotoxic. However, research has revealed that low doses of graphene family nano-materials (GFN) could be safe, as they can act as enhancers of cell proliferation at times [343]. In addition, their level of toxicity to health and environment strongly

depends on their physicochemical properties such as particle size, particulate state, surface functional groups, oxygen content and surface charges [344].

Huge environmental challenges lie in front of all of us however, the new generations of this excellent material could help. To date, insufficient information is available related to the carcinogenic effects and potential developmental toxicity of graphene. More research evidence is needed to understand the harmful potential of graphene for health and the environment since it has already gained great popularity in commercial products [345].

3.3.5. Synergic effects of hybridisation

The incorporation of two or more fillers is also known to be capable of significantly improving functionality. Many recent efforts have been made to produce enhanced mechanical properties combining different fillers as mentioned by Inam *et al.* [197]. They also explained that the purpose of producing hybrid materials is to extend the concept of modifying properties to meet requirements and to offset the disadvantages of one component by the addition of another [346, 347].

Mahrolz *et al.* reported a tremendous improvement in mechanical performances including enhancements in stiffness and tensile strength, delamination resistance, and safety factors in their epoxy-based multiscale composites [348]. Gojny *et al.* reported an increase of 20% in the interlaminar shear strength of glass fibre/CNT/epoxy composites [349]. Akil *et al.* reported 25% improvement in flexural modulus and 68% in Young's modulus of pultruded jute/glass fibre reinforced polyester hybrid composites.

Hybrid composites also exhibit superior strength compared to unfilled polyester. Muhammad *et al.* reported an enhancement in impact strength by 40% whilst flexural strength increased by 13% for hybrid glass/kenaf reinforced epoxy composite [151]. This study implied that hybrid fillers can significantly enhance the mechanical properties of the composite. Thwe and Liao reported an improvement in Young's modulus up to 60% for bamboo/glass fibre-reinforced polypropylene [350]. They also mentioned that the hybridisation is a revolutionary approach to enhance the mechanical properties and durability of the composites.

3.4. Unsaturated polyester

The polyester resin NORSODYNE O 12335 AL acquired from East Coast Fibreglass, UK, has a density of 1.2 g/cm^3. The catalyst (hardener) was methyl ethyl ketone peroxide solution in dimethyl phthalate, also acquired from East Coast Fibreglass, UK. In order to produce monolithic polyester samples, the resin was mixed with Butanox M-50 catalyst with a polyester: catalyst ratio of 98 : 2.

Unsaturated polyester (UP) is an excellent matrix for composites because of its many features which are superior to those of alternatives, including but not limited to handling characteristics, improvement in composite mechanical properties, acceptable cost and processing flexibility [22]. Although polyester resins are extensively used as a matrix in polymer composites, their curing results in brittleness due to their high cross-linking level [28].

UP resins are widely used in boat components, pipes, tanks, building panels, and automobile due to their ease of processing, low viscosity, and good chemical and corrosion resistance [3–5]. The formation of a three-dimensional cross-linking

structure in the UP from the free-radical copolymerization between a low molar mass that possesses several covalent C=C bonds and styrene, producing localised plastic deformation in front of the crack tip, which lead to brittle failure [39]. The curing process starts with the addition of unsaturated polyester resin and catalyst. When these two components mixed together, the resin starts to harden and solid composite is formed. Unsaturated polyester resin consists of long polyester chains which dissolve in solvents such as styrene. The polymer chains move freely and pass through each other. Curing starts when the catalyst is added. When heated, this catalyst breaks down into two parts called radicals. Each radical has an open double bond which then connects to all styrene molecules. This process continues until all of the polymer chains are connected and a strong 3D network is formed.

The main drawback of unsaturated polyester resin is that polymerisation occurs at high temperatures and results in significantly higher cure shrinkage compared to epoxy resins. The higher polymerization temperature of this resin will result in brittleness due to high cross-linking levels [40]. The generation of a three-dimensional cross-linking structure in the UP from the free-radical copolymerization between a low molar mass that possesses several covalent C=C bonds and the monomer (solvent) which is typically styrene generates localised plastic deformation in front of the crack tip, causing catastrophic brittle failure [353]. The brittleness of UP resins means that crack propagation and susceptible to fracture cannot be prevented. In addition, the tensile strength and stiffness of the unsaturated polyester are lower than those of epoxy resin. In the past, many studies have been conducted on unsaturated polyester to reduce its brittleness such as by reinforcing with clay particles and graphene [323, 354].

3.5. Methanol

Methanol (C.A.S number 67-56-1) with a purity 99.9% (0.1% water) was purchased from Fisher Scientific, UK. This research emphasizes the application of polyester where contact with methanol and water is possible, such as in automotive applications, which may lead to the deterioration of the resin [355].

Methanol is the most basic form of alcohol, and possess a unique smell to ethanol. It is normally used in antifreeze, solvents, fuel and as a denaturant for ethanol [356]. Methanol has gained great attention as an alternative source of energy for internal combustion (IC) as it promotes cleaner burning compared to conventional fuels. In recent years, the demand for methanol has grown rapidly as it is renewable, environmentally friendly and economically efficient.

The deterioration of polyester in methanol is greater than in other alcohols such as ethanol, isopropanol and butanol. This is because the lower molecular alcohols tend to accelerate deterioration and the penetration of liquid molecules into the resin. Methanol is considered to allow gradual chemical deterioration more rapidly which is also known as corrosion [355]. Physical deterioration is often caused by direct contact between thermosetting resin and solvent which causes the resin to swell due to its three-dimensional network structure even though the resin itself is not dissolved.

Methanol synthesis was first developed in the 1920s and improvement continued to be made over the next century [357]. Currently, dramatic advancements in methanol production entail its production from natural gas, biomass [358], or coke oven gas [359] or it can be recovered through flashing vaporation in the continuous production of biodiesel via supercritical methanol [360]. Methanol is the most

promising substitute for fossil fuels to give cleaner and more sustainable fuel. With its clean-burning qualities, methanol eliminates the smog-contribution emissions thus reduce air pollution problems and the economic cost of traditional pollution controls [361]. Interest in methanol has grown rapidly due to its diverse applications in industry.

Existing information is however inadequate, especially about the impact of nano-fillers on the mechanical properties of polymers when exposed to severe liquid media. Hojo *et al.* confirmed that methanol can cause the physical deterioration of polyester resin [355]. In this research, the effect of liquid media comprising of water-methanol on the mechanical properties of HNTs-polyester nanocomposites has been studied.

This research emphasizes on the application of polyester where contact with methanol and water is possible, such as in automotive applications, which may lead to the deterioration of the resin [355]. The influence of different weight fractions of HNTs on the barrier properties of the nanocomposites has been investigated in terms of the weight gain stemming from the liquid absorption.

Hojo *et al.* reported that methanol can cause the physical deterioration of polyester resin [355]. Robeson mentioned that methanol can cause early crazing on polystyrene [115]. Alimi *et al.* studied deterioration in HDPE (high density polyethylene) pipes exposed to toluene-methanol environment. They also mentioned that toluene-methanol is the most degrading environment, followed by sulphuric acid (H_2SO_4) and water (H_2O) [155].

3.6. Seawater

Seawater was collected from South Shields beach, United Kingdom. The samples were immersed in seawater for 7 days. Marine environmental conditions such as high salinity, high pressure, high humidity and alkaline corrosion accelerate the deterioration of polymers and severely affects the reliability of the material [362]. Wave scouring, impacts with floating debris and bacteria in sea mud can lead to the corrosion of marine vehicles, equipment, and oil exploration platforms to different degrees. The immersion of polymers in seawater environments in the long term also degrades the mechanical properties of composites and their shear strength [119, 363]. Different types of resin behave differently in seawater. Basically, the most common type of resins used for maritime applications are phenolic, polyurethane, polyester, vinylester and epoxy. However, only the effects of seawater on polyester, vinylester and epoxy resins were studied.

Polyester-based polymers are extensively used in aggressive marine environments; however, insufficient data is available on the effects of the seawater on the polyester-based nanocomposites mechanical properties. Seawater collected from South Shields, United Kingdom, was used as a secondary liquid media apart from methanol. The effect of seawater on nanocomposites is an important subject to study, especially in marine environments. Many studies in the past have used seawater to accelerate the deterioration of polymers in marine environment [364]. The assessment of the durability of polymeric-based products exposed to marine environments is crucial, particularly in oil and gas industries [364]. The major issue of FRP composites used in the marine environment is that the interface between the fibre and the matrix

could be de-bonded, and thus the thermo-mechanical properties of composites are affected.

Yian *et al.* studied the effect of seawater exposure on mode II fatigue delamination growth in a woven E-glass/bislaleimide composite. They found that the critical strain energy release rate (G_{IIC}) increased by 15.4% which was caused by the plasticization of the matrix [365]. Huang reported a decrease of 27% in the tensile strength of glass fibre/unsaturated polyester composites in a seawater environment [366]. The also stated that the material experienced physical damage and chemical degradation. The fibre/matrix interface was also damaged.

Gellert and Turley reported maximum decreases in flexural strength of up to 21% in monolithic polyester [15] while Espinal *et al.* reported decrease of 23.8% and 35.3% respectively in tensile and flexural strength decrease of epoxy/glass composites exposed to a seawater environment for 30 days [119]. From research conducted in the past, it can be concluded that exposure to seawater can cause severe deterioration effects in composites. Fang and co-workers studied the deterioration in seawater immersion of glass fibre-reinforced polymer composites using quantum dots [367]. After 6 months immersion in seawater, the tensile strength of the GFRP composite showed a significant downward trend by 13.8% [367]. They also concluded that immersion in seawater significantly reduced the mechanical properties of the composites.

3.7. Experimental techniques

3.7.1. Sample preparation

Cured nanocomposite samples are shown in Figure 15 and Figure 16.To produce monolithic polyester samples, the resin (Norsodyne O 12335 Al) was mixed with catalyst (Butanox M-50) in a polyester: catalyst ratio of 98:2. Following thorough hand mixing for 10 minutes, vacuum degassing was carried out for 10 minutes. The mixture was poured into moulds and cured at room temperature for 24 h followed by post curing at 60^{o}C. Five different fractions of HNTs (0 wt%, 0.1 wt%, 0.3 wt%, 0.7 wt% and 1.0 wt%) were used to reinforce the polyester. Hybrid nanocomposites of 0.05 wt% HNTs-0.05 wt% multi-layer graphene and 0.1 wt% of multi-layer graphene (MLG) were also used to reinforced polyester. The MLG has an average thickness of 12 nm and a 4.5 µm average lateral size with a surface area of 80 m^2/g.

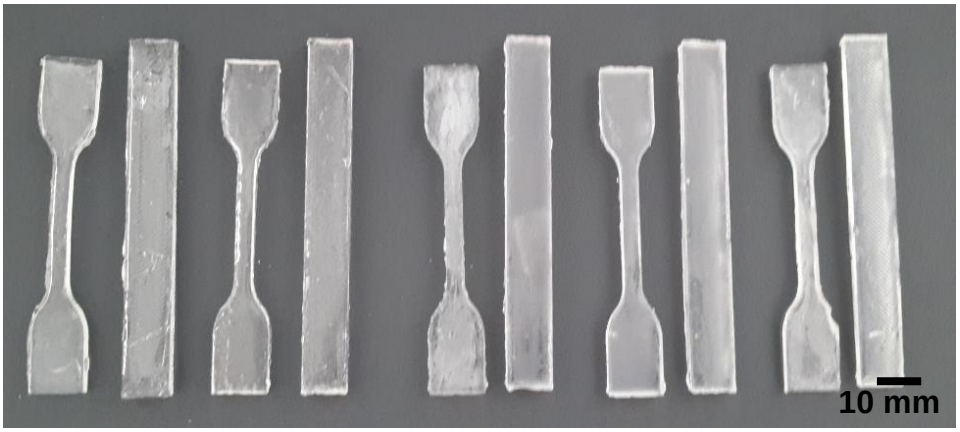

Figure 15. HNTs-polyester composites (concentration from left to right: monolithic polyester, 0.1 wt%, 0.3 wt%, 0.7 wt% and 1 wt%)

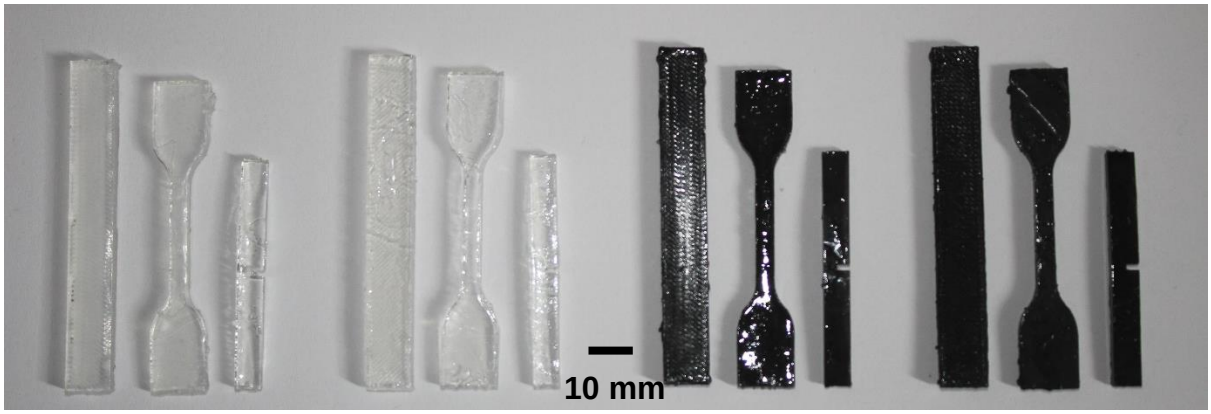

Figure 16. From left to right: monolithic polyester, 0.1 wt% HNTs-polyester, 0.05 HNTs-0.05 wt% MLG-polyester, 0.1 wt% MLG-polyester

3.7.2. Homogenisation of halloysite nanotubes (HNTs) and multi-layer graphene (MLG) in polyester

The dispersion of HNTs in polyester system is quantified using a light transmittance in UV-visible spectroscopy (Shimadzu 2600) through a series of controlled experiments. Tests were carried out immediately after the sonication of each dispersion. The light transmittance of HNTs dispersions was recorded at a fixed wavelength of 400 nm. Five specimens were tested for each set of conditions respectively and mean values were then recorded. Cured samples with concentration of 0.1wt% 0.3 wt%, 0.7 wt% and 1 wt% were fractured to observe the dispersion of HNTs.

The curing reaction of thermoset polymers like epoxy and unsaturated polyester is highly exothermic. Therefore, the incorporation of nanoparticles into thermosets could reduce exotherm heat and improve the consistency of the parts produced. The addition of nanoparticles also increased the molecular weight between cross-links, indicating the relevance of detailed cure kinetics when studying thermosets resins [368]. Adding nanoparticles gives enhancements in stiffness, fracture energy and cyclic-fatigue resistance [369].

3.7.3. Sample analysis for dispersion analysis

HNTs samples were weighed in a Sartorius MC210S analytical balance (with the readability to 0.01 mg) and dispersed in polyester resin by gentle hand-mixing for 5 seconds gently and were then sonicated in a bath sonicator (Grant MXB6) for uniform dispersion. The bath sonicator was rated for an average working power output of 89 Watt. The influence of sonication time and HNTs concentration on dispersibility was studied for cured samples.

To study the influence of concentration on the dispersibility of the cured samples, different concentrations ranging from 0.1 to 1 wt% of samples had been prepared and sonicated for 30 minutes also at 23^{o}C. The samples were then poured into a silicone mould and cured for 24 hours. Post-curing was performed at 60^{o}C for 2 hours before the light transmittance test was carried out. To prepare HNTs-polyester resin, HNTs were dispersed in polyester resin by bath sonication for different lengths of time at 23^{o}C.

3.7.4. Mould preparation

The samples were first drafted in Solidworks 2014 according to the required specifications. The drawings were then submitted to the technician for the laser-cutting process of the required object. The material used to make object was polyethylene. All objects were then attached to the bottom part of the frame with dimensions of 150 mm x 150 mm (Figure 17). Polycraft GP-3481 was purchased from Polyfibre UK which consists of two parts of moulding materials: silicone and catalyst. These two materials were mixed and stirred in a plastic container for 2 minutes and poured into the frame made earlier as shown in Figure 18. The ratio of the silicone and catalyst were 10:1

as recommended by the manufacturer. The silicone mould was left to fully cure overnight, as shown in Figure 19, and was ready to use after a trimming process which was necessary to remove any excess in dimensions. The finished moulds are shown in Figure 20.

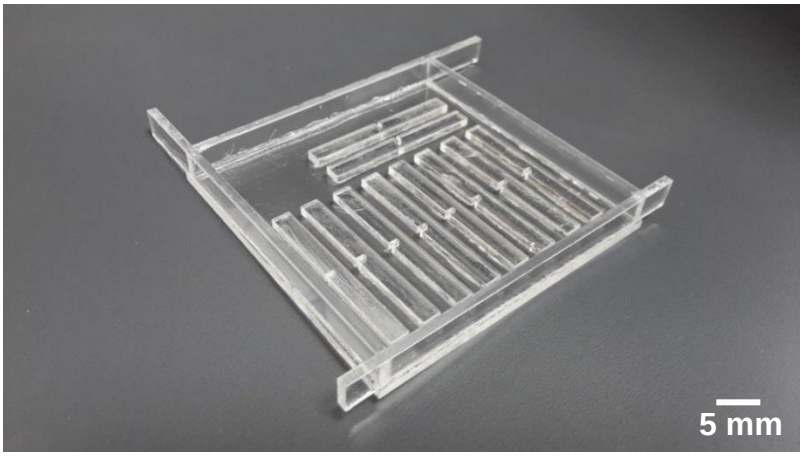

Figure 17. Samples prepared by laser cutting process according to the required specifications. The image shows single-edge-notch 3 point-bend samples according to ASTM D5045

Figure 18. Mixture and stirring process of silicone and catalyst

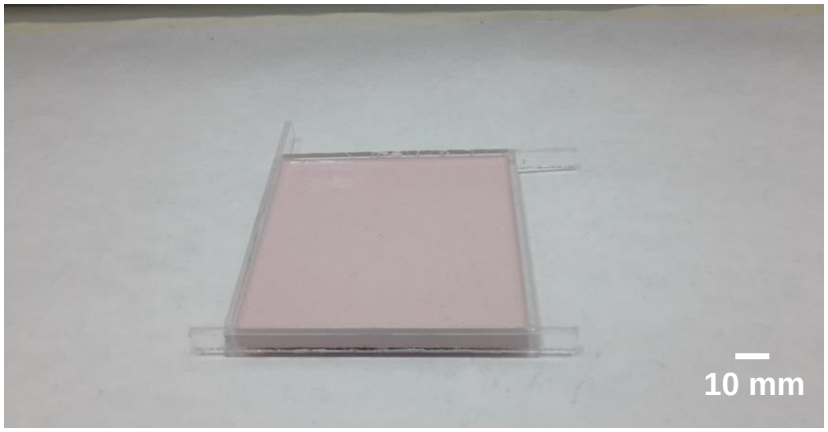

Figure 19. Curing process of silicone mould for 24 hours

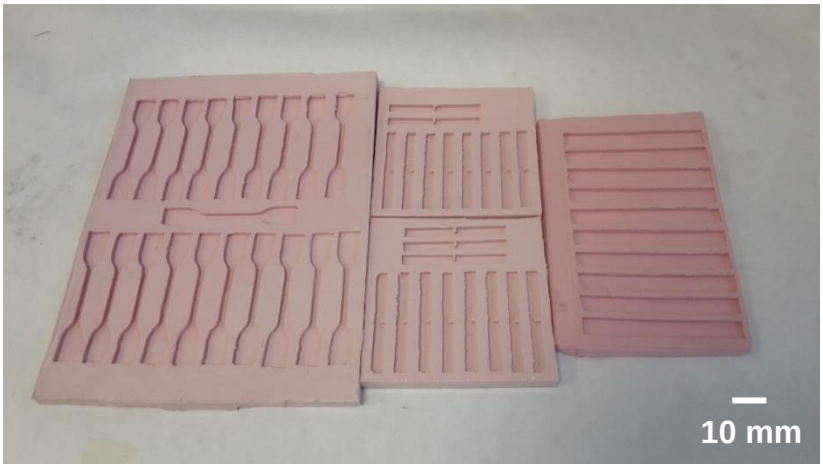

Figure 20. Finished moulds which are ready to use for sample fabrication

3.7.5. Bent strip test preparation

Flat test specimens measuring 80 mm x 10 mm x 4 mm were clamped across steel templates of different radii and placed in contact with media to examine the resistance of plastics to stress cracking. The specimens remained clamped for seven days prior to the impact test in accordance with ISO 178. The bent strip templates as shown in Figure 21 were first drafted in Solidworks 2014 with 1000 m diameter corresponding to an outer fibre strain of 0.1%. Figure 22 shows the clamped specimen immersed in water-methanol liquid.

It can be observed from visual inspection that the physical properties of the test specimens had undergone significant changes after placing the plastics under the influence of chemical agents.

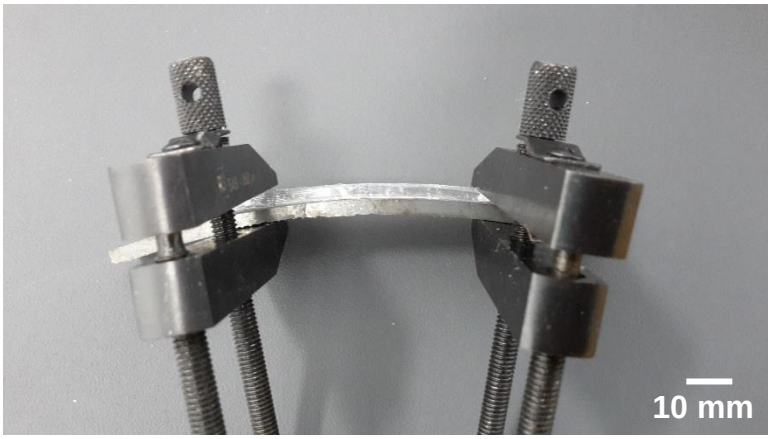

Figure 21 (a) Bent strip steel template

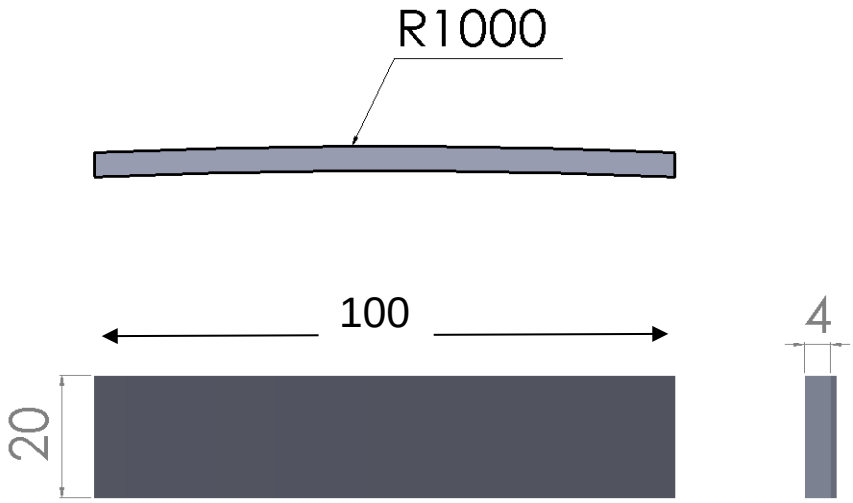

Figure 21 (b) Bent strip drawing in Solidworks (mm)

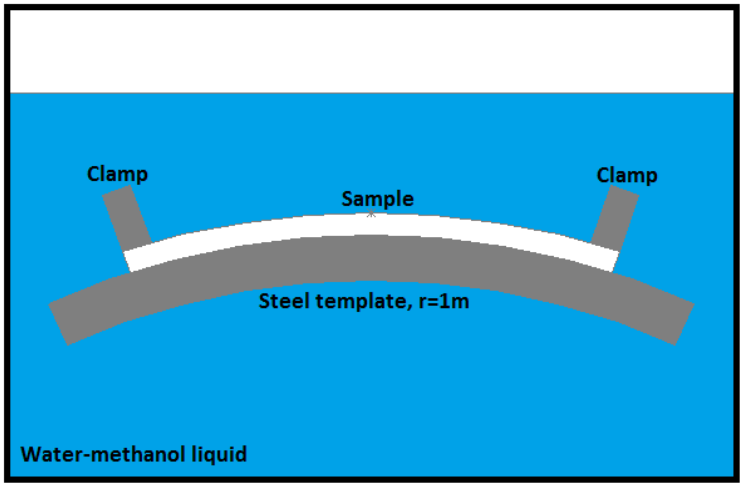

Figure 22. Test specimen clamped across steel template of 1-meter radius corresponding to 0.1% outer fibre strain (not drawn to scale)

3.8. Mechanical testing

3.8.1. Dynamic mechanical analysis

A dynamic mechanical analyzer (DMA 8000, Perkin-Elmer) was used to investigate the dynamic storage modulus (E'), and loss modulus (E'') of the samples. The loss factor tanδ was calculated as the ratio (E''/E'). The glass transition temperature (T_g) was taken as the value of temperature at the peak of the tanδ curves. Rectangular test specimens of dimensions 20 x 6 x 3 mm were used with a single cantilever clamp. All tests were conducted using the temperature sweep method with temperature ramp from 30 °C to 130 °C at 5 °C min^{-1}) at a constant frequency of 1 Hz. The temperature applied was within the range used by Jawahar *et al.*[370] and Inceogul *et al.* [371]. A maximum force of DMA of 10 N was applied during all DMA tests. Scanning electron microscopy (SEM) analysis using a FEI Quanta 200 was carried out of the fractured surfaces of tensile specimens to evaluate the fracture modes in the samples. The fractured portions were cut from the specimens and a layer of gold was applied using an Emscope sputter coater model SC500A.

3.8.2. Densification

The densification of samples was calculated according to ASTM D792. The densities of polyester, hardener, HNTs and water were 1.2, 1.18, 2.53 and 0.9975 g cm^{-3} respectively. The following equations were used to obtain the experimental density and densification.

$$\text{Experimental density} = \frac{\text{weight in air}}{\text{weight in air-weight in water}} \text{ x density of water…} \quad \text{Equation 3}$$

$$\text{Densification (\%)} = \frac{\text{experimental density}}{\text{theoretical density}} \text{ x 100} \quad \text{…. Equation 4}$$

3.8.3. Liquid absorption test

To measure the extent of liquid media absorption, rectangular specimens with dimensions 80 × 10 × 4 mm were clamped on 1 m steel template and immersed in the water-methanol (ratio 1:1) at room temperature. The weight was measured after 24 h immersion using 0.01 mg accurate weighing balance. Before weighing a specimen, any retained liquid was removed from its surface with an absorbent paper. The samples were kept at room temperature for 24 h and increases in weight were measured with respect to initial weight (before immersion) and final weight after the immersion and cleaning of samples. The water-methanol content in the sample was measured as a % weight increase. Equation 5 [52] was used to calculate the liquid absorption in the specimens, where W_t is the weight of specimen at time *t* (i.e. after immersion in the liquid) and W_o is the initial weight of the sample, before being placed in the water-methanol mixture. The effect of liquid absorption on the mechanical properties of HNTs-polyester nanocomposites was investigated after placing the specimens in water-methanol for 24 h at room temperature and via comparison with

the same nanocomposites in dry conditions without immersion in any liquid. The same procedures were applied for samples immersed in seawater (7 days) and water (24 h exposure).

$$Wc=(W_t-W_o)x(\frac{100}{W_o})$$….Equation 5 [52]

3.8.4. Vickers microhardness

The Vickers microhardness test was performed using the Buehler Micromet II for the monolithic polyester and its nanocomposites in air and after exposure to methanol. The load applied was 200 g for 10 seconds and measurements were made according to standard ISO 178.

3.8.5. Tensile, flexural and fracture toughness tests.

Tensile, three-point bending and fracture toughness tests were performed using an Instron Universal Testing Machine (Model 3382). Five specimens were tested for each composition and the displacement rate used was 1 mm/min. Tensile properties were carried out according to ISO 527 Figure 23(a) with a specimen thickness of 3 mm. The three-point bending test was performed according to ISO 178 with dimensions 80 × 10 × 4 mm (Figure 23 (b)). A Charpy impact specimen is shown in Figure 23 (c). A single edge notch three-point bending (SEN-TPB) was used to investigate mode-I fracture toughness K_{1C} according to ASTM D5045. The dimensions were 3 × 6 × 36 mm with a crack length of 3 mm (Figure 23 (d)). The notch was made at the middle of the sample and tapped to sharpen with a razor blade. The K_{1C} was determined from the following equation:

$$K_{1C}=\frac{P_{max}(\frac{a}{W})}{BW^{1/2}}$$……..Equation 6.

$$f\left(\frac{a}{w}\right) = \frac{\left[\left(2+\frac{a}{w}\right)\left\{0.0866+4.64\left(\frac{a}{w}\right)-13.32\left(\frac{a}{w}\right)-13.32\left(\frac{a}{w}\right)^2+14.72\left(\frac{a}{w}\right)^3-5.6\left(\frac{a}{w}\right)^4\right\}\right]}{\left(1-\frac{a}{w}\right)^{\frac{3}{2}}} \quad \text{.....Equation 7}$$

where, P_{max} is the maximum load of displacement curve (N), $f_{(a/w)}$ is a constant related to the geometry of the sample which was calculated using Equation 7 [311], B is the thickness of the sample, W is its width (mm) and a is crack length (between 0.45 W and 0.55 W).

3.8.6. Impact toughness test

Charpy impact tests were carried out using samples as illustrated in Figure 23 (c). Impact toughness was calculated using Equation 8 [372],

$$\text{Impact toughness} = \frac{mgh\,(\cos\beta-\cos\alpha)}{wt} \quad \text{…….Equation 8}$$

where m is the mass of the hammer (kg), g is standard gravity (9.8 m/s^2), h is the length of hammer arm (m), β is the hammer swing angle of the fractured sample (rad), α is the hammer lifting angle (rad), w is the sample width (mm), and t is the sample thickness (mm).

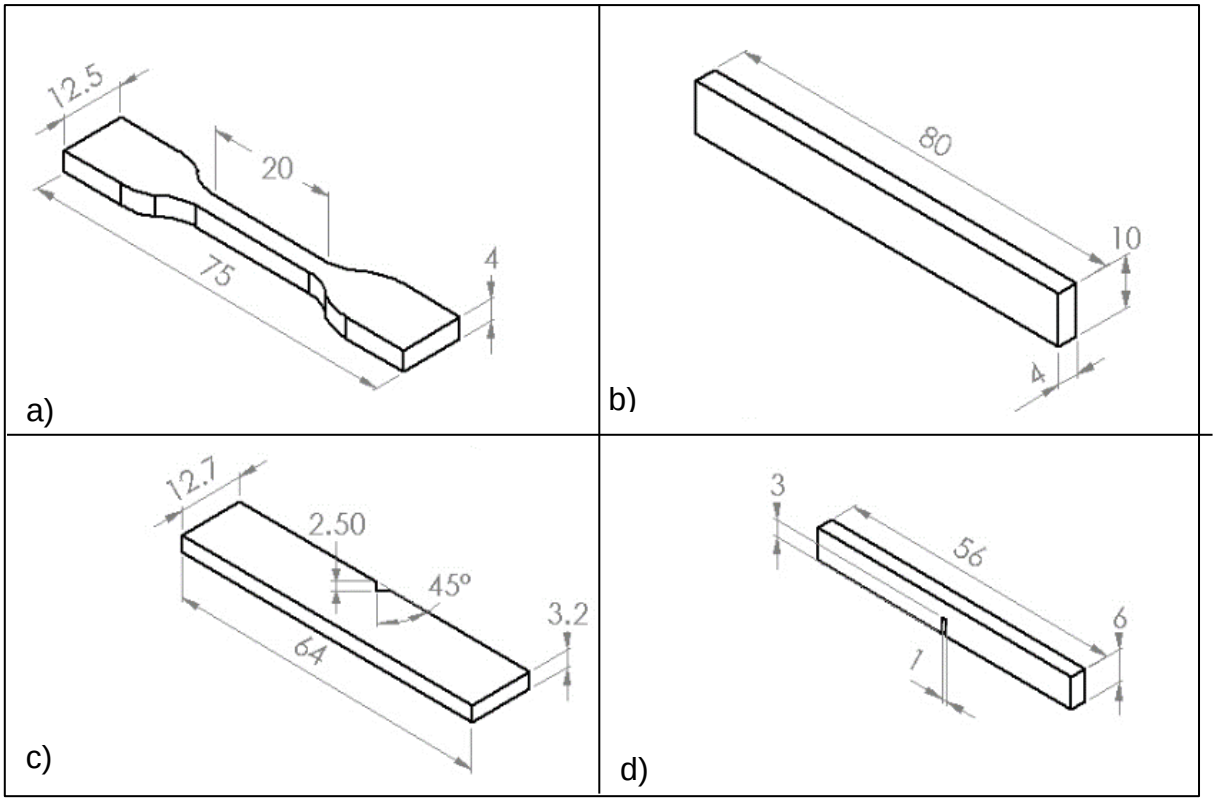

Figure 23. Schematic of specimens: (a) tensile (b) 3-point-bend, (c) impact toughness and (d) single-edge-nodge-three-point bend (mode I fracture toughness K_{1C})

4. Homogenisation of halloysite nanotubes (HNTs) and multi-layer graphene (MLG) in polyester

4.1. Clay particles dispersion

The nano materials bridge the range of molecular and micro scales and allow the connectivity of interactions which enhance the mechanical characteristics of composites. Molecular interactions will range from 0.1 to 2nm, and typical fibre reinforcements will involve dimensions from 0.1µm to mm. Nano materials normally range between the 1nm to 1 µm scale and can be used to distribute and transfer stress.

The volume of a sphere is proportional to the third power of the radius ($V = \frac{4\pi r^3}{3}$), while the surface area is proportional to the second power ($SA = 4\pi r^2$) . Hence, the surface area to volume ratio is inversely proportional to the radius. This has numerous effects on the nature of the particles and their functioning as smaller particles which are expected to aggregate. Likewise, the surfaces of particles can be functionalized to optimize binding to specific receptors. Compared to a large particle, a smaller particle has better binding for a unit of particle mass. This explains why a nanomaterial formed by exfoliated and organically modified clay could increase the strength, modulus, thermal resistance and toughness of the material even at a low weight % of addition [369].

The particles of clay do not themselves promote the enhancement of material properties, but the dispersion of clay particles produces a nanomaterial. The ability of the nanomaterial to disperse nanoparticles in a controlled manner through the material

is the key point in obtaining the enhancement of properties. The correct dispersion of nanomaterial clay can ensure a remarkable enhancement in properties.

Clay is formed naturally as a layered structure with sheets which are ~1 nm thick and extend in the other directions for distances of the order of between 100 to 1000 nm platelets. Clay naturally stacks in the form of columns and adopts a pseudo spherical form with particle sizes of the order of 1-10 microns, and it does not enhance materials properties. Exfoliated clay however does enhance physical properties [373].

4.2. Method of dispersion of clay particles

4.2.1. Ultrasonication

The increase in HNTs research in recent years, as the subject of the present work, is of interest both for the scientific community and industry [267, 281, 288]. In many previous studies, it has been noted that achieving a uniform dispersion of HNTs, particularly in epoxy nanocomposites, has remained a challenge. The dispersion of HNTs in epoxy resin can be improved using sonication which reduces air bubbles at the interface between clay platelets and resin molecules. Dispersion also easily achieves the exfoliation of particles. However, the added curing agent cause the viscosity to increase rapidly. It has been suggested that sonication is only possible for up to 3% clay loading due to the higher viscosity of the mixture [132]. The potential separation of clay fillers should be around 30-50 nm with a loading of 3 to 5 wt% [132]. However, the incorporation of HNTs at a maximum 1 wt% reinforcement is preferred in this research, following the results of the study dispersion study carried out by Sancaktar and Kuznicki,[269]. They mentioned that dispersion at higher weight fractions (more than 1wt % clays) is difficult and agglomerated clay deteriorate

mechanical properties. Asadi *et al.* also found optimal clay reinforcement was in the case of 1 wt% in their fabrication of epoxy-HNTs nanocomposite samples [270]. The dispersion of clay platelets in a polymer matrix can be enhanced using numerous techniques such as high speed stirring, high shear mixing and more commonly, ultrasonication [374].

4.2.2. Shear mixing

Shear mixing does not offer sufficient energy to produce an exfoliated state in the liquid phase due to the increase in viscosity. Through shear mixing, the solution becomes more viscous with a dispersion of clay particles. For instance, the viscosity increases with clay content and it is projected that the basal spacing of clay platelets in epoxy resin will increase due to the extra shear force produced by high viscosity [375]. Yasmin *et al.* studied the processing of clay/epoxy nanocomposites by shear mixing [375]. A three-roll mill was used to disperse clay nanoparticles in an epoxy matrix and it was found that the technique was very efficient and environmentally friendly in achieving a high quality of dispersion within a short period of time. However, the processing of nanocomposites by shear mixing tended to create high viscosity solutions which make degassing very difficult. As a result, some nanovoids were observed inside the silicate clay layers. Albdiry *et al.* studied the fracture toughness and toughening mechanisms of unsaturated polyester-based MMT nanocomposites [280]. The uniform dispersion of unsaturated polyester/MMT nanocomposites prepared by high shear mixing and sonication was observed. At higher clay content (3 wt%), several agglomerates of micro-particles were observed. The presence of which was attributed to the structure of MMT being composed of platelets with an inner octahedral layer surrounded by two silicate tetrahedral layers [280]. Another reason

for the formation of agglomerates was associated with the nature of MMT particles which exist as stacks of several platelets.

4.3. Liquid barrier properties and anticorrosion effects.

4.3.1. Introduction

From the point of view of industrial application, studies in the absorption and transport properties of water and other types of liquid are very significant in various applications such as packaging in the food industry, pharmaceuticals and electronics. In the food industry, the water barrier properties of polymer films are very important criteria in product durability [376].

Recently, new findings have shown the improved the barrier properties of polymer nanocomposites with low contents of reinforcement, not greater than 5 wt%. The new developments in barrier properties reduces gas and water vapour absorption rates. Nowadays, unsaturated polyester and epoxy are found in coating material to improve metallic reinforcements, as these materials are easily processed, have good environmental resistance, and insulating properties, and strong bonding to diverse materials [377].

Shi *et al.* reported the influence of halloysite nanoclay-epoxy on the anti-corrosion and mechanical properties of epoxy coating [378]. When mixed together, the liquid barrier properties of epoxy coatings were improved by the reinforcement of halloysite, which was well-suited to the epoxy polymer. This was achieved by reducing the voids and lengthening the diffusion path for liquid [378].

Inorganic filler particles such as clay at nano-size can be used as reinforcements in epoxy to produce nano-composites. Nanoparticle dispersion into epoxy resins could be the best way to improve the integrity and sturdiness of coatings because the fillers will eliminate micro-voids by filling gaps and providing crack bridging [379]. Moreover, dispersed nanoparticles can also prevent the epoxy from forming aggregates, especially during the curing process. As a result, a more homogenous coating can be produced. This is because nano-fillers can reduce micro-pore formation due to shrinkage during curing, and act as connections joining more molecules together. Therefore, total free volume can be reduced and cross-link density increased. Epoxy coatings including the addition of nanoparticles provide excellent corrosion protection and reduce the formation of clusters or blisters.

The improvement in barrier properties in polymer-clay composites can be tailored with relatively low concentrations, and for example huge reductions in permeability are observed to gases and water vapour. Yano *et al.* [340] revealed a significant decrease of up to 90% of permeability in a polyimide-montmorillonite composite with only 2 wt% of clay reinforcement. Well-dispersed montmorillonite reinforced into the polyimide matrix and was oriented parallel to the film surface. Their research demonstrated that longer filler particles improve permeability.

The Nielsen permeability model [380] was established on the principle that the presence of impermeable filler particles increase the penetration path. This model is normally called the ‘tortuous path’, which is illustrated in Figure 24.The hypothesis suggests that the filler particles are rectangular platelets oriented perpendicular to the direction of penetration. Despite its simplicity, this Nielsen equation does manage to accurately predict the reduction in permeability in polymer/clay nano-composite

systems. For instance, accurate predictions of the effect of montmorillonite concentration on the water permeability of polyimide nanocomposites can be given using this equation [340].

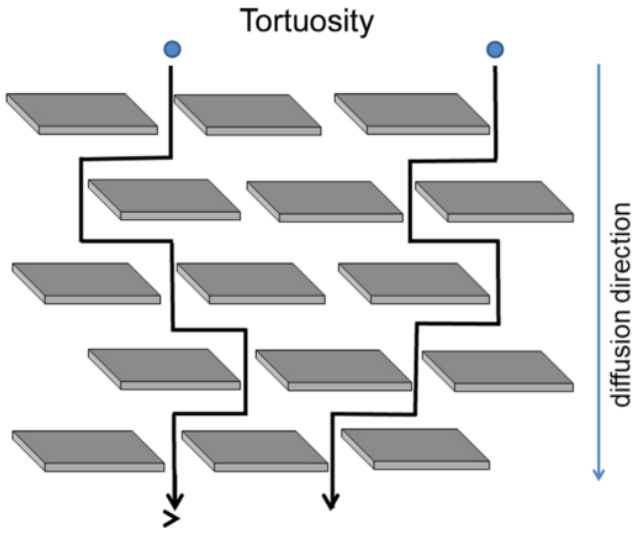

Figure 24. Tortuous path model [380]

In exfoliated nanocomposites, the clay particles are separated and dispersed individually inside the polymer matrix. The highest surface area of interaction between the clay nanoplatelets and fine polymer can only be achieved with homogenous dispersion. Exfoliated clay particles obtained from homogenous dispersion in polymer lead to improvements in barrier properties. However, homogeneous dispersion of most clays in polymers can be challenging because of the parallel stacking of the clay nano-platelets and the hydrophilicity of its surface. In a study by Abdulayev *et al.* HNTs were used for the encapsulation and controlled release of a number of corrosion inhibitors [381]. The HNTs of 15 nm of diameter and 1000 nm in length were used as nanocontainers to carry corrosion inhibitors. As a result, the anticorrosion performance of polyurethane and acrylic was significantly improved.

Only a few studies have been conducted of the self-healing coatings of halloysites nanotubes, even though preliminary results attracted considerable interest. It was reported that the HNTs produce an incredibly strong interlayer adhesion of coatings. HNTs are a promising candidate for self-healing anticorrosion coating formulations as they are easily dispersed in thermosetting resins of medium and high polarity.

4.3.2. Morphology

The structure of HNTs is illustrated in Figure 25. Their composition is identical to Kaolin except for higher hydration water content. Their ideal chemical formula is written as $Al_2Si_2O_5(OH)_4 \cdot nH_2O$, where n (representing the hydrated and dehydrated forms) is equal 2 and 0 respectively [382]. There are two types of hydroxyl groups in HNTs; the inner and outer, which are located between the clay layers and on the surface of the nanotubes. O—Si—O groups covere the outer surface while the inner surface is governed by the (Al—OH) groups.

Nanofillers with different morphologies such as platelets, nanotubes, and fibres can produce “tortuosity” and introduce additional restrictions. As a consequence, longer and more twisted path lengths are produced in the penetration of water vapor molecules, pure or mixed gas. The tortuous path is then responsible in leading the changes of polymer composites inherent permeation properties. Clearly, an exfoliated morphology proves to be better in increasing the path length due to a high aspect ratio. In addition, several factors could influence permeability proprieties, including the weight percentage of nanofiller, orientation, state of aggregation and surface treatments.

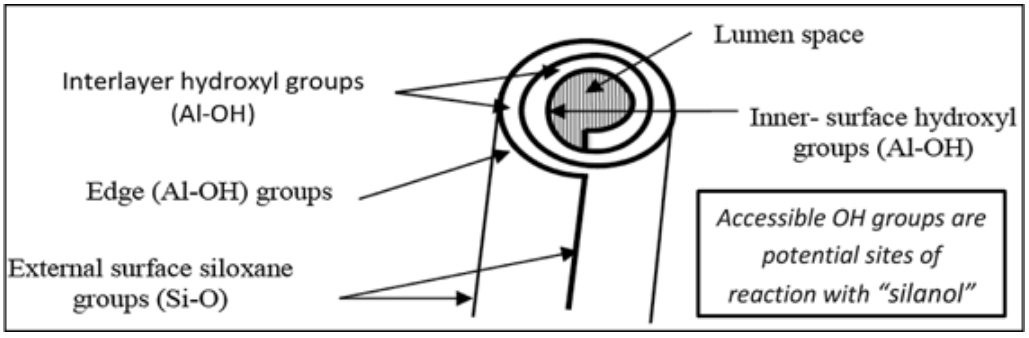

Figure 25. HNTs internal structure [382]

4.3.3. Liquid absorption test

Various specimens were immersed in water-methanol with a ratio 1:1 in order to examine the barrier properties of monolithic polyester and HNTs-polyester nanocomposites. In another study, pure water was used to evaluate the barrier properties of monolithic polyester, 0.1 wt% HNTs-polyester, 0.05 wt% HNTs 0.05 wt% MLG and 0.1 wt% MLG. The effect of water-methanol absorption on the mechanical properties of nanocomposites was studied after immersing the specimens in water for 72 hours period at room temperature compared to the same nanocomposites in dry conditions. Readings were taken every 12 hours. Figure 26 shows the weight gained after water-methanol absorption in percentage terms. The amount of absorption has a linear relationship with immersion time. The addition of HNTs significantly reduced water-methanol absorption. The reaction between water and methanol is likely to produce a thin layer on the surface of nanocomposites, as shown in Figure 27 and Figure 28. In contrast, monolithic polyester tends to absorb the water-methanol liquid that penetrates through plasticized microvoids.

Figure 29 shows a water absorption curve for polyester and its nanocomposites. Multi-layer-graphene recorded the lowest water absorption

compared to HNTs at the same of concentration 0.1 wt%. Figure 30 shows the visual appearance of the nanocomposites after 72 hours of exposure to water.The surface of MLG-polyester nanocomposites was very unlikely to deteriorate after water exposure as in Figure 31 (d). The effect of liquid absorption on the mechanical properties of HNTs-polyester nanocomposites is discussed in chapter 5, 6 and 7.

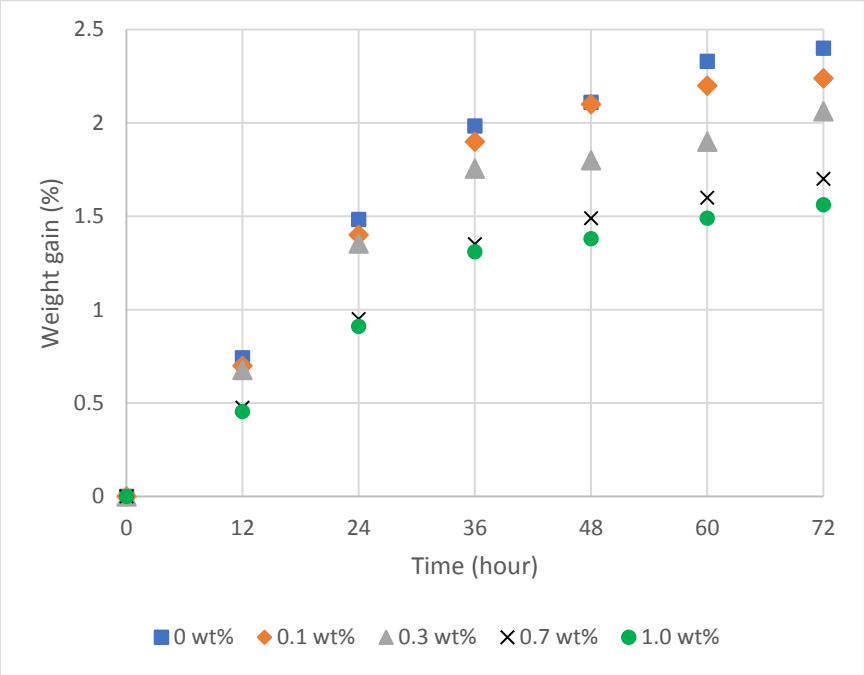

Figure 26. Water-methanol absorption curve of HNTs-polyester nanocomposites.

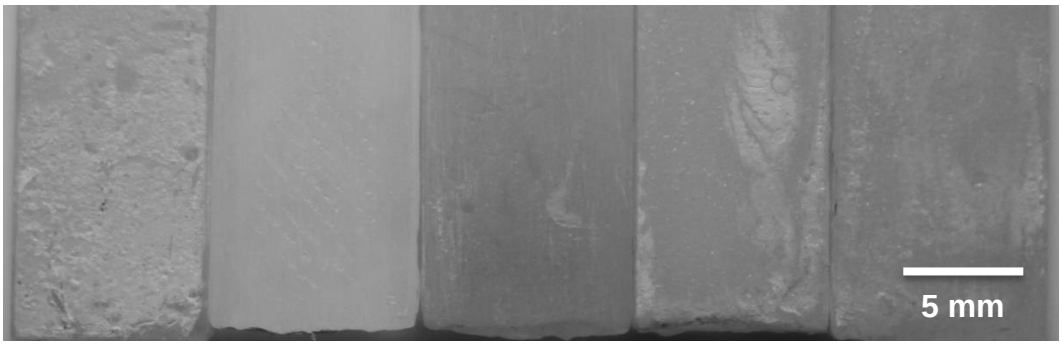

Figure 27. Visual appearance of nanocomposites after 72 hours of water-methanol exposure.

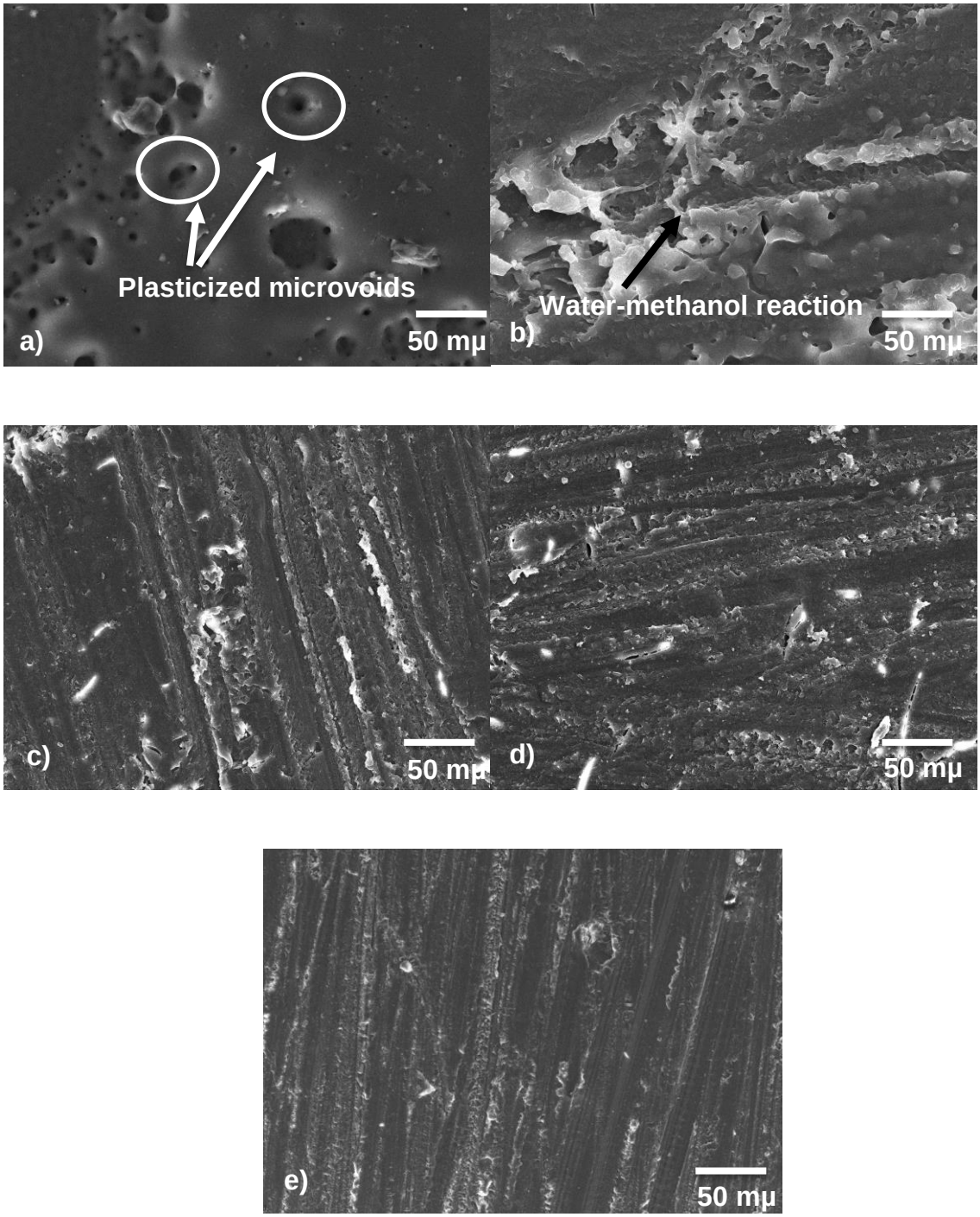

Figure 28. SEM images of HNTs-polyester after 72 hours water-methanol exposure: (a) monolithic polyester (b) 0.1 wt% HNTs-polyester (c) 0.3 wt% HNTs-polyester, (d) 0.7 wt% HNTs-polyester and (e) 1 wt% HNTs-polyester

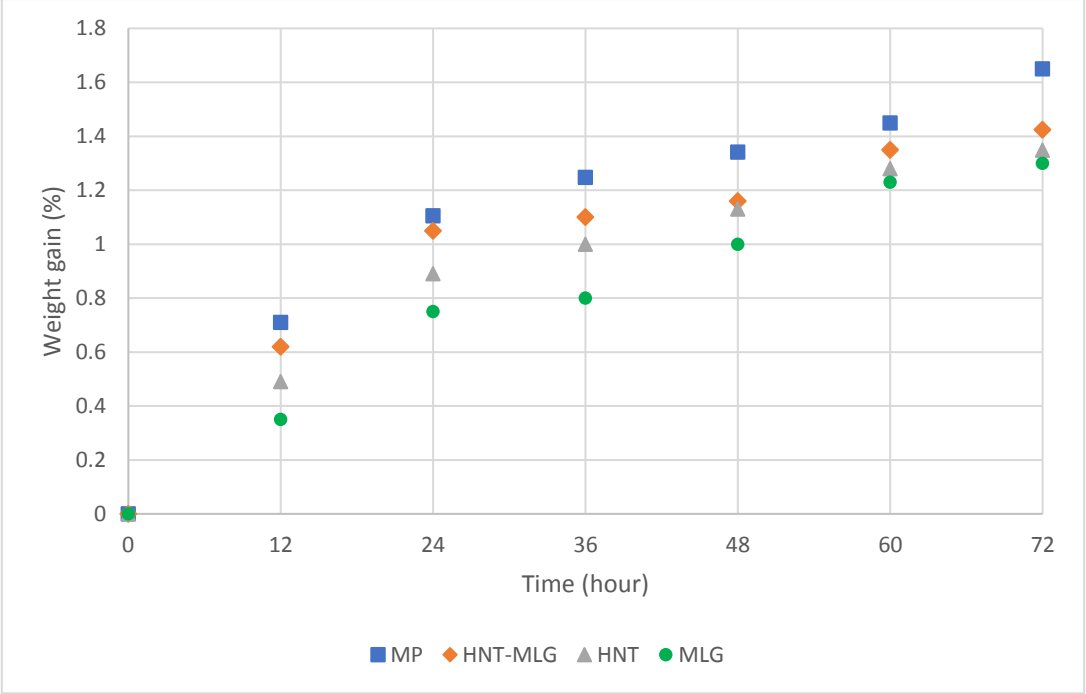

Figure 29. Water absorption curve of polyester and its nanocomposites

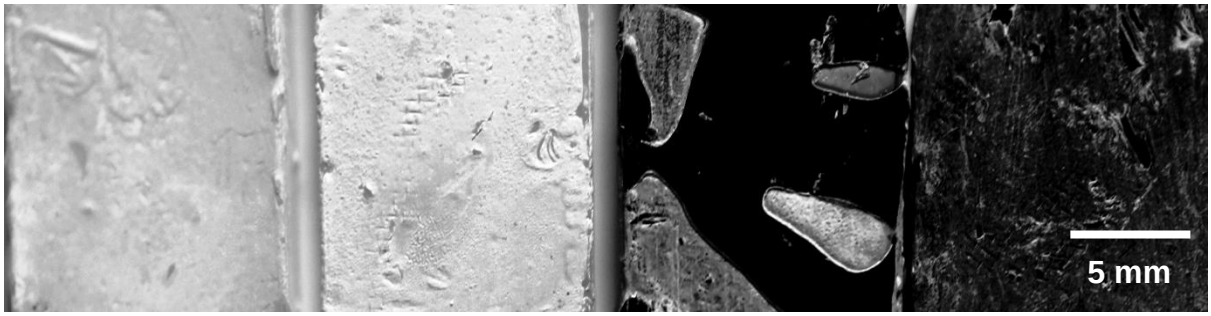

Figure 30. Visual appearance of nanocomposites after 72 hours of water immersion; from left to right (monolithic polyester, 0.1 wt% HNTs, 0.05 HNTs-0.05 MLG polyester and 0.1 wt% MLG)

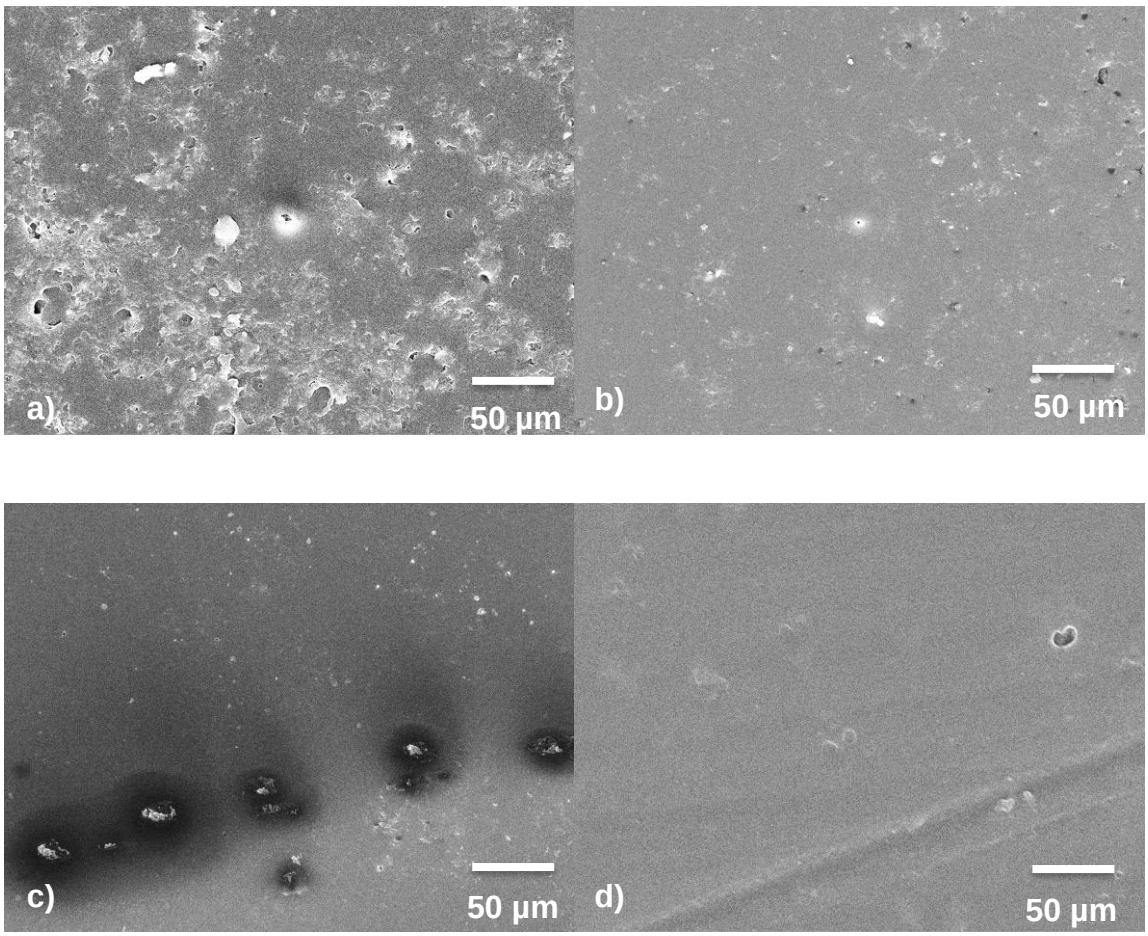

Figure 31. SEM images of HNTs-polyester exposed to water immersion for 72 hours: (a) monolithic polyester (b) HNTs-poyester (c) HNTs-MLG polyester (d) MLG-polyester

4.3.4. Physical deterioration of nanocomposites

It is observed that the resin did not dissolve when the nanocomposites were immersed in the water-methanol mixture but was rather swollen. The swelling effect of monolithic polyester can be seen, since it has a three-dimensional network structure. The swelling effect does not relate to cross-link density as the physical changes only occur on the surface of the samples.

Physical deterioration is severe for the monolithic polyester; however, the degree of corrosion was slightly reduced with the incorporation of nano-fillers. Water clustering was detected for specimens immersed in water-methanol and pure water; causing a decrease in water diffusivity and in the neighbourhood of nano-fillers [125]. Water clusters also possibly reduce the glass transition temperature and have an influence on the interaction between polymer chains.

The methanol chain interacts with water molecule clusters of different sizes with the presence of water and bends the chain into stable open-ring structures. New ordered structures of water and methanol molecules are formed proving that the liquids have blended incompletely at the microscopic level [383]. It is noted that the polyester matrix is sensitive to environmental conditioning after liquid immersion.

The addition of HNTs improved the barrier properties of the polyester by lengthening the diffusion path of the permeating water molecules due to the increase in tortuosity. However, as nanocomposites consist of difference morphological features, different kinds of lengthening of the diffusion path may be observed. The free volume in the matrix, the interfacial regions between the two different phases and the

degree of delamination of the nano-filler layers leads to different kinds of interactions between the polyester and HNTs.

In order to choose the ideal nanocomposite composition, an accurate estimation of the barrier properties of a general nanocomposite is urgently required. The HNTs dispersion state is an important factor in control line water transport properties. The findings showed that the inorganic layers in the composite considered were well dispersed in the polymer phase. The enhancement in the barrier properties of all of the polyester nanocomposites prepared in this study projected them to be used in coatings, storage tanks and packaging where liquid barriers are needed the most. Nevertheless, more systematic measurement to clarify the effects of the inorganic particles on the permeation process are needed.

Apart from that, liquid absorption measurements for samples containing the same matrix with different halloysite particle concentrations and different matrices with the same dispersed particles should be conducted. It is worth to note that water clustering which leads to reductions in water diffusivity and in the neighbourhood of nano-platelets, plasticization and agglomeration effects, could influence the moisture barrier properties of polymer nanocomposites.

4.3.5. Light transmittance and sonication

Sonication is a common method used to disperse clay-based particles in a polymer matrix, and has been proven to have very good efficiency. HNTs particles show very minimal optical clarity which makes the qualitative approach to analysis unsuitable. Figure 32 shows polyester resin and polyester-HNTs mixture. It is difficult to distinguish the effect of HNTs as the resin with HNTs looks almost the same as polyester with unfilled HNTs. However, quantitative measurement using UV-visible spectroscopy can be used to study the influence of HNTs on light transmittance. UV-visible spectroscopy (Shimadzu 2600) is normally used to quantify the dispersion state of nano-fillers at a fixed wavelength of 400 nm. Apart from that, optical clarity of samples before and after exposure to liquid can be assessed.

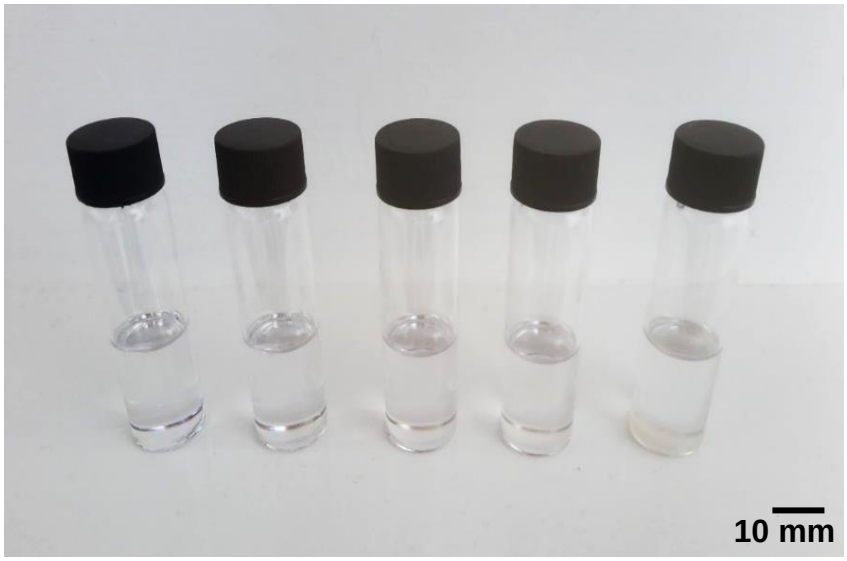

Figure 32. Images of HNTs-polyester (concentration from left to right: 0wt%, 0.1 wt%, 0.3 wt%, 0.7 wt& and 1wt%)

This chapter shows the dispersion of halloysite nanotubes (HNTs) in polyester resins before and after the sonication process. Figure 33 shows HNTs at different concentrations against sonication. In general, the light transmittance decreased with increased of HNTs concentration. Before the sonication process was performed the light transmittance of 0.1 wt% HNTs recorded the highest average value at 86.7%. This then dropped to 68.4% and 60.9% in the cases of 0.3 wt% and 0.7 wt% respectively. The lowest light transmittance was 57.5% at 1 wt% reinforcement. Increasing sonication time up to 30 minutes leads to significant reductions in light transmittance. Sonication for 30 minutes reduced the light transmittance of 1wt% HNTs from 57.5% to 52.2%. The shielding effect of HNTs aggregates dispersed into small particles causes an increase in light absorption or reduced light transmittance.

The quantitative data acquired from the graph in Figure 33 was used as a guide to produce cured nanocomposites samples for HNTs dispersion analysis. Monolithic polyester, 0.1 wt% HNTs-polyester, 0.3 wt% HNTs-polyester, 0.7 wt%-HNTs polyester and 1 wt% HNTs-polyester were cured and tested using the UV-vis spectroscopy machine. Monolithic polyester gave the highest light transmittance value at 74.3% followed by 0.1 wt% HNTs-polyester with 73%. At 0.3 wt% HNTs addition, the light transmittance further dropped to 72%.

The lowest light transmittance was observed for samples of 1 wt% HNTs at 68%. Figure 34 shows the quantitative analysis of light transmittance for the cured samples. These values confirm that light transmittance drops with increased concentrations of HNTs for both cured and uncured samples.

Figure 35 shows the light transmittance of cured nanocomposites for monolithic polyester, 0.1 wt% HNTs-polyester, 0.05 wt% HNTs-0.05 wt% MLG-polyester and 0.1 wt% MLG-polyester. It can be observed that the addition of 0.05 wt% MLG reduced light transmittance by 4% while the addition of 0.1 wt% of MLG reduced the light transmittance by 0.2%. The average value of light transmittance of graphene reported here is in line with the findings of Wei *et al*. [384]. The incorporation of MLG reduced the optical clarity of the composites.

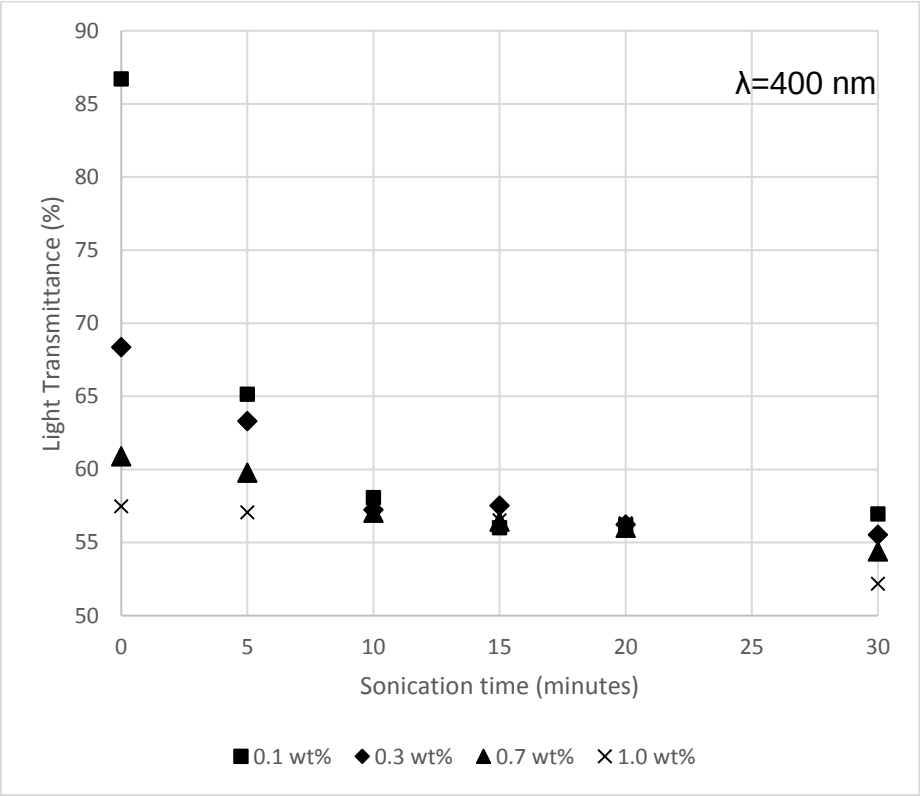

Figure 33. Light transmittance of HNTs dispersion against sonication time.

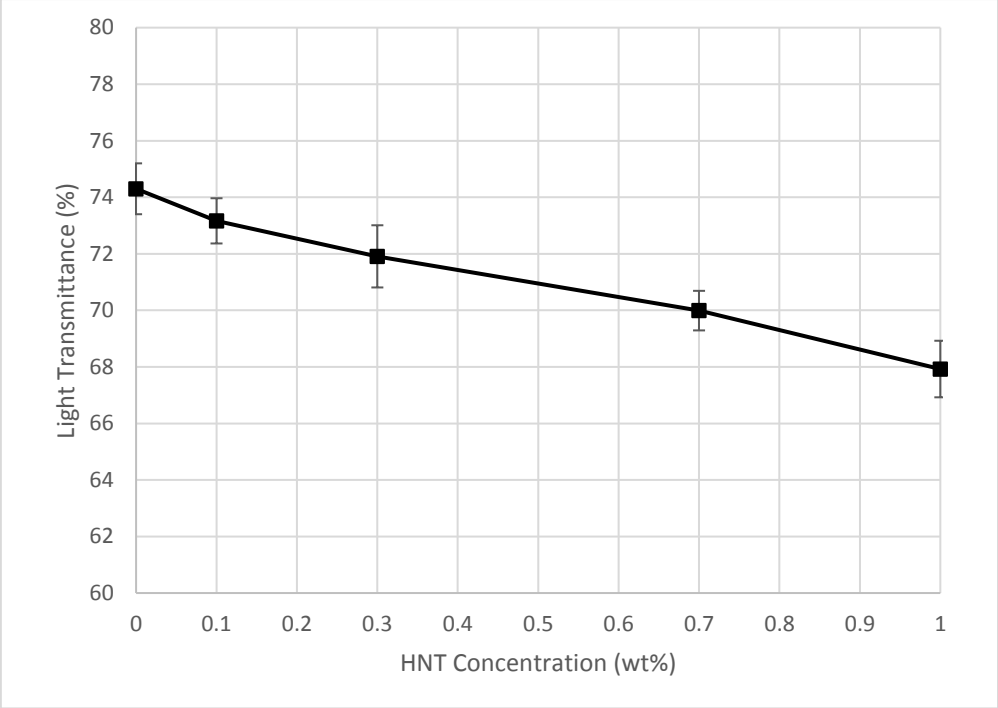

Figure 34. Light transmittance against HNTs concentration of cured samples

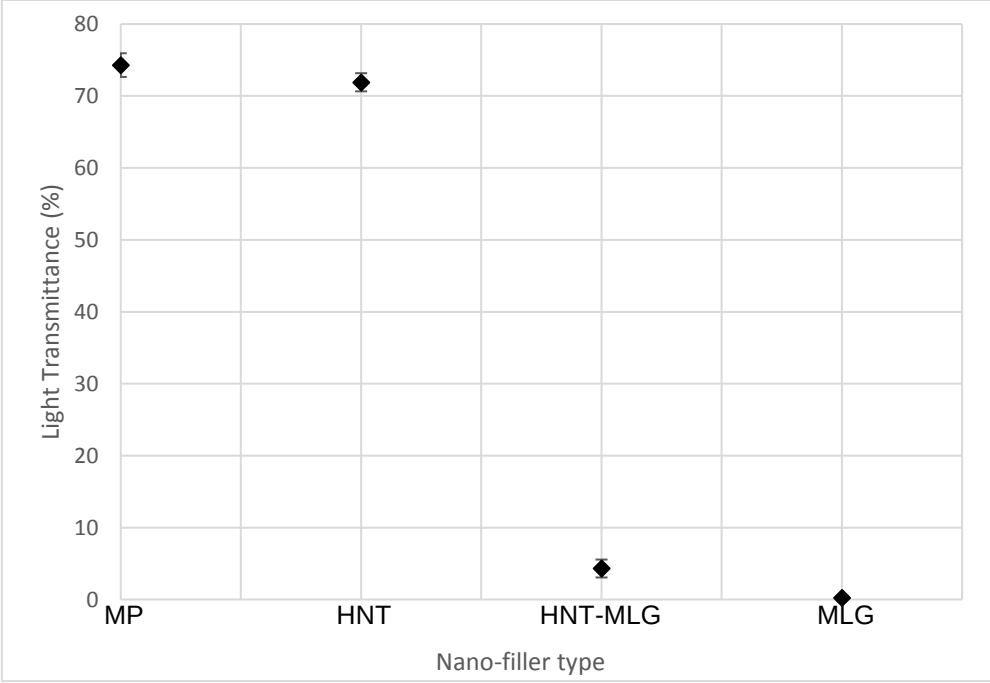

Figure 35. Light transmittance of nano-filler against different filler

Based on the degree of HNTs dispersion, there are three types of morphologies: aggregated, intercalated and exfoliated [281, 285, 385]. In the aggregated structure, the HNTs tactoids are evenly distributed in the polymer matrix, but the single clay layers are not delaminated. Conversely, the clay tactoids are delaminated in the intercalated structure, and thus polymer chains can diffuse into the galleries between them. Interestingly, the clay tactoids are completely broken apart into single layered platelets, which are homogeneously dispersed in the matrix in the exfoliated structure, making this the most desirable state to deliver excellent thermal and mechanical properties with a small amount of clay contents [1].

Figure 36 shows SEM images of various samples. At micron scale the fractured surfaces revealed in all samples reinforced with HNTs were well dispersed. The fracture surface of monolithic polyester as shown below is featureless which exhibiting brittle fracture. Pronounced surface roughness was observed with increased HNTs content. At 0.1 wt% the SEM image shows long and straight crack lines. At 0.3wt% of HNTs, the crack started to emanate radially. At 0.7 wt% and 1 wt% reinforcement, the fractured surface show pronounced increased in surface roughness. At higher filler reinforcement particularly at 2 wt% HNTs-polyester, the surface was fractured. Even though the surface roughness increased, the size of aggregates also increased as shown in Figure 36 (f).

Agglomerates 5-7 μm in diameter can be clearly seen in the 2 wt% HNTs reinforcement. Several authors have made similar observations, and this could be associated to impurities or unmodified clay in the commercial products [132, 279]. The presence of non-cylindrical particles or impurities as shown in Figure 37 (g) could contribute to lower tensile properties. The high magnification of SEM images shows

well dispersed individual HNTs at different percentages of reinforcement. Evidently, the presence of HNTs intensifies the roughness of fracture surfaces, which indicates a crack deflection mechanism. The crack length is increased during deformation. The good dispersion of individual HNTs in the polyester matrix can be attributed to good interaction and compatibility. However, HNTs aggregates at nano-sized level could still occur due to intercalation without complete exfoliation, and as a result the tortuous path is reduced accordingly [376]. Polymer nanocomposites have been identified to have better mechanical, thermal and barrier properties compared to neat polymer matrix owing to their unique structure which makes them useful for food packaging applications.

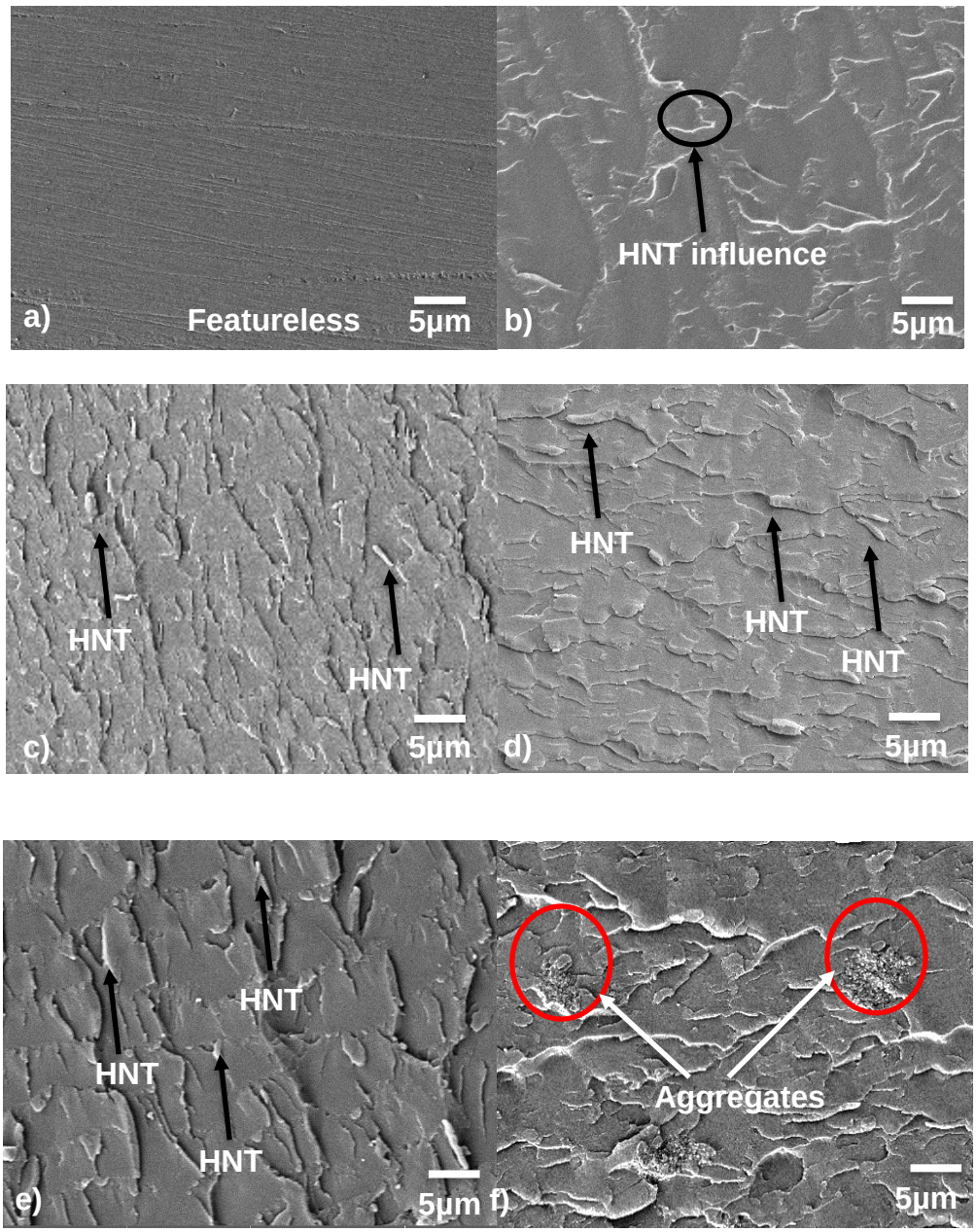

Figure 36. Scanning electron micrographs of fracture surface from left: (a) monolithic polyester, (b) 0.1wt% HNTs-polyester (c) 0.3 wt% HNTs-polyester (d) 0.7 wt% HNTs-polyester, (e)1wt% HNTs-polyester and (f) 2wt% HNTs-polyester.

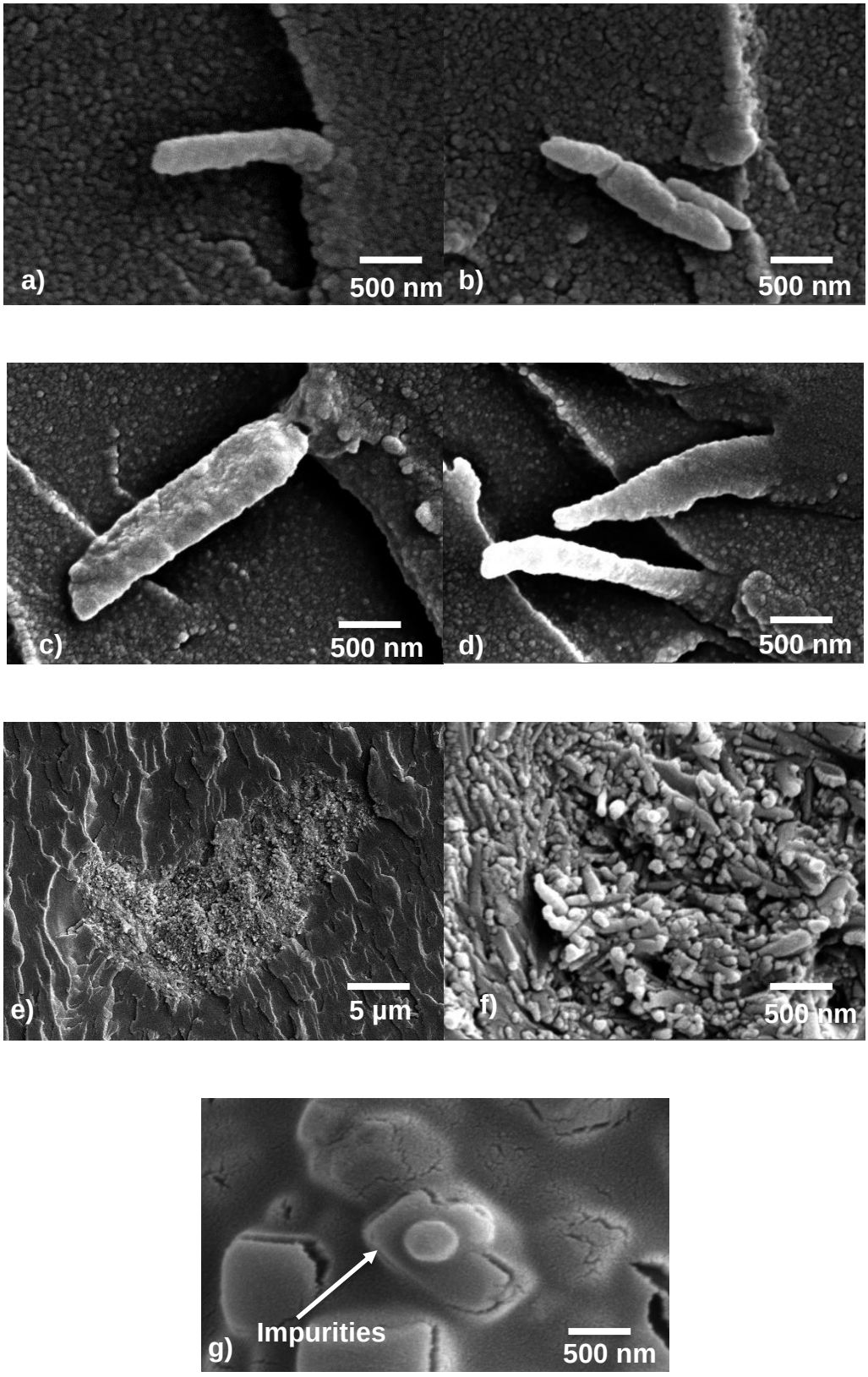

Figure 37. SEM images of dispersed HNTs at different concentrations: (a) 0.1 wt% HNTs-polyester, (b) 0.3 wt% HNTs-polyester, (c) 0.7 wt% HNTs-polyester (d) 1 wt% HNTs-polyester (e) aggregates (f) aggregates at higher magnification (g) impurities

4.3.6. Conclusions

The effects of HNTs concentration and sonication time on the dispersion of HNTs was studied. The study also aimed to achieve complete exfoliation through an appropriate sonication time to ensure better dispersion and to prevent the aggregation of HNTs in a polymer matrix. It was observed that appropriate sonication time improved the dispersion of the nano-sized filler. Furthermore, the incorporation of HNTs below 1 wt% is a good way to achieve fine dispersion. Many researchers have reported that the ideal clay reinforcement is below 1wt%, as dispersing higher weight fraction is difficult and increases clay-based particles agglomerations and hence the mechanical properties deteriorate since the agglomerates act as stress concentration sites [299].

This study applies the same approach as what was recommended by other researchers. The dispersion procedure involves sonication in a bath for a period of time. The mechanical energy generated during sonication overcomes the van der Waals forces between the nanotube bundles or HNTs leading to better exfoliation of the filler. Partially intercalated and disordered HNTs-polyester nanocomposites were obtained via the bath sonication process. From SEM images, it can be concluded that exfoliated HNTs dispersions were achieved at a maximum of 1wt% reinforcement and 30 minutes of sonication in bath sonicator. Vahedi and Paksbakhsh [297] also achieved well-dispersed HNTs after the same duration of sonication. At higher HNTs content, agglomerations are likely to occur as also shown in Figure 37 (e). Agglomerated HNTs creates stress concentrations in the polymer matrix and decreases tensile strength and elongation at break [61]. Therefore, in this study the HNTs content will be kept below 2 wt% in order to produce good clarity, processing stability and mechanical properties of the composites. The HNTs dispersion quality is

a very important factor among the mechanical properties of nanocomposites and sonication is useful to improve the dispersion of HNTs in resins and reduce agglomeration [132].

5. Deterioration of mechanical properties of halloysite nanotubes polyester composites exposed to water-methanol

5.1. Background

Its efficient combustion, and ease of availability and distribution often makes methanol a great alternative as transportation fuel [386]. Organic solvents such as methanol can significantly reduce the mechanical properties of polymers [32, 42, 58, 115, 387, 388]. For instance, Alimi *et al.* reported that the tensile modulus of high density polyethylene (HDPE) decreased by 64% when exposed to methanol [155]. Arnold revealed the effects of diffusion on crack initiation in poly(methyl methacrylate) (PMMA) and reported that methanol had the highest diffusion rate and led to the greatest degree of swelling compared to other solvents [52].

Polyester resins are among the most commonly used thermosetting polymers because of their low cost and versatility [29, 218]. These properties make them a potential candidate as a polymer matrix to produce composites for various applications. Most dinghies, yachts and workboats [223] are now built using composites based on various polyester resins. Unsaturated polyesters are also used as coatings, headlamp reflectors, body panels and fenders in the automotive industry [389]. During service, there is possibility that polyesters and methanol-based fuel encounter each other. As a result, products made from polyester will lose some of its mechanical properties. In extreme cases, applications which expose polyesters to methanol can result in the deterioration of T_g, strength and modulus [125].

In addition, when used as a polymer matrix, the degree of cross-linking of polyester resins is a crucial factor in achieving the desired mechanical properties, especially in

the presence of nano-fillers, which can significantly influence the degree of cross-linking. The incorporation of nano-fillers in polyester resins has garnered significant interest in recent years. Nano-fillers exhibit and impart a suit of remarkable properties [1] to polyester resins, as compared to other conventional micro or macro-sized fillers [40]. To improve the mechanical properties of polyester nanocomposites, layered materials of natural origin such as clay-based compounds have been widely used for decades [374]. Clay-polyester nanocomposites offer excellent improvement in a wide range of physical and engineering properties with low filler content [11, 59, 152, 379, 385, 390]. Over the last one-a-and half decades, research in this particular field has advanced tremendously [134, 391, 392].

5.2. Results

5.2.1. Dynamic mechanical analysis

The incorporation of HNTs can produce two different results on the glass transition temperature of polymers. The possibility is a decrease in T_g associated with the reduced entanglements and interactions among polymer chains and halloysite HNTs thereby enhancing the motion of polymer chains [298]. Another possibility is an increase in T_g caused by the restriction of the segmental motion of polymer chains located near the HNTs surface [393]. In this research, the addition of HNTs increased values of T_g as shown in Figure 38. The maximum increment was observed in the case of 1 wt% reinforcement, where the value of T_g markedly increased from 79.7 °C to 85.2 °C. After exposure to liquid media, the T_g values slightly decreased in all cases. Monolithic polyester recorded the lowest T_g with 77.1 °C. The highest T_g among nanocomposites exposed to water-methanol was obtained in the case of 1 wt%

reinforcement with an average of 84.2 °C. The storage moduli of the nanocomposites in air and after exposure to methanol are shown in Figure 39. The storage moduli increased with increasing clay loading, as is normally observed in other polymer-clay systems [134, 394].

A shift in storage moduli can be observed in all cases of reinforcement, which can be attributed to the stiff nature of the clay fillers and the combined effect of high aspect ratio and the fine dispersion of HNTs [134]. Exposure to water-methanol has reduces the storage moduli of the nanocomposites and increased the ductility of the polymer matrix due to the plasticising effect [293]. This phenomenon can be attributed to the methanol-water molecules entering through the polymer chain and microvoids [395]. As a result, swelling occurs and causes a reduction in the structural integrity of the nanocomposites.

The variation in loss moduli of the nanocomposites in air and after water-methanol exposure is shown in Figure 40. The loss modulus characterizes the viscous performance of the nanocomposite and also represents the dissipated energy which changes to heat [396]. After exposure to water-methanol, it can be noticed that the loss moduli were shifted to the left compared to unexposed samples. The loss modulus abruptly decreases between 60^{o}C – 90^{o}C, and falls almost to zero between temperatures of 90 ^{o}C to 100 ^{o}C. An explanation for the decreasing storage moduli and loss moduli can be that of chemical bond deterioration between HNTs and the polyester matrix as a result of exposure to the water-methanol environment [397].

5.2.2. Optical transmittance

The optical transmittance of the nanocomposites was investigated and shown in Figure 41. It can be observed that monolithic polyester is essentially very high transparent at 400 nm wavelength. The monolithic polyester recorded 74%, this value dropped to 72% in case of 0.1 wt% reinforcement. The transmittance value further dropped to 70% at 0.3 wt%. The minimum optical transmittance was observed in case of 1 wt% reinforcement with just 65% transmittance value. The reduction of transmittance value decreased with the increase of HNTs. The reduction of light transmittance is because of the presence of halloysite particles, since light interacts with clay particles and some of the particles could absorb some of the energy [398].

After water-methanol exposure, the optical transmittance for all samples were slightly reduced due to presence of moisture (from methanol and water). The penetration of water-methanol into the matrix could have change the size of halloysite as a result, the light transmittance decreased [399]. Monolithic polyester optical transmittance was reduced from 74% to 69%. At 1 wt% reinforcement, the light transmittance reduced from 65% to 58.5%. It is noted from this experiment that HNTs presence slightly reduced the optical transmittance of polymer composites. Apart from that the presence of clusters as a result of chemical reaction by water-methanol on the surface of the composites further reduced the light transmittance percentage.

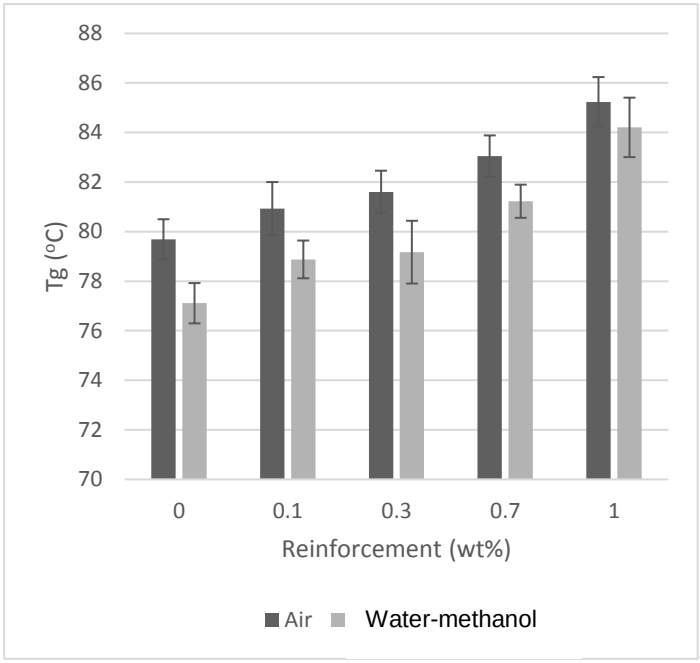

Figure 38. Glass transition temperature of nanocomposites in air and after water-methanol exposure.

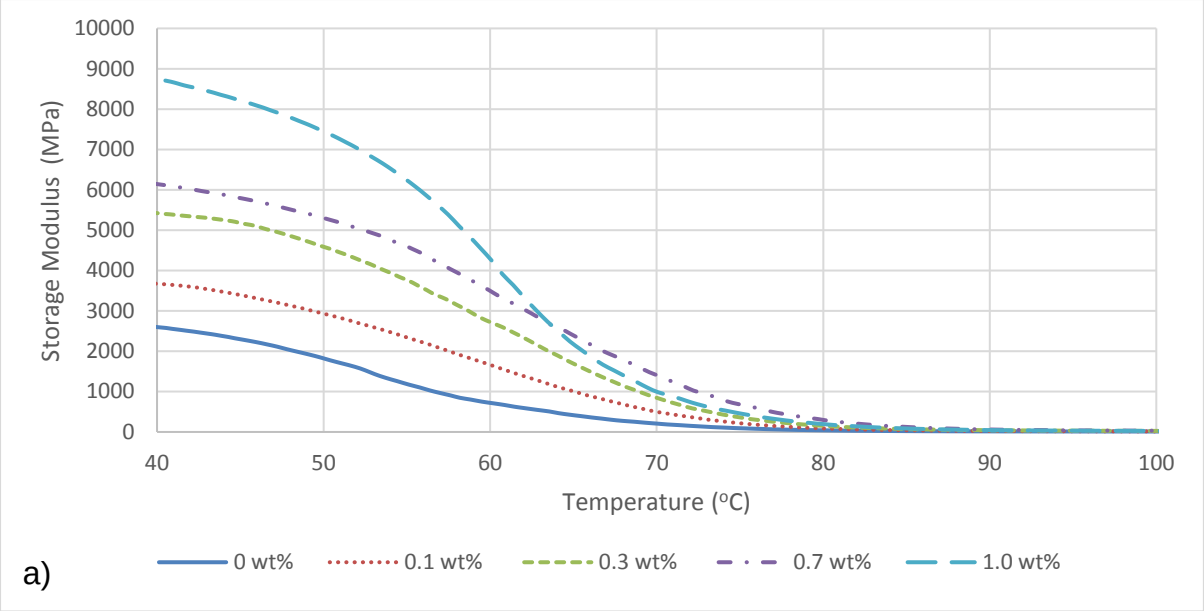

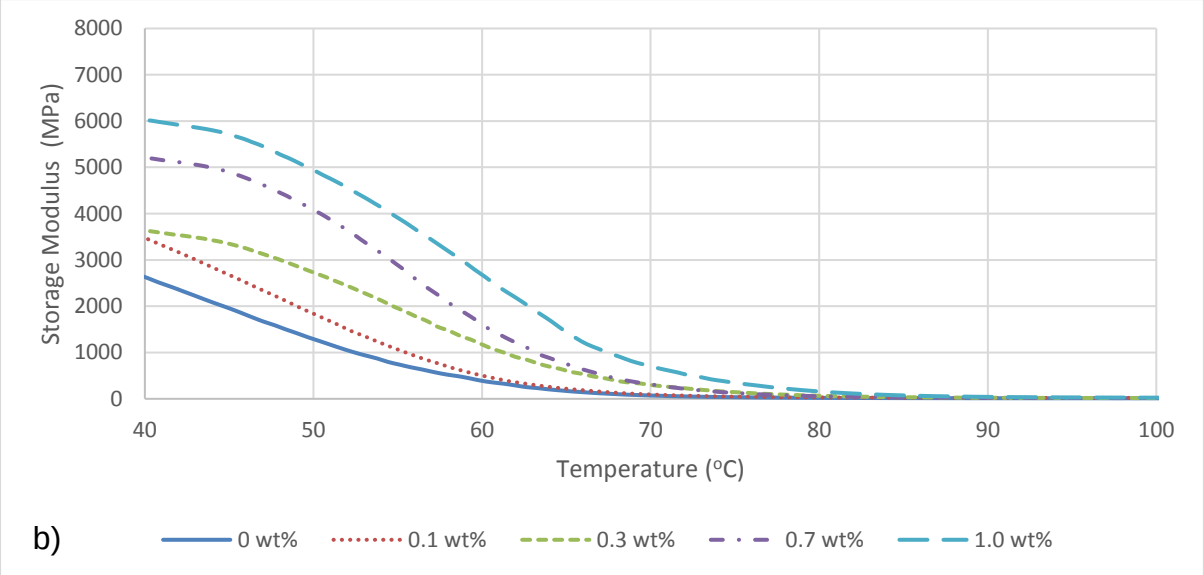

Figure 39. Storage modulus of nanocomposites in air (a) and after water-methanol exposure (b)

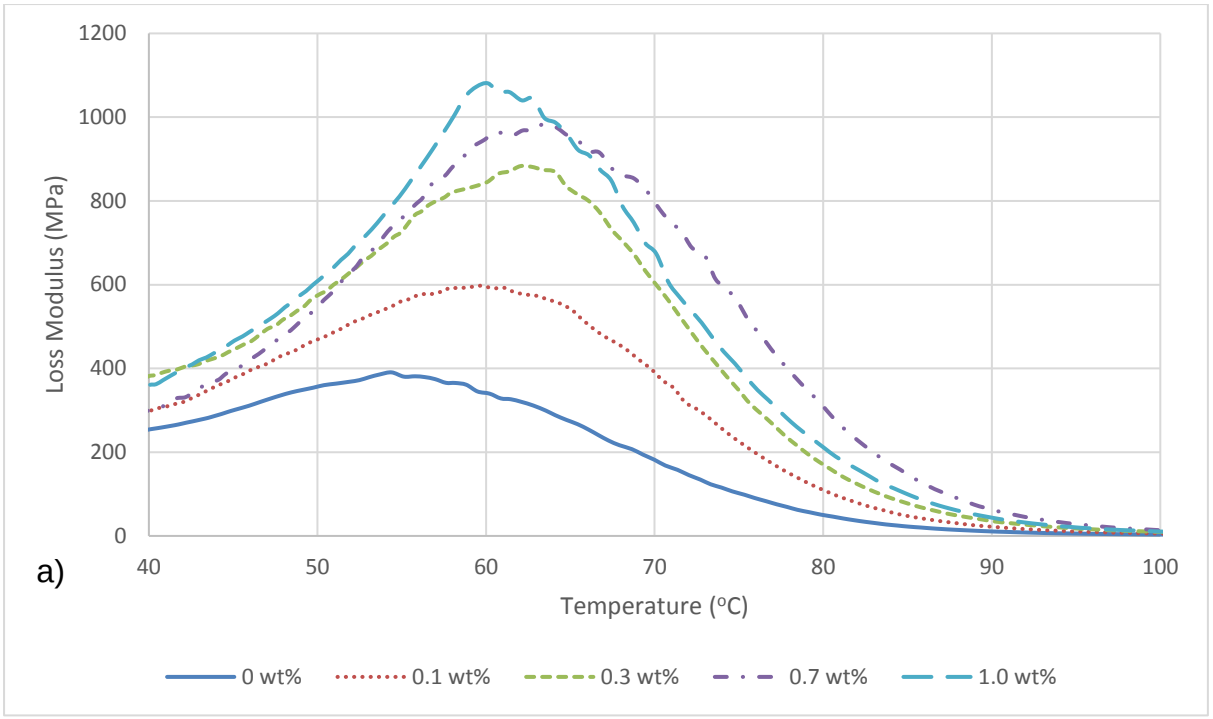

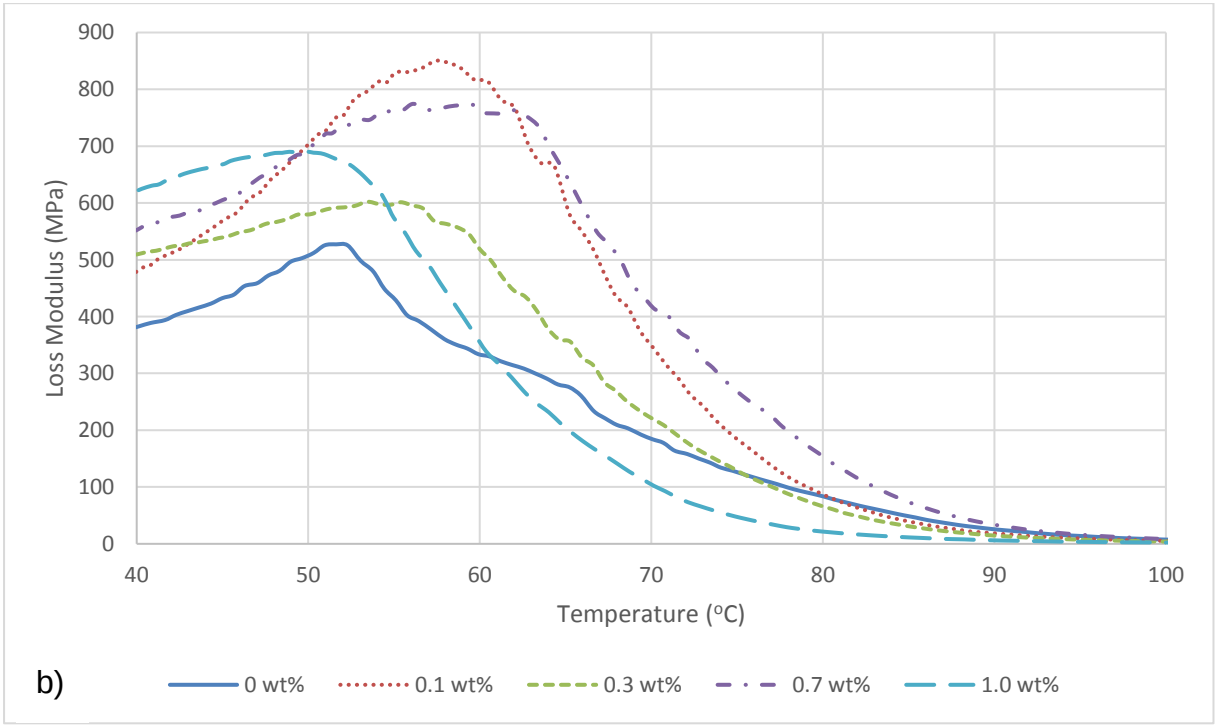

Figure 40. Loss modulus of samples in air (a) and after water-methanol exposure (b)

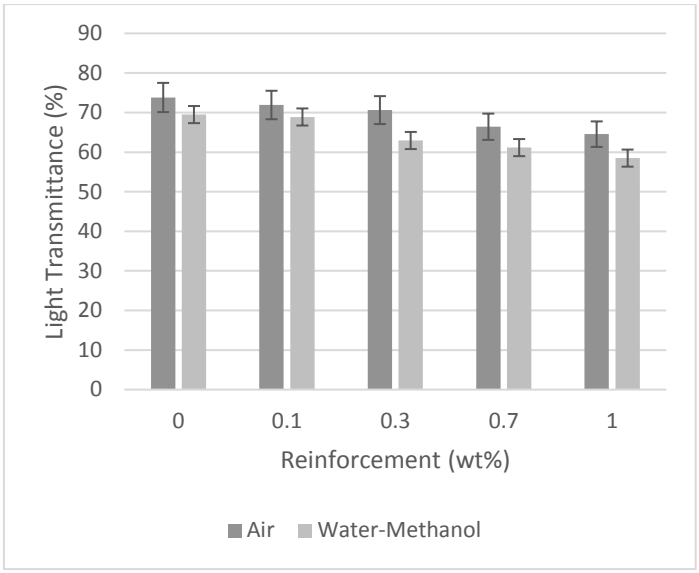

Figure 41. Light transmittance of nanocomposites before and after water-methanol exposure.

5.2.3. Densification

The densification percentage of HNTs-polyester nanocomposites is presented in Figure 42(a) where the maximum densification was observed with 0.3 wt% HNTs-polyester. The decrease in densification with increase in weight fraction of HNTs can be attributed to agglomeration and the bridging of reinforcement materials. On the other hand, trapped air bubbles in the resin remain as micropores after curing. Another possible reason is the fast curing of polyester resin when mixed with curing agent, where the volatiles could not escape during the curing process.

5.2.4. Liquid absorption test

The results of liquid absorption analysis are presented in Figure 42(b) where monolithic polyester showed the highest liquid absorption (1.48%) followed by 0.1 wt% HNTs-polyester system (1.4%). In the case of 0.3 wt% HNTs, the absorption decreased to 1.36% and at 0.7 wt% HNTs, absorption of liquid was 0.95%. The lowest

methanol absorption was observed in the case of 1 wt% reinforcement at 0.9% absorption. The increase in weight shows that the samples filled with water-methanol by diffusion. The liquid absorption results in this study are in line with previous work which reported that HNTs layers dispersed at the nanometer scale in the matrix could reduce the mean free path of liquid molecules in penetrating through the nanocomposite network compared to the monolithic polyester, which then leads to lower water absorption [124, 128]. The presence of water clusters was observed in the samples exposed to water-methanol. Water clusters during penetration have been reported in many publications [400–403]. Marais *et al.* found that water absorption produced a positive plasticization effect particularly in polar polymers (PA6, PA12, PET) [400]. Microvoids present in the samples, on the other hand also influence liquid absorption as they can provide paths for water-methanol absorption. Apart from that, better halloysite dispersion could significantly reduce water-methanol absorption by restricting the free mean path for water-methanol molecules. On the other hand, exfoliated halloysite particles also increased the path length and slowed down water-methanol penetration.

5.2.5. Vickers microhardness

Figure 42(c) shows the variation in Vickers microhardness before exposure to liquid media. At 0.1 wt% HNTs, microhardness improved from 234 HV to 264 HV (13% increase). The maximum microhardness was observed in the case of 1.0 wt% HNTs (44% increase). After exposure to liquid media, monolithic polyester recorded the lowest microhardness (203 HV). At 0.1 wt% HNTs, the microhardness improves by 8%. In the case of 0.3 wt% HNTs, a 26% improvement in microhardness was observed. The 0.7 wt% HNTs system showed a 27% improvement after exposure to

liquid media compared to the monolithic polyester. The maximum microhardness was observed in the case of 1 wt% halloysite HNTs reinforcement (45% increase). In conditions of both air and after exposure to water-methanol, HNTs significantly improved the microhardness of polyester. The HNTs tend to restrict the movement of polymer chains thereby increasing microhardness.

5.2.6. Tensile properties

The variations in Young's modulus are presented in Figure 42 (d). HNTs improved the modulus compared to monolithic polyester in the dry condition. At 0.1 wt% HNTs, the Young's modulus slightly increased from 0.59 GPa to 0.61 GPa (3.4% increase). An improvement of 48.6% was observed in the case of 0.3 wt% nanoclaly. The highest improvement in Young's modulus was observed in the case of 1 wt% HNTs where 75% improvement was recorded.

After 24 hours exposure to water-methanol, the Young's modulus dropped for all weight fractions of HNTs. In the case of the monolithic polyester, the modulus was 0.49 GPa. In comparison with monolithic polyester exposed to liquid media, a 37% increase in Young's modulus was observed in the case of 0.3 wt% reinforcement. At 1 wt% HNTs, the maximum improvement of the modulus found was from 0.49 GPa to 0.83 GPa (70% increase).

The same trend of improvement was observed in tensile strength, as shown in Figure 42(e). The minimum increase in tensile strength was from 26 MPa to 27 MPa (4% increase) in the case of 0.1 wt% HNTs. The maximum tensile strength was observed in the case of 1 wt% HNTs (increased by 38%). After exposure to water-methanol, the maximum tensile strength was 27 MPa also in the case 1 wt% HNTs

reinforcement. The tensile strain was obtained as the % value corresponding to tensile strength, as shown in Figure 42 (f). These results also indicate that tensile strain decreased with the addition of HNTs. The maximum value of tensile strain was obtained for monolithic polyester (11%). At 0.1 wt% reinforcement, the decrease in tensile strain observed was 10% followed by 9.8% and 8.2% in the cases of 0.3 wt% and 0.7 wt% HNTs, respectively. The minimum tensile strain reduction was observed in the case of 1 wt% reinforcement at 7%.

After exposure to water-methanol the tensile strain increased for all composite systems. Monolithic polyester recorded the highest mean value of tensile strain (11.5%). At 1 wt% HNTs reinforcement, the minimum tensile strain value was only 8.8%. Exposure to water-methanol increased the mobility of the polymer chain resulting in an increase in tensile strain in the nanocomposites [126]. It can be concluded that tensile properties increased due to the high surface area of the HNTs. Higher surface area gives more opportunity for filler-matrix interactions [279] and thus excellent halloysite-polyester interaction is responsible for stiffening the nanocomposites by constraining the mobility of polyester matrix and slowing down crack initiation, which results good in tensile properties [404, 405].

5.2.7. Flexural properties

The variations in flexural modulus are presented in Figure 42(g). The minimum improvement in flexural modulus was recorded at 0.1 wt% reinforcement with 3% increase. The maximum increase was observed in the case of 1 wt% reinforcement. High quality dispersion of HNTs contain thinner particles compared to a poorly

dispersed system. The effective modulus to increase with decreasing numbers of individual clay minerals within the intercalated particles [282].

The flexural modulus of composites increased by up to 65% compared to that of the monolithic polyester. The variations in flexural strength are presented in Figure 42 (h). Monolithic polyester recorded the lowest flexural strength of 20 MPa while the highest flexural strength value was 41.3 MPa for 1 wt% HNTs. The values of flexural strain of the nanocomposites are presented in Figure 42 (i). Monolithic polyester recorded the highest flexural strain for the samples tested in air. The incorporation of HNTs decreased the flexural strain of all nanocomposite systems. Exposure to water-methanol reduced the flexural modulus of nanocomposites compared to unexposed samples. At 0.1 wt% reinforcement, the flexural modulus increased from 0.61 MPa to 0.67 MPa, increased by 9.8%. At 1 wt% reinforcement, the flexural modulus recorded the highest value, increasing from 0.61 MPa to 1 MPa (increase by 64%). After exposure to water-methanol, the flexural strength slightly decreased but the HNTs were able to improve flexural strength from 19.4 MPa to 41.3 MPa (113% increase) in water-methanol. All samples recorded slightly higher flexural strain compared to dry samples. It was observed that the mechanical behaviour of polyester and its composites differs considerably compared in the dry state. After exposure to water-methanol, the modulus and strength dropped significantly. The variations in energy absorbed are shown in Figure 42 (j). Energy absorbed by the nanocomposites increased with loading up to 1 wt% HNTs. The results in Figure 42(j) indicate a remarkable enhancement in the energy absorbed by samples which incorporated with HNTs. The minimum increase of energy absorbed was observed in the case of 0.1 wt% reinforcement, from 1.36 J to 1.6 J (an improvement of 18%). The maximum

energy absorbed was observed to be from 1.4 J to 3.5 J in the case of 1 wt% reinforcement (an increase of 158%). A similar trend was also observed for samples exposed to water-methanol. Monolithic polyester recorded the lowest energy absorbed at only 1 J. The amounts of energy absorbed increased steadily with the increase of HNTs reinforcement. For instance, at 0.1 wt% reinforcement, the energy absorbed increased 40% compared to unfilled polyester. This value then increased up to 160% for samples reinforced with 1 wt% HNTs. A deterioration in mechanical properties can be associated with water-methanol absorption, but the addition of filler considerably reduced the deterioration effect.

5.2.8. Fracture toughness

The critical stress intensity factor (K_{1C}) as a function of HNTs loading is shown in Figure 42(k). In this figure, K_{1C} linearly increased with increasing filler content up to 1.0 wt% reinforcement. The maximum increase in K_{1C} was from 0.18 MPa.m$^{1/2}$ to 0.24 MPa.m$^{1/2}$ in the case of 1 wt% of HNTs reinforcement. After exposure to methanol, the K_{1C} values were found to increase due to the plasticizing effect caused by water-methanol absorption. The plasticization of the resin matrix by water-methanol appears to lower the yield stress and increase the size of the plastic zone, thereby causing the observed increase in K_{1C} after exposure to water-methanol [406]. Increases in fracture toughness after liquid exposure were also observed by Buehler *et al.* [407] and Alamri [133] for epoxy-based polymers. The plasticization effect was reduced with the incorporation of HNTs. The HNTs particle increase the diffusion path length by increasing the tortuosity effect and thus improve the liquid barrier properties of the nanocomposites.

The maximum K_{1C} after exposure to methanol was observed in the case of monolithic polyester with an average of 0.56 MPa.m$^{1/2}$. It was also noted that only 0.28 MPa.m$^{1/2}$ fracture toughness was recorded in the case of 1 wt% reinforcement.

5.2.9. Impact toughness

Inorganic fillers such as HNTs are typically used as reinforcements for polymer nanocomposites due to their capability to increase toughness while retaining high modulus and thermal stability [272]. In this research, the incorporation of HNTs significantly improved the Charpy impact toughness of all produced nanocomposites as shown in Figure 42 (l). In dry conditions, the monolithic polyester recorded the lowest impact toughness of 0.23 kJ/m^2. In the case of 0.1 wt% HNTs, the impact toughness was slightly increased to 0.27 kJ/m^2. The impact toughness values for 0.3 wt% and 0.7 wt% HNTs were 0.37 kJ/m^2 and 0.57 kJ/m^2 respectively. The impact toughness further increased to 0.75 kJ/m^2 at 1 wt% HNTs. The incorporation of HNTs as cross-linkers can promote stress transfer from matrix to filler, suppression of polymer chain mobility and the amount of energy dissipation at crack initiation and propagation, and hence toughness is enhanced [272].

After immersion in water-methanol, the impact toughness of both the monolithic polyester and nanocomposites decreased. For monolithic polyester, the lowest value of impact toughness was observed (0.19 kJ/m^2). An improvement of 8% was observed in the case of 0.1 wt% while with 0.3 wt% HNTs, an improvement of 40% was recorded. The highest value of impact toughness was observed for 1 wt% reinforcement where the value of impact toughness was 0.54 kJ/m^2. Water-methanol absorption caused the reduction in impact toughness due to a weaker HNTs-matrix

interface [127]. Failure of the composites can be associated with voids and increased porosity. The liquid diffuses along the HNTs-matrix interface through capillarity action after the composite matrix has cracked and become damaged [60].

Water-methanol molecules actively attack the interface, resulting in the disentanglement of the fibres and matrix which explains the reduction in impact toughness after exposure to water-methanol [408]. Even though the mechanical properties of the composites are reduced after exposure to water-methanol. Their reductions in mechanical properties are far lower than those of the monolithic polyester. Water-methanol in the form of molecules attacks the surface of the composites and diffuses through the gaps. The water-methanol molecules actively attack the polymer interface resulting in the swelling of the composites and hence affecting the structural integrity of their surface.

Table 8. Mechanical properties of HNTs-polyester nanocomposites before and after water-methanol exposure.

Sr.	Properties / HNT Wt%	In air					After water-methanol exposure				
		0	0.1	0.3	0.7	1.0	0	0.1	0.3	0.7	1
1	Microhardness (HV)	234±9.2	264±7	283±4.6	288±9.2	337±21	203±19	219±11	255±10	257.3±13	294.3±9
2	Young's modulus (MPa)	0.59±0.03	0.61±0.04	0.87±0.03	1.01±0.04	1.03±0.07	0.49 ± 0.02	0.52 ± 0.03	0.67± 0.05	0.71± 0.04	0.83±0.06
3	Tensile strength (MPa)	25.8 ± 2.0	26.9 ± 2.1	27.3± 3.6	32.3± 3.2	35.6± 2.4	22.9± 2.0	24.6±3.0	26.4± 3.1	26.9± 2.1	27.4± 3.1
4	Tensile strain (%)	11 ± 1.4	10 ± 1.2	9.8 ± 1.5	8.2 ± 1.4	7.44 ± 1.4	11.5 ± 2.1	10.6 ± 2.5	10.7 ± 2.5	8.6 ± 2.5	8.8 ± 2.4
5	Flexural modulus (MPa)	0.74 ± 0.1	0.76 ± 0.8	0.9 ± 0.06	0.97± 0.07	1.2 ± 0.08	0.61± 0.08	0.67± 0.04	0.86± 0.1	0.93± 0.08	0.99± 0.07
6	Flexural strength (MPa)	54.5±4.4	57±3.7	63.4±5	73.2 ± 2.6	81± 3.5	41.3± 2.5	46.5± 6.15	55.3± 3.3	58.9± 4.4	60± 5.5
7	Flexural strain (%)	9 ±0.7	8.2 ±0.4	6.6 ±0.8	6.6 ±0.8	4.6 ±0.7	10.1 ± 2.2	8.6 ±1	7.6 ± 2	6.9 ±1.3	6.6 ±1
8	Energy absorbed (J)	1.4 ± 0.4	1.6± 0.2	2.5± 0.5	3.3± 0.2	3.5± 0.5	1± 0.3	1.4± 0.29	1.8± 0.22	2.3± 0.3	2.6± 0.3
9	Fracture toughness K_{1C} ($MPa.m^{1/2}$)	0.18±0.02	0.21±0.05	0.23±0.06	0.24±0.04	0.25±0.04	0.56±0.05	0.41±0.06	0.4±0.07	0.33±0.06	0.28±0.06
10	Impact toughness (kJ/m^2)	0.23±0.19	0.27±0.2	0.48±0.3	0.57±0.3	0.75±0.5	0.2 ±0.02	0.21±0.01	0.36±0.06	0.37±0.02	0.54±0.03

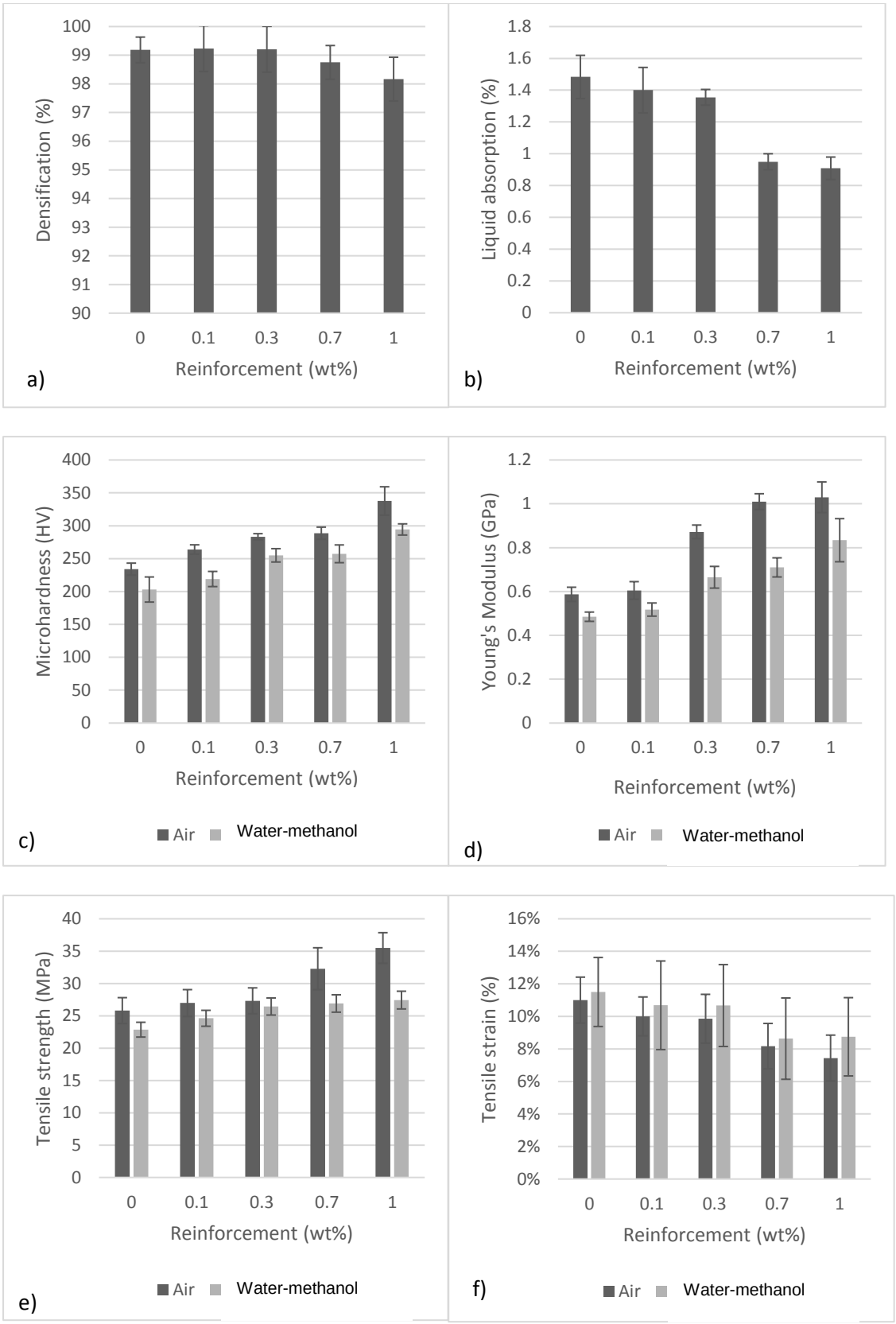

Figure 42. *Cont.*

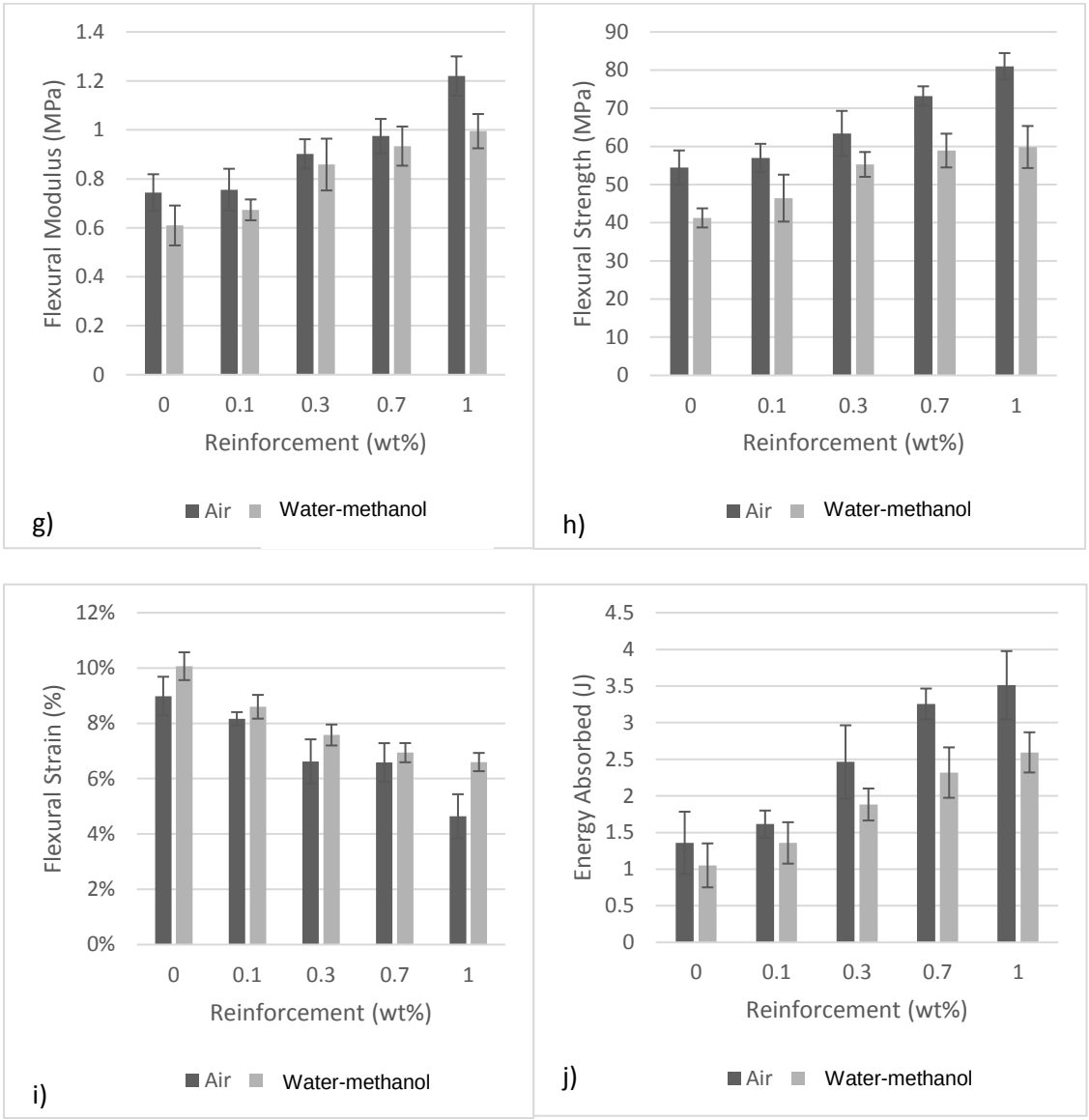

Figure 42. *Cont.*

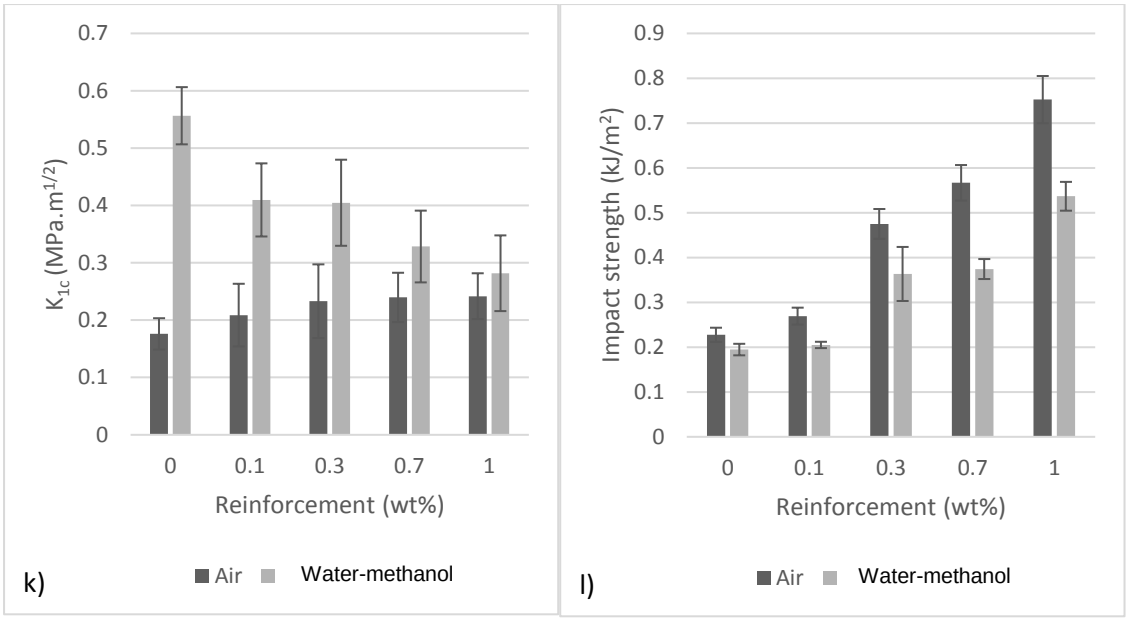

Figure 42. Mechanical properties of HNTs polyester nanocomposites (a) densification (b) liquid absorption (c) Vickers microhardness, (d) Young's modulus, (e) tensile strength, (f) tensile strain (g) flexural modulus (h) flexural strength (i) flexural strain (j) energy absorbed (k) K_{1C} and (l) impact strength

5.2.10. Topographical profile

The analysis of the surface roughness of the samples indicated that nano-fillers significantly influence fracture patterns [311]. On the other hand, a detailed examination of the topographical features of fractured surfaces could be used to evaluate the dispersion state of the fillers, interfacial interactions, and the presence of any agglomerates of filler which can be estimated based on surface parameters such as maximum surface roughness (Rz), the average surface roughness (Ra), and the root mean square parameter of roughness (Rq) [354]. The topographical study was carried out on fractured three-point bend samples. The surface roughness average (Ra) of monolithic polyester and composites with 0.1 wt%, 0.3 wt%, 0.7 wy% and 1 wt% HNTs reinforcement are shown in Figure 43 (a) below. In dry conditions, monolithic polyester recorded the lowest surface roughness, at just 0.3 µm. At 0.1 wt%

reinforcement the value of Ra increased to 0.37 μm. This is the minimum enhancement of surface roughness among the nanocomposites. Further increases of Ra were observed in the cases of 0.3 wt% and 0.7 wt% with Ra values were 0.46 μm and 0.0.49 μm respectively. The maximum enhancement in surface roughness was observed in the case of 1 wt% reinforcement, showing an Ra increase from 0.3 μm to 0.51 μm (70% higher). The fractography analysis of the samples suggested that nano-fillers significantly influence fracture patterns.

For samples immersed in water-methanol, it can be observed that the Ra values were slightly increased compared to the dry condition. The minimum surface roughness Ra was observed for monolithic polyester with 0.38 μm surface roughness. The maximum Ra values were observed in the case of 1 wt% reinforcement at 1.1 μm. In general, the root-mean-square roughness of the profile (Rq) also followed a similar trend. In dry condition, the minimum Rq value was observed for the monolithic polyester (0.4 μm) as shown in Figure 43 (b). The maximum Rq on the other hand, was observed in the case of 1 wt% reinforcement (0.63 μm). After immersion in water-methanol, Rq mean value in the case of monolithic polyester became 0.48 μm. As for 1 wt% reinforcement, the value of Rq increased to 1.6 μm. The mean-peak-to valley height of roughness profile (Rz) also showed a similar trend for all nanocomposite systems in dry conditions and after exposure to water-methanol. In dry conditions, the maximum height of the profile (Rz) was observed in the case of 1 wt% reinforcement at 2.3 μm. The Rz value then increased to 5.7 μm for the 0.1 wt% HNTs-polyester immersed in water-methanol. This can be attributed to the plasticization of deep craters or trenches on the surface measured. HNTs de-bonded from the polyester matrix also resulted in void growth and hence increased distance between the highest

peak and lowest valley. The topographic profiles for dry samples and those exposed to water-methanol are shown in Figure 44.

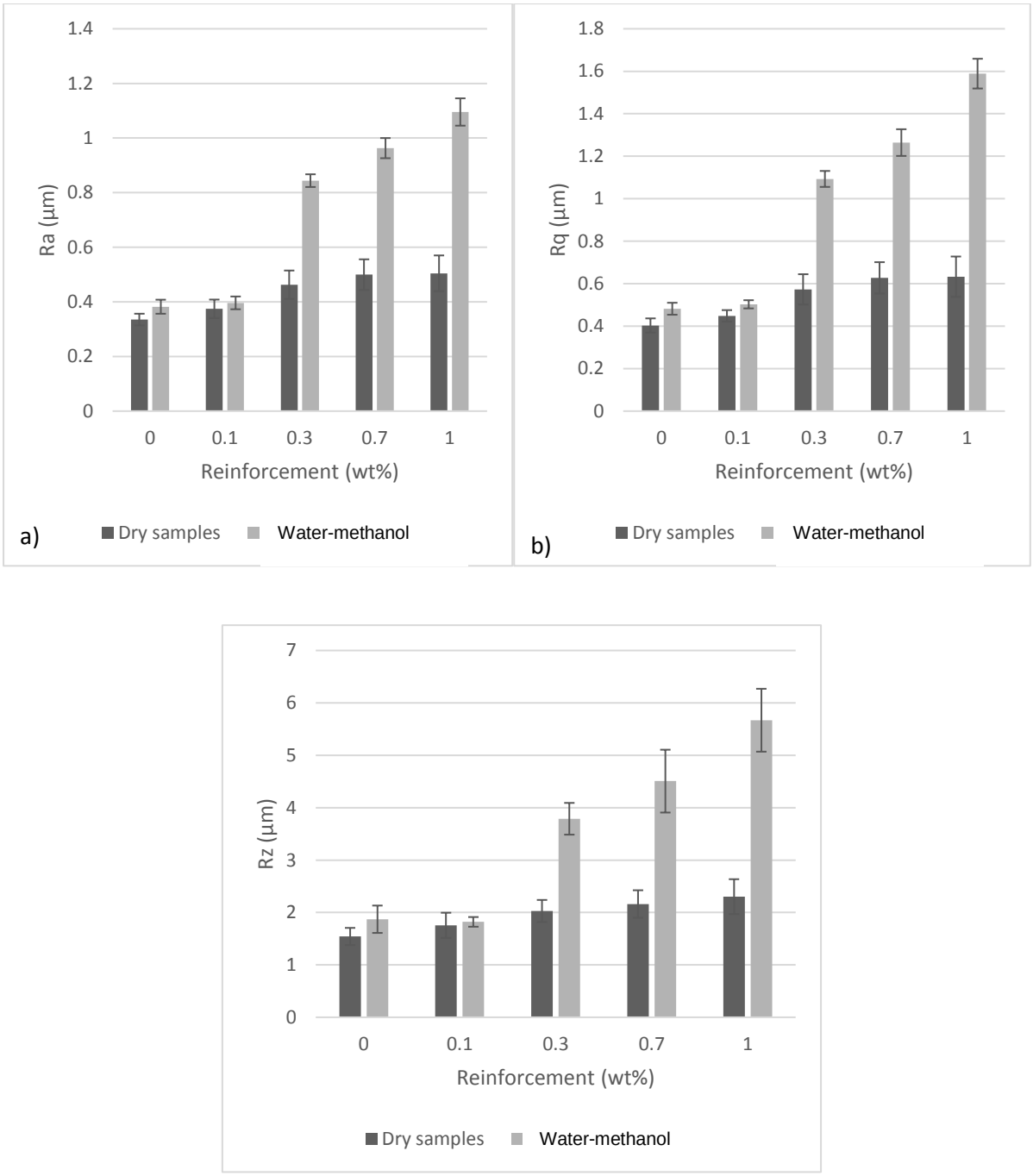

Figure 43. Surface roughness R_a, (a) R_q, (b) and R_z (c) for dry samples and immersed samples.

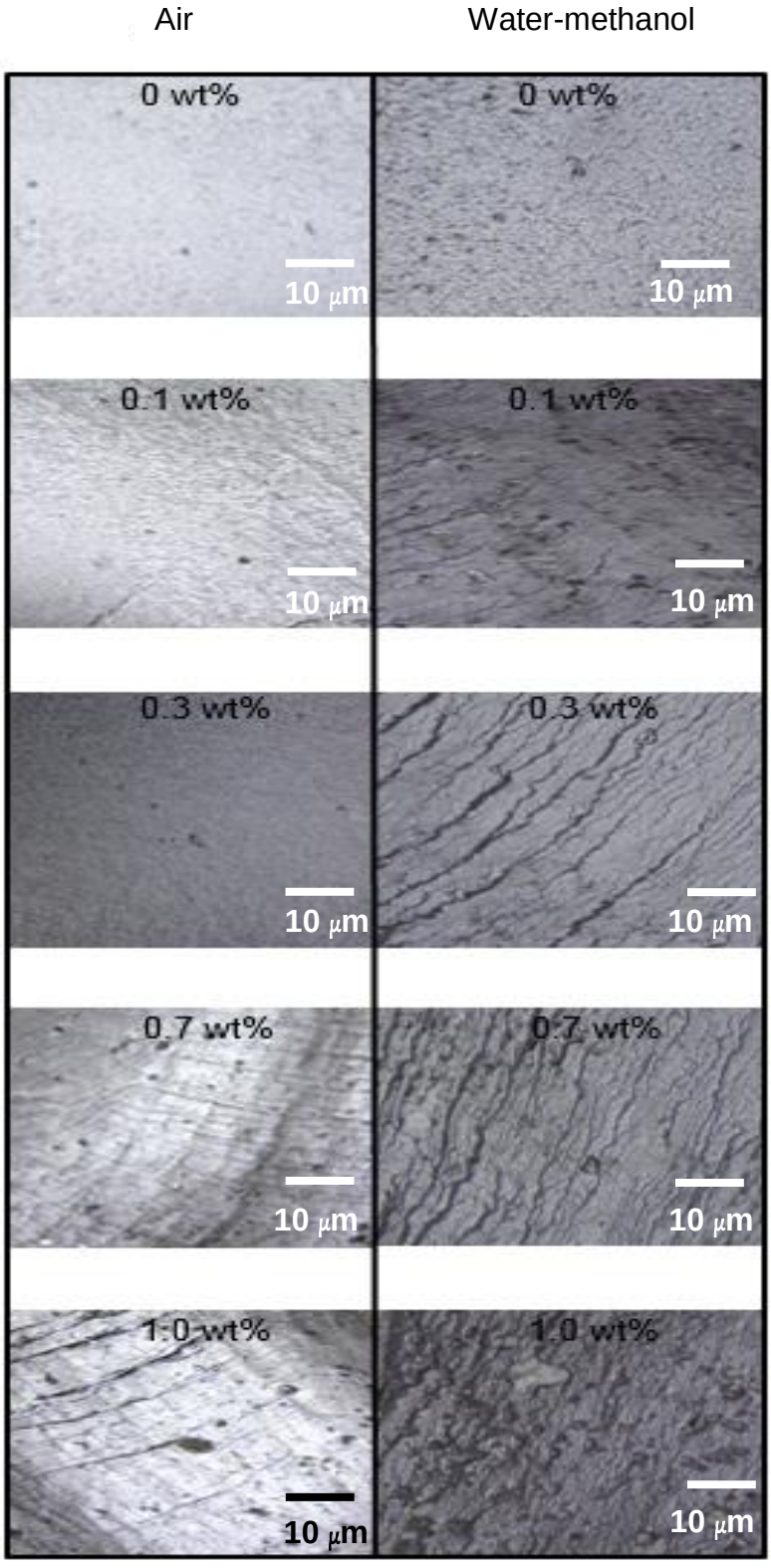

Figure 44. Topographic profiles for dry samples and those exposed to water-methanol

5.2.11. SEM images

The fractured surfaces of specimens were viewed by SEM to study the influence of HNTs on the possible fracture modes in the nanocomposites. The monolithic polyester in dry conditions is shown in Figure 45 (a). It can be observed that the image shows a surface with river marking as a result of very quick and straight crack propagation [126, 297]. The effect of methanol immersion can be seen in Figure 45 (b). The non-reinforced matrix is vulnerable to liquid diffusion. The plasticization of monolithic polyester occurs because of liquid media absorption which causes deteriorations in mechanical properties. The liquid absorption was severe in monolithic polyester. Straighter crack lines can be clearly seen for monolithic polyester as shown in Figure 45 (a). Figure 45 (b) shows the increased surface roughness of the 0.3 wt% sample. After exposure to water-methanol, the surface showed decreased in surface roughness as evidently shown in Figure 45 (d). Figure 45 (e) shows the fractured surface of the 1.0 wt% reinforcement sample. The increase in surface roughness and fluted topography can be associated with the cracks deflection by the HNTs. Figure 45 (f) shows micro-cracks in the 1.0 wt% HNTs-polyester sample. The filler acted as a barrier to the liquid. A round-ended surface can be seen which corresponds to higher resistance to crack propagation due to the presence of HNTs [297]. The swelling and plasticization effect of polymer matrix, however, were observed at all reinforcement fractions. On the other hand, the short round-ended shape can also be seen indicating that the polyester chains had been affected by exposure to liquid media. The presence of HNTs also evidently increases the surface roughness, indicating a crack deflection mechanism which increases energy absorbed during fracture [126]. Figure 46 illustrates how water-methanol molecules flow along the matrix interfaces and act as

a plasticizer, thereby weakening the mechanical integrity of the nanocomposites. Water-methanol also caused swelling and filler-matrix de-bonding.

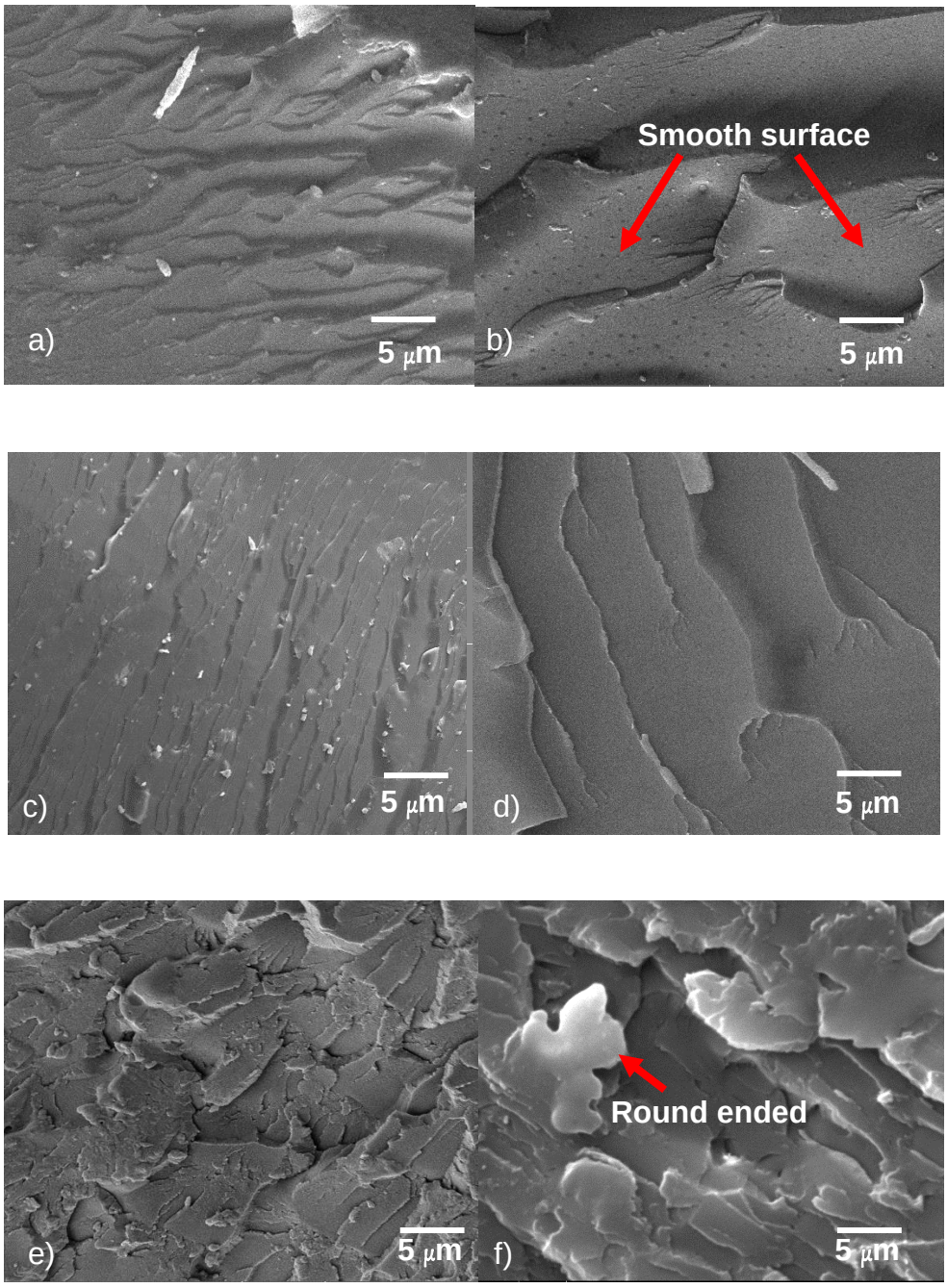

Figure 45. SEM images of fractured specimens: (a) Monolithic polyester in air (b) monolithic polyester after water-methanol exposure, (c) 0.3 wt% HNTs-polyester in air, (d) 0.3 wt% HNTs-polyester after water-methanol exposure (e) 1wt% HNTs-polyester in air (f) 1 wt% HNTs-polyester after water-methanol exposure

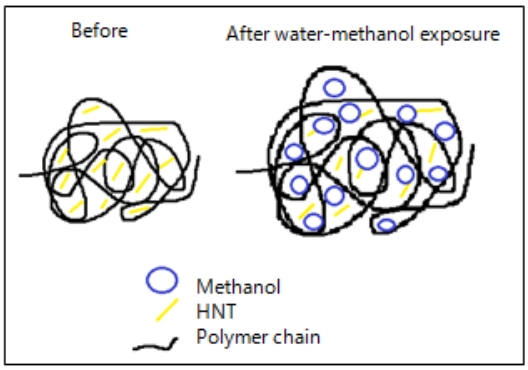

Figure 46. Schematic image of plasticized HNTs-polyester nanocomposites before and after water-methanol exposure

5.3. Conclusion

Nanocomposites of five different weight fractions of HNTs reinforcement were successfully produced and the deterioration in their mechanical properties was studied after exposure for 24 h in a water-methanol system by clamping test specimens across steel templates. HNTs have the ability to increase the storage modulus and glass transition temperature (T_g) by increasing the stiffness of nanocomposites and restricting the polymer chains. In this research, the addition of HNTs strengthens the polyester matrix up to a concentration of 1.0 wt% as shown in Table 8. HNTs also improved the mechanical properties of produced nanocomposites compared to monolithic polyester exposed to water-methanol. The plasticization effect caused by water-methanol contributed to the detrimental effect on mechanical properties such as T_g, modulus and strength. After immersion in water-methanol, the maximum microhardness, tensile, flexural and impact toughness values were observed at 1 wt% of HNTs. The microhardness increased from 203 HV to 294 HV (45% increase). The Young's modulus increased from 0.49 GPa to 0.83 GPa (by 70%) and the tensile strength increased from 23 MPa to 27 MPa (by 17.4%). Likewise, the flexural strength also recorded an increase of 113% in water-methanol system. The impact toughness

increased from 0.19 kJ/m^2 to 0.54 kJ/m^2 in the water-methanol system (184% increase). Surprisingly, the fracture toughness of all types of nanocomposites was found to increase after exposing to water-methanol due to the plasticization effect. The maximum value of K_{1C} after exposure to water-methanol was observed in the case of monolithic polyester with an average of 0.56 MPa.m$^{1/2}$. However, in the case of 1 wt% reinforcement, the K_{1C} mean value dropped to 0.29 MPa.m$^{1/2}$. This can be attributed to the liquid barrier property from the HNTs reinforcement, where the plasticization effect was reduced with increasing nano-filler content. SEM images of the fractured surfaces of tensile specimens revealed that the methanol increased the ductility of the polyester matrix and reduced the mechanical properties of the nanocomposites. However, the HNTs have the ability to improve the mechanical properties of polyester even when exposed to water-methanol.

6. Effect of seawater on the mechanical properties of halloysite nanotubes-polyester nanocomposites

6.1. Background

Sea water is a very complicated environment for polymer composites. It contains many microorganisms, animals, salt, sunlight, and fluctuating of water and rain. Their presence in sea water play an important role in the deterioration of polymer composites. The word “deterioration” is commonly used by engineers to describe processes that lead to a loss of inherent properties. Chemists focus more on chemical reactions which cause the breakdown of polymers, and the potential risks related with chemicals causing their deterioration [409].

All kinds of micro and macro-organisms can be linked with the deterioration of polymers. According to Lobelle and Cunliffe, biofilm formation leading to biofouling, develops via four distinct forms [410], the adsorption of dissolved organic molecules, attachment of bacterial cells, attachment of unicellular eukaryotes and finally the attachment of larvae and spores [410].

Muthukumar *et al.* pointed out that all surfaces in an aquatic environment become fouled due to the attachment of marine flora and fauna [411]. In the marine environment, there is a complex community of microorganisms and macro-foulants, including bio-macro molecules responsible for the occurrence of this process to occur. The first step always begins with the formation of a biofilm which is made up of carbohydrate, proteins, exopolysachrides and microorganisms, and as a result the material experiences physical, chemical and biological changes [411].

Attached cells produce extracellular polymers to form structured and complex matrixes [412]. In contrast, bacterial attachment is a highly controlled and regulated process. Microbial biofilms can subsequently trigger the attachment of specific organisms which increases the degree of biofouling such as barnacles and algae [413].

According to Dulik *et al.*, the first step of the deterioration of polyethylene exposed to marine environments is oxidation [414]. Photooxidation increases the amount of low molecular weight material by breaking bonds and increasing the surface area. The second step is when microorganisms may utilize the abiotic deterioration products and the low molecular weight of polymers [414].

To date, no studies have discussed the effect of seawater environments on the mechanical properties of HNTs-polyester nanocomposites. Understanding the mechanisms that influence the mechanical properties and deterioration behaviour of polyester composites exposed to marine environments is essential due to the application demand lifetime of 15 to 50 years [14]. The integrity of HNTs-polyesters over time is still unknown.

Thermosetting polymers are used in various industrial applications. In marine environments, complex conditions such as high salinity, high pressure, high humidity and alkaline corrosion accelerate the deterioration of polymers and greatly reduce the reliability of the material [362]. Bottles, vessels and pipes are common applications where contact with seawater is unavoidable and can lead to the loss of inherent mechanical properties [41].

Durability data for seawater immersion over prolonged periods of immersion have to be obtained in order to determine precisely the durability of HNTs composite material when exposed to seawater. In this study, the seawater was collected from South Shield beach. The location is shown in Figure 47, and the beach is located in the North East of the UK.

Figure 47. Location of the collected seawater, South Shields Beach United Kingdom.

6.2. Results

6.2.1. Liquid absorption test

The seawater absorption results are shown in Figure 48. The seawater uptake for monolithic polyester and its composites was evaluated for 168 h (7 days) at room temperature. Monolithic polyester recorded 0.98% of seawater absorption, the lowest level compared to the composite systems. In the case of 0.1 wt% reinforcement the seawater absorption was 0.07% higher compared to monolithic polyester after 168 h of immersion. At 1 wt% reinforcement, the seawater absorption was 0.6% more than

monolithic polyester. Higher HNTs content contributes to more seawater diffusion via the swelling of the matrix and nanoparticles. In our study, seawater absorption was found to increase as HNTs increased. Seawater molecules may enter through the polymer chain and microvoids. A study by Dhakal *et al.* has also revealed a similar trend of absorption in polyester nanocomposites [60]. The increased number of spaces between HNTs particles creates a higher surface area to composites which water molecules can adhere. Most likely due to its high surface area, the HNTs absorbed more seawater than unfilled polyester.

On the other hand, some authors have suggested that the water absorption of clay-polymers matrix nanocomposites is mainly influenced by two factors. The first opinion is that the clay body is water-rich and thus absorbes more liquid than nearly all the polymers used as matrix, which causes to the increase of seawater content as a function of clay content [22].

The second opinion states that clay layers dispersed at the nano-scale are able to decrease the mean free path of water molecules passing through the nanocomposite network compared to the monolithic matrix, and as a result water absorption is reduced [33-34]. Higher micro-void content at higher halloysite content in composites possibly facilitates higher absorption and creates poor interfacial bonding [415]. Seawater molecules capable of entering into the network of polyester matrix speed up the cracking that leads to poorer mechanical properties.

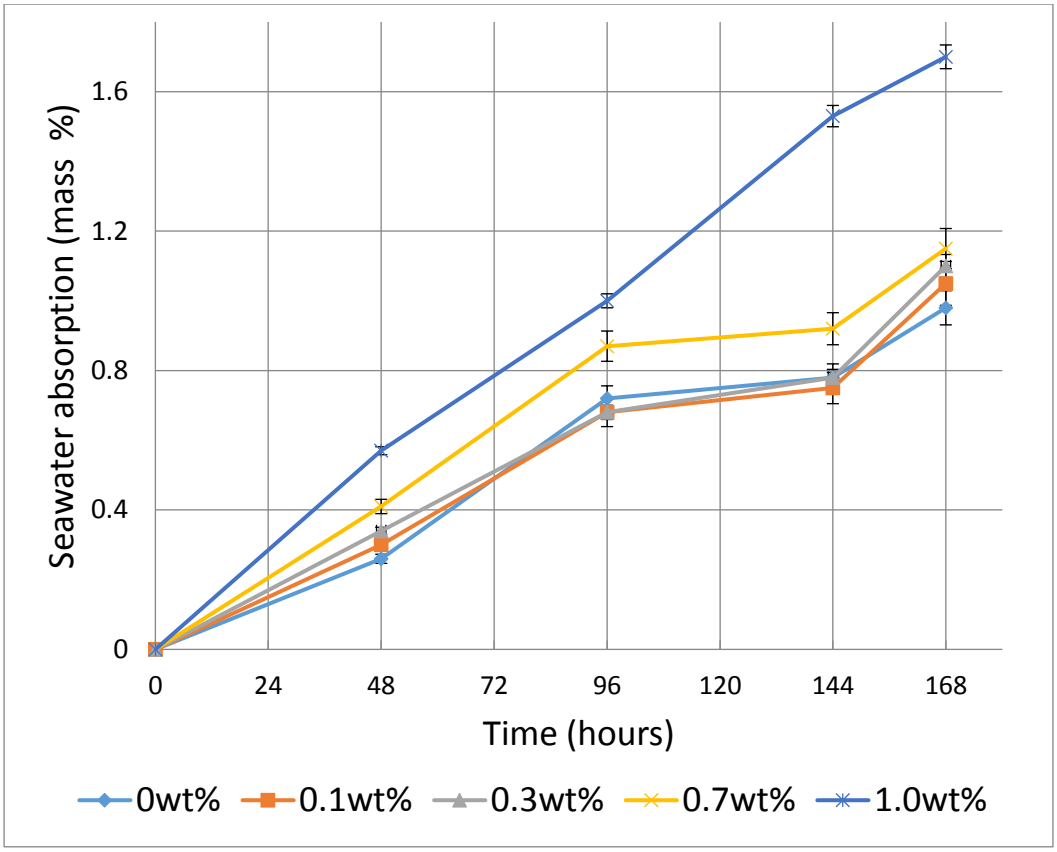

Figure 48. Seawater absorption behaviour of HNTs-polyester nanocomposites

6.2.2. Dynamic mechanical analysis

The DMA results are shown in Figure 49, Figure 50 and Figure 51. The changes in T_g depend on the percentage of filler incorporated. In dry conditions, the HNTs remarkably increased the values of the T_g. In case of monolithic polyester, the mean value of T_g was 80^{o}C. The T_g values were found to steadily increase as HNTs content increased. For instance, in the case of 0.7 wt%, an increase of 4.4 ^{o}C in T_g was recorded. However, in the case of 1 wt% reinforcement the T_g value was slightly lower than the nanocomposites of 0.7 wt% reinforcement with a 3 ^{o}C increase compared to monolithic polyester. This phenomenon could be due to the agglomeration of HNTs particles, which tend to form clay clusters or platelets as also reported by Liu *et al.* [132]. In wet conditions, it was observed that T_g values dropped considerably in

comparison to dry conditions. The seawater undoubtedly altered the structural integrity of the nanocomposites. Samples immersed in seawater were found to swell and became slightly softer compared to samples tested in dry conditions. After immersion in seawater, monolithic polyester recorded the highest T_g value at 77ºC. The minimum T_g was observed in the case of 1 wt% (74 ºC) HNTs reinforcement. The decrease in T_g with further HNTs addition, was likely to have occurred due to the plasticization effect of the matrix caused by the organic modifier of the HNTs [416]. Apart from that, plasticization may also cause by the slippage of HNTs platelets in the clustered HNTs [417]. The values of storage modulus and loss modulus of the polyester and its nanocomposites in dry conditions are shown in Figure 50 (a) and Figure 51 (a). The storage and loss moduli data were taken from the highest peak of tan δ. The storage moduli were higher at initial temperature (30 ºC) and then decreased when approaching T_g. It can be seen that the increases in stiffness and restriction in the movement of polymer chains by HNTs caused marked improvements in storage modulus.

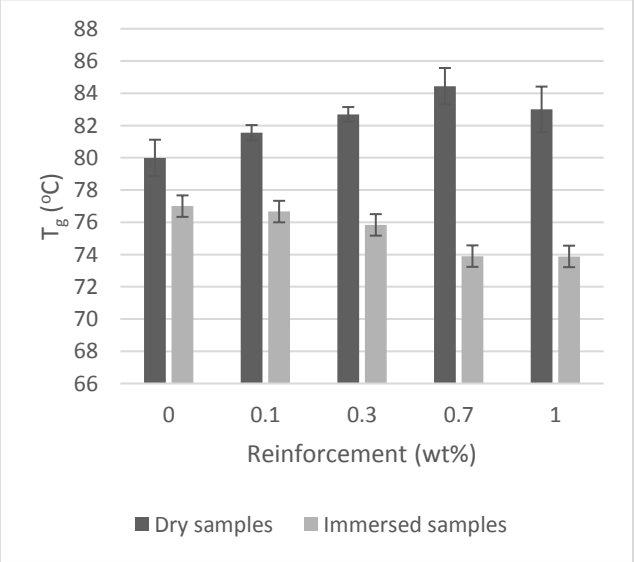

Figure 49. T_g of nanocomposites for dry and immersed samples

The lowest increase in storage modulus (162%) was recorded in the case of 0.1 wt% reinforcement. The maximum increase of 678% was observed in the case of 0.7 wt%. After seawater exposure, a different trend was observed. The seawater environment, reduced the stiffness of the samples especially the nanocomposites systems. About 27% storage modulus decreases were observed in the case of 0.7 wt%. The highest decrease of storage modulus was 43% in the case of 1 wt% reinforcement.

Based on the dynamic mechanical analysis, it is evident that monolithic polyester shows better resistance towards the seawater environment. The values of loss modulus of the polyester and nanocomposites are shown in Figure 51 (b). The curves for all nanocomposite systems were found to shift slightly to the left compared to samples tested in dry conditions. Apart from that, it can be seen from Figure 51 (b) that the loss modulus peak values decreased when the samples were immersed in seawater. After seawater immersion, monolithic polyester was found to have the highest loss modulus curve followed by samples with 0.1 wt%, 0.3 wt%, 0.7 wt% and 1 wt% reinforcement. The lowest loss modulus was from 555 MPa to 295 MPa (for 1 wt% reinforcement). The samples exposed to seawater for longer periods are softer than the dry samples and samples having absorbed water tend to be less stiff than the dry samples.

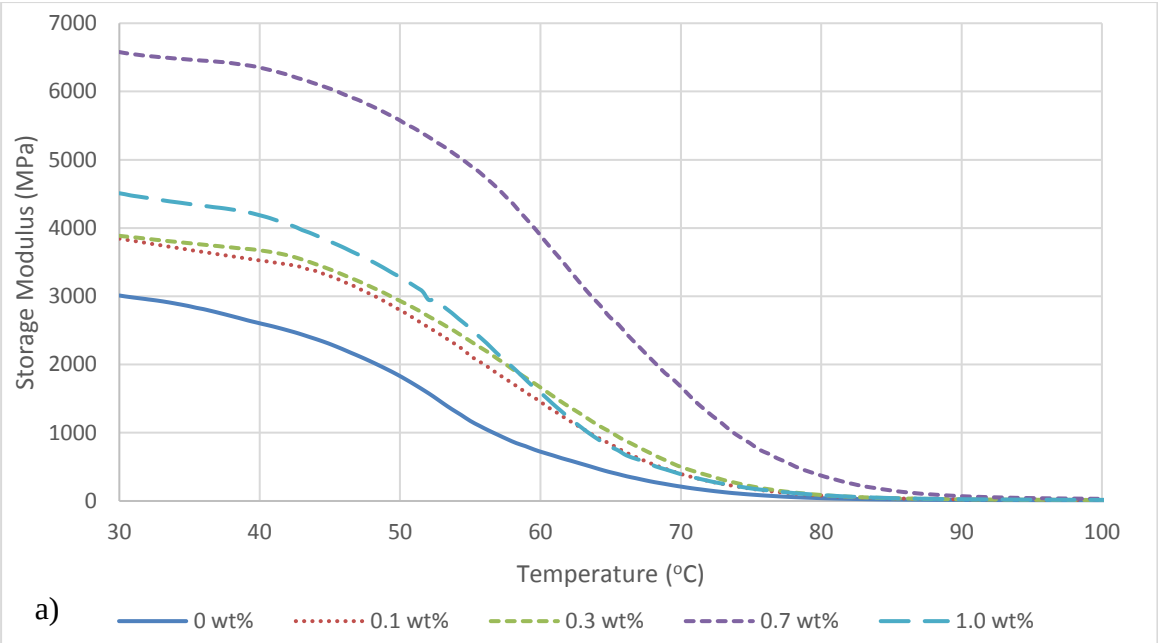

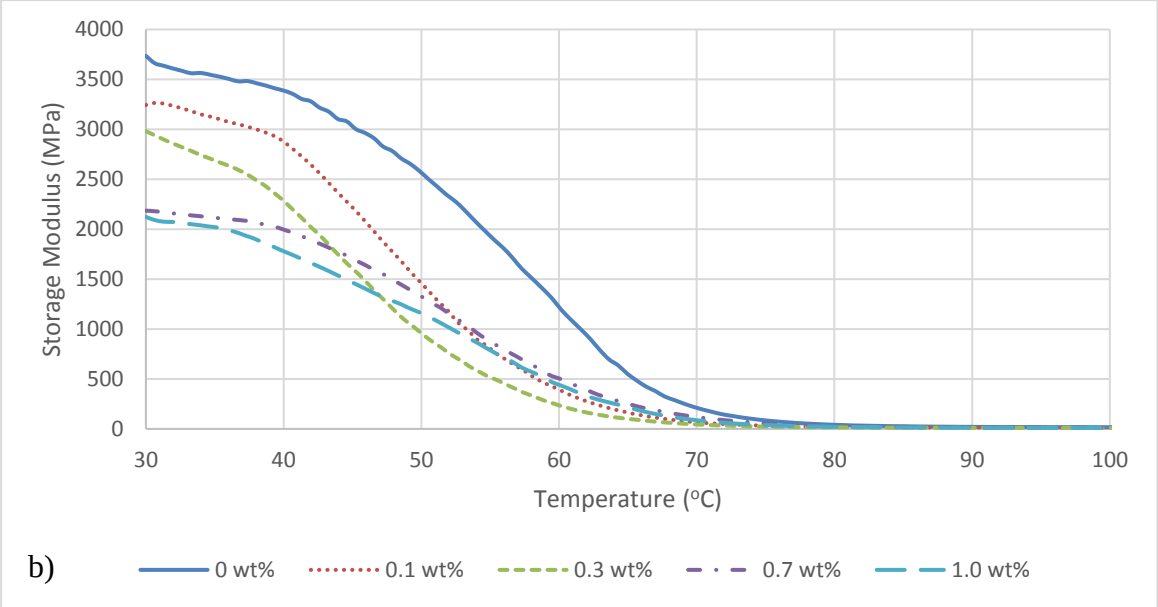

Figure 50. Storage modulus of dry (a) and immersed samples (b)

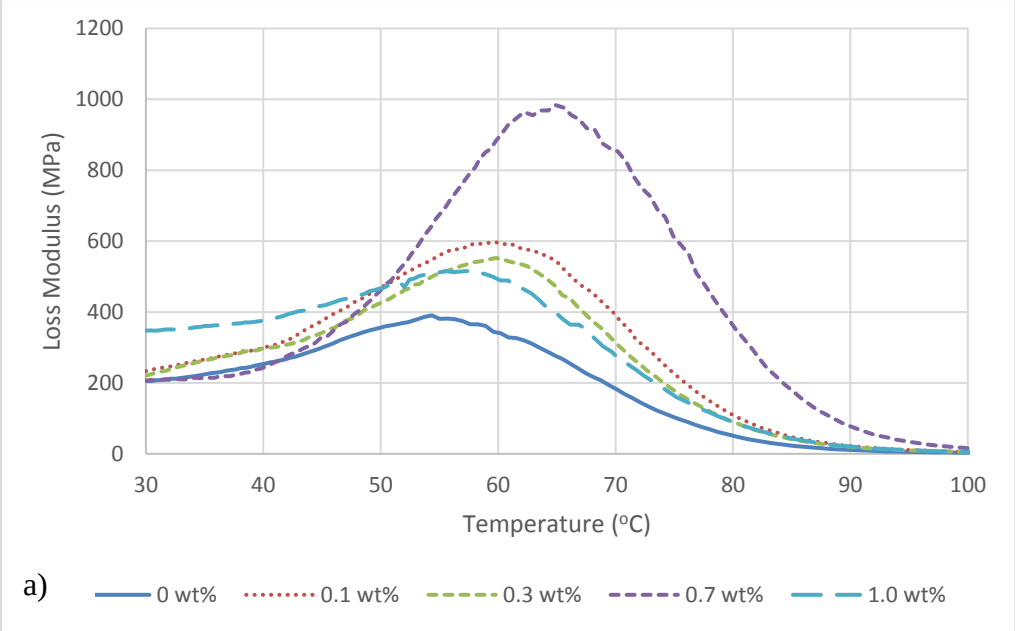

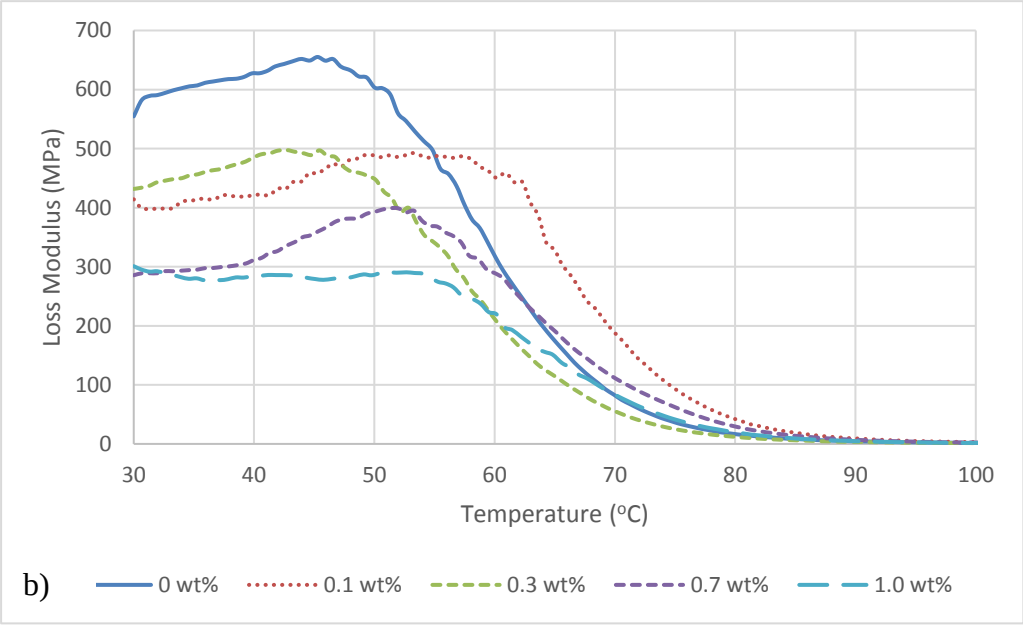

Figure 51. Loss modulus of nanocomposites in air (a) and after seawater exposure (b)

6.2.3. Optical transmittance

The optical light transmittance results are presented in Figure 52. As discussed in the previous chapter, the incorporation of halloysite nanotubes reduced optical transmittance. After seawater immersion, light transmittance values were further reduced due to seawater absorption which penetrated into the polymer matrix. After seawater immersion, the highest light transmittance value was observed in the case of monolithic polyester at 73%. The lowest light transmittance was observed for 1 wt% reinforcement at 60%. The presence of seawater on the surface of the nanocomposites can be linked to this low value.

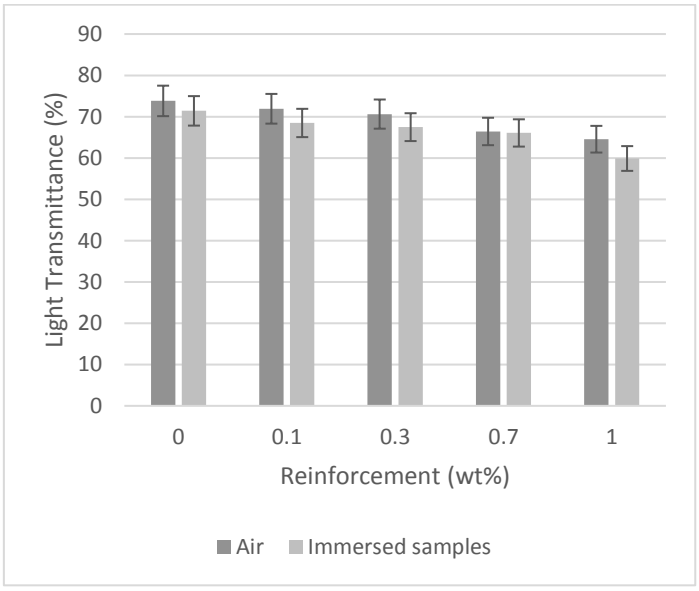

Figure 52. Light transmittance of nanocomposites before and after seawater exposure.

6.2.4. Densification

The percentages densification of HNTs-polyester nanocomposites is presented in Figure 53 (a). The large standard deviations in the graph of the nanocomposites can be attributed to the porosity in the samples produced. Trapped air bubbles in the resin remains as micropores after curing [59]. Another possibility is that, the fast curing of polyester resin when mixed with curing agent, prevents the volatiles escaping during the curing process.

6.2.5. Vickers microhardness

Surface hardness is normally investigated as one of the significant aspects that is related to the abrasion and wear resistance of nanocomposite materials [39-40]. The Vickers microhardness graph is shown in Figure 53 (b) for samples tested in air and after exposure to seawater. The incorporation of HNTs significantly improved the microhardness property, particularly in the case of 0.7 wt% reinforcement (a 44% increase). The lowest improvement in microhardness was observed in the case of 0.1 wt% at 11.4% increase. After immersion in seawater monolithic polyester showed the highest microhardness while the samples at 1 wt% reinforcement recorded the lowest values (61% reduction).

6.2.6. Tensile properties

The values of Young’s modulus (tensile modulus) of the monolithic polyester and its composites are shown in Figure 53 (c). Monolithic polyester recorded the lowest Young's ’modulus at 0.7 GPa. The lowest increase in Young’s modulus was observed in the case of 0.1 wt% with 5.4% improvement. The HNTs also showed the highest increase of 35% in the case of 0.7 wt% reinforcement. A significant reduction in

Young's modulus can be seen after immersion in seawater. At 1 wt% HNTs reinforcement, the Young's modulus dropped from 0.6 GPa to 0.4 GPa (a 33.3% decrease).

The variations in tensile strength are presented in Figure 53 (d). The maximum increase in tensile strength was from 29.5 MPa to 44.2 MPa (50% increase) in the case of 0.7 wt% HNTs. The HNTs also showed a minimum increase up to 15.3% in the case of 0.1 wt% reinforcement. After exposure to seawater, the tensile strength showed a significant decrease. The maximum decrease of tensile strength was observed in the case of 1.0 wt% reinforcement (22% decrease) compared to monolithic polyester. The HNTs composites likewise showed minimum decrease up to 2.4% in the case of 0.1 wt% reinforcement.

The variations in maximum tensile strain (%) are shown in Figure 53 (e). The value of the tensile strain was obtained from the % value of strain corresponding to the maximum tensile strength. In dry conditions, reinforcement of HNTs reduced the tensile strain. This is due to the improved stiffness of the nanocomposite materials. In the case of 0.7 wt% reinforcement, the maximum tensile strain was 4.5%. After immersion in seawater, the values of maximum tensile strain increased for all nanocomposites because of the plasticization effect. A value of about 5.2% of tensile strain value was observed for monolithic polyester. In contrast, at 1 wt% reinforcement, 9% of tensile strain was observed. The increase in tensile strain is due to the softening of the polymer matrix, which caused the time to fracture to increase. Reductions in the tensile properties (maximum tensile strength, Young's modulus and maximum tensile strain) may be associated with the plasticization of the resin matrix caused by seawater, which seems to reduce the yield stress and growth in the size of the plastic

zone ahead of the cracks [41–43]. Apart from that, the weakening of adhesion between the HNTs and matrix is also a possible reason for the decreased in tensile properties [18].

6.2.7. Flexural properties

As for the flexural modulus Figure 53 (g), the nanocomposites samples tested in air showed excellent improvements. The maximum increase in flexural modulus (61%) was achieved at 0.7 wt% reinforcement from 0.77 GPa to 1.24 GPa. In wet conditions, the flexural modulus dropped from 0.6 GPa (monolithic polyester) to 0.34 GPa (1 wt% HNTs). The flexural strength results are shown in Figure 53 (g). The maximum rise in flexural strength was observed from 55.7 MPa to 80 MPa in the case of 0.7 wt% (a 44% increase). About a 2.3% increase was obtained for 0.1 wt% reinforcement. A similar trend was also found in samples exposed to seawater, where the flexural strength dropped significantly. In the case of 1 wt%, the flexural strength was reduced by 22%. Monolithic polyester in contrast, showed the maximum flexural strength value of 51.4 MPa. The variation in flexural strain is shown in Figure 53 (h). The minimum flexural strain for unexposed samples was 8%, in the case of 0.7 wt% HNTs reinforcement. After immersion in seawater, all samples showed increased flexural strain. The lowest increase of 1% was observed for monolithic polyester, and the highest increase in flexural strain was observed in the case of 1 wt% reinforcement, where it improved from 8% to 14%.

The variations in energy absorbed are presented in Figure 53 (i). The energy absorbed is calculated by the area under the force-displacement curve. HNTs reinforcement increased the energy absorbed by 60% in the case of 0.7 wt%

reinforcement however, the amount of energy absorbed decreased at 1 wt% reinforcement, whereas compared to monolithic polyester, the energy absorbed was far better, increasing by 8%. This is an indication that agglomerates in the 1wt% samples act as flaws, reducing the energy absorbed [197]. After seawater immersion, the trend was totally different. Monolithic polyester obtained the highest energy absorbed compared to nanocomposite systems. The lowest energy absorbed was at 1 wt% reinforcement from 2.9 J dropping to 1.72 J (41% decrease).

6.2.8. Impact toughness

The variation in impact toughness results are shown in Figure 53 (j). Samples tested in dry conditions showed markedly values of Charpy impact toughness and the lowest improvement was observed at 0.1 wt% (a 54% increase). Impact toughness increased steadily and reached maximum values at 0.7 wt% reinforcement (80% increase). Exposure to seawater reduced the impact strength of the nanocomposites. Increases in impact toughness can be attributed to the good interfacial adhesion between HNTs and the polyester matrix. Good interfacial bonding between HNTs and polyester requires a higher energy absorbtion capacity, as a result producing higher impact strength. This finding is in line with those of Albdiry *et al*. [273] and Lin *et al.* [275] who reported maximum improvement in impact toughness by 61% and 300%. However, after seawater immersion, the impact strength of the nanocomposites decreased. The impact strength decreased 9% in the case of 0.1 wt% reinforcement while the lowest impact toughness was observed in the case of 1 wt%, with a 32% decrease.

6.2.9. Fracture toughness

The K_{1C} values are presented in Figure 53 (k). It can be observed that the K_{1C} increased linearly with the increasing of HNTs addition from 0.1 wt% to 0.7 wt%. For dry samples, the maximum increase in K_{1C} was obtained in the case of 0.7 wt% from 0.26 to 0.4 MPa.m$^{1/2}$ (a 54% increase). For the nanocomposites immersed in seawater, K_{1C} also increased with increasing HNTs loading due to liquid absorption which caused the plasticization of the polymer matrix. The maximum value of K_{1C} after seawater immersion was obtained in the case of 1 wt% reinforcement from 0.59 MPa.m$^{1/2}$ to 0.79 MPa.m$^{1/2}$ (a 34% increase). The seawater uptake caused the polymer matrix to soften and increase the ductility of the samples, increased and as a result the failure time also increased.

Table 9. Mechanical properties of HNTs-polyester before and after seawater exposure

Sr.	Properties / HNT Wt%	In air					After seawater exposure				
		0	0.1	0.3	0.7	1.0	0	0.1	0.3	0.7	1
1	Microhardness (HV)	234±9.2	264±7	283.3±4.6	337.7±9.2	289 ± 21.5	107.5±12	92.9±9.2	76.9± 4.7	54.4± 4.7	41.7±5
2	Young's modulus (MPa)	0.74±0.02	0.78±0.03	0.88±0.02	1±0.0.4	0.91±0.03	0.6± 0.03	0.58 ±0.035	0.58± 0.0.6	0.54± 0.07	0.4±0.06
3	Tensile strength (MPa)	29.5 ± 4	33.8 ± 3	41.3± 3.4	44.3± 3	40.2± 2.6	25.5± 1.5	24.9±.2	23.4± 1.2	22.6± 2	19.8± 1
4	Tensile strain (%)	10.5±0.8	8.9±0.6	0.8.6±0.5	8.2±0.4	8.0±0.5	12±0.7	12.2±0.8	11.3±0.6	10±0.4	10.7±0.5
5	Flexural modulus (MPa)	0.77±0.1	0.79±0.04	1±0.08	1.2±0.05	1±0.03	0.59±0.08	0.5±0.07	0.43±0.06	0.4±0.073	0.34±0.07
6	Flexural strength (MPa)	55.7±4	57±3.7	60.4±5.2	80±6.1	61±5.4	51.4±3.5	48±3.2	43.5±4	43.3±2.5	40.1±2.5
7	Flexural strain (%)	11±0.5	10±1	9±0.8	8±1	8±0.3	12±0.7	12±0.4	12±0.4	12±0.7	14±0.8
8	Energy absorbed (J)	3.25±0.4	3.6±0.4	4.8±0.51	5.2±0.46	3.5±0.6	2.85±0.2	2.75±0.3	2.6±0.4	1.88±0.2	1.72±0.11
9	Fracture toughness K_{1C} ($MPa.m^{1/2}$)	0.25±0.04	0.27±0.02	0.3±0.03	0.4±0.03	0.29±0.05	0.59±0.03	0.75±0.04	0.79±0.04	0.8±0.04	0.79±0.05
10	Impact toughness (kJ/m^2)	0.78±0.16	1.12±0.16	1.26±0.2	1.36±0.1	0.97±0.11	0.71±0.05	0.69±0.03	0.68±0.02	0.49±0.03	0.48±0.04

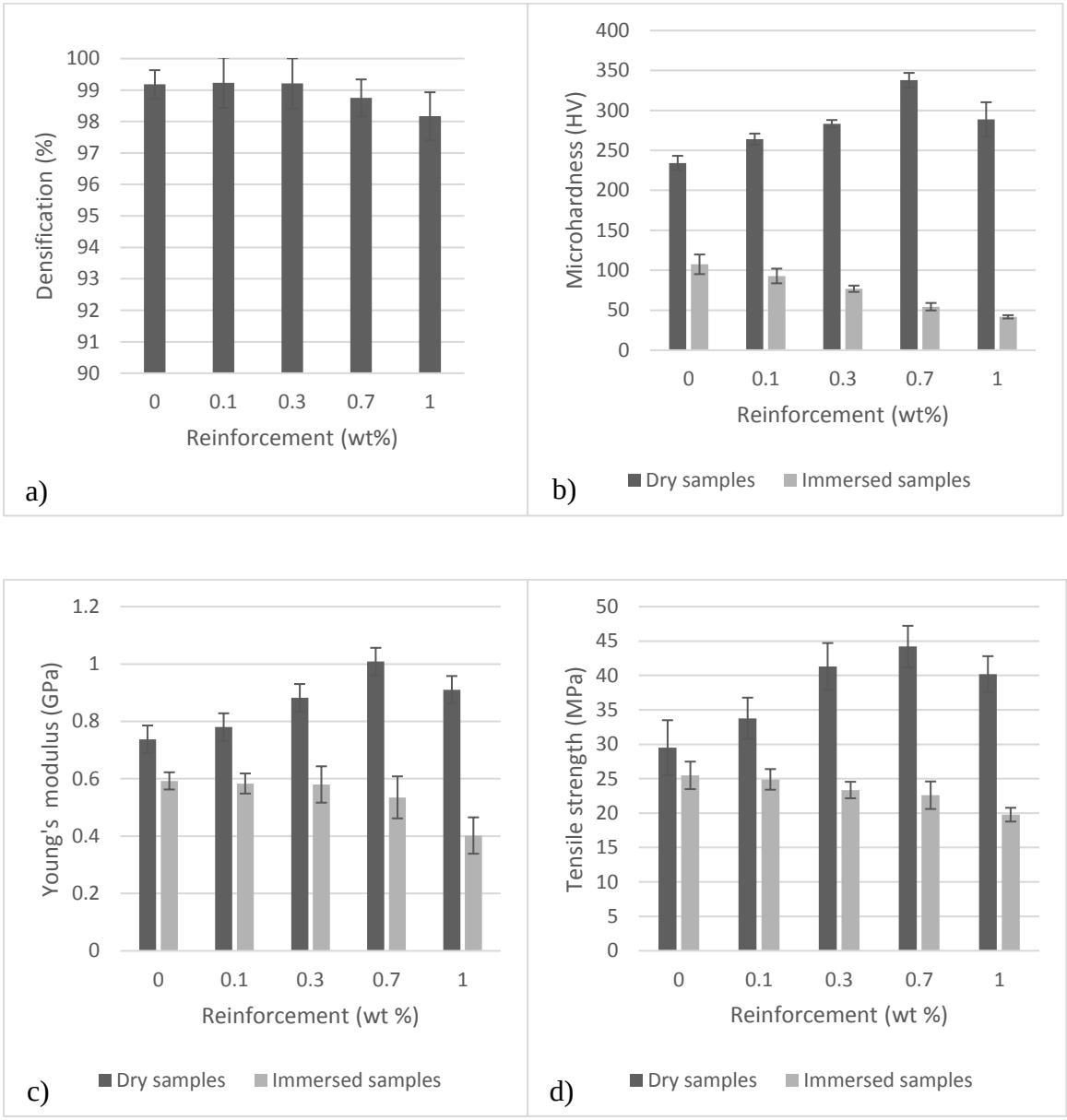

Figure 53. *Cont.*

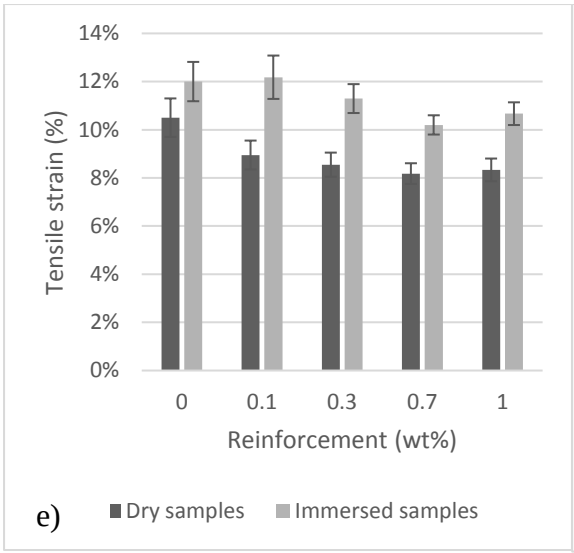

e)

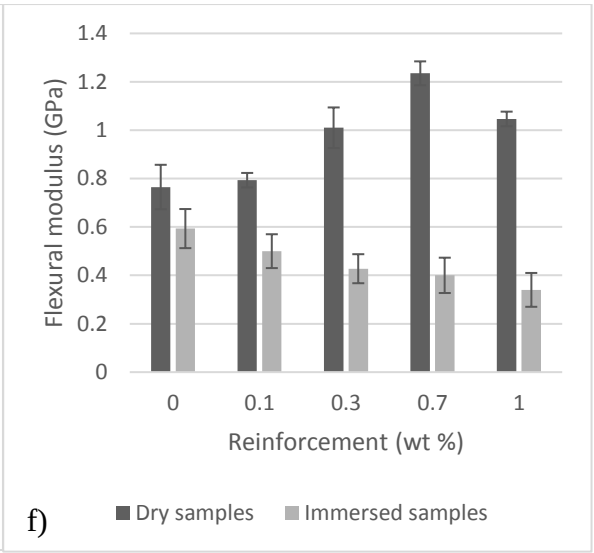

f)

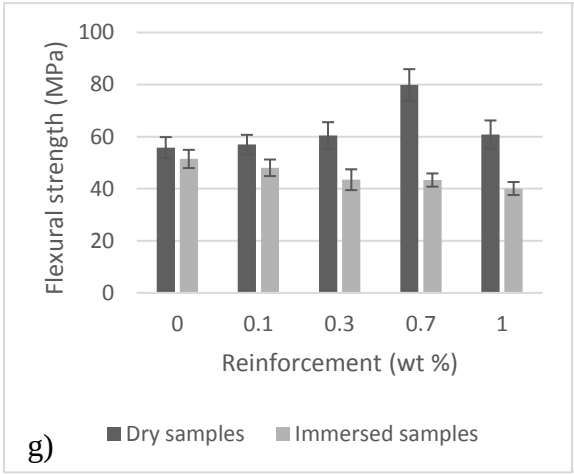

g)

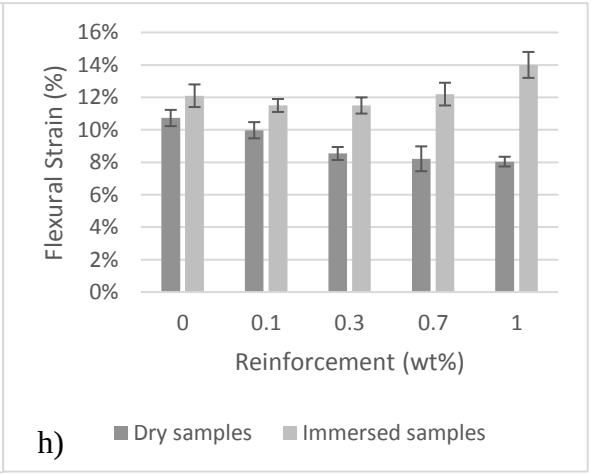

h)

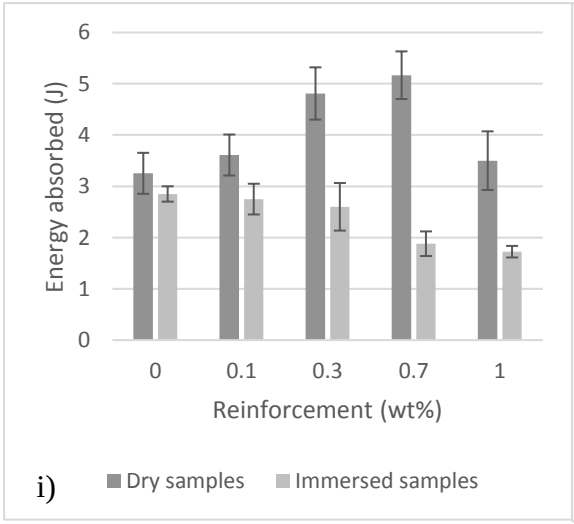

i)

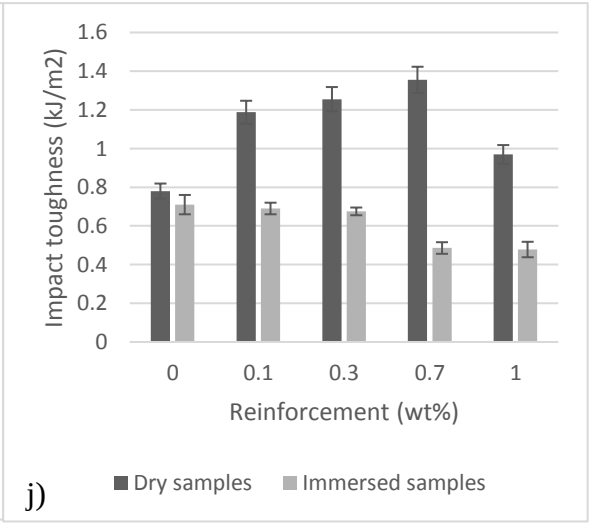

j)

Figure 53. *Cont.*

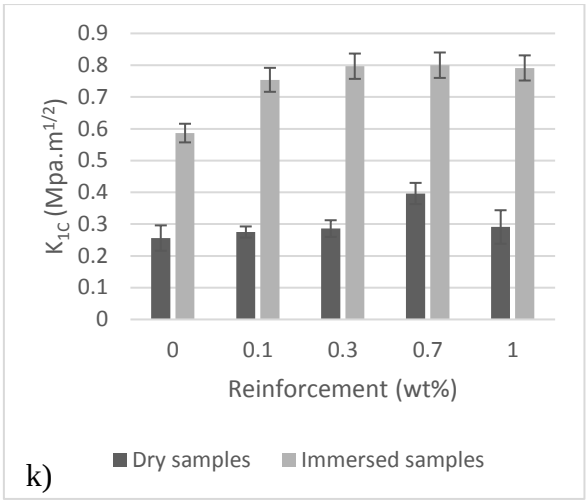

Figure 53. Mechanical properties of HNTs-polyester nanocomposites in dry and wet conditions

6.2.10. Topographical profile

A topographical study was carried out on fractured three-point bend samples. The values of surface roughness (Ra) of monolithic polyester, and 0.1 wt%, 0.3 wt, 0.7wt% and 1wt% HNTs-reinforced polyester is shown in Figure 54. In dry conditions, the Ra (mean) for monolithic polyester was 0.36 µm. Ra reached its maximum value at 1 wt% reinforcement at 0.63 µm (an increase of 75%) as shown in Figure 54 (a). After samples were immersed in seawater, the Ra for monolithic polyester increased from 0.36 µm to 0.49 µm due to the effect of the absorption of seawater. As the amount of absorbed water reaches equilibrium, plasticization and swelling take place in the polyester matrix [420]. Moisture at the interface leads to lower modulus and high-strain-to failure, similar observations were made by other researchers [364, 420, 421].

For samples reinforced with 1wt% HNTs, the Ra value increased from 0.63 µm to 0.8 µm (by 27%). Values of the root mean square of the profile, or Rq are presented in Figure 54 (b). As expected, monolithic polyester recorded the lowest Rq at just 0.44

μm. The maximum value of Rq was observed in the case of 1 wt% reinforcement at 0.79 μm. After immersion in seawater an increase in Rq can be observed for the monolithic samples, where the Rq increased from 0.44 μm to 0.5 μm. As for the 1 wt% reinforcement, the values of Rq increased from 0.79 μm to 1.37 μm. A similar trend can be observed for Rz (peak-to-valley heights) for monolithic polyester and 1wt% HNTs reinforcement. For monolithic polyester Rz mean value was 1.54 μm. In the case of 1 wt% reinforcement, the Rz mean value was 4.7 μm. After immersion in the seawater the mean values for monolithic polyester and 1wt % reinforcement were 2.2 μm and 4.7 μm respectively. Seawater immersion increased the surface roughness of the composites due to a strong plasticization effect. Seawater induced the plasticization of the matrix, and the extension of damaged zones and enhanced the ductility of the material [365]. Images of the topographic profiles of dry and immersed samples in seawater are shown in Figure 55.

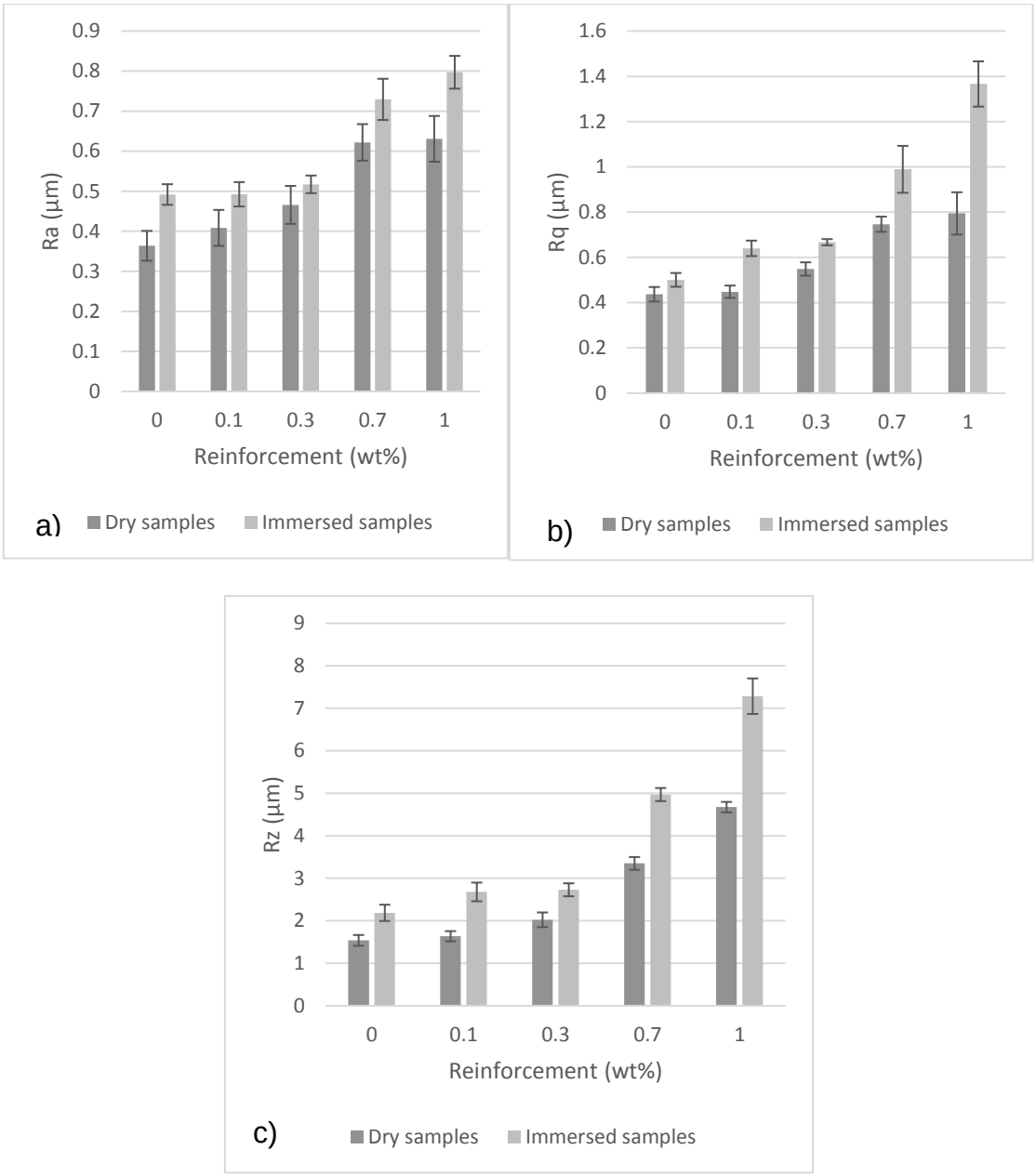

Figure 54. R_a R_q and R_z of nanocomposites in dry and wet conditions.

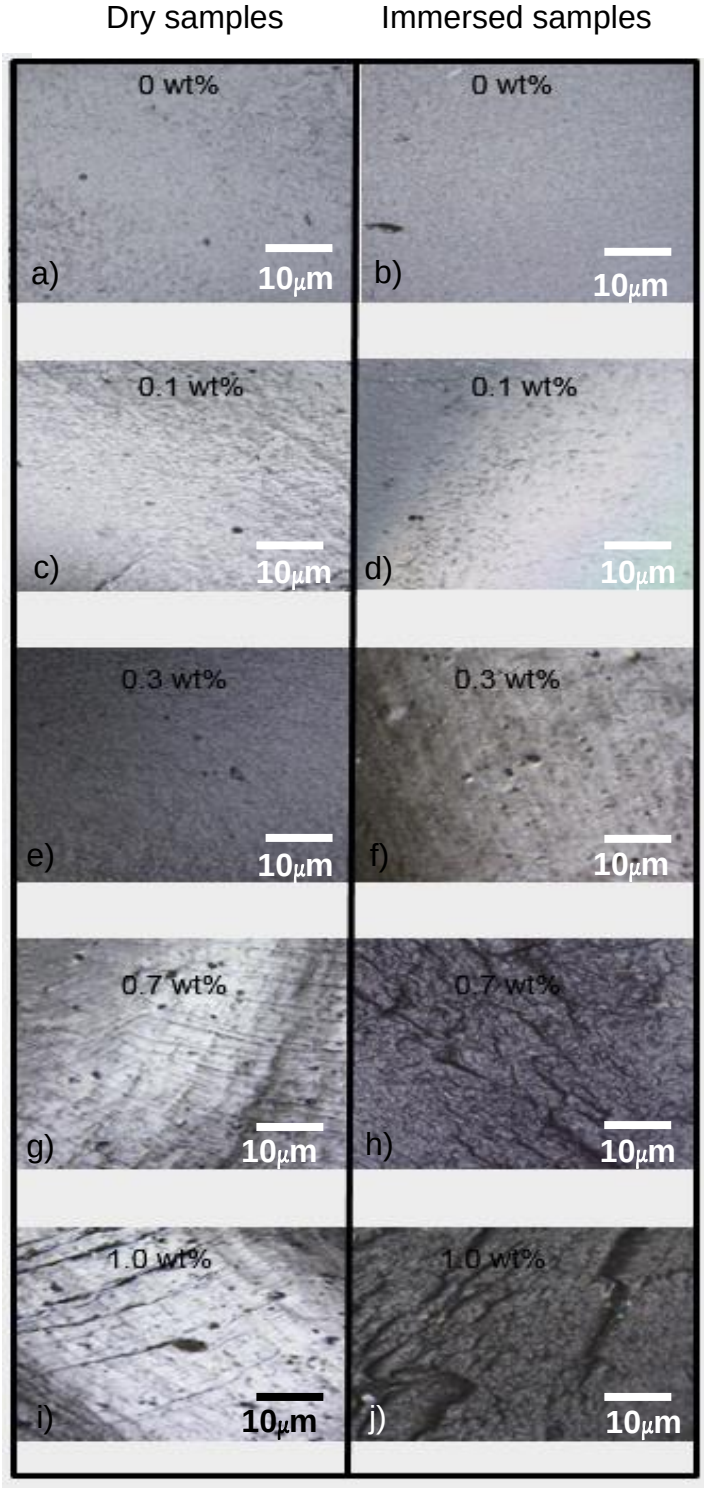

Figure 55. Topographic profiles for dry and immersed samples in seawater: (a) and (b) monolithic polyester, (c) and (d) 0.1 wt% HNTs-polyester (e) and (f) 0.3 wt% HNTs-polyester, (g) and (h) 0.7 wt% HNTs-polyester, (i) and ((j) 1 wt% HNTs-polyester.

6.2.11. SEM Images

Microscopic images show the diversity in the shapes and sizes of bacteria that live on the plastic. The pits in Figure 56, shows that the bacteria are actively breaking off hydrocarbon polymers via water molecules. Figure 57 shows SEM images of the microbial community on plastic marine debris obtained in a recent publication. Figure 58 shows the fractured surface of the monolithic polyester and its nanocomposites after expose to a seawater environment. Filamentous cyanobacteria as shown in Figure 58 (a) and (b) covering most of the fractured surface layers of monolithic polyester. This microorganism, can create a microenvironment where the polyester matrix become chemically unstable [409]. Filamentous cyanobacteria with diameters between 500-550 nm are likely to attack monolithic polyester. As for the nanocomposites reinforced with halloysite, fungi and several marine bacteria such as *Centropyxis* and *Staphylo* were found attached to the polyester matrix. Bacteria are not visible to the naked eye because of their small size between 0.2 to 3 μm. The image presented in Figure 58 is identical to what has been reported in the literature [119]. Detached bacteria create pores size between 3 to 5 μm and allow even faster seawater penetration. The rate of deterioration is believed to increase with this process. Changes in visual effects such as the yellowing of the polyester caused by biofilm formation on the surface of the samples is also observed. The deterioration at the interface is caused by hydrolysis which is caused by longer immersion times and sustained exposure to seawater led to the disintegration of the chemical bonds at the interface resulting in the separation of halloysite and polyester matrix. On the other hand, hydrolysis causes swelling in the matrix which may lead to decrease in mechanical adhesion between the halloysite and polyester matrix. Along with the

plasticization effect, the mechanical properties were weakened as the ductility of the polyester matrix increased. It has been found that seawater absorption causes plasticization and hydrolysis effects [422]. Even with microbe interference, it is also believed that the failure mode involves alteration from a brittle to ductile matrix. Aggregates of HNTs can be seen at higher HNTa reinforcement levels, particularly in the case of 1 wt%. HNTs clusters in greater size than 10 μm were found. This indicates a poor dispersing of HNTs particles, and also proves that at high concentration the movement of clay is restricted.

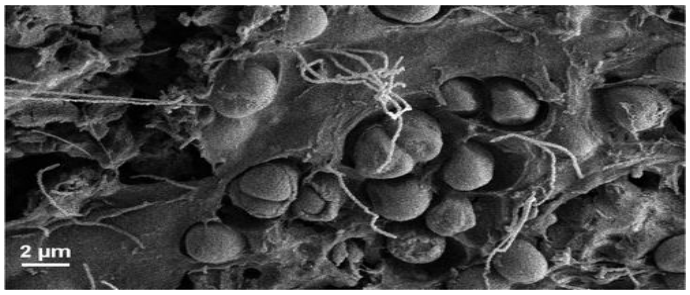

Figure 56. SEM image of polymer surface after seawater exposure [423]

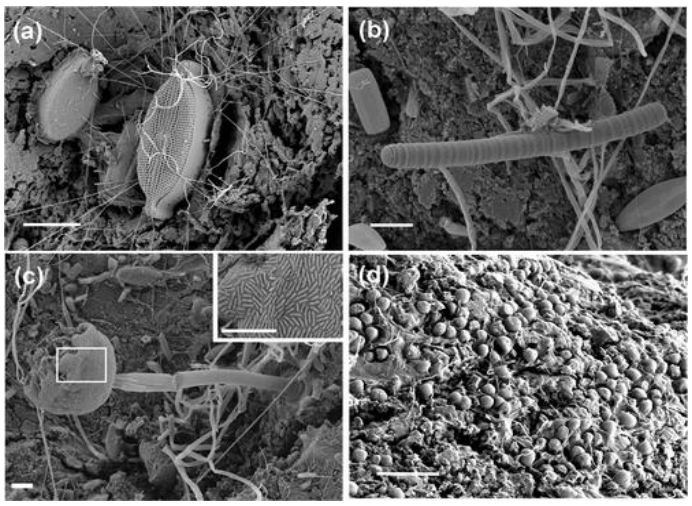

Figure 57. SEM images of the microbial community on plastic marine debris: (a) diatoms and bacteria; (b) *filamentous cyanobacteria*; (c) a ciliate in foreground covered with *ectosymbiotic* bacteria and *filamentous* cells on sample; (d) microbial cells pitting the surface of sample. Scale bars are 10 μm [423].

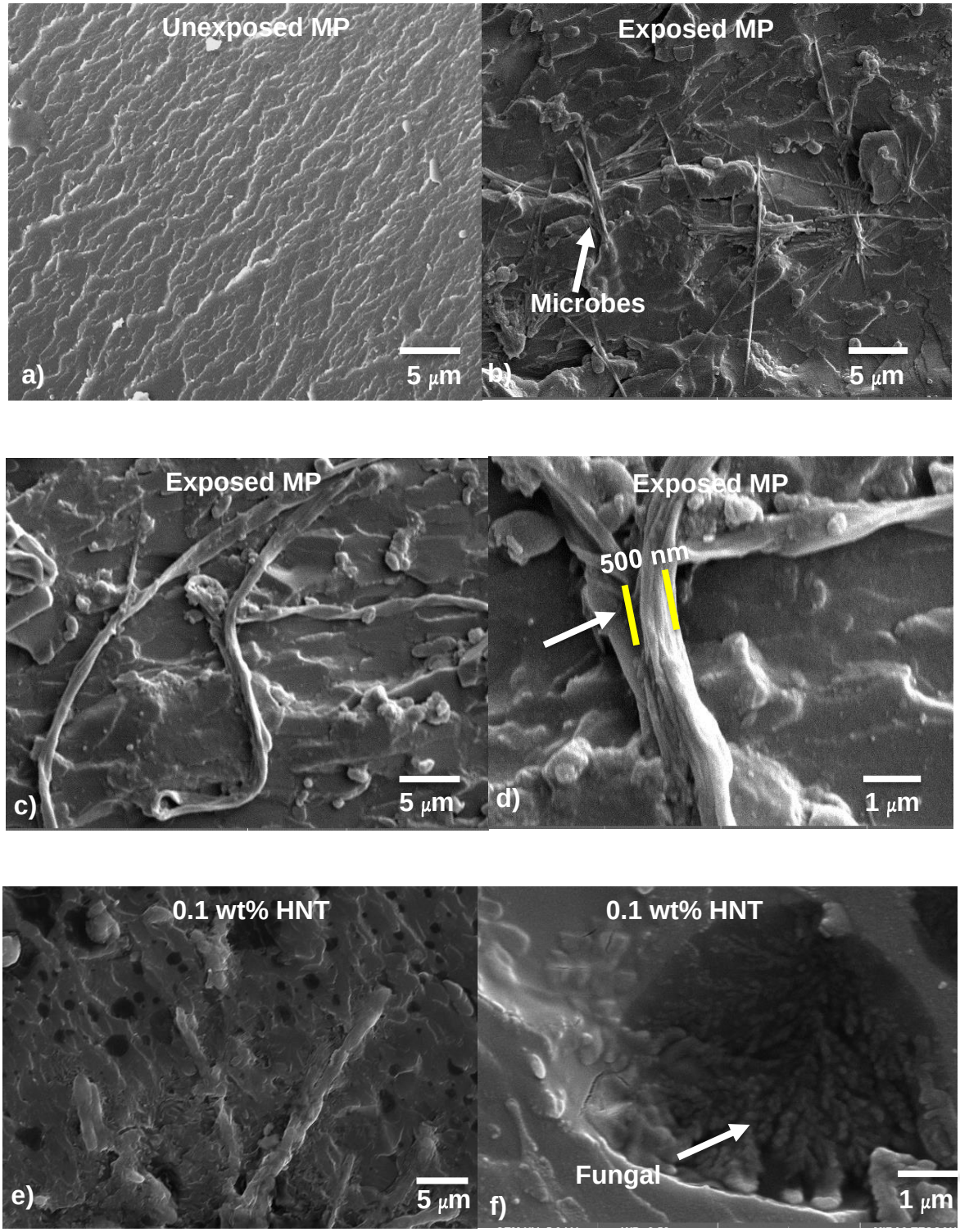

Figure 58. *Cont.*

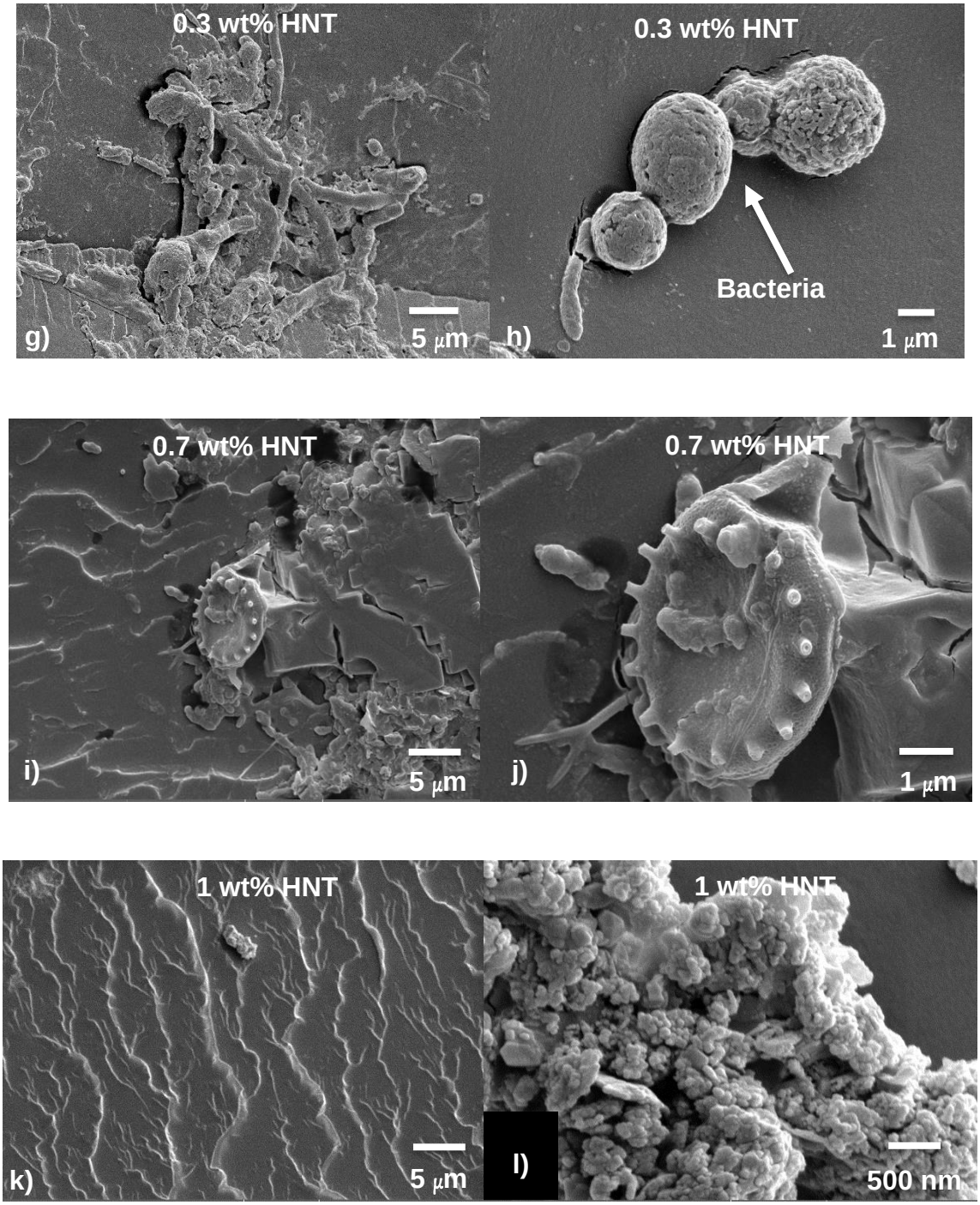

Figure 58. SEM images showing the details of fracture surfaces of polyester and its nanocomposites; (a) monolithic polyester in air (b) monolithic polyester exposed to seawater with *filamentous cyanobacteria*, (c) *filamentous cyanobacteria* in high magnification, (d) filamentous cyanobacteria diameter (e) 0.1 wt% of HNTs-polyester after seawater exposure, (f) presence of fungal in 0.1 wt% HNTs-polyester, (g) microbes at 0.3 wt% HNTs-polyester, (h) marine bacteria in 0.3 wt% HNTs-polyester, (i) 0.7 wt% HNTs-polyester, (j) *Centropyxis*, (k) 1.0 wt% HNTs-polyester, (l) *Staphylo* in 1 wt% HNTs-polyester (in cluster)

The visual effect of the HNTs enrichment of polyester was also observed. Discolouration effects and biofilm layers are clearly visible on the surface of exposed nanocomposite samples, as shown in Figure 59 (b). Biofilm formation on the surface is the initial stage of MIC (microbially influenced corrosion) where it tends to create discolouration of the surface, leading to a localised type of polymer degradation [424].

This could further make the inside of the composites vulnerable to more deterioration which could ultimately lead to embrittlement and disintegration [409]. According to Helbling *et al.*,[425] and Ipekoglu *et al.*,[426]), abiotic (mechanical, light, thermal or chemical) parameters contribute to the weakening of the polymeric structure. In some cases, these abiotic parameters are usefully seen as as a synergistic factor in initiating the biodegradation process [427]. The development of microbes growing on the surface and inside a polymer is the main contribution to physical and chemical deterioration. The environmental conditions, structure and type of polymer influence biofilms formation [428]. It seems that in this study, microbial biofilms developed rapidly on the nanocomposites and affected their mechanical properties. The microorganisms in the seawater also stick to surfaces of nanocomposites and cause them to adhere together.

Microbial biofilms exacerbate serious physical and chemical deterioration. The bacteria discharged after the formation of the microbial layer or film strengthen the adhesion of the biofilm and the nanocomposite surface. The bacteria enter the voids, growing and increasing the void size and then attacking cracks that weakened the physical properties of the plastics (Bonhomme *et al.*, [429].

In addition, the diverse microbial communities which develope on the nanocomposites and the development of the biofilm may release acid compounds including nitrous acid such as *Nitrosomonas*, nitric acid such as *Nitrobacter* or sulphuric acid as produced by *Chemolithotrophic* bacteria [423]. The *Chemoorganotrophic* communities release organic compounds with acidic features such as oxalic, gluconic, fumaric, citric and glutaric acids [423]. These acids are capable of changing the pH within microvoids and as a consequence creating gradual biodegradation of the microstructure of the polyester matrix.

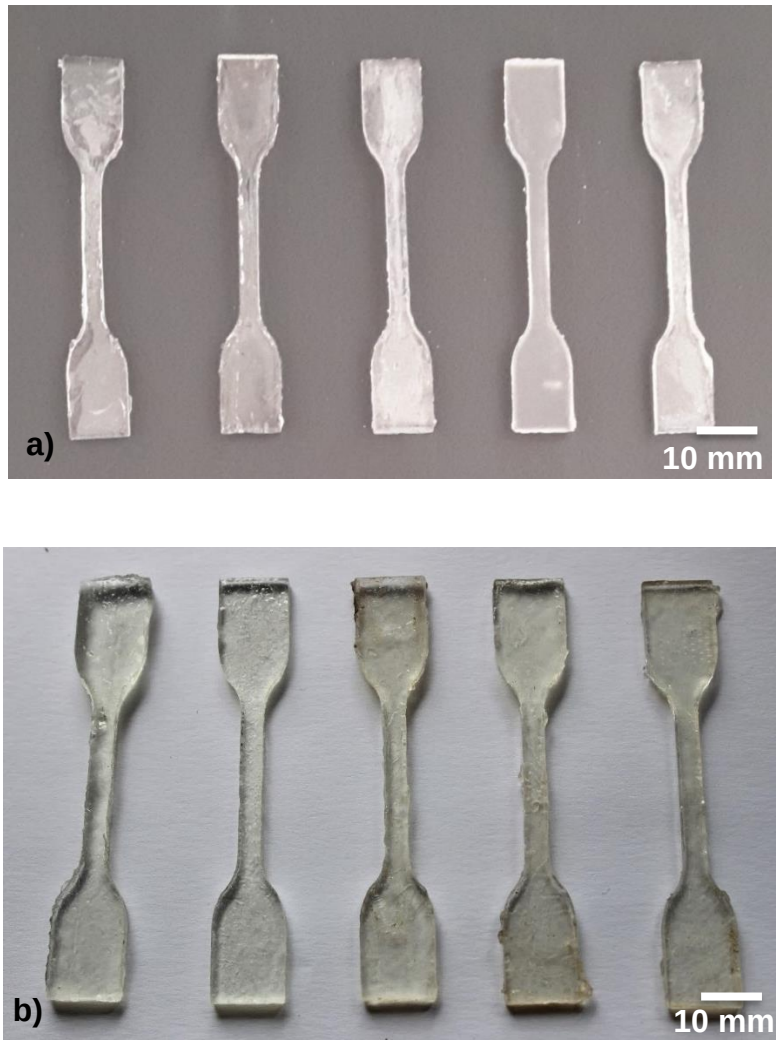

Figure 59. Visual effects of seawater on tensile samples: from left; monolithic polyester, 0.1 wt%, 0.3 wt%, 0.7 wt% and 1wt% HNTs reinforcement.

6.2.12. Conclusion

Undoubtedly, the incorporation of HNTs has enhanced the mechanical properties of unsaturated polyester as is evident in many studies. The results also showed that small amounts of HNTs considerably improved the microhardness, tensile and flexural properties, impact toughness and fracture toughness of the nanocomposites. In dry conditions, the optimal HNTs content was found to be 0.7 wt% where the microhardness was improved by 44% compared to monolithic polyester. The Young's modulus increased from 0.7 GPa to 1 GPa (a 43% increase) and the flexural modulus increased from 0.77 GPa to 1.24 GPa (a 61% increase). Furthermore, fracture toughness improved from 0.26 MPa.$m^{1/2}$ to 0.4 MPa.$m^{1/2}$ (a 54% increase).

The immersion in seawater, however significantly reduced the mechanical properties of the nanocomposites. Microhardness decreased from 107 HV to 42 HV (a 61% decrease) compared to monolithic polyester, the Young's modulus decreased 33% and the flexural modulus (decrease of 43%). The maximum value of K_{1C} after immersion in seawater was obtained in the case of 1 wt% reinforcement from 0.59 MPa.$m^{1/2}$ to 0.79 MPa.$m^{1/2}$ (a 34% increase). After the seawater immersion tests with the nanocomposites, the interface alone or possibly both the interface and nano-particles were damaged and caused deterioration of nanocomposite properties. The lack of interfacial interaction between the HNTs and polymer matrix leads to weak interfacial adhesion as shown in several SEM images (Figure 58 (g) (i) and (k)). On the other hand, the seawater diffusion into nanocomposites depends on several factors such as the volume of the fillers as well as the viscosity of the matrix. As the HNTs content increased, the high viscosity was likely to produce voids in the nanocomposites allow seawater to diffuse easily. Apart from that, seawater absorption

led to plasticization and the formation of biofilm on the surface of the nanocomposites. Environmental pollutants such as microbes entered through microvoids, further increasing the deterioration in the mechanical properties of the composites. It is believed that several deterioration pathways are likely to take place concurrently after exposure to seawater.

Once a material is immersed in a marine environment, its physical and chemical properties change due to the adsorption of macromolecules and early colonisers known as Proteobacteria. Recent research suggests, that these bacteria are the predominant bacterial microorganisms in the biofilm within 24 h of seawater exposure. They are also the most abundant and highly diverse phylum of the biofilm community. Proteobacteria are normally more abundant than other microorganisms because of their massive populations 43.3% of the total compared to Actinobacteria (8.6-12.2%), Bacteroidetes (8.3-12.2%) and Deltaproteobacteria (5.5-7.8%) [430].

The polyester and its composites were adversely affected by the microbial species. It is important to underline that the results indicate that the interfacial region in HNTs-polyester nanocomposites may be more vulnerable to damage due to seawater absorption. Based on SEM images, it can be concluded from this study, that the mechanical properties of HNTs-polyester nanocomposites were significantly affected by seawater immersion due to a biodegradation process caused by the bacteria entering through microvoids, growing and increasing the size of cavities before attacking cracks, all of which weakened the physical properties and microstructure of the nanocomposites. Microbes can cause chemical degradation and the breakage of hydrocarbons using seawater molecules. Nanocomposite biodegradation is highly undesirable for material integrity as these plastics are used mostly in structural designs

in marine applications. Damage to the structure may result in premature weakening, which often translating to system failure and enormous economic losses. Evidence indicates that polymers are likely to be the most abundant form of chemical waste present in the marine environment. Thus, there is a need for plastics from marine debris to be biodegradable in order to reduce the abundance of plastic waste in the sea. However, in terms of the nanocomposites used for marine applications, they need to withstand the effect of seawater to enhance their life cycles and to prevent degradation to insfrastructure due to environmental effects and microbial attack. Therefore, further study needs to address the importance of both, environmental and application needs.

7. Effect of short term exposure to water on the mechanical properties of HNTs-MLG reinforced polyester nanocomposites

7.1. Background

Graphene-based polymer composites have good thermal, gas barrier, flame retardant and excellent mechanical properties in comparison to unfilled polymers [34, 431, 432]. Developments in graphene research have been very rapid because the laboratory procedures to make high-quality graphene are fairly easy and cheap [433]. Apart from that, graphene-based materials have been used in different fields such as composites and coatings, electronics devices, energy storage, sensors and biomedical applications [34]. Atif *et al.* reported that MLG improves Young's modulus and microhardness by 25.7% and 18.3%, respectively [323]. MLG also exhibits increased T_g and storage modulus compared to unfilled epoxy [321, 354, 372].

In this work, the effect of short-term water absorption on the mechanical properties of polyester-based nanocomposites reinforced with HNTs, multi-layer graphene (MLG) and HNTs-MLG (hybrid filler) has been studied. The influence of HNTs, MLG and HNTs-MLG has been tested in terms of the weight gain of nanocomposites due to water absorption. The mechanical properties in dry and wet conditions has also been investigated

Knowledge of the effects of moisture absorption on flexural, tensile and impact properties is not easily found in literature for hybrid polyester composites reinforced with HNTs and MLG. This appears to be important with a view to broadening the possible industrial applications of these nanocomposites with reference to the coating industry. Hybrid nanocomposites were produced to study whether or not synergistic

effects can reduce the deterioration effect caused by water absorption at low weight fractions of 0.1 wt %.

7.2. Results and discussion

7.2.1. Dynamic mechanical analysis

In this research, the addition of 0.1 wt% of HNTs and MLG increased values of T_g as shown in Figure 60. An increase in T_g with HNTs and MLG indicates that the fillers were uniformly dispersed [41, 321]. As for HNTs, the change in T_g associated with inorganic fillers has been and discussed and discussed by other authors [288]. The two common factors were rigid phase reinforcement and the destruction of the epoxy-based polymer network structure [434]. Other authors have also proposed that HNTs and other clay particles restrict the mobility of polymer chains [416, 435]. In the case of MLG, when it is uniformly dispersed the resulting wrinkled texture and high surface area influence the maximum exothermic heat flow temperature by restricting polymer chain mobility and thereby causing an increase in T_g [372]. A previous study suggested that the wrinkled structure could play an important role in enhancing mechanical interlocking and efficient load transfer distribution within the matrix [329]. Apart from that, these wrinkles from overlapping graphene sheets can link individual graphene sheets effectively and improve interfacial interactions with polymer chains [313, 321].

In dry conditions, monolithic polyester (MP) recorded the lowest value of T_g at 77.9°C. The values of T_g increased to 78.3°C for HNTs-MLG polyester nanocomposites and increased to 80.4°C in the case of 0.1 wt% HNTs-reinforced polyester. The maximum T_g was found in 0.1 wt% MLG-reinforced polyester at 82.6°C (a 6% increase). After exposure to water, values of T_g decreased for all

nanocomposites (compared to the dry nanocomposite systems). The lowest T_g was observed for MP, dropping from 77.9°C to 70°C. The highest T_g was observed for 0.1 wt% MLG-reinforced polyester (77.34°C). The lowering of T_g is an evidence of plasticization caused by water [14]. Moisture wicking along the fibre-matrix interface degrades the interfacial bond strength, resulting in loss of micro-structural integrity [14]. Values of storage modulus of dry samples of nanocomposites are shown in Figure 61(a). The increase in storage modulus at T_g can be associated with a decrease in polymeric chain mobility [396] and the enhancement of stiffness [61]. In the cases of 0.1 wt% HNTs and 0.1 wt% MLG significant improvements in storage modulus were observed particularly at lower temperature. The maximum storage modulus at 40 °C was recorded for MLG filler. The storage modulus for all reinforced polyesters later decreased as they approached the glass transition temperature (T_g). It can be observed that storage modulus increases while loss modulus decreases for the hybrid (0.05 wt% HNTs-0.05 wt% MLG), 0.1 wt% HNTs and 0.1 wt% MLG-reinforced polyester compared with the monolithic polyester. Values of storage modulus for nanocomposites exposed to water are shown in Figure 61 (b). It can be seen the storage modulus and loss modulus (Figure 61 (a)) and Figure 62 (b)) considerably decreased as a result of matrix softening [18].

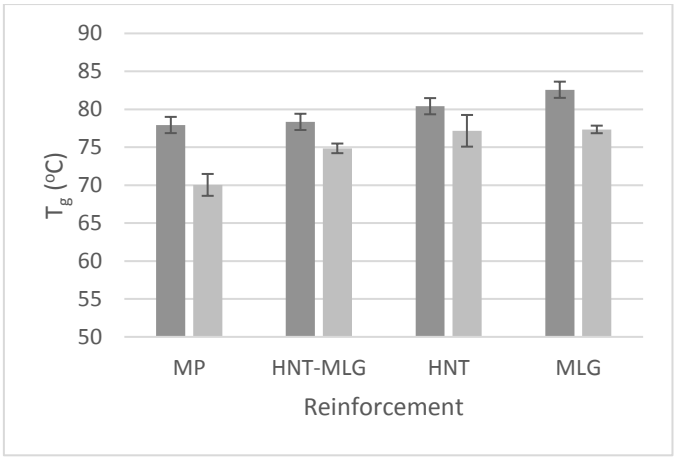

Figure 60. T_g of nanocomposites in dry conditions and after water exposure

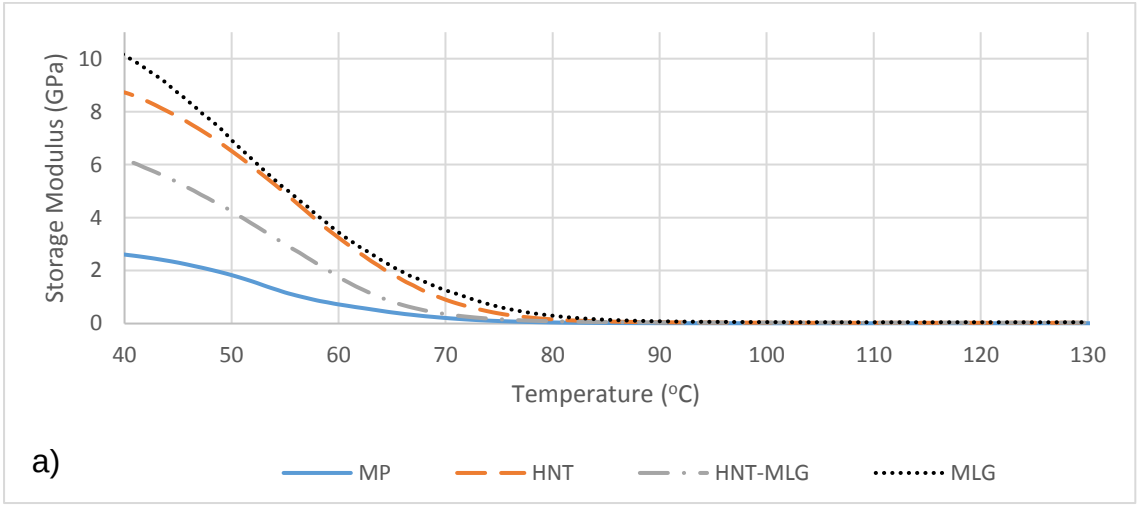

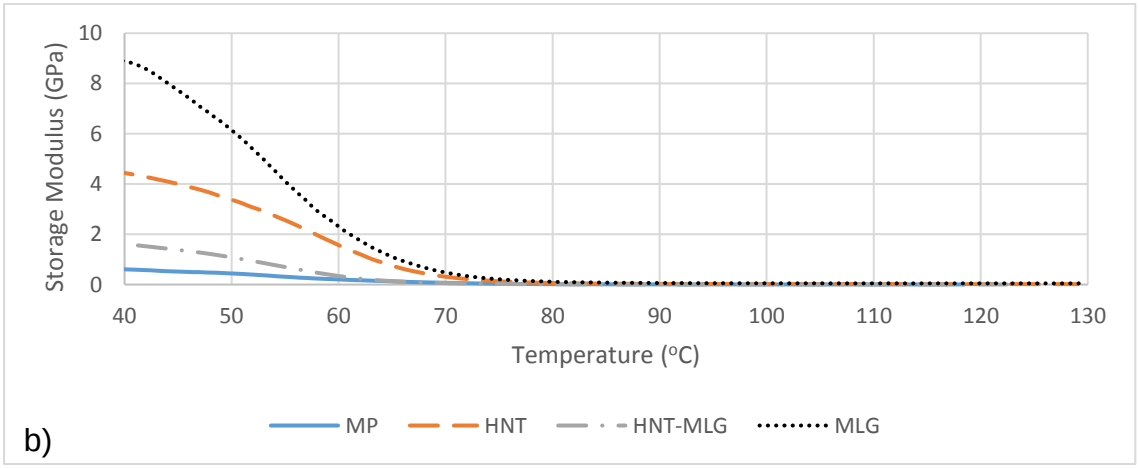

Figure 61. Storage modulus of nanocomposites in dry condition (a) and after water exposure (b)

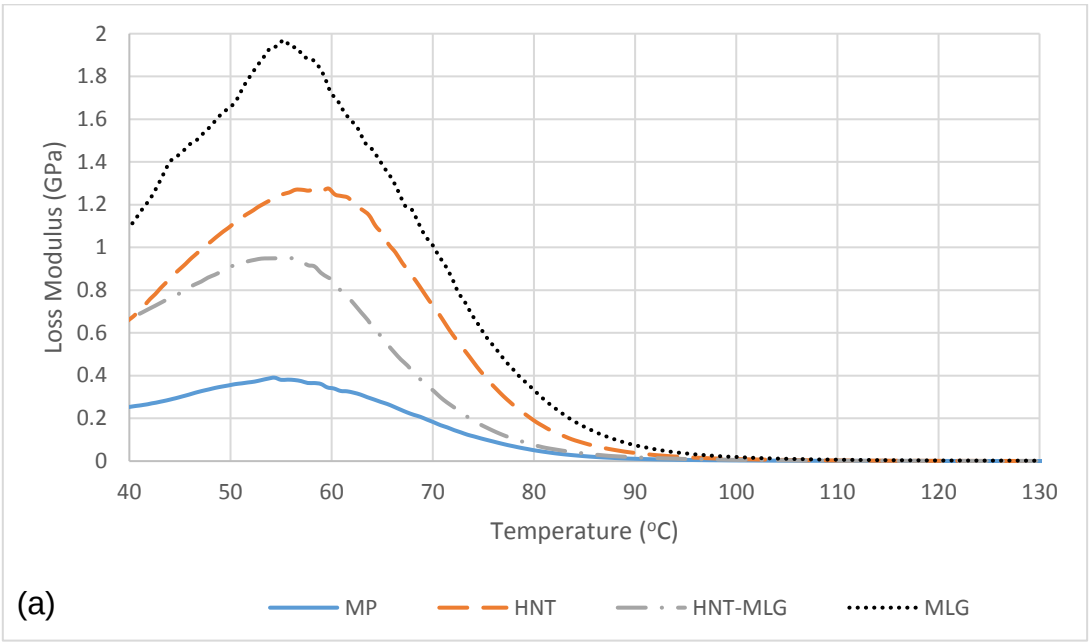

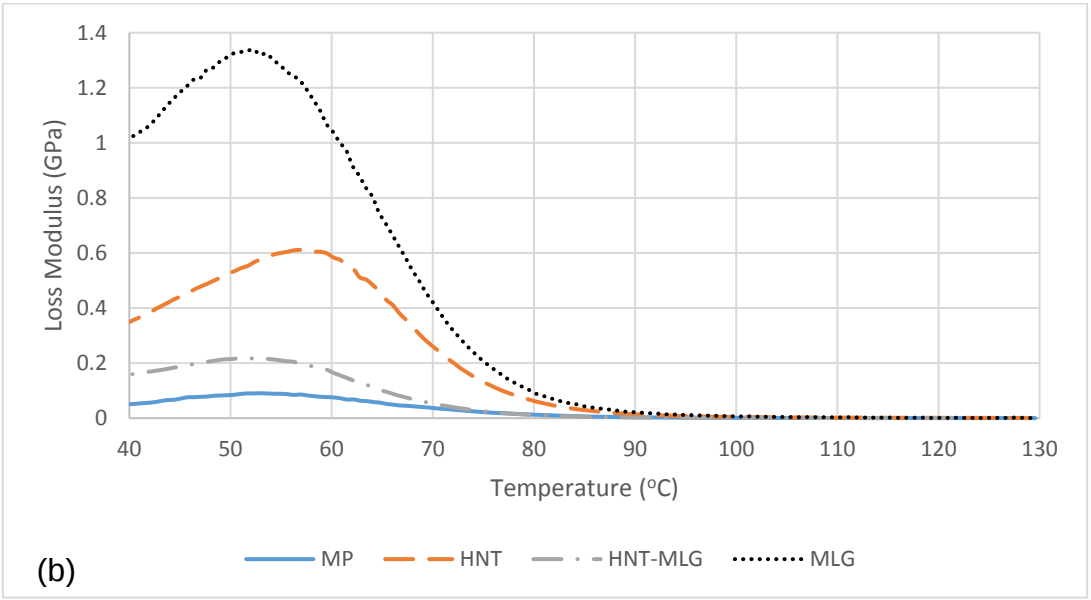

Figure 62. Loss modulus of nanocomposites in dry conditions (a) and after water exposure (b)

7.2.2. Optical transmittance

The optical transmittance of the nanocomposites was then investigated. In Figure 63 (a) and (b), it can be observed that MP (monolithic polyester) is essentially highly transparent over the 400-1400 nm wavelength. The average transmittance value of MP is 72.9%. At 0.1 wt% HNTs, average value of 57.6%was recorded. The 0.05 wt% HNTs-0.05 wt% MLG reinforced polyester recorded only 4.3% optical transmittance. The 0.1 wt% MLG had an optical transmittance of 0.29%. It can be seen that, even at 0.05 wt% HNTs-0.05 wt% MLG, the optical transmittance dropped significantly. After exposure to water, a similar trend was observed where monolithic polyester had the highest optical transmittance. However, exposure to water significantly reduced the optical transmittance of MP (monolithic polyester decrease of 46.3% compared to the dry condition). The 0.1 wt% HNTs reinforced polyester lost 37% of its optical transmittance due to water absorption. The optical transmittance for 0.05 wt% HNTs-0.05 wt% MLG reinforced polyester and 0.1 wt% MLG-reinforced polyester was also found to have decreased but the changes were statistically not significant.

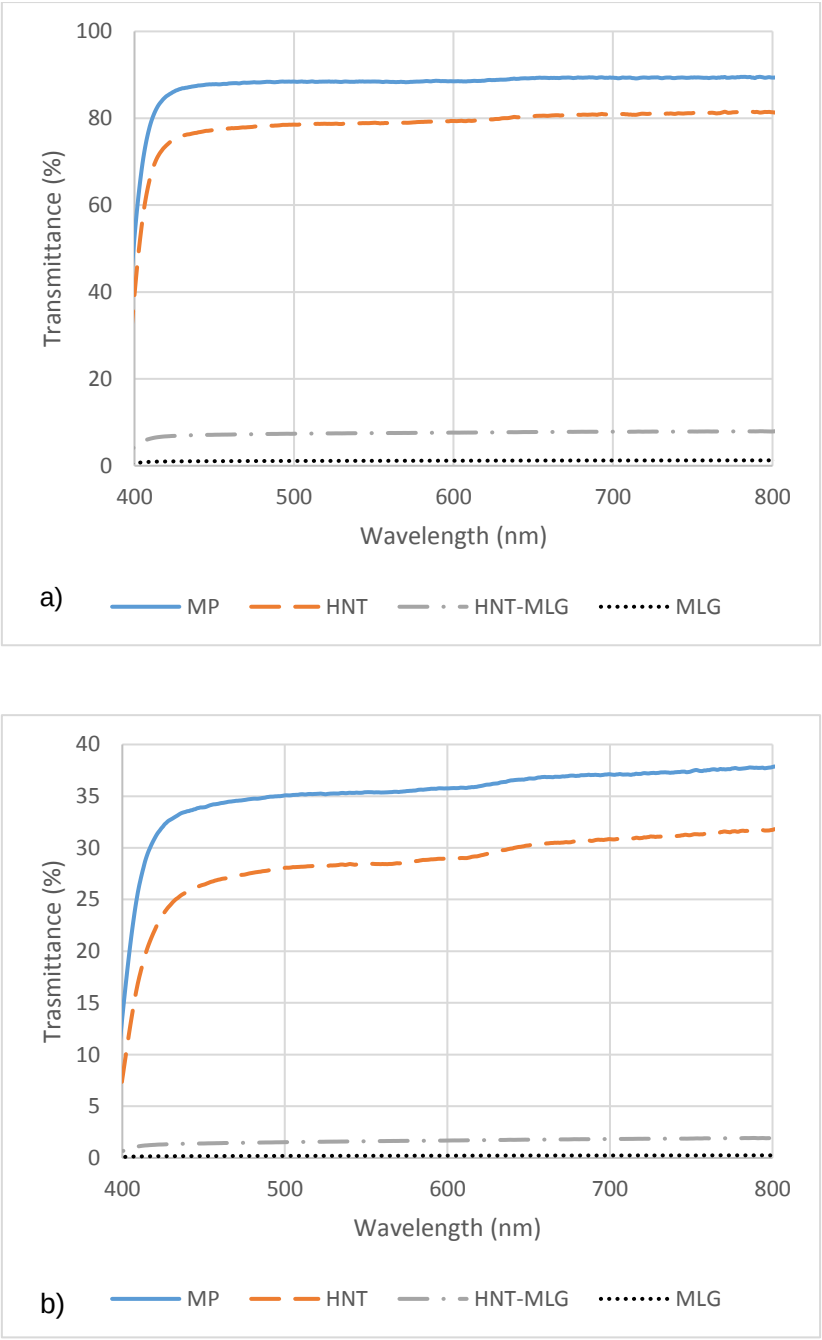

Figure 63. Optical transmittance curves of nanocomposites for dry conditions (a) and after water exposure (b)

7.2.3. Densification

The levels of densification of samples versus type of reinforcement are shown in Figure 64 (a). The large standard deviations in densification for monolithic polyester indicate porosity within the samples, indicating air entrapment during processing [436] possibly from the intense mechanical mixing that produces air bubbles in the mixture which would increase void content in the nanocomposites [318, 417]. The casting technique used, on the other hand, is not usually considered to be 100% reproducible like latex technology [372].

7.2.4. Water absorption test

The water absorption results are shown in Figure 64 (b). It can be seen that the monolithic polyester absorbed more water than the nanocomposite systems with 1.1% weight gain after 24 hours. For 0.05 wt% HNTs-0.05 wt% MLG-reinforced polyester recorded water absorption was 1.05%. The 0.1 wt% HNTs reinforced polyester recorded 0.89% and 0.1 wt% MLG-reinforced polyester showed 0.75% of water absorption. In the literature, it is reported that polymer/graphene-based nanocomposites could offer dramatic improvements in moisture barrier properties. Kousalya *et al.* in their publication reported that the graphene layer structure can act as a liquid barrier even under vigorous flow boiling conditions, indicating a broad application space for few-layer graphene as an ultra-thin oxidation barrier coating [338]. The results also suggest that MLG reduced water absorption more than HNTs at similar loadings. This can be attributed to the higher aspect ratio of MLG compared to HNTs [437].

7.2.5. Vickers microhardness

The Vickers microhardness results are shown in Figure 64 (c). Compared to monolithic polyester, the 0.05 wt% HNTs-0.05 wt% MLG-reinforced polyester showed improved microhardness from 177 HV to 221 HV (a 25% increase). The microhardness increased steadily in the case of 0.1 wt% HNTs (49% increase) and 0.1 wt% MLG (50.3% increase). After exposure to water, the monolithic polyester recorded a value of only 111 HV. The microhardness for nanocomposites exposed to water improved in the case of 0.05 wt% HNTs-MLG, 0.1 wt% HNTs and 0.1 wt% MLG; however, the values were lower than those in dry conditions. The reduction of microhardness was caused by the surface softening of polyester matrix by water [355, 438]. Exposure to water had reduced the microhardness of the samples due to swelling and matrix softening [14]. Researchers have also found that environmentally exposed composites are primarily dominated by matrix rather than fibre failure [439]. Therefore, reduction in microhardness is expected in this context.

7.2.6. Flexural properties

Values of flexural modulus of the nanocomposites are shown in Figure 64 (d). For dry samples, the maximum flexural modulus was observed in the case of 0.1 wt% MLG (60.6% increase) followed by 0.1 wt% HNTs (increase of 50.6%). For samples exposed to water, a similar trend was observed. The maximum flexural modulus was recorded in the case of 0.1 wt% MLG, increasing from 0.62 GPa to 1.15 GPa (increase of 85.5%). The flexural strengths of nanocomposites in dry and wet conditions are presented in Figure 64 (e). Minimum flexural strength was recorded in the case of MP and maximum in the case of the 0.1 wt% MLG-reinforced polyester. Where it increased

from 55.7 MPa to 71.9 MPa (by 29%). After exposure to water, the flexural strength showed deterioration compared to unexposed samples. The lowest flexural strength was observed for the MP at only 45 MPa. The flexural strength then steadily increased in the case of 0.05 wt% HNTs-0.05 wt% MLG (47 MPa), 0.1 wt% HNTs (63 MPa) and 0.1 wt% MLG (65 MPa). The variation in the flexural strain of nanocomposites in dry and wet conditions is shown in Figure 64 (f). In comparison with MP, the flexural strain decreased with the incorporation of nano-filles, as the increase in strength and stiffness reduced flexural strain. After exposure to water, the flexural strain increased in all samples. Water absorption leads to an increase of the plastic zone ahead of a crack hence increasing the strain values of all nanocomposites [406]. The higher flexural strain to failure for the samples exposed to water is due to softening and plasticization effects as mentioned in the literature [14]. This can be associated with water filling the gaps between the filler and polymer matrix, eventually leading to a decrease in flexural strength [60]. The degradation of nanocomposites in this respect is dominated by losses of matrix interface strength. Water molecules entering the network of the matrix accelerate cracking, which contributes to the decrease in flexural modulus and strength [440]. Results for the energy absorbed as calculated in terms of the area under the force-displacement curve, are presented in Figure 64 (g). At 0.1 wt% MLG reinforcement, the energy absorbed was improved by 32% compared to monolithic polyester. Short term water exposure on the other hand reduced the energy absorbed for all nanocomposite systems. For instance, at 0.1 wt% MLG reinforcement. The energy absorbed decreased from 2.5 J to 2.1 J, which is a reduction of about 16%. The same trend was observed for monolithic polyester and other composite systems.

7.2.7. Tensile properties

The variations in Young's modulus are shown in Figure 64 (h). Monolithic polyester obtained a Young's modulus of 0.75 GPa. This increased by 7% in the case of 0.1 wt% HNTs. The highest Young's modulus was obtained for 0.1 wt% MLG reinforcement with an improvement of 60%. After exposure to water, 0.1 wt% MLG reinforcement also recorded the highest Young's modulus with an increase by 98% compared to MP. The variations in tensile strength are shown in Figure 64 (i). At 0.1 wt% MLG reinforcement, the highest tensile strength was observed, with an increase from 32.4 MPa up to 47.3 MPa (by 46%) for dry samples. In wet samples, the tensile strength increased from 28.3 MPa to 39.5 MPa. The tensile strain graph is shown in Figure 64(j). In dry conditions, the tensile strain tends to have lower values than for samples exposed to water environments. Dry samples show high stiffness and higher strength than samples tested after water exposure.

7.2.8. Impact toughness

The variations in impact toughness are shown in Figure 64(k). For dry samples, the MP recorded a value of 0.78 kJ/m^2. In the case of 0.05 wt% HNTs-0.05 wt% MLG, the impact toughness increased to 1 kJ/m^2. Further increases in impact toughness can also be seen for samples reinforced with 0.1 wt% HNTs (1.4 kJ/m^2). The maximum increase in impact toughness was found for samples reinforced with 0.1 wt% MLG (1.6 kJ/m^2). The improvement in impact toughness can be linked to the reinforcing effect of the carbonaceous fillers [323].

7.2.9. Fracture toughness

The fracture toughness values (K_{1C}) are shown in Figure 64 (l). The maximum fracture toughness was observed in the case of 0.1 wt% MLG reinforcement. The fracture toughness of this polyester system has been enhanced with the addition of 0.05 wt% HNTs-0.05 wt% MLG, 0.1 wt% HNTs and 0.1 wt% MLG from 0.3 MPa.m$^{1/2}$ to 0.6 MPa.m$^{1/2}$ (a 100% increase). In general, exposure to water increased the fracture toughness of the nanocomposites. Polyester reinforced with 0.1 wt% MLG recorded the highest fracture toughness which increased from 0.48 MPa.m$^{1/2}$ to 0.8 MPa.m$^{1/2}$ (by 67%).

Table 10. Mechanical properties of nanocomposites in air and after water exposure

Sr.	Properties / Filler %	In air				After water exposure			
		MP	HNTs-MLG	HNTs	MLG	MP	HNTs-MLG	HNTs	MLG
1	Microhardness (HV)	177±14	221±11	264±7	276.5±	111±4	125±11.6	148.3±5.5	188.3±21
2	Young's modulus (MPa)	0.75±0.09	0.8±0.09	1.1±0.04	1.2±0.08	0.54±0.1	0.73±0.08	1.01±0.07	1.07±0.08
3	Tensile strength (MPa)	32.4±3	33.4±6	45.8±5	47.3±3	28.3±4.7	30.2±5	39±2.1	39.5±5.1
4	Tensile strain (%)	7±3	6.6±1	6.2±1	4±2	8.5±1	7±1	6.5±1	5.7±2
5	Flexural modulus (MPa)	0.8±0.1	0.86±0.13	1.21±0.11	1.28±0.18	0.62±0.13	0.7±0.17	1.07±0.1	1.15±0.2
6	Flexural strength (MPa)	55.68±5	62.3±4.8	68.14±6	71.9±8	44.9±7	46.7±7	63.4±6	65.4±8.4
7	Flexural strain (%)	9±0.4	7±0.4	6±0.4	6±0.6	15±2	8±1.3	7±1	7±0.8
8	Energy absorbed (J)	1.93±0.2	2.2±0.35	2.33±0.4	2.51±0.45	1.48±0.3	1.96±0.26	2.07±0.2	2.1±0.3
9	Fracture toughness K_{1C} ($MPa.m^{1/2}$)	0.34±0.05	0.45±0.06	0.57±0.05	0.6±0.05	0.48±0.04	0.5±0.04	0.61±0.05	0.80±0.07
10	Impact toughness (kJ/m^2)	0.78±0.12	1±0.12	1.4±0.13	1.57±0.14	0.62±0.1	0.74±0.1	0.88±0.13	0.98±0.13

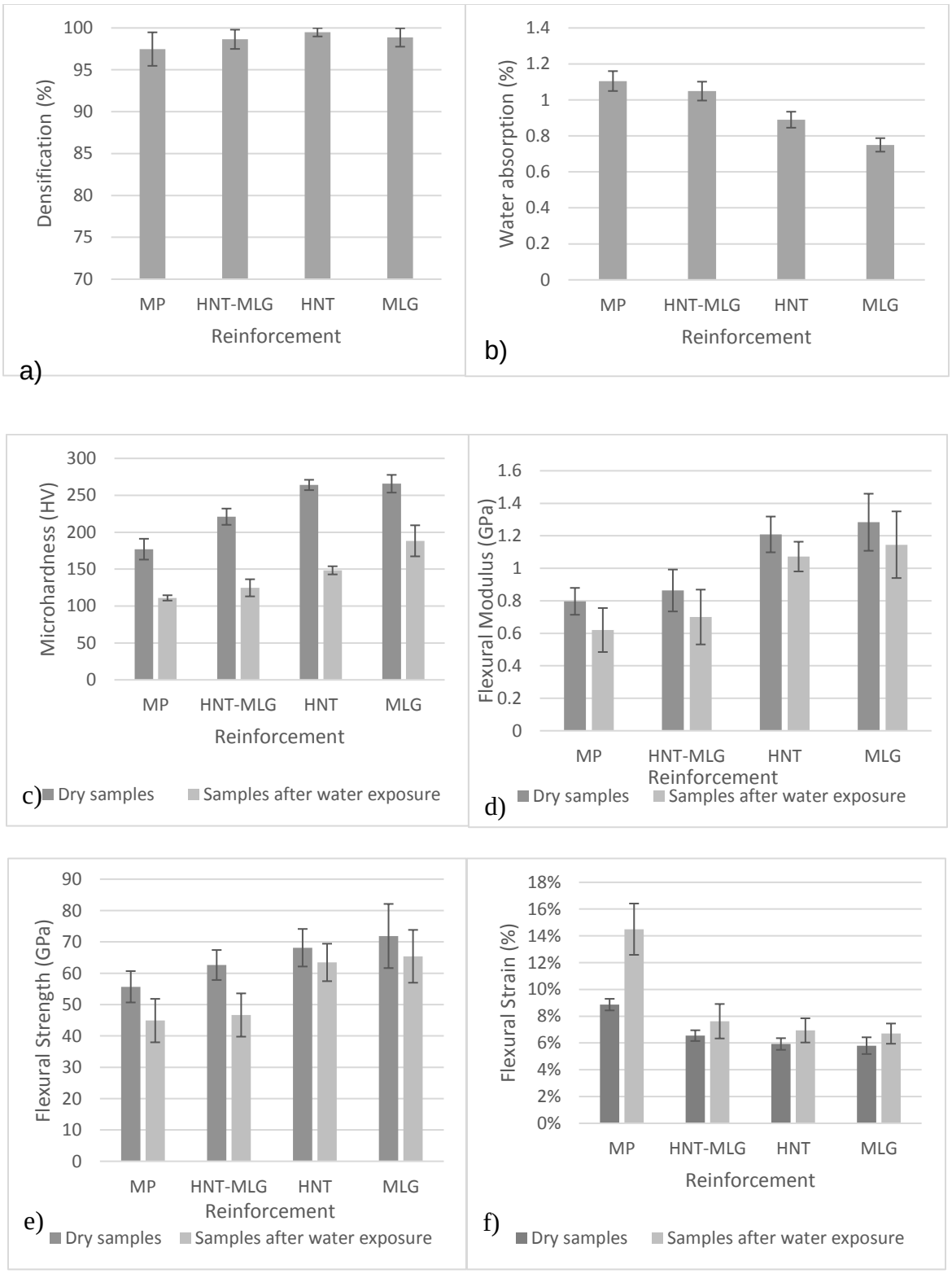

Figure 64. *Cont.*

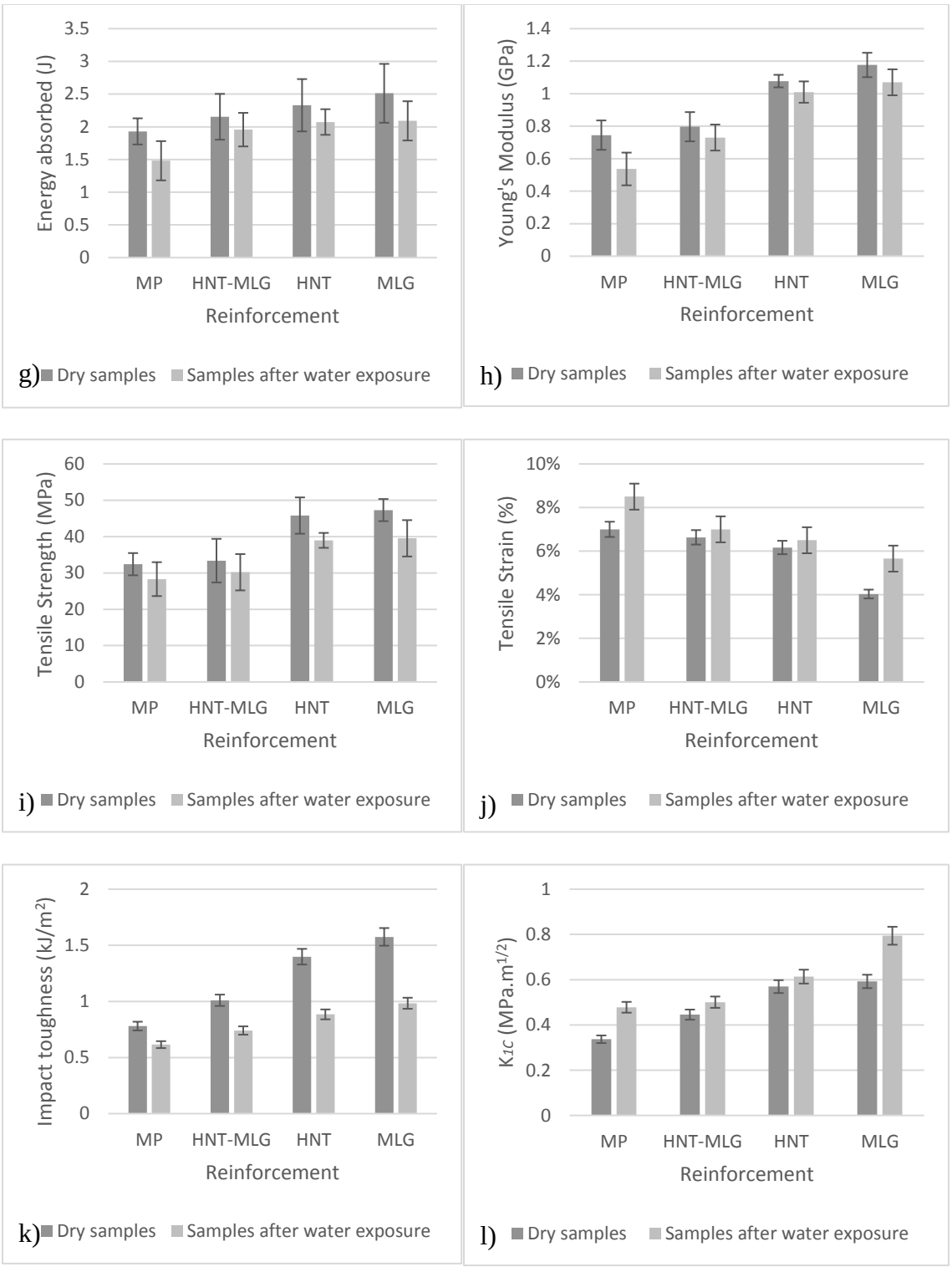

Figure 64. Mechanical properties of nanocomposites in dry conditions and after water exposure

7.2.10. Topographic profile

A topographical study was carried out on fractured three-point bend samples. The surface roughness (R_a) of monolithic polyester, 0.05 wt% HNTs-0.05 wt% MLG, 0.1 wt% HNTs and 0.1 wt% MLG are shown in Figure 65. R_a is defined as the mean of the roughness profile and is superimposed on the surface waviness [372]. Values of R_a (Figure 65 (a)) value for monolithic polyester was 0.32 µm. The R_a then increased steadily for samples reinforced with 0.05 wt% HNTs-MLG (0.48 µm), 0.1 wt% HNTs (0.68 µm) and 0.1 wt% MLG (0.8 µm). R_a values for samples exposed to water increased compared to those in dry conditions. The water molecules diffused through the polymer matrix and congregating around the particles [269]. This led to increases in the plastic zone which then increased the surface roughness of the nanocomposites.

A similar trend also observed in values of R_q and R_z for nanocomposites tested in dry conditions and after exposure to water. R_q is the root mean square of the profile and is sensitive to surface variation. The peak-to-valley height R_z measures the difference between the highest and lowest points of the profile. R_q for 0.1 wt% MLG-reinforced polyester in air was 0.71 µm and R_z was 4.43 µm. After exposure to water the maximum R_q and R_z for 0.1 wt% MLG-reinforced polyester were 1µm and 5.5 µm. A high value of R_a (with low R_z value) can be an indicator of smoother sample surfaces, the absence of agglomerates and the uniform dispersion of nano-fillers. A low value of R_a but high R_z value shows the existence of deep surface notches, agglomerates, and the non-uniform dispersion of nano-fillers. In general, values of R_q (Figure 65 (b)) and R_z (Figure 65 (c)) were lower in dry conditions and higher after exposure to water. When a coarser

topography was observed. Values for flexural strain samples (from the three point-bend test) used for the surface roughness measurement kept increasing with the coarser topography. This can be attributed to lower stiffness and strength value. A schematic illustration of the topographical difference between polyester nanocomposites tested in air and after exposure to water is given in Figure 66. The topographical profile after exposure to water became coarser because of the plasticization effect. The increase in high peaks can be linked to water absorption. The topographical surface profiles of nanocomposites for samples tested in air and wet conditions are presented in Figure 67. It can be observed that, after water exposure, the surface profiles were coarser than those of dry samples. The toughening effect with the incorporation of HNTs and MLG is due to crack deflection and plastic deformation initiated around particles, which promotes the formation of cavities [285]. These cavities when combined with water tend to plasticize and become bigger in size hence producing a coarser topography where a smooth surface is impossible to obtain in the cross section of samples.

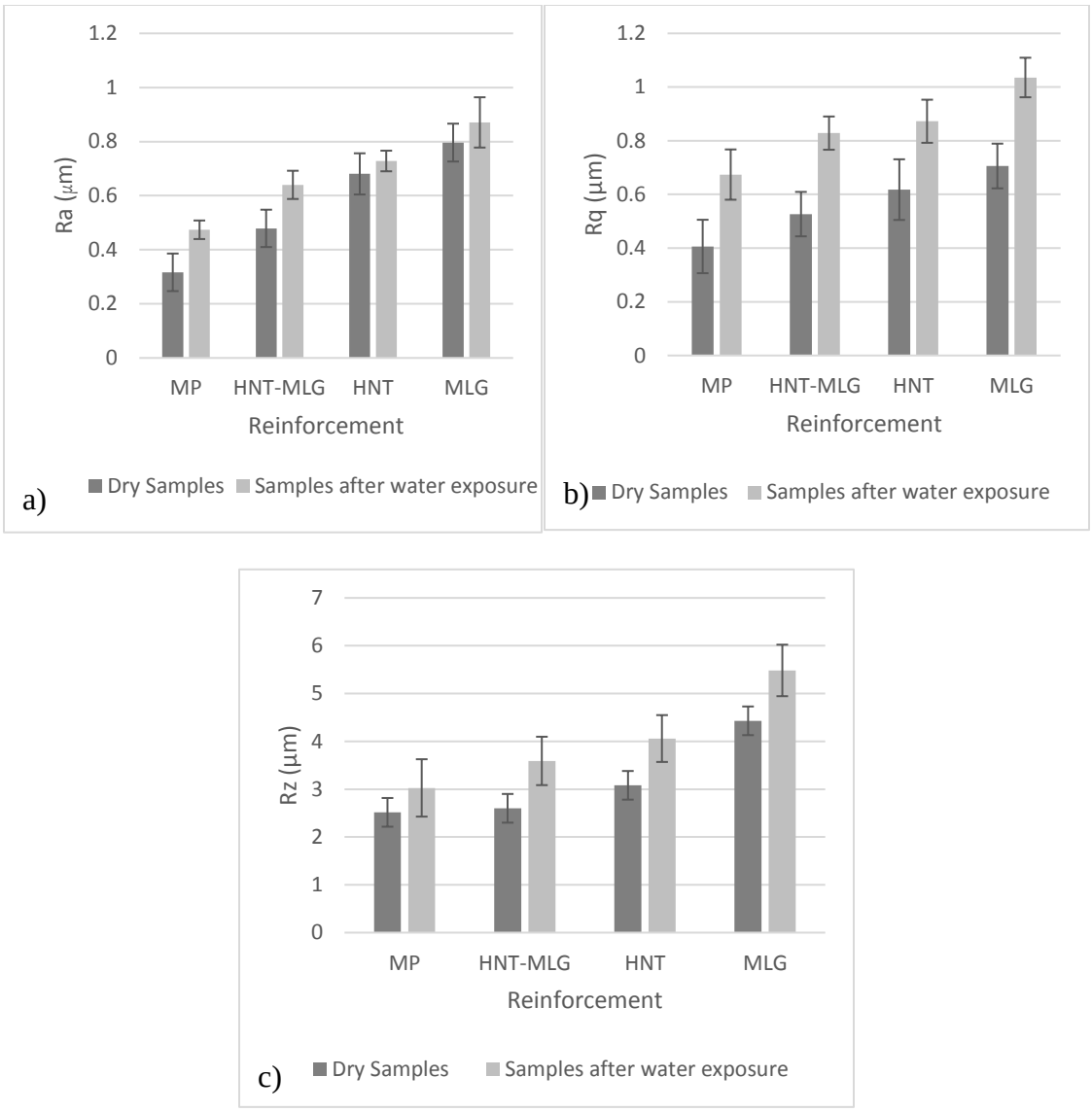

Figure 65. Topographic characteristics of nanocomposites in dry conditions and after water exposure

Figure 66. Topographic profile of samples (a) dry conditions (b) after water exposure (not drawn to scale)

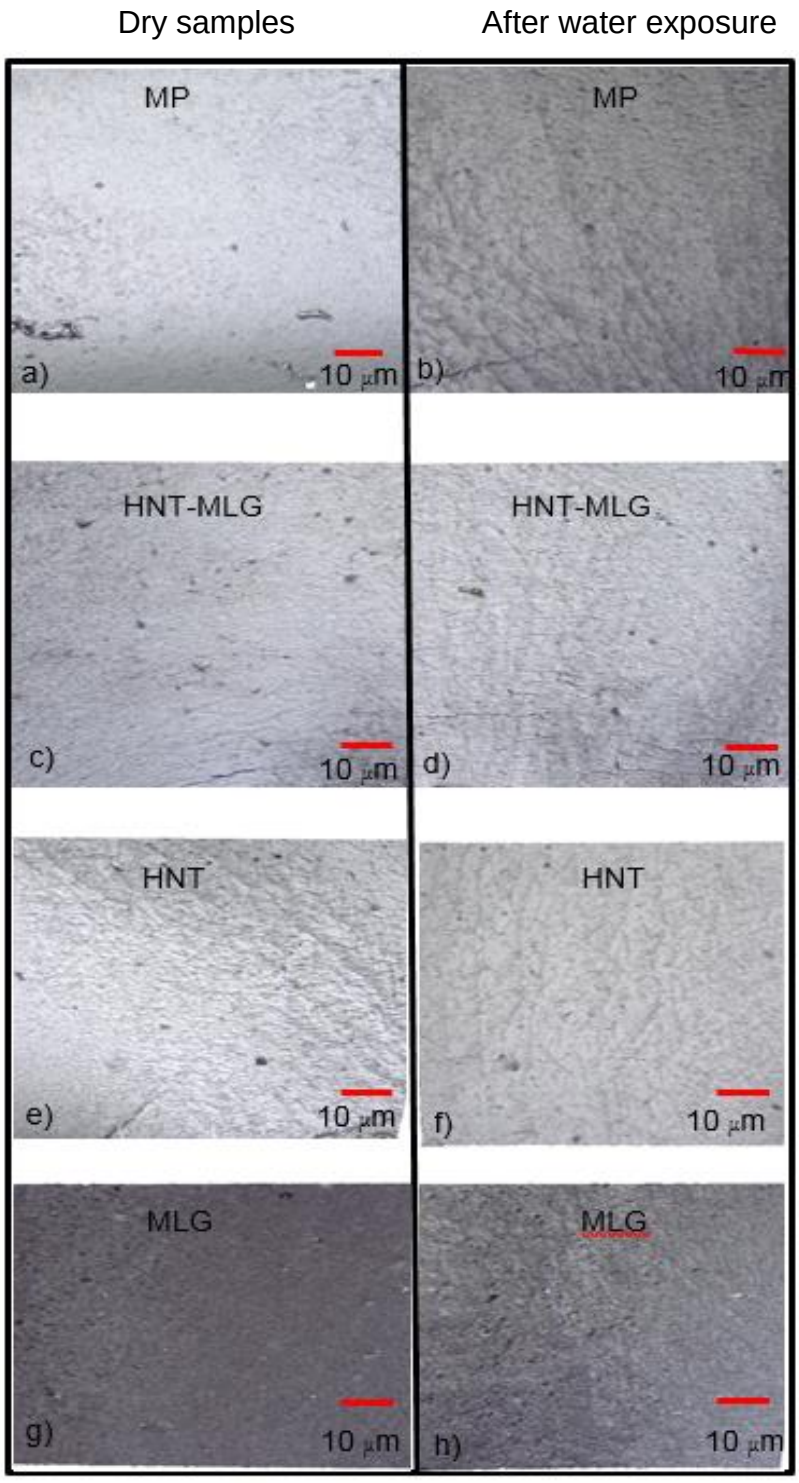

Figure 67. Surface profile of nanocomposites before and after water exposure

7.2.11. SEM Images

SEM images of fractured surfaces are shown in Figure 68. As the cracks propagate, material is lost, most likely in the form of round particles as can be observed in Figure 68 (a). The image also reveals that the monolithic sample showed river markings which can be associated with a fast brittle fracture mode [297]. This is an evident that there are no crack bridging mechanisms available in monolithic polyester. When the cracks propagate, they move with less diversion. After exposure to water, the monolithic polyester shows a smoother surface with weaker crack lines. De-bonding for the MP is in the form of long and straight lines.

Synergistic effects are not effective at filler concentrations of 0.1 wt% to produce considerable improvements in the mechanical properties of the hybrid nanocomposites produced [441]. Clusters of fillers from de-bonded polyester matrix can be seen for the hybrid sample (Figure 68 (c)). The size of the clusters is relatively small with considerably small spacing. The material in the vicinity of the clusters and the distance between them may not have a significant effect on mechanical properties [303].

The effect of MLG was also noticeable on the surface of the 0.05 wt% HNTs-0.05 wt% MLG nanocomposites. The crumpled structure of MLG is shown in Figure 68 (d). The effect of water on hybrid nanocomposites suggests that surface roughness was reduced compared to samples tested in dry conditions [103]. De-bonding and the pull-out of fillers were observed in hybrid samples, which are responsible for the moderate toughening in Figure 68 (d) [442].

For the HNTs samples, the interlocking effect can alter the crack formation mechanism. In Figure 68 (e), the crack starts from a defect point and emanates radially. Similar phenomena have been reported elsewhere [297]. Crack lines are straighter after the HNTs-reinforced polyester samples were exposed to water. The nanocomposites containing HNTs particles showed a plasticization effect where crack propagation became easier and faster.

Graphene based materials are often compliant, and when dispersed in a polymer matrix, they are typically not observed as rigid discs but rather as bent or crumpled platelets [36]. The wrinkle structure of MLG gives better interfacial interaction than the tubular structure of HNTs [316]. The wrinkled structure significantly improves the interfacial interactions with polyester chains. The Figure 68 (g) shows no particular crack orientation. This is because MLG has the ability to prevent the propagation of cracks and cracks detour around the MLG to proceed [443]. After water exposure, micro-cracks and pronounced river markings can be observed for the MLG reinforced sample. It is evident that the presence of HNTs and MLG fillers increased the fracture surface roughness. That is an indicator of crack deflection mechanisms, which increase the energy absorbed by the fracture by increasing crack length during deformation [437].

The nature of fracture between monolithic polyester, hybrid, HNTs and MLG reinforced polyester. Lower resistance to crack propagation shows more straight paths and smooth surface. This can be observed in the case of monolithic polyester and hybrid nanocomposites. Hybrid nanocomposites showed a moderate toughening mechanism which was slightly better than unfilled polyester. It can be observed that 0.1 wt% HNTs

reinforced polyester shows high resistance to crack propagation compared to monolithic polyester and hybrid nanocomposites with round ended cracks. The high aspect ratio of MLG, however, showed superior toughening compared to other nanocomposite systems. The force required for crack propagation in 0.1 wt% MLG reinforced polyester was higher based on the SEM images obtained. The results suggest that there were no significant improvements in water barrier properties and mechanical performance in hybrid nanocomposites. This is because either 0.05 wt% of HNTs and MLG is not enough to produce significant synergistic effects or no synergistic effects between HNTs and MLG are possible.

Based on the SEM images, there was no evidence that HNTs and MLG were poorly dispersed. The weight fraction used was only 0.1%, and therefore an inferior dispersion state can be ruled out as a cause of the deterioration in mechanical properties. It is noted from the literature that the diffusion of moisture can be distributed throughout the polymer matrix or water clusters may form [444]. In this research, the formation of water clusters was not observed in SEM images but plasticization was clearly noticed. Therefore, the plasticization of the matrix is suggested to be mainly responsible for the deterioration in mechanical properties of all nanocomposite systems (MP, HNTs-MLG, HNTs and MLG reinforced polyesters).

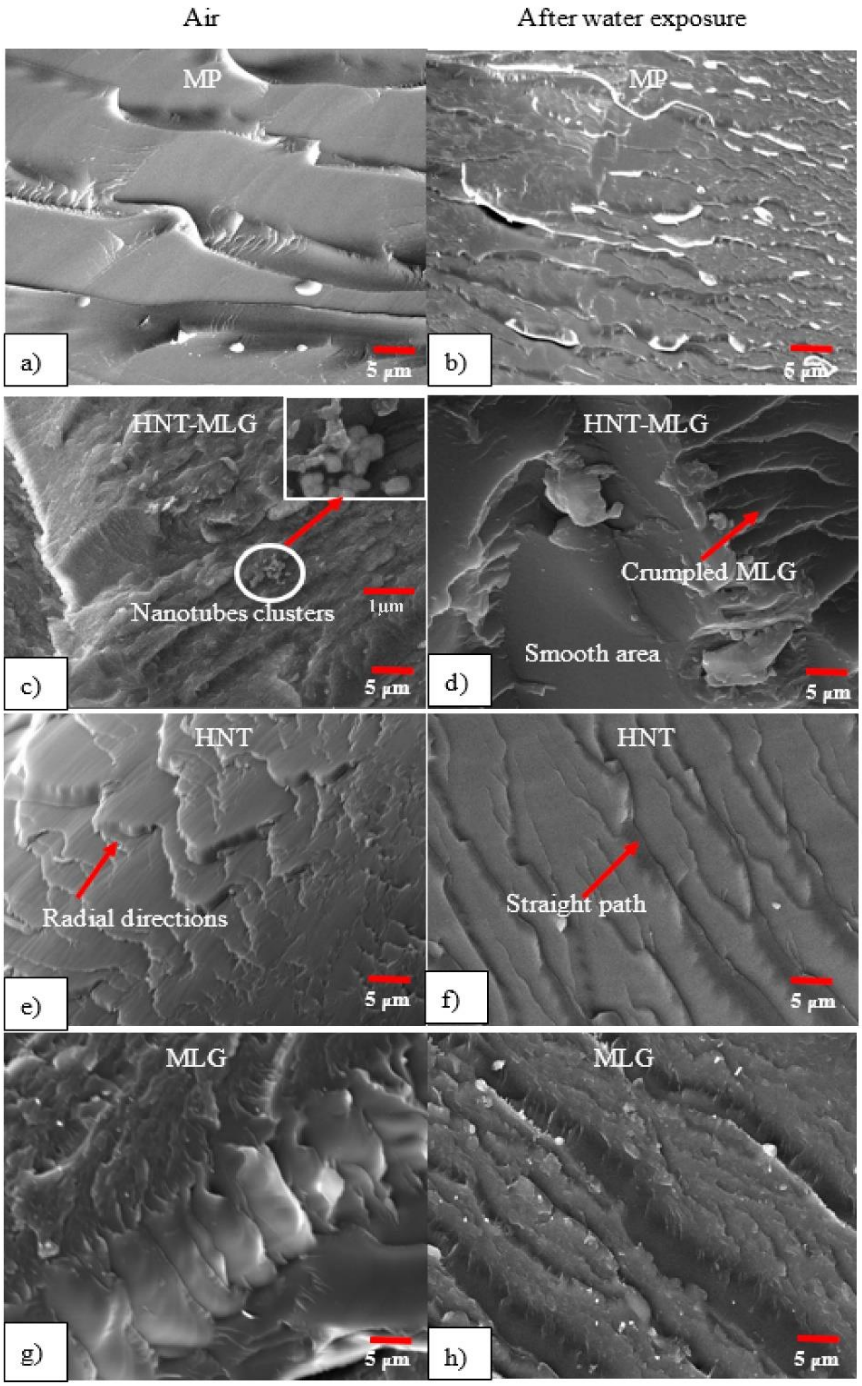

Figure 68. SEM images of nanocomposites before and after water exposure: (a) Monolithic polyester in air, (b) monolithic polyester after water exposure, (c) HNTs-MLG polyester in air, (d) HNTs-MLG after water exposure, (e) HNTs polyester in air, (f) HNTs polyester after water exposure, (g) MLG polyester in air, (h) MLG polyester after water exposure.

7.2.12. Conclusions

The effect of short periods of water absorption on the mechanical properties of HNTs and multi-layer graphene (MLG) reinforced polyester has been studied. It is shown that the polyester matrix is vulnerable to the deleterious effects of exposure to water. The addition of small amounts of HNTs and MLG decreased the weight gain of the nanocomposites compared to monolithic polyester. MLG reinforced polyester showed superior strength compared to hybrid and HNTs composites in dry conditions and after exposure to water. SEM images revealed fewer cracks in all samples exposed to water. Nano-filler and matrix interface weakening was the main failure mechanism induced by expose to water. The deterioration in mechanical properties related to water absorption caused a softening of the polymer matrix which lowered the strength of the nanocomposites. Their fracture toughness after exposure to water increased because of the plasticization effect. The surface roughness of all nanocomposite systems increased after exposure to water. This can be attributed to the high peaks and plasticized crack zone which then produced a coarser topography. This study provides evidence that the synergistic effects of HNTs-MLG hybrid nanocomposites at low content (0.05 wt% HNTs-0.05 wt% MLG) were insufficient to produce marked improvements in mechanical properties in dry conditions and after exposure to water. More research can be conducted to improve the mechanical properties of hybrid composites exposed to different liquid environment at different temperatures.

8. Conclusions

1. HNTs reinforcement enhanced the stiffness of polyester by restricting the movement of polymer chains. The storage modulus, loss modulus and T_g were considerably improved by HNTs reinforcement.
2. The short-term and long-term exposure to liquid can cause a loss of the mechanical properties of polyester composites. In contrast, the fracture toughness, tensile strain and flexural strain of the polyester composites increased. This indicates the ductility of the composites caused by liquid absorption. Moreover, liquid tends to fill the gaps between the polyester matrix and HNTs.
3. Agglomerations of clay particles and the presence of microvoids are some of the factors that are responsible for poor mechanical properties. The formation of microvoids normally occurs in high viscosity resin. HNTs also tend to agglomerate at high loading (2wt%) due to poor matrix-filler interaction.
4. Diffused liquid causes swelling, the loss of structural integrity and a softening of the polyester matrix. The microhardness of the composites deteriorated due to the liquid penetration into the matrix. Lower microhardness after exposure to liquid also can be attributed to the presence of voids and poor resistance to indenter due to surface matrix softening.
5. Surface roughness increased significantly for all polyester composites exposed to liquid media. Methanol is corrosive and promotes surface modification. Water and seawater induced the plasticization of the polyester matrix. The damage zone was further extended and the ductility of the material was enhanced.

6. The incorporation of 0.1 wt% multi-layer graphene improved the microhardness, flexural and tensile properties of the composites more than HNTs reinforcement. This can be linked to the higher aspect ratio and orientation of graphene compared to hallloysite nanotubes.
7. Synergistic effects are not effective at 0.1 wt% concentrations of hybrid fillers. No marked improvements can be seen for 0.05 wt% HNTs-0.05 wt% MLG.

Future work

There are some issues that can be further studied to improve the understanding of halloysite nanotube-polyester composite deterioration behaviour. Future work should focus on the following issues.

i) Higher percentages of HNTs

In this research, the HNTs incorporation was between 0.1 wt% to 1 wt%. This range was selected based on the previous literature suggesting that, at 1wt% and higher concentrations, agglomeration tends to occur which reduces the mechanical properties of nanocomposites. Apart from that, more time should be allowed for the nano-filler to evenly disperse in resin. This can be achieved by increasing the sonication time. The suggested sonication time is between 40 minutes to one hour or even longer.

ii) Different solvents and liquids

The main liquid media used in this research were methanol and seawater. Methanol was used because the effect of the immersion of nanocomposites is more severe than in any other solvent such as ethanol and isopropanol. In term of applications, methanol is preferred in automotive applications. It is worth investigating how other solvents influence the deterioration behaviour of nanocomposites.

iii) Higher temperature

Variations in temperature (i.e 25^{o}C, 30^{o}C, 35^{o}C and 40^{o}C) can be investigated in the future to study the effect of short-term water exposure on the mechanical properties of HNTs-multi-layer graphene-reinforced polyester nanocomposites.

iv) Crack propagation study using fracture mechanics approach

It would be interesting to see the effect of higher concentrations of HNTs/polyester composites monitored using a fracture mechanics approach to study the stress intensity factor $K_{I,E}$ of a compact tension specimen of mode I.

v) HNTs filled thermoplastics

To date there is no published research on the environmental stress cracking resistance of HNTs-reinforced thermoplastics. Such a study could be performed by applying force-displacement and liquid contact simultaneously. The main challenge here remains the high installation cost of an environmental chamber to the Universal Testing Machine.

vi) Biodegradation study of graphene-polyester nanocomposites

Various microbial and bacterial communities which develop on nanocomposites may release acid compounds, as stated in the literature. These acids create so-called gradual biodegradation on the microstructure of the polyester matrix. Deterioration at the interface is caused by hydrolysis which is caused by longer immersion times, and sustained exposure to seawater leads to the disintegration of the chemical bonds at the interface, resulting in the separation of halloysite and the polyester matrix. Graphene has

outstanding liquid barrier properties; its defect-free monolayers are impermeable to all atoms and molecules. A study of biodegradation effects could be performed on graphene-polyester nanocomposites to investigate whether or not microbes and bacteria can enter and damage their mechanical properties.

vii) Linking physical chemistry with the mechanical properties of nanocomposites to understand in detail what is happening in the matrix

It is also recommended that a new study be carried out applying the branch of chemistry concerned with the application of the techniques and theories of physics to study chemical changes in nanocomposites exposed to liquid media.

List of publications

1. Saharudin, Mohd Shahneel, Atif, Rasheed, Shyha, Islam and Inam, Fawad (2016) The degradation of mechanical properties in halloysite nanotubes-polyester nanocomposites exposed to diluted methanol. *Journal of Composite Materials*. ISSN 1530-793X.
2. Saharudin, Mohd Shahneel, Atif, Rasheed, Shyha, Islam and Inam, Fawad (2016) The degradation of mechanical properties in polymer nanocomposites exposed to liquid media - A review. *RSC Advances*, 6. pp. 1076-1089. ISSN 2046-2069.
3. Saharudin, Mohd, Wei, Jiacheng, Shyha, Islam and Inam, Fawad (2016) The degradation of mechanical properties in halloysite nanoclay-polyester nanocomposites exposed in seawater environment. *Journal of Nanomaterials* (JNM), 2016. p. 2604631. ISSN 1687-4110.
4. Saharudin, Mohd Shahneel, Atif, Rasheed and Inam, Fawad (2017) Effect of short-term water exposure on the mechanical properties of halloysite nanotube-multi layer graphene reinforced polyester nanocomposites. *Polymers,* 9 (1). p. 27. ISSN 2073-4360.
5. Saharudin, Mohd, Wei, Jiacheng, Shyha, Islam and Inam, Fawad (2017) Flexural Properties of Halloysite Nanotubes-Polyester Nanocomposites Exposed to Aggressive Environment. *International Journal of Chemical, Molecular, Nuclear, Materials and Metallurgical Engineering*, 11 (4). pp. 278-282.

6. Saharudin, Mohd Shahneel, Shyha, Islam and Inam, Fawad (2016) The effect of methanol exposure on the flexural and tensile properties of halloysite halloysite nanotubes/polyester. *International Journal of Advances in Science Engineering and Technology*, 4 (1*). pp. 42-46. ISSN 2321-9009.
7. Saharudin, Mohd Shahneel, Shyha, Islam and Inam, Fawad (2016) Viscoelastic and Mechanical Properties of Multi-layered Graphene Polyester Composites. In: *ICAME2016 - 2nd International Conference on Advances in Mechanical Engineering*, 10th - 13th May 2016, Istanbul, Turkey.
8. Wei, Jiacheng, Mohd Shahneel Saharudin, Thuc Vo, and Fawad Inam. "N, N-Dimethylformamide (DMF) usage in epoxy/graphene nanocomposites: problems associated with reaggregation." *Polymers* 9, no. 6 (2017): 193.

References

[1] Saharudin MS, Jumahat A, Kahar AZ, et al. The Influence of Alumina Filler on Impact Properties of Short Glass Fiber Reinforced Epoxy. In: *Applied Mechanics and Materials*, pp. 88–93.

[2] Day R, Reznik S, Rumyantsev S. Design of Temperature Measurements in Carbon Epoxy Polymer Structures under Microwave Treatment. *ACMTAA-2013* 2014; 24.

[3] Lewis PR. Environmental stress cracking of polycarbonate catheter connectors. *Engineering Failure Analysis* 2009; 16: 1816–1824.

[4] Crosby AJ, Lee J. Polymer Nanocomposites: The 'Nano' Effect on Mechanical Properties. *Polymer Reviews* 2007; 47: 217–229.

[5] Paul DR, Robeson LM. Polymer nanotechnology: Nanocomposites. *Polymer* 2008; 49: 3187–3204.

[6] Friedrich K, Schlarb AK. *Tribology of polymeric nanocomposites: friction and wear of bulk materials and coatings*. Elsevier, 2011.

[7] Bouty A, Petitjean L, Degrandcourt C, et al. Nanofiller structure and reinforcement in model silica/rubber composites: A quantitative correlation driven by interfacial agents. *Macromolecules* 2014; 47: 5365–5378.

[8] Bindu P, Thomas S. Viscoelastic behavior and reinforcement mechanism in rubber nanocomposites in the vicinity of spherical nanoparticles. *The journal of physical chemistry B* 2013; 117: 12632–48.

[9] Balazs AC, Emrick T, Russell TP. Nanoparticle polymer composites: where two small worlds meet. *Science (New York, NY)* 2006; 314: 1107–1110.

[10] Schmidt G, Malwitz MM. Properties of polymer-nanoparticle composites. *Current Opinion in Colloid and Interface Science* 2003; 8: 103–108.

[11] Gao F. Clay/polymer composites: the story. *Materials Today* 2004; 7: 50–55.

[12] Njuguna J, Pielichowski K, Desai S. Nanofiller-reinforced polymer nanocomposites. *Polymers for Advanced Technologies* 2008; 19: 947–959.

[13] Hill S. Mystery of the Titanic: A case of brittle fracture? *Materials World* 1996; 4: 334–335.

[14] Zainuddin S, Hosur M V., Zhou Y, et al. Durability studies of montmorillonite clay filled epoxy composites under different environmental conditions. *Materials Science and Engineering A* 2009; 507: 117–123.

[15] Gellert EP, Turley DM. Seawater immersion ageing of glass-fibre reinforced

polymer laminates for marine applications. *Composites Part A: Applied Science and Manufacturing* 1999; 30: 1259–1265.

[16] Kootsookos A, Mouritz AP. Seawater durability of glass- and carbon-polymer composites. *Composites Science and Technology* 2004; 64: 1503–1511.

[17] Berketis K, Tzetzis D, Hogg PJ. The influence of long term water immersion ageing on impact damage behaviour and residual compression strength of glass fibre reinforced polymer (GFRP). *Materials and Design* 2008; 29: 1300–1310.

[18] Huang G, Sun H. Effect of water absorption on the mechanical properties of glass/polyester composites. *Materials and Design* 2007; 28: 1647–1650.

[19] Neogi P, Zahedi G. Environmental Stress Cracking of Glassy Polymers. *Industrial & Engineering Chemistry Research* 2014; 53: 672–677.

[20] Henry LF. Prediction and evaluation of the susceptibilities of glassy thermoplastics to environmental stress cracking. *Polymer Engineering & Science* 1974; 14: 167–176.

[21] Andena L, Castellani L, Castiglioni A, et al. Determination of environmental stress cracking resistance of polymers: Effects of loading history and testing configuration. *Engineering Fracture Mechanics* 2013; 101: 33–46.

[22] Ollier R, Rodriguez E, Alvarez V. Unsaturated polyester/bentonite nanocomposites: Influence of clay modification on final performance. *Composites Part A: Applied Science and Manufacturing* 2013; 48: 137–143.

[23] Patel P. *Environmental stress cracking in thermoplastics polyurethanes*. Environmental stress cracking in thermoplastic polyurethanes, 1982.

[24] Blaga A, Yamasaki RS. Mechanism of breakdown in the interface region of glass reinforced polyester by artificial weathering. *Journal of Materials Science* 1973; 8: 654–666.

[25] Jansen J. The plastics killer. In: *Advanced Materials and Processes*. Winconsin, 2004, pp. 50–53.

[26] Sadler JM, Toulan FR, Palmese GR, et al. Unsaturated polyester resins for thermoset applications using renewable isosorbide as a component for property improvement. *Journal of Applied Polymer Science*; 132.

[27] Parashar A, Mertiny P. Impact of scaling on fracture strength of adhesively bonded fibre-reinforced polymer piping. *Procedia Engineering* 2011; 10: 455–459.

[28] Bonnia NN. Mechanical properties and environmental stress cracking resistance of rubber toughened polyester/kenaf composite. *eXPRESS Polymer Letters* 2010; 4: 55–61.

[29] Fink JK. Unsaturated Polyester Resins. *Reactive Polymers Fundamentals and Applications* 2008; 1–67.

[30] Parashar A, Mertiny P. Impact of scaling on fracture strength of adhesively bonded fibre-reinforced polymer piping. *Procedia Engineering* 2011; 10: 455–459.

[31] Wright DC. *Environmental stress cracking of plastics*. iSmithers Rapra Publishing, 1996.

[32] Wright D. *Failure of Plastics and Rubber Products*. Rapra Technology Limited, 2006.

[33] Osswald T, Menges G. Failure and damage of polymers. *Mater Sci Polym Eng Munich: Hanser Publishers* 2003; 447–519.

[34] Das TK, Prusty S. Graphene-Based Polymer Composites and Their Applications. *Polymer-Plastics Technology and Engineering* 2013; 52: 130227104444003.

[35] Holbery J, Houston D. Natural-Fiber-Reinforced Polymer Composites in Automotive Applications.

[36] Potts JR, Dreyer DR, Bielawski CW, et al. Graphene-based polymer nanocomposites. *Polymer* 2011; 52: 5–25.

[37] Friedrich K. *Application of fracture mechanics to composite materials*. Elsevier, 2012.

[38] Wright DC. *Environmental Stress Cracking of Plastics*. iSmithers Rapra Publishing, 1996.

[39] Young RJ, Lovell PA. *Introduction to polymers*. CRC press, 2011.

[40] Bonnia NN, Ahmad SH, Surip SN, et al. Mechanical Properties and Environmental Stress Cracking Resistance of Rubber Toughened Polyester/Clay Composite. In: *Advanced Materials Research*. Trans Tech Publications, 2012, pp. 318–321.

[41] Saharudin MS, Atif R, Shyha I, et al. The degradation of mechanical properties in polymer nano-composites exposed to liquid media – a review. *RSC Adv* 2016; 6: 1076–1089.

[42] Saharudin MS, Shyha I, Inam F. The effect of methanol exposure on the flexural and tensile properties of halloysite nanoclay polyester. In: *The IRES 17th International Conference, United Kingdom*. London, 2015, pp. 40–44.

[43] Saharudin MS, Rasheed A, Shyha I, et al. The degradation of mechanical properties in halloysite nanoclay – polyester nanocomposites exposed to diluted methanol. *Journal of Composite Materials* 2016; 1–12.

[44] Khodabandelou M, Razavi Aghjeh MK, Rezaei M. Fracture behavior and

environmental stress cracking resistance (ESCR) of HIPS/PE blends and the effect of compatibilization on their properties. *Engineering Fracture Mechanics* 2009; 76: 2856–2867.

[45] Cicek V. *Corrosion Engineering*. 2014. Epub ahead of print 2014. DOI: 10.1002/9781118720837.

[46] Kain V. Stress Corrosion Cracking. *Stress Corrosion Cracking* 2011; 199–244.

[47] Papavinasam S. *Corrosion Control in the Oil and Gas Industry*. 2014. Epub ahead of print 2014. DOI: 10.1016/B978-0-12-397022-0.00005-4.

[48] Ehrnstén U. 5.05 – Corrosion and Stress Corrosion Cracking of Austenitic Stainless Steels. *Comprehensive Nuclear Materials* 2012; 93–104.

[49] Fyfitch S. Corrosion and stress corrosion cracking of ni-base alloys. In: *Comprehensive Nuclear Materials*. 2012, pp. 69–92.

[50] Turnbull A, Wright L, Crocker L. New insight into the pit-to-crack transition from finite element analysis of the stress and strain distribution around a corrosion pit. *Corrosion Science* 2010; 52: 1492–1498.

[51] Deanin RD, Hauser DI. Recent developments in environmental stress-crack resistance of plastics. *Polymer-Plastics Technology and Engineering* 1981; 17: 123–137.

[52] Arnold JC. The effects of diffusion on environmental stress crack initiation in PMMA. *Journal of Materials Science* 1998; 33: 5193–5204.

[53] Borisova B, Kressler J. Environmental Stress- Cracking Resistance of LDPE/EVA Blends. *Macromolecular Materials and Engineering* 2003; 288: 509–515.

[54] Gent AN. Hypothetical mechanism of crazing in glassy plastics. *Journal of Materials Science* 1970; 5: 925–932.

[55] Knight AC. Stress crazing of transparent plastics. Computed stresses at a nonvoid craze mark. *Journal of Polymer Science Part A: General Papers* 1965; 3: 1845–1857.

[56] Hansen CM. On predicting environmental stress cracking in polymers. *Polymer Degradation and Stability* 2002; 77: 43–53.

[57] Widiastuti I, Sbarski I, Masood SH. Creep behavior of PLA-based biodegradable plastic exposed to a hydrocarbon liquid. *Journal of Applied Polymer Science* 2013; 127: 2654–2660.

[58] Kjellander CK, Nielsen TB, Ghanbari-Siahkali A, et al. ESC resistance of commercial grade polycarbonates during exposure to butter and related chemicals. *Polymer Degradation and Stability* 2008; 93: 1486–1495.

[59] Jawahar P, Gnanamoorthy R, Balasubramanian M. Tribological behaviour of clay - thermoset polyester nanocomposites. *Wear* 2006; 261: 835–840.

[60] Dhakal H, Zhang Z, Richardson M. Effect of water absorption on the mechanical properties of hemp fibre reinforced unsaturated polyester composites. *Composites Science and Technology* 2007; 67: 1674–1683.

[61] Gabr MH, Phong NT, Abdelkareem MA, et al. Mechanical, thermal, and moisture absorption properties of nano-clay reinforced nano-cellulose biocomposites. *Cellulose* 2013; 20: 819–826.

[62] Ramakrishna S, Mayer J, Wintermantel E, et al. Biomedical applications of polymer-composite materials: A review. *Composites Science and Technology* 2001; 61: 1189–1224.

[63] Lee LJ. Polymer nanoengineering for biomedical applications. *Annals of Biomedical Engineering* 2006; 34: 75–88.

[64] Brendel CM. *Biocompatibility of Polymer Implants for Medical Applications*. Biocompatibility of Polymer Implants for Medical Applicationshttp://etd.ohiolink.edu/send-pdf.cgi/Brendel Christopher M.pdf?acc_num=akron1246892895 (2009).

[65] Ikada Y, Tsuji H. Biodegradable polyesters for medical and ecological applications. *Macromolecular rapid communications* 2000; 21: 117–132.

[66] Li X. Environmental stress cracking resistance of a new copolymer of bisphenol-A. *Polymer Degradation and Stability* 2005; 90: 44–52.

[67] Isayev AI. Thermal Stresses. *Encyclopedia of Polymer Science and Engineering* 1987; 16: 747–767.

[68] Lustiger A, Ishikawa N. An analytical technique for measuring relative tie-molecule concentration in polyethylene. *Journal of Polymer Science Part B: Polymer Physics* 1991; 29: 1047–1055.

[69] Portnoy RC. *Medical plastics: degradation resistance and failure analysis*. William Andrew, 1998.

[70] Papavinasam S. *Corrosion Control in the Oil and Gas Industry*. Epub ahead of print 2014. DOI: 10.1016/B978-0-12-397022-0.00005-4.

[71] Bobić B, Mitrović S, Babić M, et al. Corrosion of Metal-Matrix composites with aluminium alloy substrate. *Tribology in Industry* 2010; 32: 3–11.

[72] Farshad M, Necola A. Strain corrosion of glass fibre-reinforced plastics pipes. *Polymer Testing* 2004; 23: 517–521.

[73] Dai J, Yao X, Liang X, et al. Experimental study of micro-cracks in stress corrosion

of fiber reinforced composites. *Polymer Testing* 2006; 25: 758–765.

[74] Farshad M, Necola A. Effect of aqueous environment on the long-term behavior of glass fiber-reinforced plastic pipes. *Polymer Testing* 2004; 23: 163–167.

[75] Hull D, Kumosa M, Price JN. Stress corrosion of aligned glass fibre-polyester composite material. *Materials Science and Technology* 1985; 1: 177–182.

[76] Kumosa M, Hull D, Price JN. Acoustic emission from stress corrosion cracks in aligned GRP. *Journal of materials science* 1987; 22: 331–336.

[77] Megel M, Kumosa L, Ely T, et al. Initiation of Stress Corrosion Cracking in Unidirectional Glass / Polymer Composite Materials. *Science* 2001; 61: 231–246.

[78] Kumosa L, Benedikt B, Armentrout D, et al. Moisture absorption properties of unidirectional glass/polymer composites used in composite (non-ceramic) insulators. *Composites Part A: Applied Science and Manufacturing* 2004; 35: 1049–1063.

[79] Kumosa L, Kumosa M, Armentrout D. Resistance to stress corrosion cracking of unidirectional ECR-glass/polymer composites for high voltage composite insulator applications. *Composites Part A: Applied Science and Manufacturing* 2003; 34: 1–15.

[80] Kumosa MS, Kumosa LS, Armentrout DL. Failure analyses of nonceramic insulators Part 1: Brittle fracture characteristics. *IEEE Electrical Insulation Magazine* 2005; 21: 14–27.

[81] Odegard G, Searles K, Kumosa M. A continuum elastic-plastic model for woven-fabric/polymer-matrix composite materials under biaxial stresses. *Composites Science and Technology* 2001; 61: 2501–2510.

[82] Chughtai AR, Smith DM, Kumosa MS. Chemical analysis of a field-failed composite suspension insulator. *Composites Science and Technology* 1998; 58: 1641–1647.

[83] Qiu Q, Kumosa M. Corrosion of E-glass fibers in acidic environments. *Composites Science and Technology* 1997; 57: 497–507.

[84] Kumosa M, Armentrout D, Kumosa L, et al. Analyses of composite insulators with crimped end-fittings: Part II - Suitable crimping conditions. *Composites Science and Technology* 2002; 62: 1209–1221.

[85] Shokrieh MM, Memar M. Stress corrosion cracking of basalt/epoxy composites under bending loading. *Applied Composite Materials* 2010; 17: 121–135.

[86] Noble B, Harris SJ, Owen MJ. Stress corrosion cracking of GRP pultruded rods in acid environments. *Journal of Materials Science* 1983; 18: 1244–1254.

[87] Caddock BD, Evans KE, Masters IG. Diffusion behaviour of the core-sheath

structure in E-glass fibres exposed to aqueous HCl. *Journal of materials science* 1989; 24: 4100–4105.

[88] Rodriguez EL. Corrosion of glass fibres. *Journal of materials science letters* 1987; 6: 718–720.

[89] Phillips MG. Prediction of long-term stress-rupture life for glass fibre-reinforced polyester composites in air and in aqueous environments. *Composites* 1983; 14: 270–275.

[90] Norwood LS, Millman AF. Strain limited design criteria for reinforced plastic process equipment. *Composites* 1980; 11: 39–45.

[91] Aveston J, Sillwood JM. Long-term strength of glass-reinforced plastics in dilute sulphuric acid. *Journal of Materials Science* 1982; 17: 3491–3498.

[92] Hsu P-L, Yau S-S, Chou T-W. Stress-corrosion cracking and its propagation in aligned short-fibre composites. *Journal of materials science* 1986; 21: 3703–3709.

[93] Hull D, Kumosa M, Price JN. Stress corrosion of aligned glass fibre-polyester composite material. *Materials Science and Technology* 1985; 1: 177–182.

[94] Kumosa M, Hull D, Price JN. Acoustic emission from stress corrosion cracks in aligned GRP. *Journal of materials science* 1987; 22: 331–336.

[95] Friedrich K. Stress corrosion crack propagation in glass fibre reinforced/thermoplastic PET. *Journal of Materials Science* 1981; 16: 3292–3302.

[96] Azwa ZN, Yousif BF, Manalo AC, et al. A review on the degradability of polymeric composites based on natural fibres. *Materials & Design* 2013; 47: 424–442.

[97] Sreekala MS, Kumaran MG, Thomas S. Water sorption in oil palm fiber reinforced phenol formaldehyde composites. *Composites - Part A: Applied Science and Manufacturing* 2002; 33: 763–777.

[98] Schmitz GK, Metcalfe AG. Stress corrosion of E-glass fibers. *Industrial & Engineering Chemistry Product Research and Development* 1966; 5: 1–8.

[99] Le Duigou A, Davies P, Baley C. Seawater ageing of flax/poly(lactic acid) biocomposites. *Polymer Degradation and Stability* 2009; 94: 1151–1162.

[100] Maurin R, Perrot Y, Bourmaud A, et al. Seawater ageing of low styrene emission resins for marine composites: Mechanical behaviour and nano-indentation studies. *Composites Part A: Applied Science and Manufacturing* 2009; 40: 1024–1032.

[101] Akil HM, Santulli C, Sarasini F, et al. Environmental effects on the mechanical behaviour of pultruded jute/glass fibre-reinforced polyester hybrid composites. *Composites Science and Technology* 2014; 94: 62–70.

[102] Lu X, Brown N, Bassani JL. The correlation of slow crack growth in linear polyethylene by the J-integral. *Polymer* 1989; 30: 2215–2221.

[103] Rothon R. *Particulate-Filled Polymer Composites*. 2003.

[104] Chan M, Lau K, Wong T, et al. Mechanism of reinforcement in a nanoclay/polymer composite. *Composites Part B: Engineering* 2011; 42: 1708–1712.

[105] Chen Y. Investigations of environmental stress cracking resistance of HDPE/EVA and LDPE/EVA blends. *Journal of Applied Polymer Science* 2014; 131: 1–8.

[106] Schellenberg,J Fienhold G. Environmental Stress Cracking Resistance of Blends of High-Density Polyethylene With Other Polyethylenes. *Polymer Engineering and Science*; 38.

[107] Hawkins WL. *Polymer degradation and stabilization*. Springer Science & Business Media, 2012.

[108] Pandey JK, Raghunatha Reddy K, Pratheep Kumar A, et al. An overview on the degradability of polymer nanocomposites. *Polymer Degradation and Stability* 2005; 88: 234–250.

[109] White JR, Turnbull a. Weathering of polymers: mechanisms of degradation and stabilization, testing strategies and modelling. *Journal of Materials Science* 1994; 29: 584–613.

[110] Lin L, Schlarb A. A study on environmental stress cracking in nano-SiO2-filled polycarbonate. *Journal of Materials Science* 2012; 47: 6614–6620.

[111] Nomai J, Schlarb AK. Environmental stress cracking (ESC) resistance of polycarbonate/SiO_2 nanocomposites in different media. *Journal of Applied Polymer Science* 2017; 45451: 45451.

[112] Soares JBP, Abbott RF, Kim JD. Environmental stress cracking resistance of polyethylene: The use of CRYSTAF and SEC to establish structure-property relationships. *Journal of Polymer Science, Part B: Polymer Physics* 2000; 38: 1267–1275.

[113] George J, Bhagawan SS, Thomas S. Effects of environment on the properties of low-density polyethylene composites reinforced with pineapple-leaf fibre. *Composites Science and Technology* 1998; 58: 1471–1485.

[114] Stuart HA, Markowski G, Jeschke D. Kunststoffe 54 (1964) 618. *Google Scholar*.

[115] Robeson LM. Environmental stress cracking: A review. *Polymer Engineering & Science* 2013; 53: 453–467.

[116] Ji-Hua Z, Mao-Sheng Z. Visual experiments for water absorbing process of fiber-reinforced composites. *Journal of composite materials* 2004; 38: 779–790.

[117] Mazuki AAM, Akil HM, Safiee S, et al. Degradation of dynamic mechanical properties of pultruded kenaf fiber reinforced composites after immersion in various solutions. *Composites Part B: Engineering* 2011; 42: 71–76.

[118] Joseph P., Rabello MS, Mattoso LH., et al. Environmental effects on the degradation behaviour of sisal fibre reinforced polypropylene composites. *Composites Science and Technology* 2002; 62: 1357–1372.

[119] Garcia-Espinel JD, Castro-Fresno D, Parbole Gayo P, et al. Effects of sea water environment on glass fiber reinforced plastic materials used for marine civil engineering constructions. *Materials & Design* 2015; 66: 46–50.

[120] Yan L, Chouw N, Jayaraman K. Effect of UV and water spraying on the mechanical properties of flax fabric reinforced polymer composites used for civil engineering applications. *Materials & Design* 2015; 71: 17–25.

[121] Abral H, Kadriadi D, Rodianus A, et al. Mechanical properties of water hyacinth fibers--polyester composites before and after immersion in water. *Materials & Design* 2014; 58: 125–129.

[122] Espert A, Vilaplana F, Karlsson S. Comparison of water absorption in natural cellulosic fibres from wood and one-year crops in polypropylene composites and its influence on their mechanical properties. *Composites Part A: Applied Science and Manufacturing* 2004; 35: 1267–1276.

[123] Garcia-Espinel JD, Castro-Fresno D, Parbole Gayo P, et al. Effects of sea water environment on glass fiber reinforced plastic materials used for marine civil engineering constructions. *Materials & Design* 2015; 66: 46–50.

[124] Rull N, Ollier RP, Francucci G, et al. Effect of the addition of nanoclays on the water absorption and mechanical properties of glass fiber/up resin composites. *Journal of Composite Materials* 2015; 49: 1629–1637.

[125] Moghbelli E, Banyay R, Sue H-J. Effect of moisture exposure on scratch resistance of PMMA. *Tribology International* 2014; 69: 46–51.

[126] Alamri H, Low IM. Effect of water absorption on the mechanical properties of nano-filler reinforced epoxy nanocomposites. *Materials & Design* 2012; 42: 214–222.

[127] Athijayamani A, Thiruchitrambalam M, Natarajan U, et al. Effect of moisture absorption on the mechanical properties of randomly oriented natural fibers/polyester hybrid composite. *Materials Science and Engineering A* 2009; 517: 344–353.

[128] Liu X, Wu Q, Berglund LA, et al. Polyamide 6-clay nanocomposites/polypropylene-grafted-maleic anhydride alloys. *Polymer* 2001; 42: 8235–8239.

[129] Ward WJ, Gaines GL, Alger MM, et al. Gas barrier improvement using vermiculite and mica in polymer films. *Journal of Membrane Science* 1991; 55: 173–180.

[130] Ishak MR, Sapuan SM, Leman Z, et al. Sugar palm (Arenga pinnata): Its fibres, polymers and composites. *Carbohydr Polym* 2013; 91: 699–710.

[131] Bachtiar D, Sapuan SM, Zainudin ES, et al. The tensile properties of single sugar palm (Arenga pinnata) fibre. *IOP Conference Series: Materials Science and Engineering* 2010; 11: 12012.

[132] Liu W, Hoa S V., Pugh M. Fracture toughness and water uptake of high-performance epoxy/nanoclay nanocomposites. *Composites Science and Technology* 2005; 65: 2364–2373.

[133] Alamri H, Low IM. Microstructural, mechanical, and thermal characteristics of recycled cellulose fiber-halloysite-epoxy hybrid nanocomposites. *Polymer Composites* 2012; 33: 589–600.

[134] Pramoda KP, Liu T. Effect of moisture on the dynamic mechanical relaxation of polyamide-6/clay nanocomposites. *Journal of Polymer Science, Part B: Polymer Physics* 2004; 42: 1823–1830.

[135] Rhim JW, Hong SI, Ha CS. Tensile, water vapor barrier and antimicrobial properties of PLA/nanoclay composite films. *LWT - Food Science and Technology* 2009; 42: 612–617.

[136] Müller CMO, Laurindo JB, Yamashita F. Effect of nanoclay incorporation method on mechanical and water vapor barrier properties of starch-based films. *Industrial Crops and Products* 2011; 33: 605–610.

[137] Karmaker AC, Hoffmann A, Hinrichsen G. Influence of water uptake on the mechanical properties of jute fiber-reinforced polypropylene. *Journal of Applied Polymer Science* 1994; 54: 1803–1807.

[138] Kim CH, Youn JR. Determination of residual stresses in injection-moulded flat plate: Simulation and experiments. *Polymer Testing* 2007; 26: 862–868.

[139] Postawa P, Kwiatkowski D. Residual stress distribution in injection molded parts. *Journal of Achievements in Materials and Manufacturing Engineering* 2006; 18: 171–174.

[140] Chen X, Lam YCC, Li DQQ. Analysis of thermal residual stress in plastic injection molding. *Journal of Materials Processing Technology* 2000; 101: 275–280.

[141] Zhou H, Li D. Residual stress analysis of the post-filling stage in injection moulding. *International Journal of Advanced Manufacturing Technology* 2005; 25: 700–704.

[142] Pons N, Bergeret A, Benezet JC, et al. An environmental stress cracking (ESC) test to study the ageing of biopolymers and biocomposites. *Polymer Testing* 2011; 30: 310–317.

[143] Borisova B. *Investigations on Environmental Stress Cracking Resistance of LDPE*

/ *EVA Blends Dissertation*. Martin-Luther-Universität Halle-Wittenberg, 2004.

[144] Brown N, Lu X. A fundamental theory for slow crack growth in polyethylene. *Polymer* 1995; 36: 543–548.

[145] Huang Y-L, Brown N. Slow crack growth in blends of HDPE and UHMWPE. *Polymer* 1992; 33: 2989–2997.

[146] Ward AL, Lu X, Huang Y, et al. The mechanism of slow crack growth in polyethylene by an environmental stress cracking agent. *Polymer* 1991; 32: 2172–2178.

[147] Evans A. Slow crack growth in brittle materials under dynamic loading conditions. *International Journal of Fracture* 1974; 10: 251–259.

[148] Akdemir A, Tarakcioglu N, Avci A. Stress corrosion crack growth in glass / polyester composites with surface crack. *Stress: The International Journal on the Biology of Stress* 2001; 32: 123–129.

[149] Lim JK. *Stress Corrosion Cracking*. Epub ahead of print 2011. DOI: 10.1533/9780857093769.3.485.

[150] Farias R, Canedo E, Wellen R, et al. Environmental Stress Cracking of Poly (3-hydroxibutyrate) Under Contact with Sodium Hydroxide 3 . Results and Discussion. *Materials Research* 2015; 18: 258–266.

[151] Muhammad YH, Ahmad S, Bakar MAA, et al. Mechanical properties of hybrid glass/kenaf fibre-reinforced epoxy composite with matrix modification using liquid epoxidised natural rubber. *Journal of Reinforced Plastics and Composites* 2015; 34: 896–906.

[152] Ruban Y, Mon S, Roy D. Chemical resistance / thermal and mechanical properties of unsaturated polyester-based nanocomposites. *Applied Nanoscience* 2014; 233–240.

[153] Alperstein D, Knani D, Borchmann N, et al. Prediction of environmental stress cracking in polycarbonate by molecular modeling. *Polymers for Advanced Technologies* 2014; 1433–1438.

[154] Grassi VG, Dal Pizzol MF, Forte MMC, et al. Influence of small rubber particles on the environmental stress cracking of high impact polystyrene. *Journal of Applied Polymer Science* 2011; 121: 1697–1706.

[155] Alimi L, Chaoui K, Ghabeche W, et al. Short-term HDPE pipe degradation upon exposure to aggressive environments. *Mat{é}riaux & Techniques* 2013; 101: 701.

[156] Dashtizadeh A, Abdouss M, Mahdavi H, et al. Acrylic coatings exhibiting improved hardness, solvent resistance and glossiness by using silica nano-composites. *Applied Surface Science* 2011; 257: 2118–2125.

[157] Byoung-Ho Choi, Jeffrey Weinhold, David Reuschle MK. Modeling of the Fracture Mechanism of HDPE Subjected to Environmental Stress Crack Resistance Test. *Polymer Engineering and Science* 2009; 47: 2085–2091.

[158] Lagarón JM, Dixon NM, Gerrard DL, et al. Cold-Drawn Material As Model Material for the Environmental Stress Cracking (ESC) Phenomenon in Polyethylene. A Raman Spectroscopy Study of Molecular Stress Induced by Macroscopic Strain in Drawn Polyethylenes and Their Relation to Environmental Stress Cr. *Macromolecules* 1998; 31: 5845–5852.

[159] Teofilo ET, Silva SML, Rabello MS. Stress cracking and chemical degradation of poly(ethylene terephthalate) in NaOH aqueous solutions. *Journal of Applied Polymer Science* 2010; 118: 3089–3101.

[160] Sahin OS, Akdemir A, Avci A, et al. Fatigue crack growth behavior of filament wound composite pipes in corrosive environment. *Journal of Reinforced Plastics and Composites* 2008; 2957–2970.

[161] Wood CA, Bradley WL. Determination of the effect of seawater on the interfacial strength of an interlayer E-glass/graphite/epoxy composite by in situ observation of transverse cracking in an environmental SEM. *Composites science and Technology* 1997; 57: 1033–1043.

[162] Zhou J, Lucas JP. The effects of a water environment on anomalous absorption behavior in graphite/epoxy composites. *Composites Science and Technology* 1995; 53: 57–64.

[163] Cho K, Lee MS, Park CE. Environmental stress cracking of rubber-modified styrenic polymers in Freon vapour. *Polymer* 1997; 38: 4641–4650.

[164] Ramsteiner F, McKee G., Breulmann M. Influence of void formation on impact toughness in rubber modified styrenic-polymers. *Polymer* 2002; 43: 5995–6003.

[165] Skudra M. *Strength of fibrous composites*. 1974. Epub ahead of print 1974. DOI: 10.1007/BF00856375.

[166] Arbelaiz A, Fernández B, Cantero G, et al. Mechanical properties of flax fibre/polypropylene composites. Influence of fibre/matrix modification and glass fibre hybridization. *Composites Part A: Applied Science and Manufacturing* 2005; 36: 1637–1644.

[167] Hufenbach W, Böhm R, Thieme M, et al. Polypropylene/glass fibre 3D-textile reinforced composites for automotive applications. *Materials and Design* 2011; 32: 1468–1476.

[168] Santulli C. Impact properties of glass/plant fibre hybrid laminates. *Journal of Materials Science* 2007; 42: 3699–3707.

[169] Gustin J, Joneson A, Mahinfalah M, et al. Low velocity impact of combination

Kevlar/carbon fiber sandwich composites. *Composite Structures* 2005; 69: 396–406.

[170] Cheng M, Chen W, Weerasooriya T. Mechanical Properties of Kevlar® KM2 Single Fiber. *Journal of Engineering Materials and Technology* 2005; 127: 197.

[171] Bencomo-Cisneros J a., Tejeda-Ochoa a., García-Estrada J a., et al. Characterization of Kevlar-29 fibers by tensile tests and nanoindentation. *Journal of Alloys and Compounds* 2012; 536: S456–S459.

[172] Ku H, Wang H, Pattarachaiyakoop N, et al. A review on the tensile properties of natural fiber reinforced polymer composites. *Composites Part B: Engineering* 2011; 42: 856–873.

[173] Miller W, Ren Z, Smith CW, et al. A negative Poisson's ratio carbon fibre composite using a negative Poisson's ratio yarn reinforcement. *Composites Science and Technology* 2012; 72: 761–766.

[174] Williams G, Trask R, Bond I. A self-healing carbon fibre reinforced polymer for aerospace applications. *Composites Part A: Applied Science and Manufacturing* 2007; 38: 1525–1532.

[175] Williams DF, McNamara, Turner RM. Potential of polyetheretherketone (PEEK) and carbon-fibre-reinforced PEEK in medical applications. *Journal of Materials Science Letters* 1987; 6: 188–190.

[176] Pimenta S, Pinho ST. Recycling carbon fibre reinforced polymers for structural applications: Technology review and market outlook. *Waste Management* 2011; 31: 378–392.

[177] Jenkins GM, de Carvalho FX. Biomedical applications of carbon fibre reinforced carbon in implanted prostheses. *Carbon* 1977; 15: 33–37.

[178] Rasheed A, Khalid FA. Fabrication and properties of CNTs reinforced polymeric matrix nanocomposites for sports applications. *IOP Conference Series: Materials Science and Engineering* 2014; 60: 12009.

[179] Starr T. *Glass-fibre Directory and Databook*. Springer Science & Business Media, 1996.

[180] Gamstedt EK, Berglund LA, Peijs T. Fatigue mechanisms in unidirectional glass-fibre-reinforced polypropylene. *Composites Science and Technology* 1999; 59: 759–768.

[181] Ramsaroop A, Kanny K, Mohan TP. Fracture Toughness Studies of Polypropylene-Clay Nanocomposites and Glass Fibre Reinfoerced Polypropylene Composites. *Materials Sciences and Applications* 2010; 1: 301–309.

[182] Thomason J, Jenkins P, Yang L. Glass Fibre Strength—A Review with Relation to

Composite Recycling. *Fibers* 2016; 4: 18.

[183] Wei J, Vo T, Inam F. Epoxy/graphene nanocomposites – processing and properties: a review. *RSC Adv* 2015; 5: 73510–73524.

[184] Inam F, Bhat BR, Vo T, et al. Structural health monitoring capabilities in ceramic–carbon nanocomposites. *Ceramics International* 2014; 40: 3793–3798.

[185] Kim H, Abdala A, MacOsko CW. Graphene/polymer nanocomposites. *Macromolecules* 2010; 43: 6515–6530.

[186] Verdejo R, Bernal MM, Romasanta LJ, et al. Graphene filled polymer nanocomposites. *Journal of Materials Chemistry* 2011; 21: 3301–3310.

[187] Geim AK, Novoselov KS. The rise of graphene. *Nature Mater* 2007; 6: 183–191.

[188] Yang K, Feng L, Hong H, et al. Preparation and functionalization of graphene nanocomposites for biomedical applications. *Nat Protoc* 2013; 8: 2392–2403.

[189] Geim AK. Graphene: status and prospects. *Science (New York, NY)* 2009; 324: 1530–4.

[190] Singh V, Joung D, Zhai L, et al. Graphene based materials: Past, present and future. *Progress in Materials Science* 2011; 56: 1178–1271.

[191] Ansari S, Giannelis EP. Phase equilibria and charge fractionation in polydisperse polyelectrolyte solutions. *Polymer Science* 2009; 888–897.

[192] Lee YR, Raghu A V., Jeong HM, et al. Properties of waterborne polyurethane/functionalized graphene sheet nanocomposites prepared by an in situ method. *Macromolecular Chemistry and Physics* 2009; 210: 1247–1254.

[193] Ramanathan T, Abdala AA, Stankovich S, et al. Functionalized graphene sheets for polymer nanocomposites. *Nature nanotechnology* 2008; 3: 327–331.

[194] Stankovich S, Dikin D a, Dommett GHB, et al. Graphene-based composite materials. *Nature* 2006; 442: 282–286.

[195] Xu Y, Wang Y, Liang J, et al. A hybrid material of graphene and poly (3,4-ethyldioxythiophene) with high conductivity, flexibility, and transparency. *Nano Research* 2009; 2: 343–348.

[196] Inam F, Luhyna N. Carbon Nanotubes for Epoxy Nanocomposites : A Review on Recent Developments Carbon Nanotubes for Epoxy Nanocomposites : A Review on Recent. *Carbon* 2012; 80–86.

[197] Inam F, Wong DWY, Kuwata M, et al. Multiscale Hybrid Micro-Nanocomposites Based on Carbon Nanotubes and Carbon Fibers. *Journal of Nanomaterials* 2010; 2010: 1–12.

[198] Inam F, Heaton A, Brown P, et al. Effects of dispersion surfactants on the properties of ceramic-carbon nanotube (CNT) nanocomposites. *Ceramics International* 2014; 40: 511–516.

[199] Inam F, Peijs T. Re-agglomeration of Carbon nanotubes in two-part epoxy system ; Influence of the concentration. In: *5th International Bhurbhan Conference on Applied Science and Technology (IBCAST 2007)*. 2007, pp. 38–44.

[200] Inam F, Yan H, Jayaseelan DD, et al. Electrically conductive alumina-carbon nanocomposites prepared by Spark Plasma Sintering. *Journal of the European Ceramic Society* 2010; 30: 153–157.

[201] Sahoo NG, Rana S, Cho JW, et al. Polymer nanocomposites based on functionalized carbon nanotubes. *Progress in Polymer Science* 2010; 35: 837–867.

[202] Chatterjee S, Nafezarefi F, Tai NH, et al. Size and synergy effects of nanofiller hybrids including graphene nanoplatelets and carbon nanotubes in mechanical properties of epoxy composites. *Carbon* 2012; 50: 5380–5386.

[203] Mirjalili V, Yourdkhani M, Hubert P. Dispersion stability in carbon nanotube modified polymers and its effect on the fracture toughness. *Nanotechnology* 2012; 23: 315701.

[204] Milsom B, Viola G, Gao Z, et al. The effect of carbon nanotubes on the sintering behaviour of zirconia. *Journal of the European Ceramic Society* 2012; 32: 4149–4156.

[205] Inam F. *Development of Ceramic – Carbon Nanotubes (CNTs) Nanocomposites*. Queen Mary, University of London, 2009.

[206] Tsai TY, Lin MJ, Chuang YC, et al. Effects of modified Clay on the morphology and thermal stability of PMMA/clay nanocomposites. *Materials Chemistry and Physics* 2013; 138: 230–237.

[207] Afzal A, Siddiqi HM, Iqbal N, et al. The effect of SiO2 filler content and its organic compatibility on thermal stability of epoxy resin. *Journal of Thermal Analysis and Calorimetry* 2013; 111: 247–252.

[208] Manitiu M, Horsch S, Gulari E, et al. Role of polymer–clay interactions and nano-clay dispersion on the viscoelastic response of supercritical CO2 dispersed polyvinylmethylether (PVME)–Clay nanocomposites. *Polymer* 2009; 50: 3786–3796.

[209] Dusza J, Blugan G, Morgiel J, et al. Hot pressed and spark plasma sintered zirconia/carbon nanofiber composites. *Journal of the European Ceramic Society* 2009; 29: 3177–3184.

[210] Inam F, Yan H, Peijs T, et al. The sintering and grain growth behaviour of ceramic-carbon nanotube nanocomposites. *Composites Science and Technology* 2010; 70:

947–952.

[211] Inam F, Peijs T, Reece MJ. The production of advanced fine-grained alumina by carbon nanotube addition. *Journal of the European Ceramic Society* 2011; 31: 2853–2859.

[212] Pacurari M, Castranova V, Vallyathan V. Single- and multi-wall carbon nanotubes versus asbestos: are the carbon nanotubes a new health risk to humans? *Journal of toxicology and environmental health Part A* 2010; 73: 378–95.

[213] Pacurari M, Castranova V, Vallyathan V. Single- and multi-wall carbon nanotubes versus asbestos: are the carbon nanotubes a new health risk to humans? *Journal of toxicology and environmental health Part A* 2010; 73: 378–95.

[214] Donaldson K, Aitken R, Tran L, et al. Carbon nanotubes: A review of their properties in relation to pulmonary toxicology and workplace safety. *Toxicological Sciences* 2006; 92: 5–22.

[215] Schaefer DW, Justice RS. How nano are nanocomposites? *Macromolecules* 2007; 40: 8501–8517.

[216] Ho M, Wang H, Lee J-H, et al. Critical factors on manufacturing processes of natural fibre composites. *Composites Part B: Engineering* 2012; 43: 3549–3562.

[217] Ratna Prasad AV, Mohana Rao K. Mechanical properties of natural fibre reinforced polyester composites: Jowar, sisal and bamboo. *Materials & Design* 2011; 32: 4658–4663.

[218] Aziz SH, Ansell MP. The effect of alkalization and fibre alignment on the mechanical and thermal properties of kenaf and hemp bast fibre composites: Part 1 – polyester resin matrix. *Composites Science and Technology* 2004; 64: 1219–1230.

[219] Leman Z, Sapuan SM, Saifol AM, et al. Moisture absorption behavior of sugar palm fiber reinforced epoxy composites. *Materials & Design* 2008; 29: 1666–1670.

[220] Mogea J, Seibert B, Smits W. Multipurpose palms: the sugar palm (Arenga pinnata (Wurmb) Merr.). *Agroforestry Systems* 1991; 13: 111–129.

[221] Nam TH, Ogihara S, Tung NH, et al. Effect of alkali treatment on interfacial and mechanical properties of coir fiber reinforced poly(butylene succinate) biodegradable composites. *Composites Part B: Engineering* 2011; 42: 1648–1656.

[222] Nigrawal A, Prajapati SC, Sharma R, et al. Influence of Nano Alumina Addition on Strength, Structure and Thermal Behavior of Chemically Treated Sisal Powder Filled Polyvinyl Alcohol (PVA). *Instrumentation Science & Technology* 2011; 18: 725–736.

[223] Munikenche Gowda T, Naidu a. CB, Chhaya R. Some mechanical properties of untreated jute fabric-reinforced polyester composites. *Composites Part A: Applied*

Science and Manufacturing 1999; 30: 277–284.

[224] Plackett D, Andersen TL, Pedersen WB, et al. Biodegradable composites based on L-polylactide and jute fibres. *Composites Science and Technology* 2003; 63: 1287–1296.

[225] Nishino T, Hirao K, Kotera M, et al. Kenaf reinforced biodegradable composite. *Composites Science and Technology* 2003; 63: 1281–1286.

[226] Kozłowski RM, Mackiewicz-Talarczyk M. *Handbook of Natural Fibres*. Epub ahead of print 2012. DOI: 10.1533/9780857095503.1.

[227] Wambua P, Ivens J, Verpoest I. Natural fibres: Can they replace glass in fibre reinforced plastics? *Composites Science and Technology* 2003; 63: 1259–1264.

[228] Wollerdorfer M, Bader H. Influence of natural fibres on the mechanical properties of biodegradable polymers. *Industrial Crops and Products* 1998; 8: 105–112.

[229] Oksman K, Skrifvars M, Selin JF. Natural fibres as reinforcement in polylactic acid (PLA) composites. *Composites Science and Technology* 2003; 63: 1317–1324.

[230] Jawaid M, Abdul Khalil HPS. Cellulosic/synthetic fibre reinforced polymer hybrid composites: A review. *Carbohydrate Polymers* 2011; 86: 1–18.

[231] Chan ML, Lau KT, Wong TT, et al. Interfacial bonding characteristic of nanoclay/polymer composites. *Applied Surface Science* 2011; 258: 860–864.

[232] Zilg C, Thomann R, Finter J, et al. The influence of silicate modification and compatibilizers on mechanical properties and morphology of anhydride-cured epoxy nanocomposites. *Macromolecular Materials and Engineering* 2000; 280–281: 41–46.

[233] Kornmann X, Lindberg H, Berglund LA. Synthesis of epoxy-clay nanocomposites. Influence of the nature of the curing agent on structure. *Polymer* 2001; 42: 4493–4499.

[234] Sinha Ray S, Okamoto M. Polymer/layered silicate nanocomposites: A review from preparation to processing. *Progress in Polymer Science (Oxford)* 2003; 28: 1539–1641.

[235] Voss H, Kargerkocsis J. Fatigue crack propagation in glass-fibre and glass-sphere filled PBT composites. *International Journal of Fatigue* 1988; 10: 3–11.

[236] Pegoretti A, Ricco T. Fatigue crack propagation in polypropylene reinforced with short glass fibers. *Composites Science and Technology* 1999; 59: 1055–1062.

[237] Pisanova E, Zhandarov S, Mäder E, et al. Three techniques of interfacial bond strength estimation from direct observation of crack initiation and propagation in polymer-fibre systems. *Composites Part A: Applied Science and Manufacturing*

2001; 32: 435–443.

[238] Hussain F. Polymer-matrix Nanocomposites, Processing, Manufacturing, and Application: An Overview. *Journal of Composite Materials* 2006; 40: 1511–1575.

[239] Ahmed S, Jones FR. A review of particulate reinforcement theories for polymer composites. *Journal of Materials Science* 1990; 25: 4933–4942.

[240] Coleman JN, Khan U, Blau WJ, et al. Small but strong: A review of the mechanical properties of carbon nanotube–polymer composites. *Carbon* 2006; 44: 1624–1652.

[241] Cho J, Inam F, Reece MJ, et al. Carbon nanotubes: do they toughen brittle matrices? *Journal of Materials Science* 2011; 46: 4770–4779.

[242] Timmerman JF, Hayes BS, Seferis JC. Nanoclay reinforcement effects on the cryogenic microcracking of carbon fiber / epoxy composites. *Composites Science and Technology* 2002; 62: 1249–1258.

[243] Park JH, Jana SC. The relationship between nano- and micro-structures and mechanical properties in PMMA–epoxy–nanoclay composites. *Polymer* 2003; 44: 2091–2100.

[244] Fu SY, Feng XQ, Lauke B, et al. Effects of particle size, particle/matrix interface adhesion and particle loading on mechanical properties of particulate-polymer composites. *Composites Part B: Engineering* 2008; 39: 933–961.

[245] Lewis Tb, Nielsen Le. Dynamic Mechanical Properties of Particulate-Filled Composites. *Journal of Applied Polymer Science* 1970; 14: 1449–1471.

[246] Mukherjee T, Sani M, Kao N, et al. Improved dispersion of cellulose microcrystals in polylactic acid (PLA) based composites applying surface acetylation. *Chemical Engineering Science* 2013; 101: 655–662.

[247] Pötschke P, Krause B, Buschhorn ST, et al. Improvement of carbon nanotube dispersion in thermoplastic composites using a three roll mill at elevated temperatures. *Composites Science and Technology* 2013; 74: 78–84.

[248] Liang JZ. Reinforcement and quantitative description of inorganic particulate-filled polymer composites. *Composites Part B: Engineering* 2013; 51: 224–232.

[249] Fiedler B, Gojny FH, Wichmann MHG, et al. Fundamental aspects of nano-reinforced composites. *Composites Science and Technology* 2006; 66: 3115–3125.

[250] Sun H, Yang B. In situ preparation of nanoparticles/polymer composites. *Science in China, Series E: Technological Sciences* 2008; 51: 1886–1901.

[251] Palza H, Vergara R, Zapata P. Composites of polypropylene melt blended with synthesized silica nanoparticles. *Composites Science and Technology* 2011; 71: 535–540.

[252] Sprenger S. Epoxy resin composites with surface-modified silicon dioxide nanoparticles: A review. *Journal of Applied Polymer Science* 2013; 130: 1421–1428.

[253] Chen X, Mao SS. Titanium dioxide nanomaterials: Synthesis, properties, modifications and applications. *Chemical Reviews* 2007; 107: 2891–2959.

[254] Chan C-M, Wu J, Li J-X, et al. Polypropylene/calcium carbonate nanocomposites. *Polymer* 2002; 43: 2981–2992.

[255] Varghese S, Gatos KG, Apostolov AA. Morphology and Mechanical Properties of Layered Silicate Reinforced Natural and Polyurethane Rubber Blends Produced by Latex Compounding. *Applied Polymer Science*.

[256] Kaempfer D, Thomann R, Mülhaupt R. Melt compounding of syndiotactic polypropylene nanocomposites containing organophilic layered silicates and in situ formed core/shell nanoparticles. *Polymer* 2002; 43: 2909–2916.

[257] Kornmann X, Berglund L a., Sterte J, et al. Nanocomposites based on montmorillonite and unsaturated polyester. *Polymer Engineering & Science* 1998; 38: 1351–1358.

[258] Tomić MD, Dunjić B, Likić V, et al. The use of nanoclay in preparation of epoxy anticorrosive coatings. *Progress in Organic Coatings* 2014; 77: 518–527.

[259] Fu J. Effect of Nanoclay on the Mechanical Properties of PMMA/Clay Nanocomposite Foams. *Journal of Cellular Plastics* 2006; 42: 325–342.

[260] Du M, Guo B, Jia D. Newly emerging applications of halloysite nanotubes: A review. *Polymer International* 2010; 59: 574–582.

[261] Fakhrullina GI, Akhatova FS, Lvov M, et al. Environmental Science Nano Toxicity of halloysite clay nanotubes in vivo : a Caenorhabditis elegans study †. *Environmental Science: Nano* 2015; 2: 54–59.

[262] Lvov Y, Abdullayev E. Functional polymer-clay nanotube composites with sustained release of chemical agents. *Progress in Polymer Science* 2013; 38: 1690–1719.

[263] Zeng QH, Yu AB, Lu GQ, et al. Clay-based polymer nanocomposites: research and commercial development. *Journal of nanoscience and nanotechnology* 2005; 5: 1574–1592.

[264] Chang J-H, Jang T-G, Ihn KJ, et al. Poly(vinyl alcohol) nanocomposites with different clays: Pristine clays and organoclays. *Journal of Applied Polymer Science* 2003; 90: 3208–3214.

[265] Kamble R, Ghag M, Gaikawad S, et al. Review article halloysite nanotubes and applications : A review. *Journal of Advanced Scientific Research* 2012; 3: 25–29.

[266] Joussein E, Petit S, Churchman J, et al. Halloysite clay minerals – a review. *Clay Minerals* 2005; 40: 383–426.

[267] Brantseva T V., Ilyin SO, Gorbunova IY, et al. Epoxy reinforcement with silicate particles: Rheological and adhesive properties - Part II: Characterization of composites with halloysite. *International Journal of Adhesion and Adhesives* 2016; 68: 248–255.

[268] Du M, Guo B, Jia D. Thermal stability and flame retardant effects of halloysite nanotubes on poly(propylene). *European Polymer Journal* 2006; 42: 1362–1369.

[269] Sancaktar E, Kuznicki J. Nanocomposite adhesives: Mechanical behavior with nanoclay. *International Journal of Adhesion and Adhesives* 2011; 31: 286–300.

[270] Asadi J, Ebrahimi NG, Razzaghi-kashani M. Composites : Part A Self-healing property of epoxy / nanoclay nanocomposite using poly (ethylene-co-methacrylic acid) agent. *Composites Part A* 2015; 68: 56–61.

[271] Singh B, Gilkes RJ. An electron optical investigation of the alteration of kaolinite to halloysite. *Clays and Clay Minerals* 1992; 40: 212–229.

[272] Wang M, Fan X, Thitsartarn W, et al. Rheological and mechanical properties of epoxy/clay nanocomposites with enhanced tensile and fracture toughnesses. *Polymer (United Kingdom)* 2015; 58: 43–52.

[273] Albdiry MT, Ku H, Yousif BF. Impact fracture behaviour of silane-treated halloysite nanotubes-reinforced unsaturated polyester. *Engineering Failure Analysis* 2013; 35: 718–725.

[274] Yuan P, Tan D, Annabi-Bergaya F. Properties and applications of halloysite nanotubes: recent research advances and future prospects. *Applied Clay Science* 2015; 112: 75–93.

[275] Lin Y, Ng KM, Chan C-M, et al. High-impact polystyrene/halloysite nanocomposites prepared by emulsion polymerization using sodium dodecyl sulfate as surfactant. *Journal of colloid and interface science* 2011; 358: 423–429.

[276] Carli LN, Crespo JS, Mauler RS. PHBV nanocomposites based on organomodified montmorillonite and halloysite: The effect of clay type on the morphology and thermal and mechanical properties. *Composites Part A: Applied Science and Manufacturing* 2011; 42: 1601–1608.

[277] Pavlidou S, Papaspyrides CD. A review on polymer-layered silicate nanocomposites. *Progress in Polymer Science (Oxford)* 2008; 33: 1119–1198.

[278] Zhang H, Zhang Z, Yang J-L, et al. Temperature dependence of crack initiation fracture toughness of various nanoparticles filled polyamide 66. *Polymer* 2006; 47: 679–689.

[279] Pasbakhsh P, Silva RT De, Vahedi V. The Role of Halloysite Surface Area and Aspect Ratio on the Tensile Properties of Ethylene Propylene Diene. *International Journal of Chemical, Molecular, Nuclear, Materials and Metallurgical Engineering* 2014; 8: 1363–1366.

[280] Albdiry MT, Yousif BF, Ku H. Fracture toughness and toughening mechanisms of unsaturated polyester-based clay nanocomposites. In: *13 th International Conference on Fracture*. 2013, pp. 1–10.

[281] Tang Y, Deng S, Ye L, et al. Effects of unfolded and intercalated halloysites on mechanical properties of halloysite-epoxy nanocomposites. *Composites Part A: Applied Science and Manufacturing* 2011; 42: 345–354.

[282] Kaynak C, Nakas GI, Isitman NA. Mechanical properties, flammability and char morphology of epoxy resin/montmorillonite nanocomposites. *Applied Clay Science* 2009; 46: 319–324.

[283] Bozkurt E, Kaya E, Tanoğlu M. Mechanical and thermal behavior of non-crimp glass fiber reinforced layered clay/epoxy nanocomposites. *Composites Science and Technology* 2007; 67: 3394–3403.

[284] Qi B, Zhang QX, Bannister M, et al. Investigation of the mechanical properties of DGEBA-based epoxy resin with nanoclay additives. *Composite Structures* 2006; 75: 514–519.

[285] Wang K, Chen L, Wu J, et al. Epoxy nanocomposites with highly exfoliated clay: Mechanical properties and fracture mechanisms. *Macromolecules* 2005; 38: 788–800.

[286] Kinloch AJ, Taylor AC. Mechanical and fracture properties of epoxy / inorganic micro- and nano-composites. *Journal of Materials Science Letters* 2003; 22: 1439–1441.

[287] Chozhan CK, Rajasekaran R, Alagar M, et al. Thermomechanical Behavior of Vinyl Ester Oligomer-Toughened Epoxy-Clay Hybrid Nanocomposites. *International Journal of Polymeric Materials* 2008; 57: 319–337.

[288] Ye Y, Chen H, Wu J, et al. High impact strength epoxy nanocomposites with natural nanotubes. *Polymer* 2007; 48: 6426–6433.

[289] Lepoittevin B, Devalckenaere M, Pantoustier N, et al. Poly(ε-caprolactone)/clay nanocomposites prepared by melt intercalation: mechanical, thermal and rheological properties. *Polymer* 2002; 43: 4017–4023.

[290] Manfredi LB, De Santis H, Vázquez A. Influence of the addition of montmorillonite to the matrix of unidirectional glass fibre/epoxy composites on their mechanical and water absorption properties. *Composites Part A: Applied Science and Manufacturing* 2008; 39: 1726–1731.

[291] Ji Q, Wetzel B, Friedrich K, et al. Tribological properties of surface modified nano-alumina / epoxy composites. 2004; 9: 6487–6493.

[292] Wang HT, Pan BR, Du QG, et al. The strain in the test environmental stress cracking of plastics. *Polymer Testing* 2003; 22: 125–128.

[293] Lima Sobrinho L, Ferreira M, Bastian FL. The effects of water absorption on an ester vinyl resin system. *Materials Research* 2009; 12: 353–361.

[294] Lee S-B, Rockett TJ, Hoffman RD. Interactions of water with unsaturated polyester, vinyl ester and acrylic resins. *Polymer* 1992; 33: 3691–3697.

[295] Deng S, Zhang J, Ye L, et al. Toughening epoxies with halloysite nanotubes. *Polymer* 2008; 49: 5119–5127.

[296] Albdiry MT, Yousif BF. Morphological structures and tribological performance of unsaturated polyester based untreated/silane-treated halloysite nanotubes. *Materials and Design* 2013; 48: 68–76.

[297] Vahedi V, Pasbakhsh P. Instrumented impact properties and fracture behaviour of epoxy/modified halloysite nanocomposites. *Polymer Testing* 2014; 39: 101–114.

[298] Bhuvana S, Prabakaran M. Synthesis and Characterisation of Polyamide / Halloysite Nanocomposites Prepared by Solution Intercalation Method. *Nanoscience and nanotechnology* 2014; 4: 44–51.

[299] Saharudin MS, Atif R, Shyha I, et al. The degradation of mechanical properties in halloysite nanoclay-polyester nanocomposites exposed to diluted methanol. *Journal of Composite Materials* 2016; 1–12.

[300] Gilman JW. Flammability and thermal stability studies of polymer layered-silicate (clay) nanocomposites. *Applied Clay Science* 1999; 15: 31–49.

[301] Gilman JW, Kashiwagi T, Lichtenhan JD. Nanocomposites: A revolutionary new flame retardant approach. *SAMPE Journal* 1997; 33: 40–46.

[302] Jumahat A, Soutis C, Mahmud J, et al. Compressive properties of nanoclay/epoxy nanocomposites. *Procedia Engineering* 2012; 41: 1607–1613.

[303] Liu W, Hoa S V., Pugh M. Water uptake of epoxy-clay nanocomposites: Model development. *Composites Science and Technology* 2008; 68: 156–163.

[304] Bergaya F, Lagaly G. General introduction: Clays, clay minerals, and clay science. *Developments in Clay Science* 2013; 5: 1–19.

[305] Maisanaba S, Pichardo S, Puerto M, et al. Toxicological evaluation of clay minerals and derived nanocomposites: A review. *Environmental Research* 2015; 138: 233–254.

[306] Patel HA, Somani RS, Bajaj HC, et al. Nanoclays for polymer nanocomposites, paints, inks, greases and cosmetics formulations, drug delivery vehicle and waste water treatment. *Bulletin of Materials Science* 2006; 29: 133–145.

[307] Guo M, Wang A, Muhammad F, et al. Halloysite nanotubes, a multifunctional nanovehicle for anticancer drug delivery. *Chinese Journal of Chemistry* 2012; 30: 2115–2120.

[308] Vergaro V, Abdullayev E, Lvov YM, et al. Cytocompatibility and uptake of halloysite clay nanotubes. *Biomacromolecules* 2010; 11: 820–826.

[309] Maisanaba S, Pichardo S, Puerto M, et al. Toxicological evaluation of clay minerals and derived nanocomposites: A review. *Environmental Research* 2015; 138: 233–254.

[310] Kotov NA. Carbon sheet solutions. *NATURE* 2006; 442: 254–255.

[311] Atif R, Inam F. Fractography analysis of 0.5 wt% multi layer graphene/nanoclay reinforced nanocomposites. *AIMS Materials Science* 2016; 3: 1294–1308.

[312] Wang J, Qiao J, Wang J, et al. Bioinspired Hierarchical Alumina–Graphene Oxide–Poly(vinyl alcohol) Artificial Nacre with Optimized Strength and Toughness. *ACS Applied Materials & Interfaces* 2015; 150423104146003.

[313] Kuilla T, Bhadra S, Yao D, et al. Recent advances in graphene based polymer composites. *Progress in Polymer Science* 2010; 35: 1350–1375.

[314] Saini A. EU Graphene Flagship project aims for technological breaktrough. *Cambridge University Press* 2014; 393–394.

[315] Sun X, Liu Z, Welsher K, et al. Nano-graphene oxide for cellular imaging and drug delivery. *Nano research* 2008; 1: 203–212.

[316] Stankovich S, Dikin D a, Dommett GHB, et al. Graphene-based composite materials. *Nature* 2006; 442: 282–286.

[317] López-Polín G, Gómez-Herrero J, Gómez-Navarro C. Confining Crack Propagation in Defective Graphene. *Nano Letters* 2015; 150302111347001.

[318] Atif R, Shyha I, Inam F. Mechanical, Thermal, and Electrical Properties of Graphene-Epoxy Nanocomposites—A Review. *Polymers* 2016; 8: 281.

[319] Lee C, Wei X, Kysar JW, et al. Measurement of the elastic properties and intrinsic strength of monolayer graphene. *Science (New York, NY)* 2008; 321: 385–388.

[320] Wang X, Jin J, Song M. An investigation of the mechanism of graphene toughening epoxy. *Carbon* 2013; 65: 324–333.

[321] Atif R, Shyha I, Inam F. The degradation of mechanical properties due to stress

concentration caused by retained acetone in epoxy nanocomposites. *RSC Adv* 2016; 6: 34188–34197.

[322] Zaman I, Phan TT, Kuan HC, et al. Epoxy/graphene platelets nanocomposites with two levels of interface strength. *Polymer* 2011; 52: 1603–1611.

[323] Atif R, Wei J, Shyha I, et al. Use of morphological features of carbonaceous materials for improved mechanical properties of epoxy nanocomposites. *RSC Adv* 2016; 6: 1351–1359.

[324] Wan Y-J, Tang L-C, Gong L-X, et al. Grafting of epoxy chains onto graphene oxide for epoxy composites with improved mechanical and thermal properties. *Carbon* 2014; 69: 467–480.

[325] Zhang Y, Wang Y, Yu J, et al. Tuning the interface of graphene platelets/epoxy composites by the covalent grafting of polybenzimidazole. *Polymer* 2014; 55: 4990–5000.

[326] Tang L-C, Wan Y-J, Yan D, et al. The effect of graphene dispersion on the mechanical properties of graphene/epoxy composites. *Carbon* 2013; 60: 16–27.

[327] Bortz DR, Heras EG, Martin-Gullon I. Impressive fatigue life and fracture toughness improvements in graphene oxide/epoxy composites. *Macromolecules* 2011; 45: 238–245.

[328] Rafiee MA, Rafiee J, Srivastava I, et al. Fracture and fatigue in graphene nanocomposites. *Small* 2010; 6: 179–183.

[329] Rafiee MA, Rafiee J, Wang Z, et al. Enhanced mechanical properties of nanocomposites at low graphene content. *ACS Nano* 2009; 3: 3884–3890.

[330] Kim H, Macosko CW. Morphology and Properties of Polyester/Exfoliated Graphite Nanocomposites. *Macromolecules* 2008; 41: 3317–3327.

[331] Loomis J, Panchapakesan B. Dimensional dependence of photomechanical response in carbon nanostructure composites: a case for carbon-based mixed-dimensional systems. *Nanotechnology* 2012; 23: 215501.

[332] Neto AC, Guinea F, Peres NM. Drawing conclusions from graphene. *Physics World* 2006; 19: 33–37.

[333] Ren F, Zhu G, Ren P, et al. In situ polymerization of graphene oxide and cyanate ester--epoxy with enhanced mechanical and thermal properties. *Applied Surface Science* 2014; 316: 549–557.

[334] Swain S. Synthesis and Characterization of Graphene Based Unsaturated Polyester Resin Composites. *Transactions on Electrical and Electronic Materials* 2013; 14: 53–58.

[335] Rafiq R, Cai D, Jin J, et al. Increasing the toughness of nylon 12 by the incorporation of functionalized graphene. *Carbon* 2010; 48: 4309–4314.

[336] Kyhl L, Nielsen SF, Čabo AG, et al. Graphene as an anti-corrosion coating layer. *Faraday discussions* 2015; 180: 495–509.

[337] Compton OC, Kim S, Pierre C, et al. Crumpled graphene nanosheets as highly effective barrier property enhancers. *Advanced Materials* 2010; 22: 4759–4763.

[338] Kousalya AS, Kumar A, Paul R, et al. Graphene: An effective oxidation barrier coating for liquid and two-phase cooling systems. *Corrosion Science* 2013; 69: 5–10.

[339] Tseng IH, Liao YF, Chiang JC, et al. Transparent polyimide/graphene oxide nanocomposite with improved moisture barrier property. *Materials Chemistry and Physics* 2012; 136: 247–253.

[340] Yano K, Usuki A, Okada A, et al. SYNTHESIS AND PROPERTIES OF POLYIMIDE CLAY HYBRID. *Journal of Polymer Science Part A-Polymer Chemistry* 1993; 31: 2493–2498.

[341] Dreher KL. Health and environmental impact of nanotechnology: Toxicological assessment of manufactured nanoparticles. *Toxicological Sciences* 2004; 77: 3–5.

[342] Schinwald A, Murphy FA, Jones A, et al. Graphene-based nanoplatelets: A new risk to the respiratory system as a consequence of their unusual aerodynamic properties. *ACS Nano* 2012; 6: 736–746.

[343] Ruiz ON, Fernando KAS, Wang B, et al. Graphene oxide: a nonspecific enhancer of cellular growth. *ACS Nano* 2011; 5: 8100–8107.

[344] Guo X, Mei N. Assessment of the toxic potential of graphene family nanomaterials. *Journal of Food and Drug Analysis* 2014; 22: 105–115.

[345] Wang K, Ruan J, Song H, et al. Biocompatibility of Graphene Oxide. *Nanoscale Research Letters* 2011; 6: 1–8.

[346] Peijs AAJM, de Kok JMM. Hybrid composites based on polyethylene and carbon fibres. Part 6: Tensile and fatigue behaviour. *Composites* 1993; 24: 19–32.

[347] Schrauwen B, Bertens P, Peijs T. Influence of hybridisation and test geometry on the impact response of glass-fibre-reinforced laminated composites. *Polymers and Polymer Composites* 2002; 10: 259–272.

[348] Mahrholz T, Mosch J, Röstermundt D, et al. Fibre-reinforced nanocomposites for spacecraft structures-manufacturing, characterisation and application. In: *Spacecraft Structures, Materials and Mechanical Testing 2005*. 2005.

[349] Gojny FH, Wichmann MHG, Fiedler B, et al. Influence of nano-modification on the

mechanical and electrical properties of conventional fibre-reinforced composites. *Composites Part A: Applied Science and Manufacturing* 2005; 36: 1525–1535.

[350] Thwe MM, Liao K. Effects of environmental aging on the mechanical properties of bamboo–glass fiber reinforced polymer matrix hybrid composites. *Composites Part A: Applied Science and Manufacturing* 2002; 33: 43–52.

[351] Pascault JP, Williams RJJ. Thermosetting Polymers. In: *Handbook of Polymer Synthesis, Characterization, and Processing*. 2013, pp. 519–533.

[352] Bordes P, Pollet E, Avérous L. Nano-biocomposites: Biodegradable polyester/nanoclay systems. *Progress in Polymer Science (Oxford)* 2009; 34: 125–155.

[353] Young RJ, Chung CI. Introduction to Polymers. *Journal of Engineering Materials and Technology* 1982; 104: 297.

[354] Atif R, Inam F. Influence of macro-topography on mechanical performance of 0.5 wt% nanoclay/multi-layer graphene-epoxy nanocomposites. *AIMS Materials Science* 2016; 3: 1294–1308.

[355] Hojo H, Ogasawara K, Chang W., et al. Degradation behavior of unsaturated polyester resin in alcohols. *Adv Composite Mater* 1994; 3: 341–353.

[356] Ott J, Gronemann V, Pontzen F, et al. Methanol. *Ullmann's Encyclopedia of Industrial Chemistry* 2012; 3.

[357] Lange J-P. Methanol synthesis: a short review of technology improvements. *Catalysis Today* 2001; 64: 3–8.

[358] Pellegrini LA, Soave G, Gamba S, et al. Economic analysis of a combined energy-methanol production plant. *Applied Energy* 2011; 88: 4891–4897.

[359] Bermudez JM, Fidalgo B, Arenillas A, et al. CO2 reforming of coke oven gas over a Ni/Al 2O3 catalyst to produce syngas for methanol synthesis. *Fuel* 2012; 94: 197–203.

[360] Wang C, Chen W, Wang W, et al. Experimental study on methanol recovery through flashing vaporation in continuous production of biodiesel via supercritical methanol. *Energy Conversion and Management* 2011; 52: 1454–1458.

[361] Hall J V. Potential air quality benefits of methanol as a vehicle fuel. *Energy* 1985; 10: 733–736.

[362] Han W, Chen S, Campbell J, et al. Fracture toughness and wear properties of nanosilica/epoxy composites under marine environment. *Materials Chemistry and Physics* 2016; 177: 1–9.

[363] Nguyen T, Aouadi K, Alsheh D, et al. Effect of Civil Engineering Environments on

Interfacial Properties of Polymer/Glass Fiber Composites. In: *4th International Conference on Composites Engineering*. 1997, pp. 725–726.

[364] Le Gac PY, Le Saux V, Paris M, et al. Ageing mechanism and mechanical degradation behaviour of polychloroprene rubber in a marine environment: Comparison of accelerated ageing and long term exposure. *Polymer Degradation and Stability* 2012; 97: 288–296.

[365] Yian Z, Keey SL, Boay CG. Effects of seawater exposure on mode II fatigue delamination growth of a woven E-glass/bismaleimide composite. *Journal of Reinforced Plastics and Composites* 2016; 35: 138–150.

[366] Gu H. Behaviours of glass fibre/unsaturated polyester composites under seawater environment. *Materials and Design* 2009; 30: 1337–1340.

[367] Fang Y, Wang K, Hui D, et al. Monitoring of seawater immersion degradation in glass fibre reinforced polymer composites using quantum dots. *Composites Part B: Engineering* 2017; 112: 93–102.

[368] Keller A, Masania K, Taylor AC, et al. Fast-curing epoxy polymers with silica nanoparticles: properties and rheo-kinetic modelling. *Journal of Materials Science* 2015; 51: 236–251.

[369] Wan C, Qiao X, Zhang Y, et al. Effect of different clay treatment on morphology and mechanical properties of PVC-clay nanocomposites. *Polymer Testing* 2003; 22: 453–461.

[370] Jawahar P, Balasubramanian M. Influence of nanosize clay platelets on the mechanical properties of glass fiber reinforced polyester composites. *Journal of nanoscience and nanotechnology* 2006; 6: 3973–3976.

[371] Inceogul AB, Yilmazer U. *Mechanical properties of unsaturated polyester/montmorillonite composites*. 2001.

[372] Atif R, Inam F. Influence of macro-topography on damage tolerance and fracture toughness of 0.1 wt % multi-layer graphene/clay-epoxy nanocomposites. *Polymers* 2016; 8: 335–360.

[373] Xu B, Zheng Q, Song Y, et al. Calculating barrier properties of polymer/clay nanocomposites: Effects of clay layers. *Polymer* 2006; 47: 2904–2910.

[374] Albdiry M, Yousif B, Ku H, et al. A critical review on the manufacturing processes in relation to the properties of nanoclay/polymer composites. *Journal of Composite Materials* 2012; 47: 1093–1115.

[375] Yasmin A, Abot JL, Daniel IM. Processing of clay/epoxy nanocomposites by shear mixing. *Scripta Materialia* 2003; 49: 81–86.

[376] Tan B, Thomas NL. A review of the water barrier properties of polymer/clay and

polymer/graphene nanocomposites. *Journal of Membrane Science* 2016; 514: 595–612.

[377] Rossi S, Deflorian F, Fiorenza J. Environmental influences on the abrasion resistance of a coil coating system. *Surface and Coatings Technology* 2007; 201: 7416–7424.

[378] Shi X, Nguyen TA, Suo Z, et al. Effect of nanoparticles on the anti corrosion and mechanical properties of epoxy coating. *Surface and Coatings Technology* 2009; 204: 237–245.

[379] Senthil Kumar MS, Mohana Sundara Raju N, Sampath PS, et al. Tribological analysis of nano clay/epoxy/glass fiber by using Taguchi's technique. *Materials & Design* 2015; 70: 1–9.

[380] Nielsen LE. Models for the permeability of filled polymer systems. *Journal of Macromolecular Science—Chemistry* 1967; 1: 929–942.

[381] Abdullayev E, Lvov Y, Twite RL, et al. Clay nanotubes for corrosion inhibitor encapsulation: release control with end stoppers. *Journal of Materials Chemistry* 2010; 20: 6681.

[382] Gorrasi G, Pantani R, Murariu M, et al. PLA/halloysite nanocomposite films: Water vapor barrier properties and specific key characteristics. *Macromolecular Materials and Engineering* 2014; 299: 104–115.

[383] Yarris L. Alcohol and Water Don't Mix. *Science Beat*http://www2.lbl.gov/Science-Articles/Archive/sb-ALS-alcohol-and-water.html (2003).

[384] Wei J, Atif R, Vo T, et al. Graphene Nanoplatelets in Epoxy System: Dispersion, Reaggregation, and Mechanical Properties of Nanocomposites. *Journal of Nanomaterials*; 2015. Epub ahead of print 2015. DOI: 10.1155/2015/561742.

[385] Bédoui F, Cauvin L. Elastic properties prediction of nano-clay reinforced polymers using hybrid micromechanical models. *Computational Materials Science* 2012; 65: 309–314.

[386] Bromberg L, Cheng WK. *Methanol as an alternative transportation fuel in the U.S.: Options for sustainable and/or energy-secure transportation*http://www.methanol.org/Energy/Resources/Alternative-Fuel/MIT-Methanol-Report-Final-Nov-2010.aspx (2010).

[387] Arnold JC. The influence of liquid uptake on environmental stress cracking of glassy polymers. *Materials Science and Engineering: A* 1995; 197: 119–124.

[388] Rahman M. *Degradation of Polyesters in Medical Applications*. Manitoba, Canada.: INTECH, 2012. Epub ahead of print 2012. DOI: 10.5772/47765.

[389] Bora C, Gogoi P, Baglari S, et al. Preparation of polyester resin/graphene oxide

nanocomposite with improved mechanical strength. *Journal of Applied Polymer Science* 2013; 129: 3432–3438.

[390] Lewitus D, McCarthy S, Ophir a., et al. The effect of nanoclays on the properties of PLLA-modified polymers Part 1: Mechanical and thermal properties. *Journal of Polymers and the Environment* 2006; 14: 171–177.

[391] Paul DR, Robeson LM. Polymer nanotechnology: Nanocomposites. *Polymer* 2008; 49: 3187–3204.

[392] Wildan MW, Mohd Ishak ZA, others. Preparation and properties of clay-reinforced epoxy nanocomposites. *International Journal of Polymer Science*; 2013.

[393] Guo B, Zou Q, Lei Y, et al. Structure and performance of polyamide 6/halloysite nanotubes nanocomposites. *Polymer journal* 2009; 41: 835–842.

[394] Wu Z, Zhou C, Qi R, et al. Synthesis and characterization of nylon 1012/clay nanocomposite. *Journal of applied polymer science* 2002; 83: 2403–2410.

[395] Fraga AN, Alvarez V a, Vazquez A, et al. Relationship Between Dynamic Mechanical Properties and Water Absorption of Unsaturated Polyester and Vinyl Ester Glass Fiber Composites. *Journal of Composite Materials* 2003; 37: 1553–1574.

[396] Bastiurea M, Rodeanu MS, Dima D, et al. Thermal and Mechanical Properties of Polyester Composites With Graphene Oxide and Graphite. *Digest Journal of Nanomaterials and Biostructures* 2015; 10: 521–533.

[397] Morrison ED, Malvey MW, Johnson RD, et al. Effect of chemical environments on stress cracking of poly(ethylene terephthalate) beverage bottles. *Polymer Testing* 2008; 27: 660–666.

[398] Cele HM, Ojijo V, Chen H, et al. Effect of nanoclay on optical properties of PLA/clay composite films. *Polymer Testing* 2014; 36: 24–31.

[399] Nadareishvili LI. *Polymers and polymeric materials for fiber and gradient optics*. Utrecth: VSP, 2002.

[400] Marais S, Nguyen QT, Devallencourt C, et al. Permeation of water through polar and nonpolar polymers and copolymers: determination of the concentration-dependent diffusion coefficient. *Journal of Polymer Science, Part B: Polymer Physics* 2000; 38: 1998–2008.

[401] Hansen CM. Diffusion in polymers. *Polymer Engineering & Science* 1980; 20: 252–258.

[402] Picard E, Vermogen A, Gérard JF, et al. Barrier properties of nylon 6-montmorillonite nanocomposite membranes prepared by melt blending: Influence of the clay content and dispersion state. Consequences on modelling. *Journal of*

Membrane Science 2007; 292: 133–144.

[403] Picard E, Gérard J-F, Espuche E. Water transport properties of polyamide 6 based nanocomposites prepared by melt blending: On the importance of the clay dispersion state on the water transport properties at high water activity. *Journal of Membrane Science* 2008; 313: 284–295.

[404] Forsyth M. The effect of nano-particle TiO2 fillers on structure and transport in polymer electrolytes. *Solid State Ionics* 2002; 147: 203–211.

[405] Albdiry MT, Yousif BF, Ku H. Fracture toughness and toughening mechanisms of unsaturated polyester-based clay nanocomposites. 2013; 1–10.

[406] Indrani DJ, Cook WD, Televantos F, et al. Fracture toughness of water-aged resin composite restorative materials. *Dental Materials* 1995; 11: 201–207.

[407] Buehler FU, Seferis JC. Effect of reinforcement and solvent content on moisture absorption in epoxy composite materials. *Composites Part A: Applied Science and Manufacturing* 2000; 31: 741–748.

[408] Marom G. The role of water transport in composite materials. In: *Polymer permeability*. Springer, 1985, pp. 341–374.

[409] Gewert B, Plassmann MM, MacLeod M. Pathways for degradation of plastic polymers floating in the marine environment. *Environmental science Processes & impacts* 2015; 17: 1513–21.

[410] Lobelle D, Cunliffe M. Early microbial biofilm formation on marine plastic debris. *Marine Pollution Bulletin* 2011; 62: 197–200.

[411] Muthukumar T, Aravinthan A, Lakshmi K, et al. Fouling and stability of polymers and composites in marine environment. *International Biodeterioration and Biodegradation* 2011; 65: 276–284.

[412] Costerton JW, Lewandowski Z, Caldwell DE, et al. Microbial biofilms. *Annual review of microbiology* 1995; 49: 711–45.

[413] Zardus JD, Nedved BT, Huang Y, et al. Microbial biofilms facilitate adhesion in biofouling invertebrates. *Biological Bulletin* 2008; 214: 91–98.

[414] Falkiewicz-Dulik M, Janda K, Wypych G. *Handbook of Material Biodegradation, Biodeterioration, and Biostablization: Second Edition*. Epub ahead of print 2015. DOI: 10.1016/B978-1-895198-87-4.50009-8.

[415] Pandian A, Vairavan M, Jebbas Thangaiah WJ, et al. Effect of Moisture Absorption Behavior on Mechanical Properties of Basalt Fibre Reinforced Polymer Matrix Composites. *Journal of Composites* 2014; 2014: 1–8.

[416] John B, Nair CPR, Ninan KN. Effect of nanoclay on the mechanical, dynamic

mechanical and thermal properties of cyanate ester syntactic foams. *Materials Science and Engineering A* 2010; 527: 5435–5443.

[417] Maharsia R, Gupta N, Jerro HD. Investigation of flexural strength properties of rubber and nanoclay reinforced hybrid syntactic foams. *Materials Science and Engineering A* 2006; 417: 249–258.

[418] Kajohnchaiyagual J, Jubsilp C, Dueramae I, et al. Thermal and Mechanical Properties Enhancement Obtained in Highly Filled Alumina-Polybenzoxazine Composites. *Polymer Composites* 2014; 10: 2269–2279.

[419] Landel RF, Nielsen LE. *Mechanical properties of polymers and composites*. CRC Press, 1993.

[420] Mourad AHI, Beckry Mohamed AM, El-Maaddawy T. Effect of seawater and warm environment on glass/epoxy and glass/polyurethane composites. *Applied Composite Materials* 2010; 17: 557–573.

[421] Heimowska A, Krasowska K, Rutkowska M. Degradability of Different Packaging Polymeric Materials in Seawater. In: *The 12th Annual General Assembly IAMU*. 2012, pp. 153–163.

[422] Chakraverty a P, Mohanty UK, Mishra SC, et al. Sea Water Ageing of GFRP Composites and the Dissolved salts. *IOP Conference Series: Materials Science and Engineering* 2015; 75: 12029.

[423] Zettler ER, Mincer TJ, Amaral-Zettler LA. Life in the 'plastisphere': Microbial communities on plastic marine debris. *Environmental Science and Technology* 2013; 47: 7137–7146.

[424] Hamzah E, Hussain MF, Ibrahim Z, et al. Corrosion Behaviour of Carbon Steel in Sea Water Medium in Presence of P. aeruginosa Bacteria. *Arabian Journal for Science and Engineering* 2014; 39: 6863–6870.

[425] Helbling C, Abanilla M, Lee L, et al. Issues of variability and durability under synergistic exposure conditions related to advanced polymer composites in the civil infrastructure. *Composites Part A: Applied Science and Manufacturing* 2006; 37: 1102–1110.

[426] Ipekoglu B, Boke H, Cizer O. Assessment of material use in relation to climate in historical buildings. *BUILDING AND ENVIRONMENT* 2007; 42: 970–978.

[427] Jakubowicz I, Yarahmadi N, Petersen H. Evaluation of the rate of abiotic degradation of biodegradable polyethylene in various environments. *Polymer Degradation and Stability* 2006; 91: 1556–1562.

[428] Lugauskas A, Levinskaite L, Pe??iulyte D. Micromycetes as deterioration agents of polymeric materials. *International Biodeterioration and Biodegradation* 2003; 52: 233–242.

[429] Bonhomme S, Cuer A, Delort AM, et al. Environmental biodegradation of polyethylene. *Polymer Degradation and Stability* 2003; 81: 441–452.

[430] Rampadarath S, Bandhoa K, Puchooa D, et al. Early bacterial biofilm colonizers in the coastal waters of Mauritius. *Electronic Journal of Biotechnology* 2017; 29: 13–21.

[431] Geim AK, Novoselov KS. The rise of graphene. *Nature Mater* 2007; 6: 183–191.

[432] Balandin AA, Ghosh S, Bao W, et al. Superior thermal conductivity of single-layer graphene. *Nano letters* 2008; 8: 902–907.

[433] Novoselov KS, Fal′ko VI, Colombo L, et al. A roadmap for graphene. *Nature* 2012; 490: 192–200.

[434] Preghenella M, Pegoretti A, Migliaresi C. Thermo-mechanical characterization of fumed silica-epoxy nanocomposites. *Polymer* 2005; 46: 12065–12072.

[435] Nair RR, Wu H a., Jayaram PN, et al. Unimpeded Permeation of Water Through Helium-Leak-Tight Graphene-Based Membranes. *Science* 2012; 335: 442–444.

[436] Saharudin M, Wei J, Shyha I, et al. The degradation of mechanical properties in halloysite nanoclay-polyester nanocomposites exposed in seawater environment. *Journal of Nanomaterials (JNM)*.

[437] Bhattacharya M. Polymer nanocomposites-A comparison between carbon nanotubes, graphene, and clay as nanofillers. *Materials* 2016; 9: 1–35.

[438] Hough MC, Wright DC. Two new test methods for assessing environmental stress cracking of amorphous thermoplastics. *Polymer Testing* 1996; 15: 407–421.

[439] Faruk O, Bledzki AK, Fink H-P, et al. Biocomposites reinforced with natural fibers: 2000–2010. *Progress in Polymer Science* 2012; 37: 1552–1596.

[440] Pandian A, Vairavan M, Jebbas Thangaiah WJ, et al. Effect of Moisture Absorption Behavior on Mechanical Properties of Basalt Fibre Reinforced Polymer Matrix Composites. *Journal of Composites* 2014; 2014: 1–8.

[441] Peeterbroeck S, Alexandre M, Nagy JB, et al. Polymer-layered silicate–carbon nanotube nanocomposites: unique nanofiller synergistic effect. *Composites Science and Technology* 2004; 64: 2317–2323.

[442] Zeng Y, Liu H-Y, Mai Y-W, et al. Improving interlaminar fracture toughness of carbon fibre/epoxy laminates by incorporation of nano-particles. *Composites Part B: Engineering* 2012; 43: 90–94.

[443] Feng H, Wang X, Wu D. Fabrication of spirocyclic phosphazene epoxy-based nanocomposites with graphene via exfoliation of graphite platelets and thermal curing for enhancement of mechanical and conductive properties. *Industrial &*

Engineering Chemistry Research 2013; 52: 10160–10171.

[444] Moghbelli E, Banyay R, Sue HJ. Effect of moisture exposure on scratch resistance of PMMA. *Tribology International* 2014; 69: 46–51.